

INFORMATION TO USERS

This manuscript has been reproduced from the microfilm master. UMI films the text directly from the original or copy submitted. Thus, some thesis and dissertation copies are in typewriter face, while others may be from any type of computer printer.

The quality of this reproduction is dependent upon the quality of the copy submitted. Broken or indistinct print, colored or poor quality illustrations and photographs, print bleedthrough, substandard margins, and improper alignment can adversely affect reproduction.

In the unlikely event that the author did not send UMI a complete manuscript and there are missing pages, these will be noted. Also, if unauthorized copyright material had to be removed, a note will indicate the deletion.

Oversize materials (e.g., maps, drawings, charts) are reproduced by sectioning the original, beginning at the upper left-hand corner and continuing from left to right in equal sections with small overlaps.

Photographs included in the original manuscript have been reproduced xerographically in this copy. Higher quality 6" x 9" black and white photographic prints are available for any photographs or illustrations appearing in this copy for an additional charge. Contact UMI directly to order.

**ProQuest Information and Learning
300 North Zeeb Road, Ann Arbor, MI 48106-1346 USA
800-521-0600**

UMI[®]

**Novel Approaches Towards the Synthesis of Protein Tyrosine
Phosphatase Inhibitors
and
Alternative Strategies in the Design of Transition State Analogues for
Phosphatase Abzymes**

by

Gabriel Hum

**A thesis submitted in conformity with the requirements
for the degree of Doctorate of Philosophy
Graduate Department of Chemistry
University of Toronto**

© Copyright by Gabriel Hum 2002



**National Library
of Canada**

**Acquisitions and
Bibliographic Services**

**395 Wellington Street
Ottawa ON K1A 0N4
Canada**

**Bibliothèque nationale
du Canada**

**Acquisitions et
services bibliographiques**

**395, rue Wellington
Ottawa ON K1A 0N4
Canada**

Your file Votre référence

Our file Notre référence

The author has granted a non-exclusive licence allowing the National Library of Canada to reproduce, loan, distribute or sell copies of this thesis in microform, paper or electronic formats.

The author retains ownership of the copyright in this thesis. Neither the thesis nor substantial extracts from it may be printed or otherwise reproduced without the author's permission.

L'auteur a accordé une licence non exclusive permettant à la Bibliothèque nationale du Canada de reproduire, prêter, distribuer ou vendre des copies de cette thèse sous la forme de microfiche/film, de reproduction sur papier ou sur format électronique.

L'auteur conserve la propriété du droit d'auteur qui protège cette thèse. Ni la thèse ni des extraits substantiels de celle-ci ne doivent être imprimés ou autrement reproduits sans son autorisation.

0-612-69033-4

Canada

Abstract

The work reported herein spans two different projects. In the first section, SPSOS chemistry is used to prepare two series of compounds bearing the difluoromethylene phosphonic (DFMP) acid moiety that are screened against PTP1B. Non crosslinked polystyrene (NCPS) is employed as a support for the synthesis of both series of inhibitors allowing for homogeneous reaction conditions and non-destructive monitoring of the reaction progress by ^{19}F NMR. In the first series, a Suzuki reaction is used to prepare a series of biaryl phosphonic acids while a Wittig reaction is used to synthesize the second styryl-like series of compounds. Compounds from both libraries ranged in purity from 43 to 99% and were suitable for assaying without the need for further purification. The best inhibitors from the Suzuki and Wittig libraries had K_i 's of 1.7 and 5 μM respectively.

In the second section of the thesis, isomeric 2,5-di-*p*-nitrophenyl phospholanate esters were synthesized and employed as transition state analogues for the purpose of obtaining catalytic antibodies capable of hydrolyzing model phosphotriester and phosphono diester substrates. Crucial to the hapten design was the C-P-C bond angle of the cyclic TSA's. The value of this angle was determined by X-ray crystallography of one of the final TSA products as well as various synthetic intermediates. The TSA's were conjugated to carrier proteins and immunized into mice for the purposes of isolating antibodies. One antibody, Jel 541, was found to be able to differentiate between the TSA's and exhibit catalytic activity in hydrolyzing the substrates significantly above background rates.

Acknowledgements

The work and effort that goes into working towards and assembling a thesis requires an effort for which there is no real preparation. It is an ordeal I liken to a trial by fire and would also not be possible without a supporting cast. As is customary, I would like to begin by thanking my supervisor, Scott D. Taylor, for his support and guidance.

I would like to thank the members of the Taylor group, past and present, who provided me with the occasional chemistry advice and above all, moments of levity. This group is far too numerous to name here, but it is fair to say we have all shared together many memories both good and bad.

Special mention must be made of those who assisted in a technical role. A. Young, A. Lough, and J. Venne provided and maintained services which no graduate student could ever do without.

To my family and my in-laws, your support never wavered and you have been there all the way. I thank all of you for looking out for us.

To my little angels, Kelsey, Meghan, and Riley, I am reminded about the true purpose of life every time I look at you. The past few years have not been easy, but would have been much less significant without all of you.

Finally, to my wife Stephanie, endowed with the face of an angel and patience of a saint, who has sacrificed so much to see this to an end, let us now begin the next stage of our lives together. I thank you for being who and what you are and am forever indebted to you.

Table of Contents

Abstract	ii
Acknowledgements	iii
Table of Contents	iv
Abbreviations	x
List of Schemes	xiii
List of Figures	xviii
List of Tables	xx
Appendix	xxi
CHAPTER 1 INTRODUCTION TO PROTEIN TYROSINE PHOSPHATASES AND COMBINATORIAL CHEMISTRY	
1.1 Overview and Global Objectives	1
1.2 Phosphatase Enzymes	2
1.3 Protein Tyrosine Phosphatases (PTPases)	3
1.3.1 Classes of PTPases	3
1.3.2 Structural Features of PTPases	5
1.3.3 Substrate Binding and Catalytic Mechanism	6
1.4 PTPase Substrates	13
1.5 Protein Tyrosine Phosphatase 1B (PTP1B)	16
1.5.1 PTP1B Overview	16
1.5.2 PTP1B Substrate Binding	17

1.5.3 PTP1B and Diabetes	20
1.6 PTPase Inhibitors	24
1.6.1 Peptide Based Inhibitors	24
1.6.2 Inorganic Metal Based PTPase Inhibitors	27
1.6.3 Irreversible PTPase Inhibitors	28
1.6.4 Natural Product Based PTPase Inhibitors	29
1.6.5 Therapeutic Agents as PTPase Inhibitors	31
1.6.6 Structure Based Non-Peptidyl PTPase Inhibitors	32
1.7 Combinatorial Chemistry	37
1.8 Polymer Supported Organic Synthesis	40
1.8.1 Insoluble Polymer Supports	41
1.8.2 Soluble Polymer Supports	44
1.9 Specific Objectives	48
1.10 References	51
CHAPTER 2 PSOS SYNTHESIS OF BIARYL DFMP COMPOUNDS VIA A SUZUKI REACTION	
2.1 Introduction	60
2.2 Experimental	64
General	64
2.2.1 Molecular Modeling	66
2.2.2 Organic Synthesis	67
2.2.2.1 Synthesis of Aryl DFMP Compounds	67

2.2.2.2 Synthesis and Functionalization of NCPS	73
2.2.2.3 Synthesis of Library of Biaryl DFMP Compounds	78
2.2.2.4 Synthesis of 1-hexanol functionalized NCPS	83
2.2.3 Inhibition Studies	85
2.2.4 Synthesis of Biphenyl Phosphine Ligand 2.99	85
2.3 Results and Discussion	89
2.3.1 Molecular Modeling of 1.34 Bound to PTP1B	89
2.3.2 Synthesis of Benzylic DFMP Compounds	96
2.3.2.1 The DAST Approach	96
2.3.2.2 Coupling of Aryl Iodides with Br(M)CF₂P(O)(OEt)₂	98
2.3.2.3 The Electrophilic Fluorination Approach	99
2.3.3 Synthesis of Chloromethylated NCPS	102
2.3.4 Attachment of Phosphonates to NCPS	103
2.3.5 Room Temperature Suzuki Couplings	108
2.3.6 Attaching a Linker Chain to Polymer 2.32	112
2.3.7 Reaction Sequence for Library Synthesis	114
2.3.8 Library Construction Using a C-C Linker Arm	121
2.3.9 Inhibition Studies with Biaryl Phosphonates and PTP1B	123
2.3.10 Suzuki Couplings with Novel Phosphine Ligands	127
2.4 Summary	129
2.5 Future Directions for Preparing DFMP Compounds on SPSOS	130
Using Palladium Chemistry	
2.6 Synthesis of a Biaryl DFMS Library	134

2.7 References	136
CHAPTER 3 SYNTHESIS OF STYRL BASED PTP1B INHIBITORS	
3.1 Introduction	141
3.2 Experimental	145
General	145
3.2.1 Synthesis of Protected Aryl Aldehyde DFMP Compounds	145
3.2.2 Synthesis of Sulfamide Mitsunobu Reagent	149
3.2.3 Synthesis of Protected Aryl Alcohol DFMP Compounds	150
3.2.4 Synthesis of Dess-Martin Reagent	158
3.2.5 On Polymer Reactions - Synthesis of Wittig Library	158
3.3 Results and Discussion	169
3.3.1 Studies on Model Compounds in Solution	169
3.3.2 Model Wittig Reactions	172
3.3.3 Attachment of 3.7 to the Polymer Support	175
3.3.4 Synthesis of Phosponates Bearing a Protected Alcohol	179
Moiety on the Aryl Ring	
3.3.5 Model and on Polymer Oxidation Reactions	188
3.3.6 On Polymer Wittig Reactions	191
3.3.7 Cleavage and Deprotection of Wittig Products	193
3.3.8 Purification of Phosphonic Acids by Ion Exchange	193
3.3.9 Library Synthesis	198
3.3.10 Inhibition Studies	206

3.4 Summary of the Wittig Library	207
3.5 Conclusions Concerning the Use of Soluble Polymers as Supports for PSOS	207
3.5.1 Conclusions Concerning the Synthesis of DFMP's on Polymer Supports	209
3.6 Future Directions	210
3.6.1 Future Work With Aryl Aldehyde DFMP Compounds on NCPS	210
3.6.2 Alternative Applications of Aryl DFMP Compounds	213
3.7 Recent Advances in PTP1B Inhibitor Design	213
3.7 References	218
CHAPTER 4 ANTIBODY CATALYZED HYDROLYSIS OF PHOSPHOTRIESTERS	
4.1 Introduction	223
4.1.1 Overview and Global Objectives	223
4.1.2 Antibodies	224
4.1.3 Catalytic Antibodies	227
4.1.4 Phosphatase Catalytic Antibodies	231
4.1.5 Specific Objectives	236
4.2 Experimental	240
General	240
4.2.1 Synthesis of Transition State Analogues	240
4.2.2 <i>Cis</i> TSA (4.26) Isomerization Studies	256

4.2.3 Conjugation of TSA's to Carrier Proteins	257
4.2.4 Synthesis of Antibody Substrates	258
4.2.5 Antibody Substrate Hydrolysis Studies	262
4.3 Results and Discussion	263
4.3.1 Synthesis of Transition State Analogues	263
4.3.2 Hapten Isomerization Studies	288
4.3.3 Conjugation of TSA's to Carrier Proteins	294
4.3.4 Crystal Structure Data	296
4.3.5 Synthesis of Antibody Substrates	302
4.3.6 Antibody Substrate Hydrolysis Studies	304
4.3.7 Antibody Production and Catalytic Screening	306
4.4 Summary	308
4.5 Current State of Phosphatase Abzymes	308
4.6 Future Work	315
4.7 References	317
Appendix	
Supplementary Crystallographic Data	A.i

Abbreviations

Ab	antibody
approx	approximately
Ar	argon
BSA	bovine serum albumin
DAST	diethylaminosulfur trifluoride
DEAD	diethylazido dicarboxylate
DFMP	difluoromethylene phosphonic acid
DIAD	diisopropylazido dicarboxylate
DME	1,2-dimethoxyethane
DMF	dimethyl formamide
DMSO	dimethyl sulphoxide
DTT	dithrethiol
EDC	1-(3-methyl-amino-propyl)-3-ethyl-carbodiimide
EGFR	epidermal growth factor receptor
eq	equivalent (schemes)
equiv	equivalent (text)
EtOAc	ethyl acetate
F₂Pmp	(difluorophosphonomethyl)phenylalanine
FDP	fluorescein diphosphate
hr(s)	hour(s)
IRK	insulin receptor kinase

KLH	keyhole limpet hemocyanin
LPOS	liquid phase organic synthesis
M	molar
min	minute
mmol	millimoles
NaHMDS	sodium bis(trimethylsilyl) azide
NCPS	non crosslinked polystyrene
NFSi	<i>N</i>-fluorobenzensulfonimide
NHS	<i>N</i>-hydroxy succinimide
nm	nanometer
O/N	overnight
PG	protecting group
PEG	polyethylene glycol
Ph	phenyl group
ppm	parts per million
PSOS	polymer supported organic synthesis
PTK	phosphotyrosine kinase
PTP	protein tyrosine phosphatase
R_f	migration distance on a TLC plate
RT	room temperature
SP	square pyramidal
SPOS	solid phase organic synthesis
SPSOS	soluble polymer supported organic synthesis

TBP	trigonal bipyramidal
TFA	trifluoroacetic acid
THF	tetrahydrofuran
THP	tetrahydropyranol
TMSBr	trimethylsilyl bromide
TMSCl	trimethylsilyl chloride
TMSI	trimethylsilyl iodide
TS	transition state
TSA	transition state analogue
VAZO	1,1'-azobis(cyclohexane carbonitrile)

List of Schemes

Scheme	Title	Page
1.1	Action of PTK's and PTPases.	3
1.2	Catalytic mechanism of PTPases.	8
1.3	Stabilization of a trigonal bipyramidal transition state or intermediate by a guanidinium group.	10
1.4	Possible transition states for enzyme-product formation and hydrolysis.	13
1.5	The insulin signalling cascade.	22
1.6	Inactivation by menadione.	28
1.7	Inactivation of enzyme by 1.18 and 1.19.	29
1.8	Synthesis of PTP inhibitors on Rinke resin using a Ugi reaction.	43
1.9	Synthesis of prostaglandin E ₂ methyl ester on NCPS.	47
1.10	General approach for library synthesis.	49
2.1	General approach to the synthesis of biaryl DFMP compounds.	62
2.2	DAST approach to the synthesis of 2.11.	97
2.3	Burton and Qiu's approach to the synthesis of aryl DFMP compounds.	98
2.4	Synthesis of 2.11 using Burton's cadmate procedure.	99

2.5	Synthesis of iodobenzyl phosphonate 2.18 .	100
2.6	Preparation of benzylic phosphonates and DFMP compounds.	100
2.7	Synthesis of monoacids 2.28 and 2.29 .	101
2.8	Synthesis of 3% chloromethylated NCPS (2.32).	102
2.9	Attempt to attach 2.26 to 3% chloromethylated NCPS using the tetrabutyl ammonium salt.	105
2.10	Conversion of chloromethylated NCPS to hydroxymethyl NCPS.	106
2.11	Mitsunobu coupling of phosphonic acids 2.28 and 2.29 to polymer 2.37 .	107
2.12	Model Suzuki reaction.	110
2.13	Synthesis of benzyl phosphonate ester 2.44 .	113
2.14	Functionalization of NCPS with 1,4-butanediol linker.	114
2.15	Mitsunobu and Suzuki couplings on NCPS.	116
2.16	Cleavage and deprotection of phosphonic acids from the support.	117
2.17	Synthesis of polymer 2.93 .	122
2.18	Synthesis of biaryl DFMP compounds via a Stille coupling.	126
2.19	Buchwald's Suzuki coupling conditions.	128
2.20	Pd catalyzed amination of aryl chlorides.	130
2.21	Pd catalyzed biaryl ether formation.	131
2.22	Pd catalyzed aryl <i>t</i> -butyl ether formation.	131
2.23	Room temperature Sonogashira coupling conditions.	131

2.24	Heck coupling conditions with aryl chlorides.	132
2.25	Route towards a library of triaryl DFMP bearing inhibitors.	133
2.26	Synthesis of <i>meta</i> biaryl DFMS library.	135
3.1	Stille and Heck approaches towards library construction.	142
3.2	Wittig approaches towards library construction.	143
3.3	Alternative reactions with a polymer bound aldehyde.	144
3.4	Attempted Bouveault reaction on aryl bromide 2.27 .	170
3.5	Synthesis of phosphonate 3.16 .	171
3.6	Deprotection of 3.16 .	172
3.7	Synthesis of 3.2 using Bellucci's Wittig conditions.	173
3.8	Wittig reaction using NaH and 15-crown-5.	175
3.9	Synthesis of betaine 3.22 .	177
3.10	Attempt at converting 3.16 to the acid chloride.	178
3.11	Revised approach towards library construction.	178
3.12	Synthesis of TBDPS protected alcohol 3.32 .	180
3.13	Synthesis of <i>o</i> -nitrobenzyl protected alcohol 3.37 .	182
3.14	Synthesis of allyl protected alcohol 3.42 .	184
3.15	Coupling of 3.43 to functionalized NCPS and removal of allyl group.	187
3.16	Dess-Martin oxidation of polymer-bound 3.45 .	190
3.17	On-polymer Wittig reaction using KH/18-crown-6.	192
3.18	Cleavage and deprotection of products from the support.	193

3.19	Reaction sequence for library synthesis.	199
3.20	Reductive amination as a route to diversity.	211
3.21	HWE reactions with polymer bound aldehydes.	212
3.22	Staudinger/Aza-Wittig reaction with polymer supported triphenylphosphine.	213
4.1	Ester hydrolysis by abzyme 6D4.	229
4.2	Carbonate hydrolysis by MOPC167.	230
4.3	Phosphate ester hydrolysis proceeds through a trigonal bipyramidal transition state.	233
4.4	Antibody catalyzed phosphate monoester hydrolysis.	234
4.5	Hydrolysis of a cyclic phosphate ester.	237
4.6	Hydrolysis of substrates for antibodies raised against 4.25 and 4.26 .	239
4.7	Towards the synthesis of intermediates 4.33-4.35 .	263
4.8	Retrosynthesis of 4.25 and 4.26 starting with nitrated diene 4.38 .	264
4.9	Alternative approach to TSA's 4.25 and 4.26 .	265
4.10	McCormack reaction with nitrated diene.	266
4.11	Synthesis of unnitrated precursors 4.33-4.35 .	267
4.12	Isomerization of 4.34 or 4.35 to <i>trans</i> compound 4.33 .	273
4.13	Nitration of 4.33-4.34 and deprotection of the resulting products.	274
4.14	Synthesis of allyl protected linker 4.52 .	276

4.15	Attachment of allyl protected linker arm 4.52.	277
4.16	Removal of allyl group from 4.55 and 4.56.	278
4.17	Larock's method for preparing ester 4.57.	279
4.18	Synthesis of <i>t</i> -butyl protected linker arm 4.57.	280
4.19	Synthesis of <i>trans</i> TSA 4.25.	282
4.20	Mitsunobu reaction with nitrated <i>cis</i> phospholanic acid 4.50.	283
4.21	Mitsunobu reaction of unnitrated phospholanic acid 4.45.	283
4.22	Mechanism of Mitsunobu reaction.	285
4.23	Alternative mechanism for the Mitsunobu reaction.	286
4.24	Synthesis of <i>cis</i> TSA 4.26.	287
4.25	Conjugation of TSA's to carrier proteins.	295
4.26	Synthesis of phosphate substrate 4.27.	302
4.27	Synthesis of phosphonate substrate 4.28.	303
4.28	Phosphodiester hydrolysis by 2G12.	309
4.29	Phosphodiester hydrolysis by MATT.F-1.	310
4.30	Hydrolysis of VX analog 4.85 by PAR 15.	312
4.31	P-O versus P-S hydrolysis of 4.85.	315

List of Figures

Figure	Title	Page
1.1	PTP1B C215S mutant complexed with DADEpYL peptide substrate.	17
1.2	DADEpYL substrate complexed in the PTP1B active site.	20
1.3	Combinatorial chemistry strategy.	38
1.4	Combinatorial chemistry applied to multi-step sequences.	38
2.1	1.34 docked with PTP1B.	90
2.2	1.34 docked into PTP1B active site.	91
2.3	Overlay of PTP1B active site and 1.34 at 25, 50, 75, and 100 ps.	92
2.4	Distances monitored during MD runs.	93
2.5	Fluctuations in distance over 100 ps for key 1.34 -PTP1B interactions.	94
2.6	Interaction of K120 with distal aryl ring.	95
2.7	Calibration curve for determination of Cl content.	103
3.1	Phosphonium salts which failed to give desired products.	201
4.1	A schematic representation of a IgG class antibody.	225
4.2	A ribbon representation of an IgG class antibody.	225

4.3	Abzymes catalyze reactions by lowering the energy of the transition state.	228
4.4	Development of complementary charges in antibody active site and their role in stabilizing charges in the TS of 4.19.	235
4.5	¹ H NMR of 4.43.	269
4.6	¹ H NMR of 4.42.	269
4.7	¹ H NMR spectra of 4.35.	270
4.8	¹ H NMR spectra of 4.33.	271
4.9	¹ H NMR spectra of 4.34.	272
4.10	HPLC chromatograms of 4.26 and 4.25.	289
4.11	HPLC chromatograms of <i>cis</i> TSA 4.26 in 0.1 M NaOH.	291
4.12	HPLC chromatograms of <i>cis</i> TSA 4.26 in 20 mM sodium phosphate buffer, pH 7.5.	292
4.13	HPLC chromatogram of <i>cis</i> TSA 4.26 in 20 mM NaHCO ₃ buffer, pH 8.5.	293
4.14	Crystal structure of 4.44.	298
4.15	Crystal structure of 4.46.	299
4.16	Crystal structure of 4.47.	300
4.17	Crystal structure of <i>cis</i> TSA 4.26.	301
4.18	Plot of absorbance as a function of time for hydrolysis of 4.27 and 4.28.	305
4.19	Hydrolysis of phosphonate substrate 4.28 (500 μM) in the presence and absence of Jel 541 (500 nM) in 10 mM HEPES	307

List of Tables

Table	Title	Page
2.1	Evaluation of Pd catalysts for the Suzuki coupling	111
2.2	Yields and Purities of <i>meta</i> Compounds 2.60-2.73 .	119
2.3	Yields and Purities of <i>para</i> series of compounds 2.74-2.86 .	120
2.4	Results from Rapid Screen of 2.60-2.87 for PTP1B inhibition.	124
2.5	Inhibition of PTP1B with 2.61 , 2.69 , and 2.73 constructed using conventional solution phase chemistry.	125
3.1	Allyl deprotection conditions.	186
3.2	Recovery of 3.49 from Amberlyst A21 using varying amounts of NH ₄ HCO ₃ and NH ₄ OH.	197
3.3	Product yields and purities from the 'Wittig library.'	202
4.1	Percentages of the <i>cis</i> (4.26) and <i>trans</i> (4.25) isomers in 0.1 M NaOH at various time intervals.	290
4.2	Percentages of the <i>cis</i> (4.26) and <i>trans</i> (4.25) isomers in 20 mM sodium phosphate buffer, pH 7.5.	291
4.3	Percentages of the <i>cis</i> (4.26) and <i>trans</i> (4.25) isomers in 20 mM sodium bicarbonate buffer, pH 8.5.	293
4.4	Endocyclic C-P-C bond angles of 4.44 , 4.46 , 4.47 , and 4.26 .	297

Appendix

A.1 Supplementary Crystallographic Data for 4.26	A.iii
A.2 Supplementary Crystallographic Data for 4.44	A.viii
A.3 Supplementary Crystallographic Data for 4.47	A.xiii
A.4 Supplementary Crystallographic Data for 4.46	A.xviii

CHAPTER 1 INTRODUCTION TO PROTEIN TYROSINE PHOSPHATASES AND COMBINATORIAL CHEMISTRY

1.1 Overview and Global Objectives

The phosphorylation-dephosphorylation of specific sites on certain proteins is a post translational modification that serves as a fundamental method of cellular signaling. Protein kinases carry out the phosphorylation while phosphatases catalyze the hydrolysis event. In general, these events serve as on-off switches in a variety of cellular metabolism and signal transduction processes.^{1,2} The balance between kinase and phosphatase activity is essential for maintaining viable cellular activity. The role of tyrosine phosphorylation in signaling pathways has recently become the subject of intense scrutiny. Among the many processes in which tyrosine phosphorylation is known to play a role are cell proliferation, receptor signaling, T-cell activation, and gene transcription.^{3,4} It has been demonstrated that the malfunction of certain protein tyrosine phosphatases (PTPases) interferes in cellular signaling pathways.¹ The result of this disruption often manifests itself as a disease state, which affects an organism's ability to survive. Specific inhibitors of PTPases would serve as useful tools in studying their role in signaling pathways and may also be potentially employed as therapeutic agents. The *global* objective of the work presented in chapters 2 and 3 is to prepare compounds that are capable of inhibiting a PTPase known as PTP1B. There is now considerable evidence that PTP1B is involved in the down regulation of the insulin receptor kinase.⁵ Inhibitors of PTP1B may potentially serve as therapeutics for the treatment of

non-insulin-dependent diabetes mellitus, also known as type 2 diabetes. Our approach to preparing these inhibitors is to construct a series of compounds bearing a non-hydrolyzable phosphate mimetic using polymer supported organic synthesis techniques. Towards this goal, the *specific* objective of this work is to develop methodologies for the rapid, parallel synthesis of potential PTP1B inhibitors on a soluble polymer support. These compounds bear the difluoromethylenephosphonic acid (DFMP) functionality which has previously been proven to be an effective method of obtaining PTPase inhibitors.⁶ The methodology described herein should facilitate the process of obtaining inhibitors of PTP1B, as well as other protein tyrosine phosphatases.

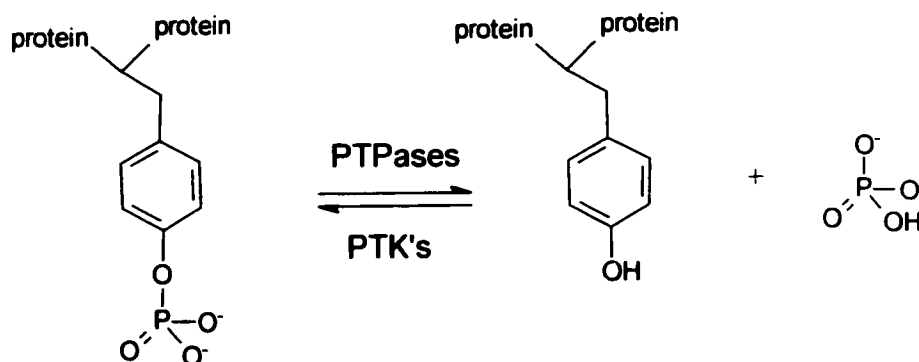
1.2 Phosphatase Enzymes

Since PTPases are central to this work, an overview of these enzymes is presented below.

Phosphatases comprise a diverse family of enzymes which can be categorized into three broad classes: nonspecific phosphatases, phosphoprotein phosphatases (PPases), and the protein tyrosine phosphatases (PTPases).⁷ Examples of nonspecific phosphatases include alkaline and acid phosphatases. These enzymes act on both protein and small molecule substrates and are considered to play the role of 'phosphate scavengers.'

PPases exhibit a sequence homology which differs from the nonspecific and protein tyrosine phosphatases. These enzymes dephosphorylate serine and threonine residues which account for the vast majority of protein phosphorylation sites. PPases are believed to share a common catalytic mechanism and require

a metal ion as a co-factor. Protein tyrosine phosphatases act on phosphorylated tyrosine residues. In conjunction with the protein tyrosine kinases, the PTPases control the phosphorylation state of tyrosine residues in proteins (Scheme 1.1). Over 100 enzymes belonging to this group have been identified.⁸ The diversity of this group of enzymes is surprising when one considers that tyrosine phosphorylation accounts for only 0.01 to 0.05% of total protein phosphorylation.



Scheme 1.1. Action of PTK's and PTPases.

1.3 Protein Tyrosine Phosphatases (PTPases)

1.3.1 Classes of PTPases

The superfamily of protein tyrosine phosphatases can be divided into three sub families based upon structural and biochemical criteria. These classifications are the tyrosine specific phosphatases, or classic PTPases, the dual specificity phosphatases, and the low-molecular weight phosphatases. The function of the low molecular weight tyrosine phosphatases has yet to be determined. Structurally, these enzymes are composed almost exclusively of a catalytic segment.

The dual specificity phosphatases are composed of three subgroups: the VH1-like phosphatases, the MAP kinase phosphatases, and the cdc25

phosphatases. These phosphatases are capable of hydrolyzing phosphate esters on tyrosine, serine and threonine residues of protein/peptide substrates.⁹

The tyrosine specific phosphatases are considered the classic PTPases. In the work reported here, the term PTPases will be used to refer to the broad superfamily of enzymes capable of hydrolyzing phosphotyrosine substrates. The term PTP's will be used to refer to the tyrosine specific subfamily of enzymes. This subfamily can be further classified into two broad categories based upon structural considerations: receptor-like and non receptor-like or cytosolic PTP's.¹⁰ The former class of PTP's are comprised of an intracellular catalytic domain, a single membrane spanning region, and a variety of receptor-like extracellular portions which are believed to play a role in cell signaling. Examples of receptor-like PTP's include PTP α and CD45. These enzymes possess tandem PTPase catalytic domains whose exact roles have yet to be ascertained. The nature of the PTPase catalytic domain is described further on. The importance of the dual PTPase segments has yet to be fully understood. It is not known whether both domains of the receptor-like PTP's are catalytically active or if one serves a regulatory purpose. The cytosolic PTP's are comprised of a single catalytic domain flanked by a variety of non catalytic segments. These flanking segments serve a regulatory and substrate targeting role. PTP1B and *Yersinia* PTPase exemplify cytosolic PTP's.

Structurally, PTPases share a common motif that is essential for catalytic activity. In addition, this family of enzymes utilizes a common catalytic mechanism to catalyze the hydrolysis of aryl phosphate esters without the need

for metal ion co-factors. Additional common biochemical properties include the ability to hydrolyze *p*-nitrophenyl phosphate and inhibition by vanadate ions.

1.3.2 Structural Features of PTPases

Though there is as little as 20% sequence homology across the sub families of PTPases, certain structural features are common to the three groups. The members of the various sub families all possess similar secondary scaffolds composed of a series of α -helices and β -sheets. At the tertiary level, the twisted β -sheet is flanked by a series of α -helices. The general three dimensional structure of VHR, *Yersinia* PTPase, PTP1B, and PTP α all exhibit a common general folding pattern⁸ which includes a common 250 amino acid sequence referred to as the PTPase catalytic domain. Within this 250 residue sequence, the sequence homology is greater than 30% from bacterial to mammalian PTPases.

Essential to the catalytic activity of the PTPases is a structural feature which has been termed the PTPase signature motif and is composed of nine amino acids. This sequence comprises conserved cysteine and arginine residues whose relative placement can be summarized as (H/V)C(X)₅R(S/T). The PTPase signature motif is located within the PTPase catalytic domain and constitutes a crucial part of the active site for this family of enzymes. It is the loop segment of a strand-loop-helix sequence which forms a crevice ~9 Å in from the enzyme surface and is therefore also referred to as the PTP loop. The cysteine residue forms the center of the active site and is located at the base of the cavity which serves as the active site. The arrangement of the amino acids

within the crevice is essential for substrate binding and is particularly suited to binding the phosphate moiety. The exact role of each residue will be elaborated upon further ahead.

A second loop, termed the movable, or WpD, loop, is also characteristic of the PTPases. The movable loop consists of only three amino acids, of which the third is invariably an aspartic acid residue that plays a role in catalysis. The tryptophan residue of this sequence acts as a hinge to impart a great degree of flexibility to this segment, which is the only portion of the enzyme that exhibits significant conformational changes upon binding a ligand. In the example of *Yersinia* PTPase, when a ligand is bound, this loop acts as a flap to cover the active site. When compared to the ligand-free enzyme, a difference of 10 Å can be observed, in the position of the movable loop, between the 'open' and 'closed' forms.^{11,12} The 'open' and 'closed' conformations are present in approximately equal amounts in the free enzyme. In the enzyme-ligand complex, the 'closed' form dominates.¹³

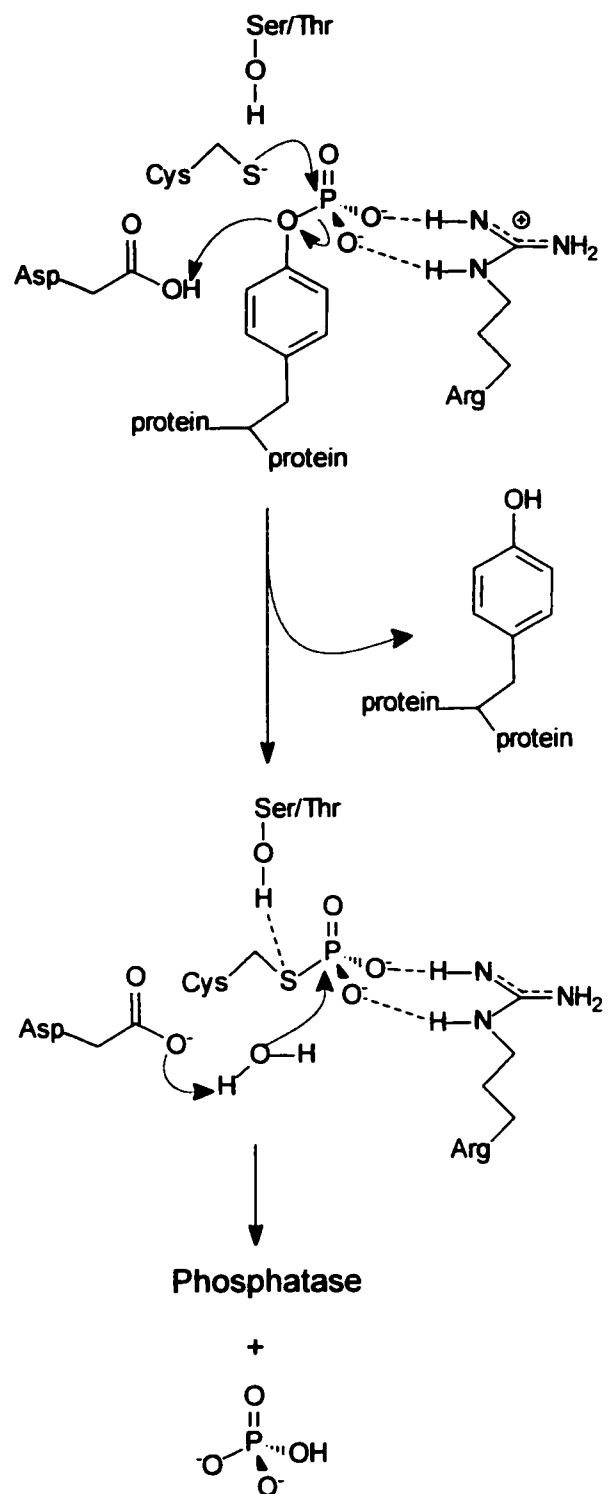
1.3.3 Substrate Binding and Catalytic Mechanism

In the PTP loop, it has been demonstrated that the cysteine and arginine residues are essential for catalytic activity, as is the aspartic acid that is located on the movable loop. The role of these residues has been determined through a variety of studies including site directed mutagenesis, kinetic, and X-ray crystallography experiments.

The catalytic mechanism of the PTP's appears to be uniform across all the PTP's regardless of species thus revealing a significant degree of evolutionary

convergence. The 'closing' of the movable loop over the active site represents the major conformational change resulting from the formation of the enzyme-substrate complex. In this conformation, the aspartic acid of the movable loop is placed into the active site in close proximity to the scissile oxygen of the substrate. The initial step of the catalytic reaction is nucleophilic attack of the thiolate anion of the conserved cysteine residue upon the phosphorous of the phosphotyrosine group to give a phosphocysteine intermediate (Scheme 1.2).⁸ The aspartic acid of the movable loop acts as an acid catalyst by donating its proton to the phenolic oxygen of the tyrosine leaving group. Nucleophilic attack by a water molecule hydrolyzes the covalent intermediate to restore the free enzyme and release inorganic phosphate. The data used to support the catalytic reaction of the PTP's and additional mechanistic detail merit further discussion.

X-ray crystallography images of *Yersinia* PTP complexed with the sulphate¹² and tungstate¹¹ anions, both of which are weak competitive inhibitors of PTPases, demonstrate that the anions occupy the active site. In the instance of the tungstate-enzyme complex, the guanidinium functionality of the arginine residue in the active site forms a bidentate electrostatic interaction with two of the oxygen atoms of the tungstate oxyanion. The amide backbone of the PTP loop contributes additional interactions in the form of hydrogen bonding. The network of electrostatic bonds serves to position the tungstate within close proximity to the nucleophilic cysteine side chain (3.6 Å).¹¹ This complex approximates the positioning of the phosphate groups of the endogenous phosphotyrosine substrates.



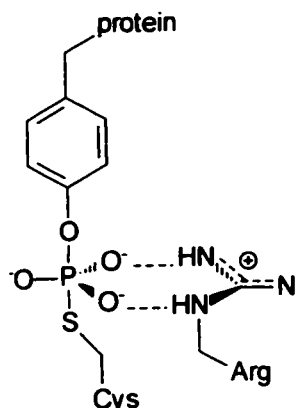
Scheme 1.2. Catalytic mechanism of PTPases.

Comparison of the enzyme-tungstate complex to the free enzyme also reveals a conformational change where the movable loop closes over the active

site in the case of the former structure. This change moves the invariant aspartic acid of the movable loop a distance of 10 Å to within 3.8 Å of the only unliganded oxygen of the tungstate which is located directly opposite the thiol group and is the equivalent to the labile oxygen of the substrate. Further evidence of the mode of phosphate binding was reported in a crystal structure of a C215S mutant of PTP1B complexed with a peptide substrate.¹⁴ The backbone nitrogens of S216 to R221 form a total of six hydrogen bonds to the terminal phosphate oxygens of the phospho tyrosine group in addition to the two salt bridges of the guanidinium side chain of R221.

The side chains of arginine residues are well suited for interaction with phosphate anions. Theoretical results have demonstrated that upon binding to the phosphate group, the guanidinium functionality has the effect of decreasing and redistributing the negative charge as to render the phosphorous atom more positive, and thus more susceptible to nucleophiles.¹⁵ There is considerable evidence that supports the idea that the role of the conserved arginine is more significant than merely substrate binding. Substitution of this residue consistently results in a dramatic decrease in catalytic activity in the case of *Yersinia* PTP¹⁶ and PTP1B.¹⁷ In the less active PTPases LAR and CD45, mutations of the conserved arginine causes a complete loss of activity.^{18,19} In the case of PTP1B, a R221K mutant bound a peptide substrate normally as indicated by similar K_m values. The activity, as reflected in the k_{cat} , was decreased by a factor of 5500. The ability of the guanidinium group to stabilize the trigonal bipyramidal transition state may contribute to the overall catalysis. The positive charges of the

guanidinium group are able to form a coplanar bidentate complex with the equatorial oxygen atoms (Scheme 1.3). In the case of the R221K mutation, the cationic lysine side chain may serve as an adequate surrogate for substrate binding, but fails in transition state stabilization.



Scheme 1.3. Stabilization of a trigonal bipyramidal transition state or intermediate by a guanidinium group.

The importance and role of the conserved cysteine residue has been determined through a variety of experiments. Substitution of serine for cysteine results in inactive C→S mutants which are capable of binding substrates but are unable to catalyze the hydrolysis reaction.²⁰ In the active site, the cysteine has a pK_a of 4.7 in *Yersinia* PTP, and therefore, exists as the thiolate anion under physiological conditions. This pK_a value is three units below what is typically expected of a free cysteine (8.3-8.5). These unique electronic properties have been attributed to the unique active site environment.²¹ Crystal structures of wild type PTP's complexed with metal ions^{11,12,22} and C→S mutants complexed with pY containing peptides show that the active site nucleophile (S in wild type structures and O in C→S mutants) is within 3-4 Å of five backbone amide groups.

These amide groups form a network of S—HN hydrogen bonds which are oriented away from the cysteine residue. This creates a network of microdipoles in which the positive charges are directed at the thiol and are able to stabilize the thiolate anion.^{23,24}

The conserved His residue in the PTP loop is also essential for catalytic activity. Mutation of this residue for asparagine or alanine results in an increase in the pK_a of the cysteine residue. While it is known that the His residue does not directly participate in catalysis,¹ it remains unclear whether it plays a vital structural role in positioning the thiol side chain in the active site or interacts through charge stabilization effects. Regardless of the nature of its role, alterations in the His residue results in a significant decrease in catalytic activity.

Kinetics experiments demonstrate that the hydroxyl group of the Ser/Thr residue participates in the catalytic process by assisting in the decomposition of the phosphoenzyme intermediate.^{24,25,26} The hydroxyl group acts as a hydrogen bond donor which stabilizes the thiolate anion leaving group.

General acid-base catalysis is provided by the Asp residue of the movable loop. During the formation of the phosphocysteine intermediate, it donates a proton to the phenolate leaving group. The same carboxylate group appears to act as a base in activating a trapped water molecule as a nucleophile.²⁷

The importance of the conserved Cys residue in PTPases has been demonstrated for a variety of enzymes^{18,28,29} in which mutation of the PTP loop Cys resulted in the loss of activity. Initial experiments employing sulfhydryl reactive compounds to inactivate PTPases alluded to the role of the Cys

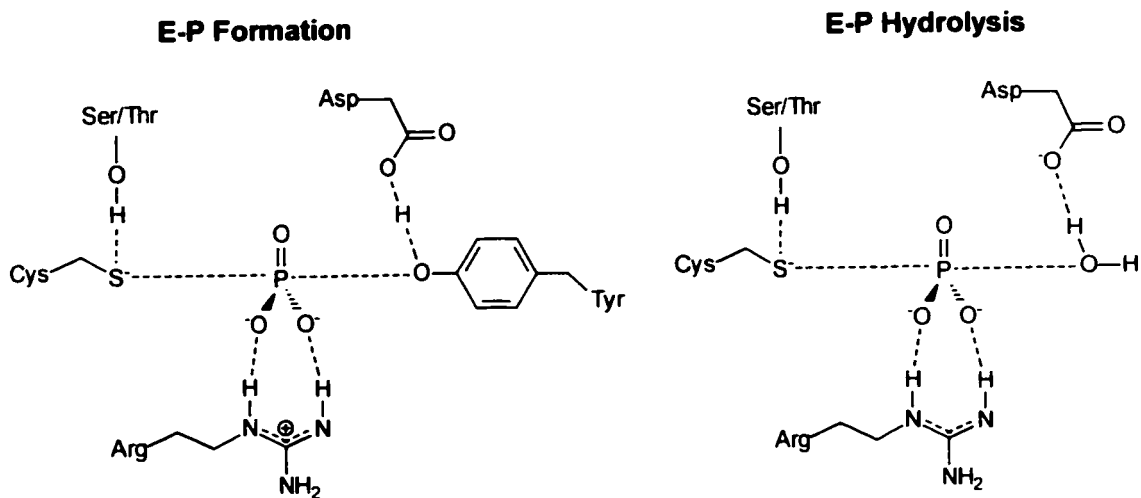
residue.^{29,30} The formation of the phosphocysteine intermediate was confirmed by using ^{32}P labeled substrates followed immediately by trapping of the phosphoenzyme intermediate by addition of SDS.^{20,29,31} The intermediate was also detected by ^{31}P NMR^{31,32} by using PTPase mutants with decreased activity.

Substitution of the Cys residue for a Ser is a net change of one atom, which nevertheless results in complete loss of catalytic ability. The C→S mutants are still able to bind substrates, but unable to form the covalent intermediate required for catalysis. Whereas a cysteine residue has a pK_a of 8.5, that of a serine is much greater at 14. Within the micro-environment of the active site, the network of hydrogen bonding is not capable of lowering the pK_a of the Ser to the degree at which it would be ionized at physiological pH. If the serine were somehow to become ionized at physiological pH, the thiolate anion would still serve as a better nucleophile than the alkoxy anion.¹

From an evolutionary convergence standpoint, the PTPases utilize a phosphocysteine intermediate due to energy considerations. The P-S bonds are more labile than P-O bonds with bond energies of 45-50 and 95-100 kcal/mol respectively.³³ Hydrolysis of the covalent intermediate is therefore facilitated by using a P-S bond over a P-O bond.

Both of the transition states for the formation of the phosphoenzyme intermediate and its subsequent hydrolysis are dissociative in nature^{8,26,34} and occur by consecutive in-line displacement reactions. Dissociative transition states are characterized by nucleophilic attack preceding departure of the leaving group resulting in a large degree of bond cleavage to the leaving group coupled

with a relatively low bond order to the incoming nucleophile.³⁵ Scheme 1.4 outlines the proposed transition states for the formation and hydrolysis of the phosphoenzyme intermediate with the role of the conserved active site residues included. The hydrolysis of the phosphoenzyme intermediate is the rate limiting step for the overall hydrolysis reaction.



Scheme 1.4. Possible transition states for enzyme-product formation and hydrolysis.

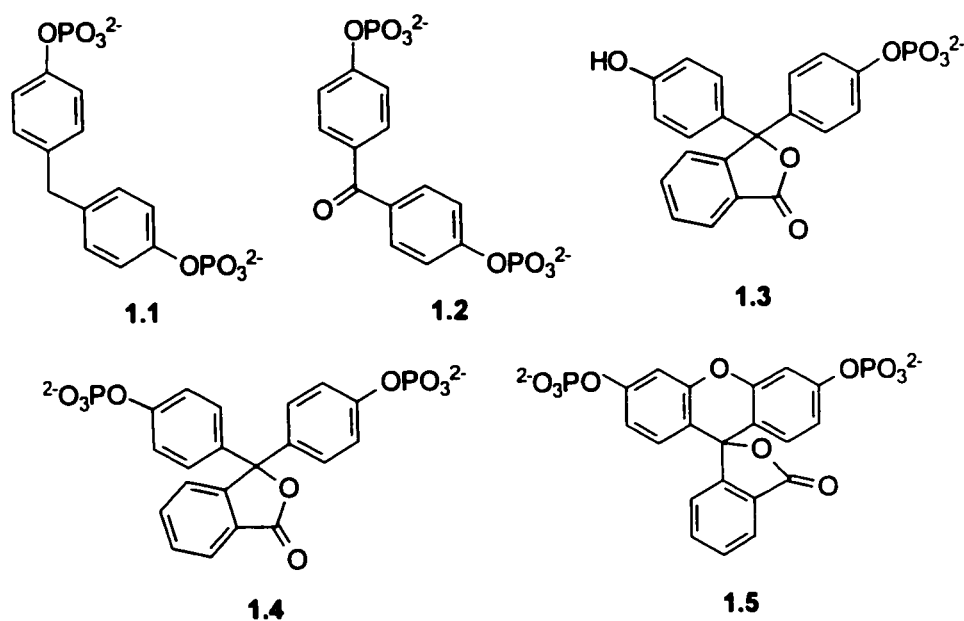
An understanding of how PTPases work represents the mere beginning of actually learning the function of these enzymes *in vivo*, and more importantly how their activity may be modulated to treat disease states.

1.4 PTPase Substrates

In order to understand the function of PTPases *in vivo*, it is potentially helpful to identify its natural substrate in order to determine what features control binding and recognition. Identification of PTPase substrates also has the potential of offering insight in to inhibitor design. For most PTPase enzymes, the physiological substrates have yet to be confirmed.¹⁰ Much of the work to identify

potential PTPase substrates have utilized peptide sequences modeled upon naturally occurring tyrosine phosphorylation sites. Free phosphotyrosine is a poor substrate for PTPases when compared to peptide sequences which incorporate this functionality. While the pY group is undoubtedly the source of primary recognition, this demonstrates the importance of the flanking residues in modulating substrate affinity and selectivity.¹⁰ A variety of peptide sequences have been evaluated to reveal that alterations in the sequence of peptidyl substrates results in changes in the value k_{cat} and K_m .³⁶ The data supports the idea that substrate specificity is at least partially dictated at the primary level of peptide sequences. Among the more effective peptide based substrates for recombinant *Yersinia* PTPase and recombinant mammalian PTPase, originally cloned from rat brain, is a sequence based upon the phosphorylation site of epidermal growth factor receptor. EGFR₉₈₈₋₉₉₈ is a undecapeptide with the sequence DADEYLIPQQG which can undergo phosphorylation at the Tyr residues at position 992 to give the phosphorylated substrate DADEpYLIPQQG.³⁷ Zhang *et al.* found that the K_m for this substrate decreases with pH, for the two recombinant PTPases studied, which indicates that the phosphate dianion is favoured for substrate binding. Further work with this substrate showed that only six residues contributed significantly towards affinity. The truncated peptide DADEpYL-NH₂ (EGFR₉₈₈₋₉₉₃) could be employed as a substrate with slight gain in K_m and an overall minor compromise in the value of k_{cat}/K_m .³⁸ These sequences indicate that acidic residues on the N-terminal side of the pY play an active role in substrate recognition and binding.

Though peptide based substrates may potentially offer significant insight into substrate recognition and affinity factors, small molecule substrates for the PTPases have also been investigated. Such substrates serve a dual purpose of facilitating continuous assay methods and acting as the foundation for novel inhibitor design. One of the most commonly used and simplest PTPase substrates is *p*-nitrophenol phosphate, which unfortunately, does not provide much information towards structural requirements on the substrate.



Monserat *et al.* offered many novel examples of PTPase substrates including some *bis*-phosphorylated species.³⁹ The K_m values ranged from the low micromolar range of 0.016 mM (1.1) to 0.130 mM (1.2) with a relatively slight modification. The use of only a single phosphate group increased the K_m to 2.2 mM (1.3) which demonstrates the contribution of the second phosphate group towards enhancing substrate affinity. Numerous fluorogenic substrates (1.4, 1.5) were also reported to have a K_m values ranging from of 20 to 200 μ M.^{40,41} These

values were found to vary with each PTPase therefore, demonstrating the possibility of designing selective substrates (and by implication inhibitors) for each enzyme.

1.5 Protein Tyrosine Phosphatase 1B (PTP1B)

1.5.1 PTP1B Overview

The work reported in this thesis focuses on one specific PTPase known as protein tyrosine phosphatase 1B or PTP1B. PTP1B is the prototypical non-receptor-like or cytosolic PTP. PTP1B was the first PTPase to be cloned and characterized.^{42,43} The enzyme is composed of a single chain which has a size of 37 kDa and is composed of 321 amino acids. This represents the N-terminal portion of a larger protein which is encoded in a cDNA segment representing 435 residues. The characteristic PTP domain spans residues 30 to 278. The 35 C-terminal residues mediate interactions between the enzyme and the cytoplasmic face of the endoplasmic reticulum.²³ The first 122 N-terminal residues are mainly hydrophilic and contain several serine phosphorylation sites.

X-ray structure analysis of PTP1B^{23,44} reveals that the enzyme comprises 8 α helices and 12 β -strands. The PTPase signature motif is situated on loop 15, which joins β -12 and α -4, and spans residues H214 to R221. Residues which merit mention include C215, which acts as the nucleophile in the formation of the covalent intermediate, and D181. D181 serves as the general acid/base catalyst during the catalytic event and is located on loop 13. The enzyme possesses all the characteristic structural and mechanistic features of the PTPases described above. PTP1B is often employed as the enzyme to which other PTP's are

compared due to the fact that much of the work towards understanding the PTPase family of enzymes was performed using PTP1B as the subject.



Figure 1.1. PTP1B C215S mutant complexed with DADEpYL peptide substrate.⁴⁵ The bound peptide and the C215S mutation are shown as a stick rendering. The movable, or WpD loop is shown in yellow while the PTP loop is shown in red.

Figure 1.1 is a ribbon rendering of a crystal structure of a PTP1B C215S mutant complexed with a tyrosine phosphorylated hexapeptide of sequence DADEpYL.⁴⁵ This sequence, which is represented as a stick rendering, is modeled on the autophosphorylation site of EGFR. Also shown as a stick rendering is the C215S mutation which is located at the bottom of the active site crevice on the PTP loop (red). The movable, or WpD, loop is shown in yellow.

1.5.2 PTP1B Substrate Binding

Crystal structures of catalytically inactive C215S mutants of PTP1B have been solved and offer insight into how the enzyme recognizes a hexapeptide substrate (DADEpYL-NH₂) corresponding to EGFR₉₈₈₋₉₉₃.¹⁴ In brief, the side chain of the pY residue is held in a 9 Å deep pocket which makes up the active site. The depth of the crevice corresponds to the length of a pY residue. The sidechains of serine and threonine residues are too short to reach the base of the active site. The base of the pocket is formed by S215, which substitutes for the nucleophilic C215 in the wild type enzyme, and R221, which forms salt bridges via its guanidinium side chain with the phosphate dianion. Additional hydrogen bonding to the phosphate functionality is provided by the main chain atoms of S216 to R221. The binding of the substrate also induces the closing of the movable loop which consists of residues W179 to S187. This conformational change brings D181 and F182 into the active site. F182 participates in π -stacking interactions with the pY aromatic ring as does Y46 on the opposite face. Additional hydrophobic interactions with the pY ring are formed by A217, I219, and V49. Several other electrostatic interactions are formed between the backbones of the substrate and enzyme which assist in orienting the peptide and maintain the substrate in a helical conformation. A water molecule, responsible for the hydrolysis of the covalent intermediate, is locked in the active site via a hydrogen bond to the backbone nitrogen of F182 and is positioned within 2.9 Å of the scissile oxygen atom. Away from the active site, notable interactions include the side chain of R47 which forms salt bridges with the side chains of the P-1 and P-2 residues (where the pY is designated P-0 so that P-1 is immediately on the

N-terminal side and P+1 is adjacent on the carboxyl terminal side). This observation accounts for the preference for acidic side chains N-terminal to the pY residue.

Mutagenesis studies carried out by Sarmiento *et al.* offer additional insight into the roles of Y46, R47, Asp48, F182, and Q262.⁴⁶ PTP1B Y46F mutants exhibited only a slight decrease in affinity and activity for the EGFR988-998 substrate. The aromatic side chain was important for substrate recognition and orientation in the active site. R47 appears to dictate the preference for acidic residues at the -1 and -2 positions of the substrates. R47A mutants have higher K_m values than the wild type enzyme. D48 plays a role in positioning peptidyl substrates for binding. This is based upon the observation that D48A mutants possess similar kinetic parameters when simple aryl phosphates are employed as substrates but have increased K_m values when the EGFR₉₈₈₋₉₈₈ sequence is used. F182 is located on the movable loop and appears to play a role in substrate recognition and loop closure. Substrate binding is achieved through π stacking with the pY ring, which also closes the movable loop to bring the D181 residue into the active site. The D181 residue acts as an acid/base catalyst for the formation and subsequent hydrolysis of the covalent phosphocysteine intermediate. F182 is required to maintain the 'closed' conformation of the loop that is required for activity. Alignment of the active site water molecule is mediated by Q262, which also orients the phenyl ring of the pY. This is based upon large decreases in k_{cat} for Q262A mutants and increases in K_m , both of which reflect a build up of covalent intermediate.

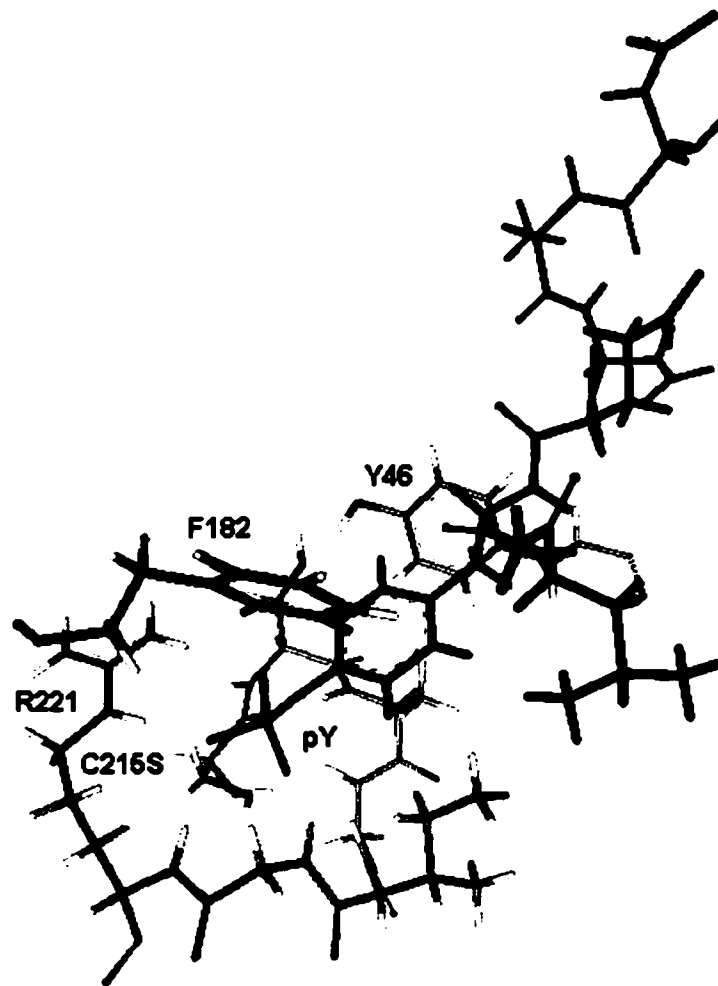


Figure 1.2. DADEpYL substrate (red) complexed in the PTP1B active site. Some of the key residues involved in substrate binding are shown.

Figure 1.2 shows the DADEpYL hexapeptide in the PTP1B C215S mutant active site. The substrate, shown in red, extends into the active site pocket where the pY residue is sandwiched between Y46 and F182. Also labeled is the C215S residue which is located at the bottom of the pocket on the PTP loop.

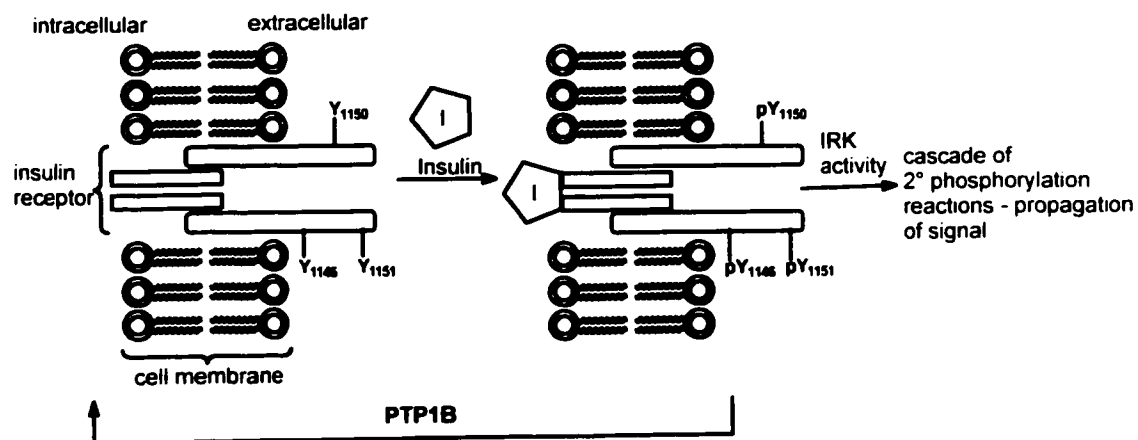
1.5.3 PTP1B and Diabetes

Type 2 diabetes, which is also known as non-insulin-dependent diabetes mellitus (NIDDM), is a disease state characterized by resistance to normal levels

of circulating insulin resulting in high blood glucose levels (hyperglycemia).⁴⁷ The occurrence of type 2 diabetes, which accounts for 80% of diabetic patients, is approaching epidemic proportions in industrialized nations.⁴⁸ Combined, type 1 and type 2 diabetes are among the leading causes of death in North America.

Insulin is a polypeptide which is the principal hormone controlling blood glucose levels, in mammals, by stimulating its intake and metabolism in muscle and adipocyte cells and inhibiting gluconeogenesis by the liver. Insulin also affects the activity of numerous enzyme and transport systems present in nearly all cells. Insulin action is mediated by the insulin receptor which is a transmembrane protein with intrinsic kinase activity. The receptor is composed of two of each α and β subunits linked via disulfide bonds in a β - α - α - β pattern. The insulin binding site is located on the extracellular α subunits. The β subunits span the cellular membrane and include intracellular segments which contain a tyrosine protein kinase. This insulin receptor kinase (IRK) requires autophosphorylation of three key tyrosine residues in order to attain an active state. Upon binding of insulin to the extracellular domain, a conformational change occurs which allows the IRK to autophosphorylate. Though there are several tyrosine phosphorylation sites on the β subunits, residues Tyr1146, Tyr1150, and Tyr1151 occur in the kinase regulatory domain.⁴⁹ Phosphorylation of these residues has the twofold effect of activating the IRK towards other intracellular substrates, such as insulin receptor substrate-1 and -2 (IRS-1, IRS-2), and the generation of docking sites for other enzymes and/or effector molecules. The result is the propagation of the insulin signal through a series of

secondary reactions carried out by the IRK and its substrates. This sequence of events is outlined in Scheme 1.5. The kinase activity of the IRK is essential for maintaining all of the cascade reactions which are responsible for the growth promoting and metabolic effects of insulin signaling.⁵⁰ One of the major effects of insulin signaling is increased glucose uptake by cells to lower the overall blood glucose levels.⁸



Scheme 1.5. The insulin signalling cascade.

The activity of the IRK and the secondary cascade reactions continues even in the absence of bound insulin. Deactivation occurs upon the dephosphorylation of the IRK by various PTPases including PTP1B. Several groups have contributed evidence to support the pivotal role of PTP1B in the down regulation of insulin signaling and its viability as a therapeutic target.^{51.52} It is beyond the scope of this thesis to present all of this evidence. However, one particular study by Echebley and co-workers⁵ warrants mention as it is now considered to be the seminal study in this area of research. This work involved engineering mice that lacked the PTP1B gene. Three sets of mice were employed: wild type, which expressed normal levels of the enzyme (PTP1B^{+/+}),

mice homozygous in the absence of the PTP1B gene (PTP1B^{-/-}), and heterozygous mice (PTP1B^{+/-}) which were the progeny of the wild type and PTP1B^{-/-} mice and expressed half the amount of PTP1B enzyme when compared to the PTP1B^{+/+} subjects. Aside from the differences in PTP1B expression, all three lines of mice were identical with none of the PTP1B^{+/-} or PTP1B^{-/-} exhibiting any abnormalities. The mice were tested in order to observe their physiological responses to glucose and insulin. It was found that the PTP1B^{-/-} mice were insulin sensitive since they were able to maintain lower blood glucose levels with significantly reduced amounts of insulin. Upon insulin injection, tyrosine phosphorylation levels of IRK and IRS-1 in muscle and liver tissue was found to be higher in the PTP1B^{-/-} mice when compared to the PTP1B^{+/+}. These results can be attributed to a prolonged tyrosine phosphorylation state of the IRK and indicate that PTP1B is the enzyme responsible for dephosphorylating the IRK and thus down regulating the insulin signal. Further experiments evaluated the effects of a high fat and high calorie diet on the mice. Over a ten week experiment, the animals consumed the same amount of food. The wild type PTP1B^{+/+} mice exhibited a weight gain coupled with increased blood glucose and circulating insulin levels as a result of obesity induced insulin resistance. The PTP1B^{-/-} and PTP1B^{+/-} mice were resistant to the weight gain. The PTP1B^{-/-} mice had normal glucose and insulin levels over the course of the experiment which serves as additional evidence of the role of PTP1B in insulin signaling.

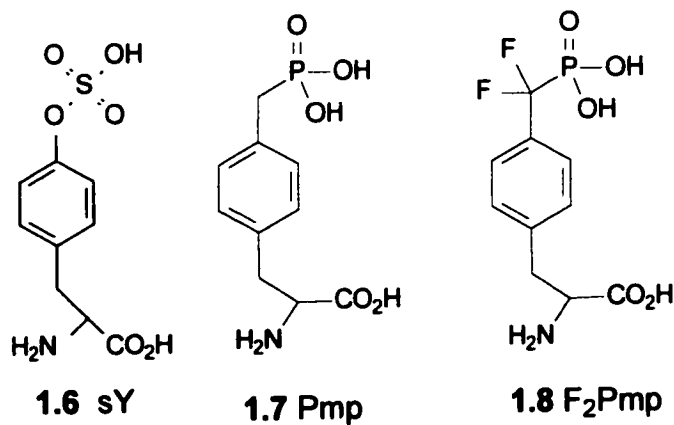
The above studies strongly indicate that inhibitors of PTP1B may prove to be effective therapeutics for the treatment of type 2 diabetes and also obesity.

Below we summarize the work that had been reported in the scientific literature on PTPase inhibitors at the time we began our own studies.

1.6 PTPase Inhibitors

1.6.1 Peptide Based Inhibitors

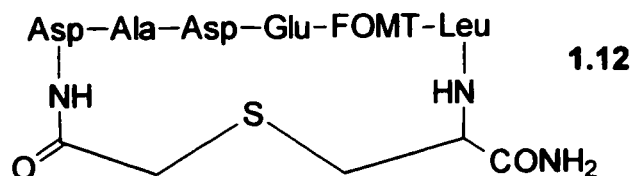
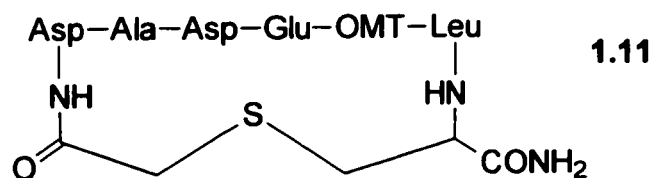
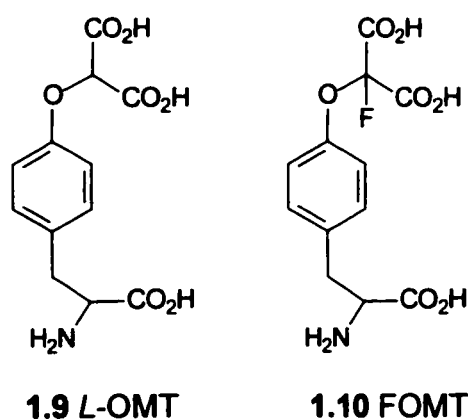
A fundamental approach towards developing PTPase inhibitors is to replace the phosphotyrosine residue in natural peptide substrates with non hydrolyzable analogues. Liotta *et al.*⁵³ incorporated three sulfotyrosyl residues (1.6) into a dodecapeptide sequence derived from residues 1142-1153 of the IRK. The peptide TRDIsYETDsYsYRK was observed to inhibit tyrosine dephosphorylation in both membrane and cellular studies presumably by inhibition of a PTPase. Desmarais *et al.* also incorporated the sulfotyrosyl residue into a series of peptides in order to study their inhibition upon the PTPase enzymes PTP1B and CD45.⁵⁴ The IC₅₀ values were in the low micromolar range (2 - >200 μ M) and were dependent upon the size of the peptide and the sequence. The most important findings of this study was that recognition elements of PTP1B and CD45 were different which allows for the possibility of designing active site specific inhibitors for each PTPase.



Burke *et al.* employed the peptide sequence Ac-DADEX-L-NH₂ where X was either a phosphonomethyl phenylalanine (Pmp, 1.7) or a phosphonodifluoromethyl phenylalanine (F₂Pmp, 1.8,) both of which replace the scissile oxygen atom with a methylene carbon.⁵⁵ The IC₅₀ of the F₂Pmp peptide was 100 nM which represented a 2000-fold improvement over the Pmp inhibitor which had an IC₅₀ of 200 μM. A study of the inhibition of PTP1B by the Pmp and F₂Pmp peptides as a function of pH showed that inhibition was independent of the pH therefore suggesting that both the monoanionic and dianionic forms of the phosphate analogs bind equally well to the enzyme.⁵⁶ This indicated the possibility that the enhanced potency of the F₂Pmp peptide was not due to lowering of the pK_{a2} value by the presence of the fluorine atoms relative to the Pmp inhibitor. It was postulated that the fluorine atoms were able to mimic the hydrogen bonding interactions normally present between the phenolic oxygen of the pY and residues in the active site. Ganesan *et al.*⁵⁷ reported the results of their inhibition studies of the phosphatases PTP α, β, and ε, by a series of dipeptidyl inhibitors which incorporated the F₂Pmp group. At inhibitor concentrations of 100 μM, greater than 50% inhibition against PTP ε was observed for 3 out of the 108 compounds synthesized, which indicated the possibility of designing selective inhibitors for each PTP.

The incorporation of the F₂Pmp and Pmp moieties allows for the design of potent inhibitors, however, it is believed that their dianionic charges may be problematic in terms of cell permeability. Also, peptides bearing this moiety will be difficult to prepare as 'caged' esters for cellular studies. As a potential

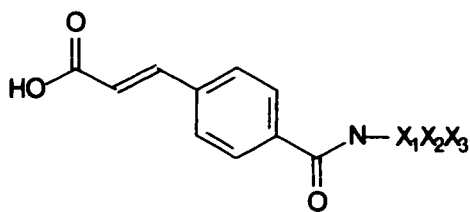
solution to this dilemma, a *L*-*O*-malonyltyrosine (**1.9**, *L*-OMT) was employed by Kole *et al.* as a pY substitute⁵⁸ since the malonic acid functionalities can be readily masked as esters for improved cell penetration. The Ac-DADE[*L*-OMT]-L-NH₂ peptide had an IC₅₀ of 10 μM against PTP1B. Introduction of a fluorine atom yields the 4'-*O*-[2-(2-fluoromalonyl)]-*L*-tyrosine (**1.10**, FOMT) surrogate, which, upon incorporation into the Ac-DADE[FOMT]-L-NH₂ peptide enhances the potency for an IC₅₀ value of 1 μM.⁵⁹



In order to introduce conformational restrictions and augment proteolytic stability, Akamatsu *et al.*⁶⁰ and Roller *et al.*⁶¹ employed cyclic versions of the DADEXL peptides incorporating both the *L*-OMT and FOMT functionalities. It was found that a cyclization scheme using a sulfide bridge between a C-terminal

cysteine and the β -carbon of a N-terminal acetyl residue yielded the most potent inhibitors. The K_i values of **1.11** and **1.12** were $0.73 \mu\text{M}$ and $0.17 \mu\text{M}$ respectively.

Moran *et al.* incorporated *p*-carboxycinnamic acid (Cinn) at the N terminus of a series of tripeptide sequences.⁶² Using a limited variety of amino acids, Moran *et al.* found the sequences CinnGEL (**1.13**) and CinnGEE (**1.14**) to have K_i values of 490 and 79 nM respectively against PTP1B. There is reason to believe that these peptides act as irreversible inhibitors via Michael addition of the active site cysteine nucleophile onto the β carbon of the cinnamic acid.⁶³



1.13 $X_1X_2X_3 = \text{GEL}$

1.14 $X_1X_2X_3 = \text{GEE}$

Though peptide based inhibitors are potent and potentially highly specific, they suffer from poor bioviability since they are easily hydrolyzed by protease enzymes and are not easily transported across cell membranes. These properties of peptides clearly demonstrate the need for the development of non-peptidyl PTPase inhibitors.

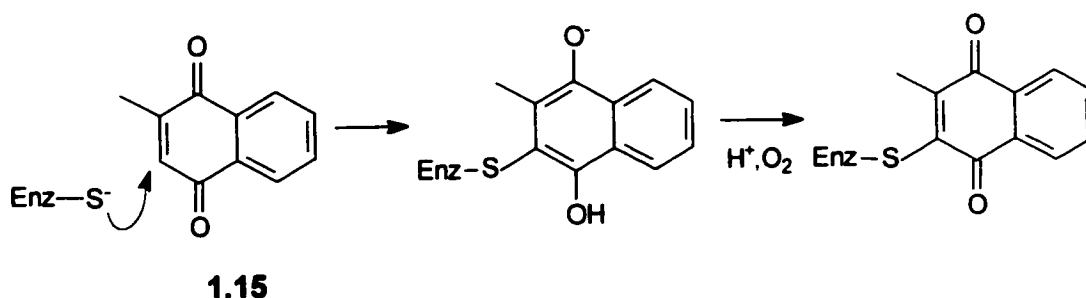
1.6.2 Inorganic Metal Based PTPase Inhibitors

There are many examples of metal based inhibitors of the PTPases including gallium nitrate⁶⁴, and vanadium and peroxovanadium compounds.^{65,66} These compounds usually exert their inhibitory by mimicking the trigonal

bipyramidal geometry of the phosphate transfer transition state or by oxidation of the active site cysteine. The metal based inhibitors display poor selectivity between the PTPases and are potentially toxic and are therefore considered to be poor candidates for cellular studies and therapeutic use.

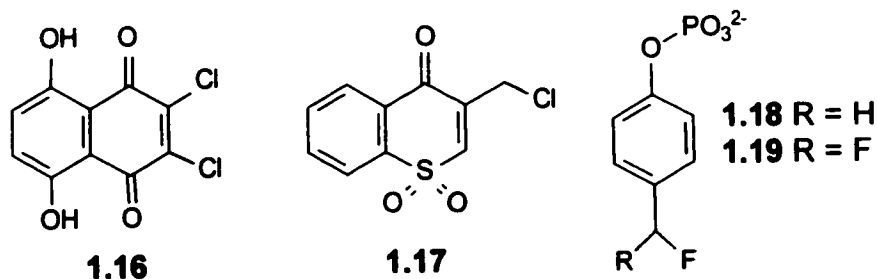
1.6.3 Irreversible PTPase Inhibitors

Numerous irreversible inhibitors of PTPases have been found both by discovery and design. Menadione (**1.15**) was found to irreversibly inhibit the PTPase *cdc25* presumably by the mechanism outlined in Scheme 1.6.⁶⁷



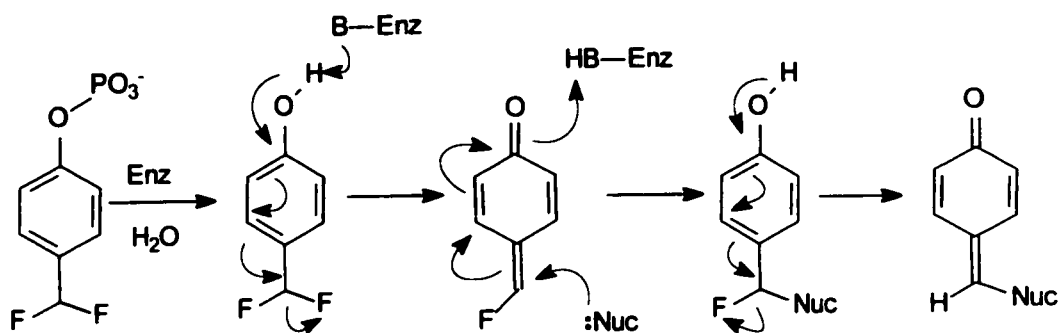
Scheme 1.6. Inactivation by menadione.

A similar type of Michael addition type inactivation was proposed for both naphthoquinone (**1.16**)⁶⁸ and the sulfone analogue of naphthoquinone (**1.17**).⁶⁹ Compound **1.17** was selective against PTP1B over the phosphatases *cdc25A*, *cdc25B*, *cdc25C*, LAR, and *Yersinia* PTP.



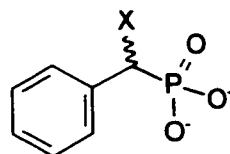
Widlanski *et al.*⁷⁰ and Withers *et al.*⁷¹ designed and employed **1.18** and **1.19** respectively as suicide inhibitors of prostatic acid phosphatase. Both

inhibitors are believed to act via the same mechanism involving a quinone methide intermediate as shown in Scheme 1.7.



Scheme 1.7. Inactivation of enzyme by **1.18** and **1.19**.

Widlanski et al.⁷² also employed α -halobenzyl phosphonates **1.20.a-c** as inactivators of *Yersinia* PTP. Two possible modes of action for these inhibitors were proposed involving either direct S_N2 attack by the active site nucleophile to displace the halogen or addition to the phosphonate to give a phosphorane. A phosphorane oxygen then displaces the α -halogen to give a three membered ring which may then be opened by water or a second active site nucleophile.

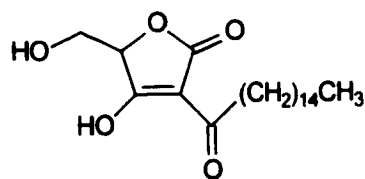


1.20 a R = F
b R = Cl
c R = Br

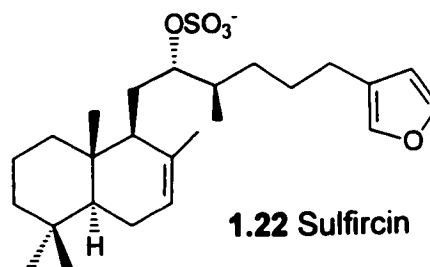
The general consensus is that though irreversible inhibitors are useful in the study of the function of the PTPases, they suffer from poor selectivity and susceptibility to reaction with other cellular nucleophiles.

1.6.4 Natural Product Based PTPase Inhibitors

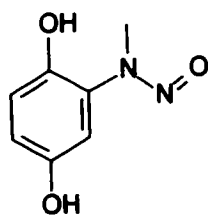
Several natural products and their synthetic analogues have been found to inhibit a variety of PTPases. A brief summary of some of these compounds and their relevant inhibition data is presented here. RK-682 from *Streptomyces* sp. 88-682 arrests cell cycle at G1 phase and *in vitro* has IC_{50} values of 54 μM and 2 μM against the PTPases CD45 and VHR.⁷³ RK-682 and its analogues exhibited 100-fold selectivity for VHR over the PPases cdc25A, cdc25B, and PP1.⁷⁴ Sulfircin and its analogs were tested for inhibitory activity against cdc25A, PTP1B, and VHR.⁷⁵ The natural product had IC_{50} values of 7.8 μM and 29.8 μM against cdc25A and PTP1B. Structure-activity studies revealed that substitution of the furyl side chain and sulfate group with malonic acid could be used to alter activity, though the compounds were consistently most effective against cdc25A. Nornuciferine⁷⁶ was found to have an IC_{50} value of 5.3 μM against CD45. Dephostatin exhibits activity against CD45 and *Yersinia* PTP, however, the mode of inhibition is unclear.^{77,78}



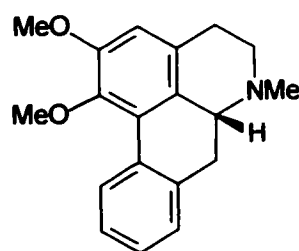
1.21 RK-682



1.22 Sulfircin



1.23 Dephostatin

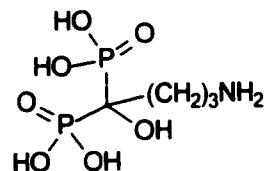


1.24 Nornuciferine

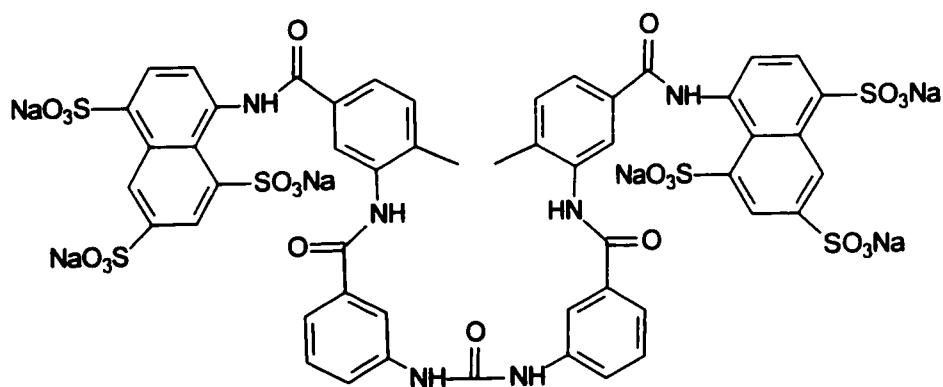
Several other natural products have shown activity against the PTPases. Due to the structural diversity among these compounds, it is apparent that a better understanding of how each of these natural products exert their inhibitory activity is required.

1.6.5 Therapeutic Agents as PTPase Inhibitors

The implication of PTP1B in a variety of metabolic diseases is still a fairly recent development so it has yet to be employed as a biological target. There are examples of compounds intended for other therapies exhibiting activity against PTPases. Alendronate, a drug employed in osteoporosis patients, has been shown to inhibit CD45 and PTP1B.⁷⁹ A detailed examination revealed that alendronate required the presence of H_2O_2 and a metal ion in order to effect inhibition by oxidation of the active site cysteine residue.



1.25 Alendronate



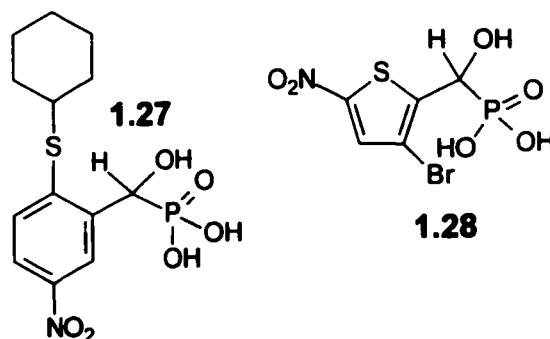
1.26 Suramin

Suramin, a drug used to treat sleeping sickness, has K_i values of 4, 1.3, and 48 μM against PTP1B, *Yersinia* PTP, and VHR respectively.⁸⁰ Against CD45, suramin exhibits noncompetitive irreversible inhibition. The unique nature of these agents necessitate detailed structure-activity studies in order to better understand how they are recognized by the PTPases.

1.6.6 Structure Based Non-Peptidyl PTPase Inhibitors

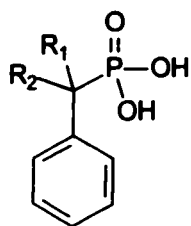
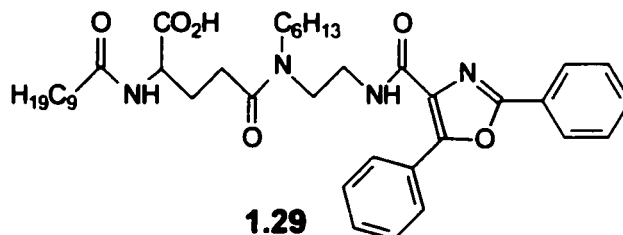
Several groups have reported progress in the synthesis and evaluation of small molecule, reversible inhibitors of PTPases. Ideally, for potential therapeutic applications, these inhibitors should bind competitively with nanomolar range potency and exhibit selectivity between the various PTPases.

Frechette *et al.*⁸¹ and Beers *et al.*⁸² employed the α -hydroxy phosphonic acid moiety attached to a phenyl ring as a surrogate for the phosphate group. The effects of varying the substituents on the phenyl ring upon the inhibition of CD45 was examined. When tested against CD45, **1.27** was found to have an IC_{50} of 1.2 μM .⁸¹ Beers *et al.* employed a thiophene scaffold and found that **1.28** also inhibited CD45 with an IC_{50} of 2 μM .⁸²



Rice *et al.* based **1.29** on the pharmacophore model of natural product inhibitors of the phosphothreonine phosphatases. The inhibition of **1.29** against

Cdc25A, -B, and -C was found to be competitive with a K_i of about 10 μM whereas PTP1B was inhibited in a non-competitive mode with a K_i of 0.85 μM . While compound **1.29** displays appreciable potency against PTP1B and is potentially cell permeable, due to its highly hydrophobic nature, its mode of inhibition makes **1.29** a poor therapeutic candidate.

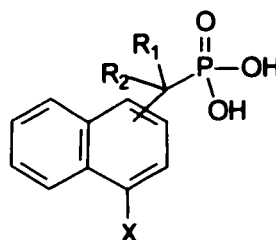


1.30a $R_1 = R_2 = \text{H}$

1.30b $R_1 = \text{H}, R_2 = \text{OH}$

1.30c $R_1 = \text{H}, R_2 = \text{F}$

1.30d $R_1 = R_2 = \text{F}$



1.31a 2-naphthyl, $R_1 = R_2 = \text{H}, X = \text{H}$

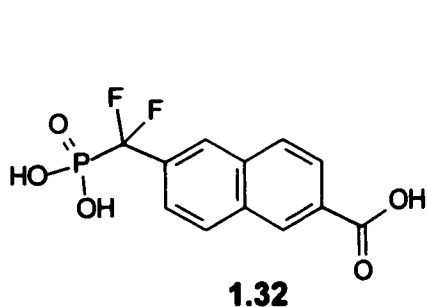
1.31b 1-naphthyl, $R_1 = R_2 = \text{F}, X = \text{H}$

1.31c 2-naphthyl, $R_1 = R_2 = \text{F}, X = \text{H}$

1.31d 2-naphthyl, $R_1 = R_2 = \text{F}, X = \text{OH}$

Kole *et al.*⁸³ reported the inhibition data for a series of phenyl and naphthyl inhibitors (**1.30a-d** and **1.31a-d**) against PP-2A and PTP1B. In general, the phenyl compounds exhibited low activity, which increased marginally with substitution at the α position ($\text{CH}_2 \rightarrow \text{CHOH} \rightarrow \text{CHF} \rightarrow \text{CF}_2$). Incorporation of the difluoromethylene phosphonic acid (DFMP) group into a naphthyl system (**1.31b-c**) resulted in greater than 85% inhibition for both PP2A (300 μM inhibitor) and PTP1B (200 μM inhibitor), when protein substrates were employed, which

was an improvement over both the phenyl compound and the unfluorinated 2-naphthyl phosphonic acid **1.31a**. Against PTP1B, **1.31b** and **1.31c** had K_i values of 255 and 179 μM respectively. X-ray analysis of the **1.31c**•PTP1B complex revealed an unconventional hydrogen bond between the pro-S fluorine and the backbone NH of F182 and it is believed that this unusual fluorine H-bond contributes significantly to the potency of this compound.⁸⁴ On the basis of the X-ray data and molecular modeling studies, **1.31d** was synthesized where the 4-hydroxyl group was believed to mimic a water molecule observed in the active site of the **1.31c**•PTP1B complex. The K_i was 93 μM , an improvement of about 2-fold. The potency of the naphthyl inhibitors was improved by appending acidic functionalities to the ring system using a series of amide bonds⁸⁵. The use of amide bonds resulted in peptide-like structures which are susceptible to protease enzymes. Compound **1.32**, displayed improved potency with a K_i of 22 μM , and was the only compound from the study which lacked a peptide-type scaffold.

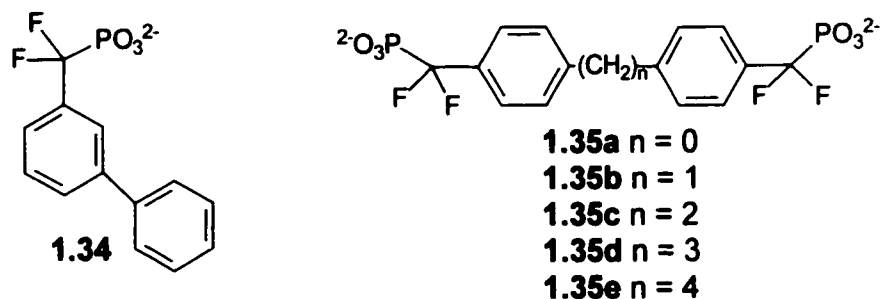


1.33a 2,7 substitution	1.33d 1,3 substitution
1.33b 2,6 substitution	1.33e 1,6 substitution
1.33c 1,5 substitution	1.33f 1,7 substitution

Also employing the naphthyl scaffold, Wang *et al.*⁸⁶ varied the substitution of bis-DFMP functionalities in compounds **1.33a-f**. The most effective inhibitor was **1.33a** which consisted of the 2,7 substitution pattern and had a K_i of 26 μM .

The 2,6 substituted compound **1.33b** had a K_i of 29 μM which was within experimental error.

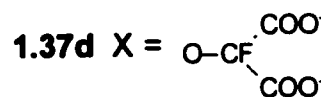
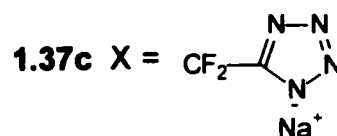
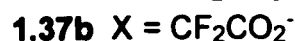
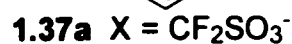
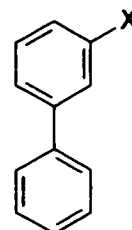
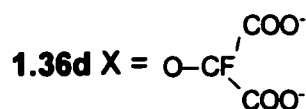
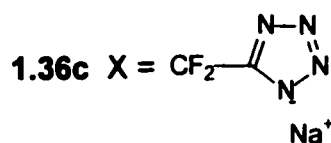
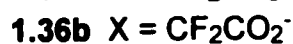
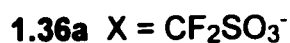
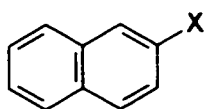
Taylor *et al.* reported a series of inhibitors with low micromolar potency against PTP1B.⁸⁷ An initial set of inhibitors consisted of a phenyl DFMP scaffold where the effects of substituents on the phenyl ring were explored. From this series, **1.34** was found to have a K_i of 17 μM . The *meta* position appeared to be crucial for activity since the structurally similar *para* biphenyl DFMP compound was found to be six fold less effective. A second set of inhibitors, **1.35a-e**, composed of a bis-aryl DFMP scaffold was found to be even more potent, as the chain length between the two aryl rings was increased. In the case of the butyl spacer (**1.35e**), the K_i was found to be 1.5 μM .



The identification of an additional non catalytic aryl phosphate binding site by Puius *et al.*⁸⁸ suggested that the potency of **1.35e** stemmed from an ability to bind with the active and non-catalytic sites simultaneously. However, this mode of interaction has recently been discounted by an X-ray structure of the **1.35e**•PTP1B complex.⁸⁹

In an effort to explore alternatives to the DFMP functionality, Kotoris *et al.*⁹⁰ synthesized several compounds bearing new monoanionic phosphate

mimetics, **1.36a-d** and **1.37a-d**, and examined these compounds as inhibitors of PTP1B. In all four DFMP substitutions, the fluorinated compounds were consistently more effective as inhibitors than the unfluorinated analogues. Of all the surrogates tested, the CF₂-sulfonate proved to be the most effective with an IC₅₀ that was still a factor of ten larger than that of the DFMP compound. These results indicate the importance of dianionic functionalites, especially phosphorus-based ones, as phosphate mimetics for PTP1B inhibition. Though the DFMP functionality is not ideal for cell studies or therapeutic use, it may serve as a means of identifying viable scaffolds for PTP1B inhibitors. Once the scaffolds are identified, the DFMP functionality may potentially be replaced with only a slight decrease, or in some cases, no compromise in potency.



It is clear from the above discussion on PTPase inhibitors that, at the time we began our studies, neither highly potent nor selective inhibitors of PTP1B, or indeed of any PTPase, had been reported. There was clearly room for

improvement in this area. In general, there are two ways by which inhibitors are obtained. One approach is known as rational inhibitor or drug design. In this approach, computer modeling is used to design compounds that bind tightly to the desired target, the structure of which is known. The other approach is less rational and involves the screening of randomly generated compound libraries in the hope that at least one of the compounds being screened will exhibit good potency. One way of generating such compound libraries is known as combinatorial chemistry. As combinatorial chemistry is central to this thesis, a brief discussion of this topic is given below.

1.7 Combinatorial Chemistry

The drive to discover novel chemical entities has given birth to the field of combinatorial chemistry (also commonly referred to as combi-chem). IUPAC borrows from Webster's Collegiate Dictionary the definition of combinatorial as '(1) of, or relating to or involving combinations; (2) of, or relating to the arrangement of, operation on and selection of discrete elements belonging to finite sets.' Combinatorial chemistry is then *strictly* defined as the use of a combinatorial procedure to prepare sets of compounds from sets of building blocks.⁹¹ In brief, rather than synthesize one compound at a time, a combinatorial approach prepares many products, with defined structures, *simultaneously*.⁹²

The key feature of combinatorial chemistry is that the synthetic route allows for the preparation of a range of analogues utilizing similar reaction conditions, either in a single batch or in parallel where separate reactions are

performed concurrently.⁹³ This procedure usually entails the systematic and repetitive covalent connection of a set of 'building blocks' to each other in order to produce an array of diverse structures.⁹⁴ This definition and the potential of combinatorial chemistry is probably better elaborated on with the aid of Figure 1.3.

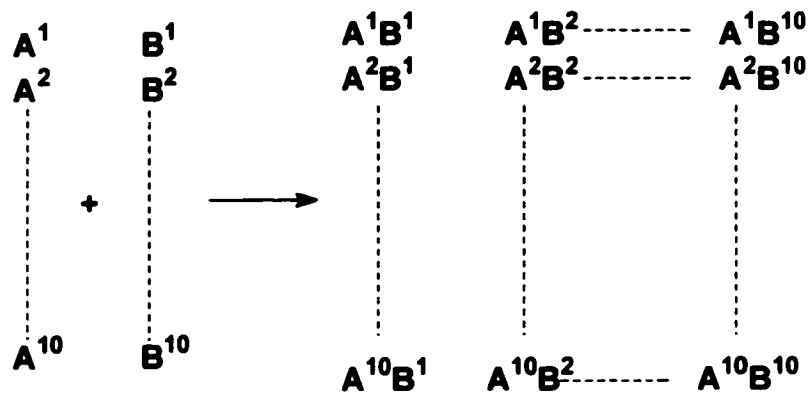


Figure 1.3. Combinatorial chemistry strategy.

In Figure 1.3, A and B represent building blocks/reagents which are composed of 10 subtypes. According to combinatorial principles, each reagent is reacted with every other reagent to give a set, or library, of 100 new compounds. If additional steps are added, where new building blocks are introduced, this simple principle would result in the exponential growth of the library (Figure 1.4).

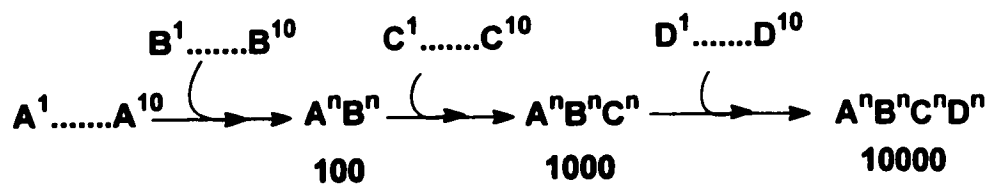


Figure 1.4. Combinatorial chemistry applied to multi-step sequences.

Today, the term combinatorial chemistry has a much broader definition and is used to refer to a wide range of practices that have the *potential* to create large collections of compounds. These practices include polymer supported

synthesis, combinatorial synthesis, reaction monitoring, and compound identification (ie. tagging) strategies. The many facets of combi-chem serve to convey the potential and promise of the field.

The development of combinatorial chemistry methodologies has the potential of accelerating the chemical discovery process. The most attractive feature of combi-chem is the efficient use of time and material resources. Rather than synthesizing one compound of interest at a time, combi-chem permits the rapid synthesis of potentially thousands of candidates which can be evaluated for a desired property. The potential applications of combi-chem include the discovery of new drug candidates,⁹⁴ catalysts, and materials.⁹⁵

As applied to drug discovery, combi-chem can be employed in both lead determination/discovery and optimization. In the absence of any structural information, the screening of compound libraries against a biological target may potentially yield an active compound or a 'hit.' The activity of this lead structure can then be optimized by the parallel generation of structural analogues in order to define structure-activity relationships (SAR's). The generation and use of synthetic libraries complements the traditional lead discovery process which involves the screening of natural product libraries.

In the generation of chemical libraries, several key criteria must be maintained. Ideally, the compounds are produced in a relatively pure form or a method of parallel purification is developed, such that the activity of any hit can be attributed to the compound and not a contaminant. Most importantly, the compounds must be identifiable. A means must exist such that the identity of

any hit can be determined with ease. This can be a simple process if each compound is synthesized in its own unique reaction vessel in parallel. Compounds synthesized in a batch procedure may be tagged as a means of identification or elucidated using recursive deconvolution tactics. Today, the methods of synthesizing combinatorial libraries are as diverse as the compounds synthesized, employing a vast arsenal of strategies including polymer supported synthesis, solution phase synthesis, and hybrid techniques combining the benefits of both approaches.

1.8 Polymer Supported Organic Synthesis

The origins of combinatorial synthesis are intrinsically linked with the use of polymer supported organic synthesis (PSOS). Traditionally, this has involved the covalent attachment of a substrate to an inert polymer. The substrate is then chemically modified in order to introduce diversity and produce a set of related compounds. The final step of the synthesis involves removal of the compound(s) from the support to allow for evaluation/assay. The advantage of constructing compounds on polymers is that an excess of reagents can be used to drive reactions to completion. When the reaction is complete, the excess reagents are removed by filtration. Thus, the main advantage of using PSOS is that the compounds can be purified rapidly after each step. Much of the initial work in the area of polymer supported chemistry was dominated by the preparation of oligomeric type structures such as peptides, nucleotides, and oligosaccharides.⁹⁶ Due to the limited chemistry and diversity achievable by such means, the prominence of oligomeric type chemistry on polymer supports has since given

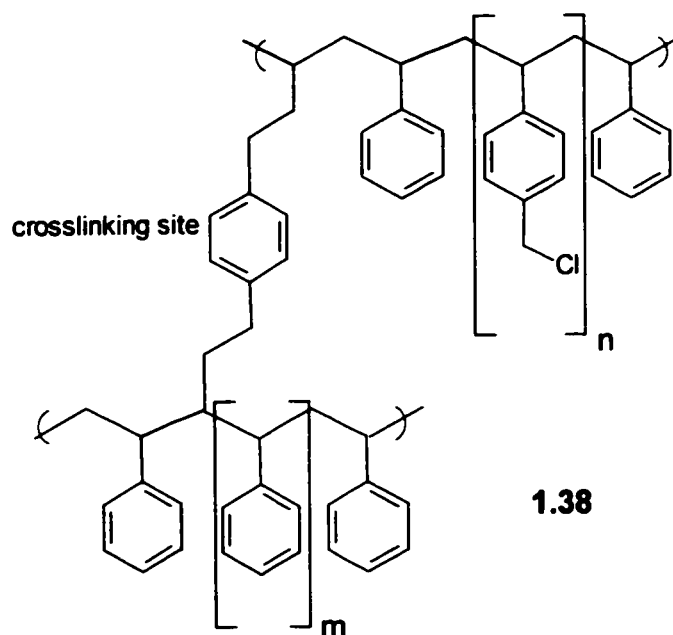
way to the synthesis of low molecular weight compounds by traditional synthesis pathways.

1.8.1 Insoluble Polymer Supports

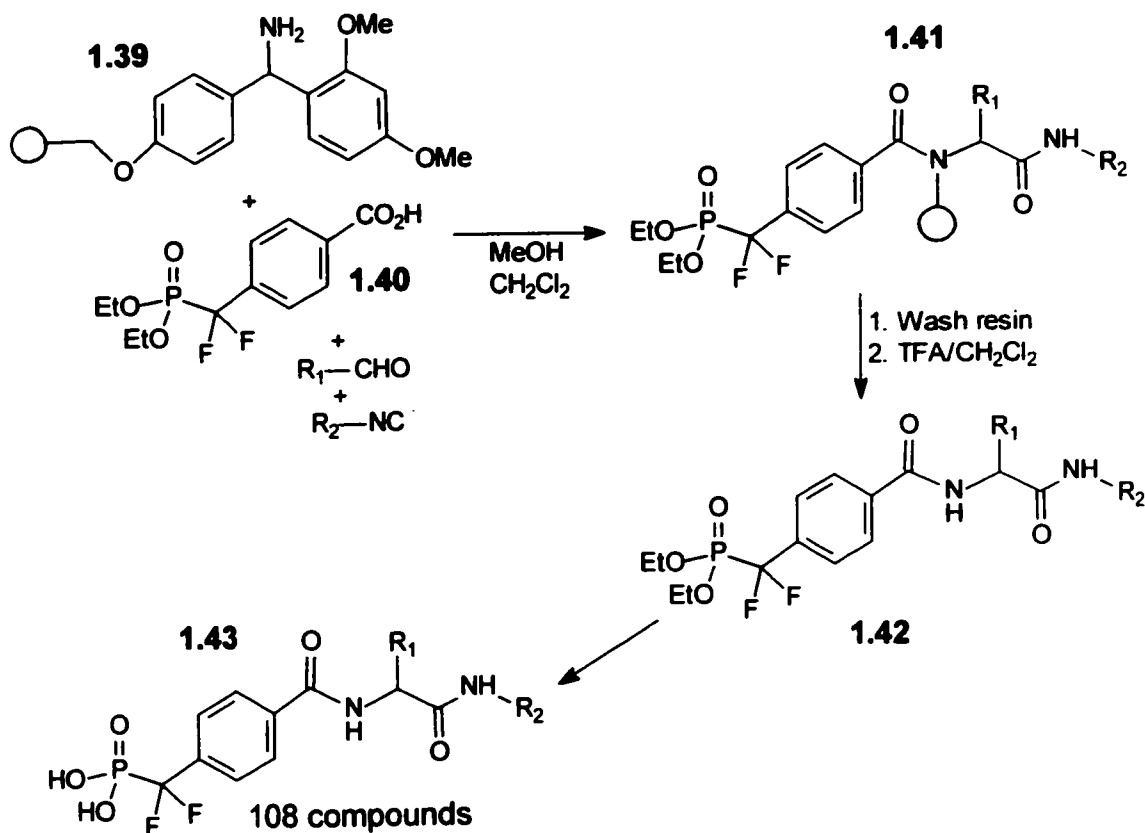
The vast majority of the work on polymer supported synthesis employs insoluble supports and is called solid phase organic synthesis (SPOS). In this approach, the substrate is attached covalently to a functionalized site on a polymer. A linker or spacer arm is often used to distance the substrate from the polymer backbone and to improve the stability of the linkage. The polymer matrix is insoluble and inert to the reaction conditions to be employed. The main advantage of employing insoluble polymer supports is that an excess of reagents can be used to drive each reaction step to completion. The polymer bound intermediates and products can be readily purified by filtration followed by extensive washing. Merrifield's solid phase peptide synthesis methodology is a classic example of SPOS.⁹⁷ This technique is carried out on functionalized cross-linked polystyrene, which is an insoluble polymer. Merrifield resin is composed of styrene, crosslinked with divinyl benzene, and containing reactive chloromethylated sites, which allow for the attachment of the substrates (1.38).

Numerous variations of the Merrifield resin have been employed where the chloromethyl group is replaced with alternative functionalities. A review of these substitutions has been compiled by Winter.⁹⁸ Merrifield resin is typically 1 to 8% crosslinked. The cross linking renders the polymer insoluble in most organic solvents, and affects physical properties such as swelling and

mechanical stability. Higher cross linking results in decreased swelling properties and improved mechanical stability.



A good example of the use of a Merrifield-type insoluble resin for the construction of a compound library is the work of Ganesan *et al.*⁵⁷ who prepared a series of PTP inhibitors using a Ugi reaction (Scheme 1.8). Rink amide resin (**1.39**), a polystyrene based polymer with an acid labile functionality, was used as the amine component for the condensation reaction. An excess of the phenyl DFMP benzoic acid (**1.40**), aldehyde, and isonitrile was used to produce a series of polymer bound di-amide intermediates (**1.41**) which were purified using repeated wash and rinse cycles. The compounds were cleaved using a TFA solution, and the desired phosphonic acids obtained by deprotecting the ethyl groups using TMSBr. By using 8 isonitriles and 18 aldehydes, Ganesan and co-workers prepared a total of 108 compounds based on a di-amide scaffold (**1.43**).



Scheme 1.8. Synthesis of PTP inhibitors on Rinke resin using a Ugi reaction.

Alternatives to the crosslinked polystyrene matrix have been developed and employed in a diverse range of applications. These include polystyrene-polyethylene glycol graft copolymers, polyacrylamide based matrices, and controlled pore glass. The applications and advantages of each matrix extend beyond the scope of the work presented herein.

Though commonly used, it is widely acknowledged that SPOS methods do suffer from several notable drawbacks. The use of heterogeneous reaction conditions requires that traditional solution phase synthetic methodologies be adapted to the solid phase, therefore, requiring new reaction optimization studies. In addition, SPOS methods are often plagued by non-linear reaction

kinetics as well as poor or unequal access to the reaction sites or reactants. The ability to follow the progress of reactions in a non-destructive manner is also compromised. Due to these drawbacks, several groups have investigated alternative means of polymer supported chemistry which still provide the advantages of SPOS.

1.8.2 Soluble Polymer Supports

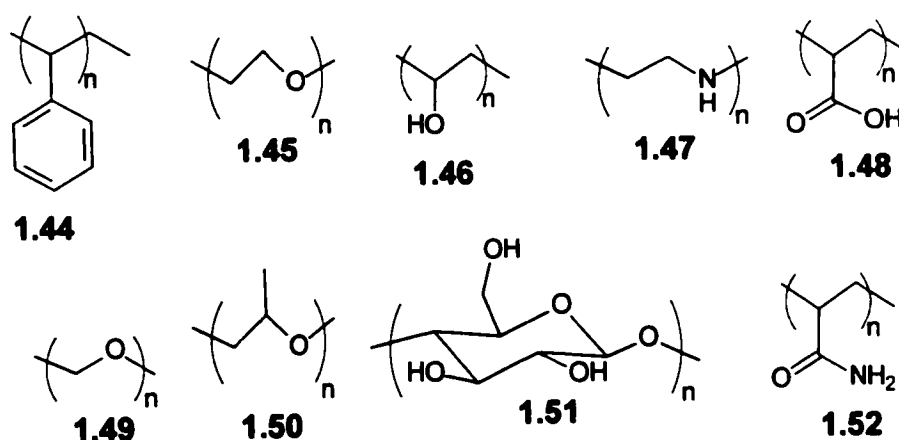
Shortly after Merrifield published his seminal papers on solid phase peptide synthesis in 1963 and 1964, Shemyakin *et al.*⁹⁹ pointed out some of the above-mentioned shortcomings in the context of solid phase peptide synthesis (SPSS). In their words, some of these shortcomings “could be overcome in a novel way by carrying out the peptide synthesis on a support (for instance polymer) not in the solid phase but in solution.” In 1965, Shemyakin *et al.* described the synthesis of a simple tetrapeptide on 25% chloromethylated non-crosslinked polystyrene (NCPS, 1.44). NCPS differs from the Merrifield resin in that divinyl benzene is omitted in the co-polymerization step. As a result, NCPS is soluble in a wide range of organic solvents which allows for many synthetic avenues. However, precipitation can be induced by addition to methanol, hexanes, and/or water. Each step of Shemyakin's synthesis was carried out in solvents in which the polymer was soluble (eg. dioxane, DMF, methylene chloride). When each step of the synthesis was complete, purification was achieved by addition of the reaction mixture to water, which resulted in the precipitation of the polymer-bound products. The peptide was obtained in a 65% yield and was practically homogeneous before chromatography.

The use of soluble polymer supports offer some advantages over classic SPOS and solution phase methodologies. Reactions are carried out under conditions where the polymer is soluble thereby taking advantage of homogeneous reaction conditions. Such reaction conditions allow greater access to reactive sites and reactants, as well as allow for linear kinetic behaviour. The solubility of the polymer also allows for the progress of the reactions to be followed by conventional solution phase NMR spectroscopy methods. Upon completion of the reaction, the polymer is precipitated in a solvent in which it is insoluble to yield the bound products or intermediates. At this stage, the precipitated polymer can be manipulated as if it were insoluble (ie. filtered and washed). In essence, the support serves as a solubility control device. The solubility behaviour of the bound substrate is dictated by the bulk properties of the support. The ability for soluble polymer supports to harness the advantages of insoluble supports and classic solution phase methodologies make it a potentially powerful tool for combi-chem and parallel synthesis methods.

In Shemyakin *et al.*'s⁹⁹ initial report they concluded "this method permitting construction of a chain in solution by ordinary methods will prove to be very convenient not only in the synthesis of polypeptides, but also of other natural oligomers such as nucleotides." However, since Shemyakin's initial report, to our knowledge, only two groups¹⁰⁰⁻¹⁰² have employed NCPS as a support for the synthesis of peptide segments. Much of Shemyakin's enthusiasm was echoed

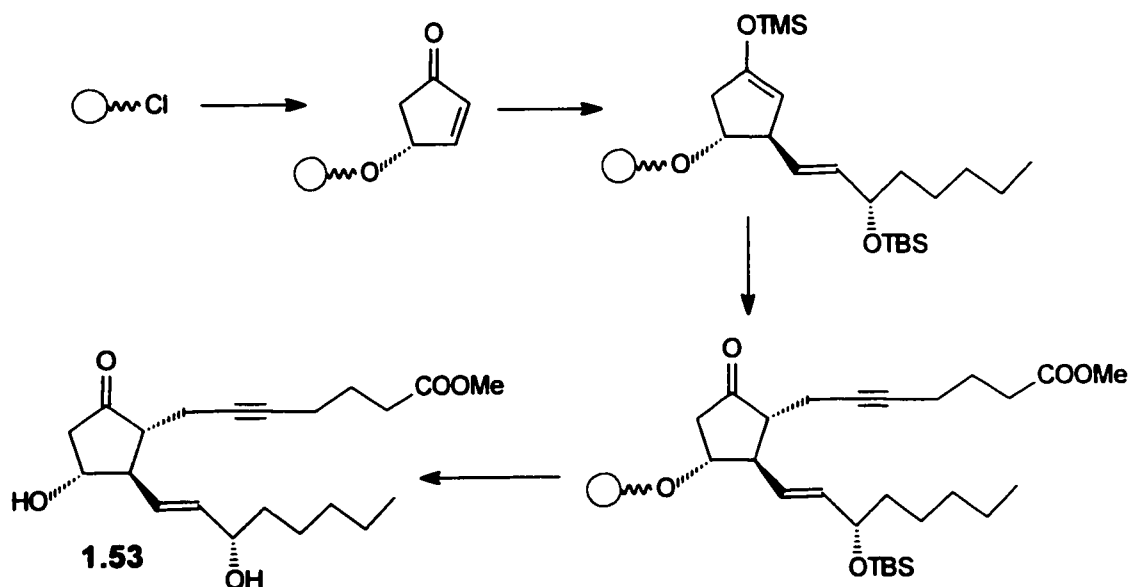
by Narita^{100,101} and Green,¹⁰² who have also used NCPS as a support for the synthesis of polypeptides.

Polyethylene glycol (PEG, **1.45**), polyvinyl alcohol (**1.46**), polyethylene imine (**1.47**), polyacrylic acid (**1.48**), polymethyleneoxide (**1.49**), polypropylene oxide (**1.50**) cellulose (**1.51**) and polyacrylamide (**1.52**) have also been used as soluble supports for peptide synthesis, oligonucleotide synthesis and oligosaccharide synthesis, with PEG being the most popular since it is commercially available and relatively inexpensive. The extent of functionalization, or loading, can be controlled by increasing or decreasing the chain length, since the only loading sites are located on the termini. Despite of Shemyakin *et al.*'s initial optimism, the use of soluble polymers as supports for oligomer synthesis has never attained the popularity of its insoluble counterparts which still dominate the field of PSOS of oligomeric molecules. One possible reason for this may be due to the changes in solubility properties of the soluble polymers when large oligomeric molecules are attached to them.



Janda *et al.* are generally credited for 'rediscovering' soluble polymers for preparing organic compounds.^{103,104,105} Janda originally called this approach to

PSOS 'liquid phase organic synthesis' (or LPOS).¹⁰⁶ This term has recently lost popularity due to its ambiguity, in favour of the term soluble polymer supported organic synthesis (SPSOS).¹⁰⁷ Unlike previous work in this area, most of the current work has focused on preparing small molecules as opposed to oligomers. Unlike oligomers, the attachment of small molecules to a soluble polymer has little effect on the solubility properties of the polymer. Almost all of the current work on the synthesis of small molecules using soluble polymer supports has been conducted on PEG or NCPS with PEG being by far the more popular of the two, probably due to the fact that functionalized NCPS is not commercially available.¹⁰³ Indeed, at the time we began our work in the area of SPOS, to our knowledge, there was only a single example in the literature describing the synthesis of small molecules on NCPS.



Scheme 1.9. Synthesis of prostaglandin E₂ methyl ester on NCPS.

This was reported by Janda who demonstrated the utility of NCPS as a support for the synthesis of a prostaglandin methyl ester¹⁰³ (Scheme 1.9) and

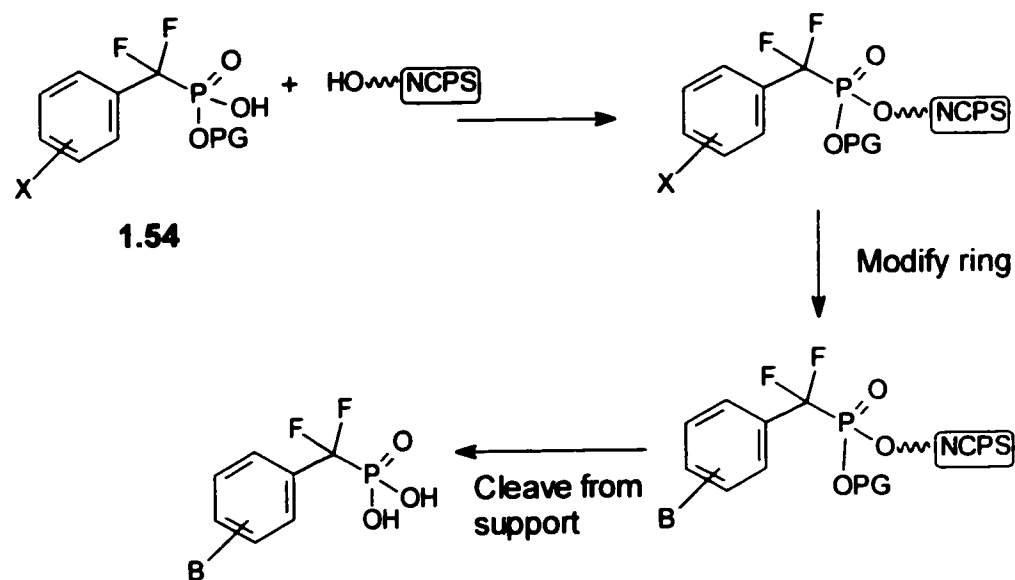
later applied to methodology towards the preparation of a prostanoid library.^{105,108} The use of NCPS as a support allowed a wide range of flexibility in the chemistry that was employed. Conventional solution phase reactions could be used in conjunction with traditional solution phase workup conditions that involved multiple solvent extraction steps. Purification of the intermediates was accomplished by precipitation of the polymer in methanol. Using the NCPS support, the overall yield for the synthesis of prostaglandin E₂ methyl ester (**1.53**) was 37% over 8 steps.

1.9 Specific Objectives

Due to the potential of polymer-supported methodologies as a means of preparing large numbers of compounds rapidly and efficiently, we decided to examine this technique as a route to preparing potential inhibitors of PTP1B. The class of compound we chose to prepare were aryl difluoromethylenephosphonic acids (aryl DFMP's). We targeted these compounds due to their potential to inhibit PTP1B (see Section 1.6.6). The main objective of the work presented in the following two chapters is to develop the chemistry that will allow for the synthesis of aryl DFMP's using SPSOS. The general approach is outlined in Scheme 1.10.

In brief, a mono-protected aryl DFMP compound of type **1.54** is attached to NCPS via a phosphonate ester linkage. The polymer bound substrate is then functionalized on the aryl ring to create a series of analogous compounds which are then cleaved from the support and deprotected in a single step. We report the preparation of two sets of aryl DFMP's. The first set of compounds are based

upon a biphenyl structure and are prepared using a Suzuki reaction where the second aryl ring is varied to introduce diversity (chapter 2). The second set of compounds are prepared using a Wittig reaction where the diversity is introduced by the use of various Wittig reagents (chapter 3).



Scheme 1.10. General approach for library synthesis.

We chose to work with a soluble support because of the apparent advantages listed above. Of these advantages, we considered the ability to monitor the progress of the reactions using conventional solution phase NMR to be particularly attractive. Since all of the compounds are attached to the support by a phosphonate ester linkage, all subsequent transformations on the polymer could be followed using ^{19}F -NMR or ^{31}P -NMR. ^{19}F -NMR is a particularly attractive nucleus for this purpose since it is a fairly sensitive technique and has a broad chemical shift range.^{109,110,111,112} As a result, chemical modifications remote from the DFMP functionality may effect a change in chemical shift. Also, since the polymer does not contain fluorine, the ^{19}F -NMR spectra would be

uncomplicated by signals from the polymer. We chose to use NCPS, as opposed to more commonly used PEG, as the soluble support, since we were concerned that PEG would not be stable to some of our reaction conditions.

With the exception of Janda's studies, no other reports had appeared in the literature using NCPS for small molecule library construction when we began our studies. Thus, another objective of the work described in the following two chapters, was to evaluate NCPS as a support for preparing small molecule libraries in general, using the synthesis of aryl DFMP's as a model system. We conclude from these studies that there are both definite advantages as well as disadvantages to this approach to small molecule library construction.

1.10 REFERENCES

- 1 Zhang, Z-Y.; Dixon, J. E. *Advances in Enzymology and Related Areas of Molecular Biology* **1994**, *68*, 1-36.
- 2 Tonks, N. K.; Neel, B. G. *Cell*. **1996**, *87*, 365-368.
- 3 Neel, B. G.; Tonks, N. K. *Curr. Opin. Cell. Biol.* **1997**, *9*, 193.
- 4 Walton, K. M., Dixon, J. E. *Annu. Rev. Biochem.* **1993**, *62*, 101-120.
- 5 Elchebley, M.; Payette, P.; Michaliszyn, E.; Cromlish, W.; Collins, S.; Loy, A. L.; Mormandin, D.; Cheng, A.; Himms-Hagen, J.; Chan, C-C.; Ramanchandran, C.; Gresser, M. J.; Tremblay, M. L.; Kennedy, B. P. *Science* **1999**, *283*, 1544-2548.
- 6 Burke, T.R.; Kole, H.K.; Roller, P. P. *Biochem. Biophys. Res. Commun.* **1994**, *204*, 129-134.
- 7 Stone, R. L.; Dixon, J. E. *J. Biol. Chem.* **1994**, *269*, 31323-31326.
- 8 Zhang, Z-Y. *Critical Reviews in Biochemistry and Molecular Biology* **1998**, *33*, 1-52.
- 9 Fauman, E. B.; Saper, M. A. *TIBS* **1996**, *21*, 413-417.
- 10 Ripka, W. C. *Annual Reports in Medicinal Chemistry* **2000**, *35*, 231-250.
- 11 Stuckey, J. A.; Schubert, H. L.; Fauman, E.; Zhang, Z-Y.; Dixon, J. E.; Saper, M. A. *Nature* **1994**, *370*, 571-575.
- 12 Schubert, H. L.; Fauman, E.; Stuckey, J. A.; Dixon, J. E.; Saper, M. A. *Protein Sci.* **1995**, *4*, 1904-1913.
- 13 Juszczak, L. J.; Zhang, Z-Y.; Wu, L.; Gottfried, D. S.; Eads, D. D. *Biochemistry* **1997**, *36*, 2227-2236.

-
- 14 Jia, Z.; Barford, D. A.; Flint, A. J.; Tonks, N. K. *Science* **1995**, *268*, 1754-1758.
- 15 Cotton, F. A.; Hazen Jr., E. E.; Norman Jr., J. G.; Wong, S. T. K.; Johnson, K. H. *J. Am. Chem. Soc.* **1973**, *95*, 2367-2369.
- 16 Zhang, Z-Y.; Wang, Y.; Wu, L.; Fauman, E.B.; Stuckey, J. A.; Schubert, H. L.; Saper, M. A.; Dixon, J. E. *Biochemistry* **1994**, *33*, 15266-15270.
- 17 Flint, A. J.; Taganis, T.; Barford, D.; Tonks, N. K. *Proc. Natl. Acad. Sci. USA* **1997**, *94*, 1680-1685.
- 18 Streuli, M.; Krueger, N. X.; Thai, T.; Tang, M.; Saito, H. *EMBO J.* **1990**, *9*, 2399-2407.
- 19 Johnson, P.; Ostergaard, H. L.; Wasden, C.; Trowbridge, I. S. *J. Biol. Chem.* **1992**, *267*, 8035-8041.
- 20 Guan, K. L.; Dixon, J. E. *J. Biol. Chem.* **1991**, *266*, 17026-17030.
- 21 Zhang, Z-Y.; Dixon, J. E. *Biochemistry* **1993**, *32*, 9340-9345.
- 22 Zhang, M.; Zhou, M.; Van Etten, R. L.; Stauffacher, C. V. *Biochemistry* **1997**, *36*, 15-23.
- 23 Barford, D.; Flint, A. J.; Tonks, N.K. *Science* **1994**, *263*, 1397-1404.
- 24 Zhang, Z-Y.; Palfey, B. A.; Wu, L.; Zhao, Y. *Biochemistry* **1995**, *34*, 16389-16396.
- 25 Denu, J. M.; Dixon, J. E. *Proc. Natl. Acad. Sci. USA* **1995**, *92*, 5910-5914.
- 26 Zhao, Y.; Zhang, Z-Y. *Biochemistry* **1996**, *35*, 11797-11804.
- 27 Wu, L.; Zhang, Z-Y. *Biochemistry* **1996**, *35*, 5426-5434.
- 28 Guan, K. L.; Dixon, J. E. *Science* **1990**, *249*, 553-556.

-
- 29 Pot, D. A.; Woodford, T. A.; Remboutsika, E.; Haun, R. S.; Dixon, J. E. *Proc. Natl. Acad. Sci. USA* **1991**, *87*, 19688-19696.
- 30 Tonks, N. K.; Diltz, C. D.; Fischer, E. H. *J. Biol. Chem.* **1990**, *265*, 10674-10608.
- 31 Cho, H.; Krishnaraj, R.; Kitas, E.; Bannwarth, W.; Walsh, C. T.; Anderson, K. S. *J. Am. Chem. Soc.* **1992**, *114*, 7296-7298.
- 32 Denu, J.; Lohse, D. L.; Vijayalakshmi, J.; Saper, M. A.; Dixon, J. E. *Proc. Natl. Acad. Sci. USA* **1996**, *93*, 2493-1498.
- 33 Bruice, T. C.; Benkovic, S. J. Phosphate esters. *Bioorganic Mechanisms*. **1966**, Vol. II, pp. 1-103, Benjamin, W. A., Inc., New York.
- 34 Hengge, A. C.; Sowa, G.; Wu, L.; Zhang, Z-Y. *Biochemistry*. **1995**, *34*, 13982-13987.
- 35 Cleland, W. W.; Hengge, A. C. *FASEB J.* **1995**, *9*, 1585-1594.
- 36 Pinna, L. A.; Donella-Deana, A. *Biochem. Biophys. Acta* **1994**, *1222*, 415-431.
- 37 Zhang, Z-Y.; Thieme-Seffler, A. M.; Maclean, D.; McNamara, D. J.; Dobrusin, E. M.; Sawyer, T. K.; Dixon, J. E. *Proc. Natl. Acad. Sci. USA* **1993**, *90*, 4446-4450.
- 38 Zhang, Z-Y.; Maclean, D.; McNamara, D. J.; Sawyer, T. K.; Dixon, J. E. *Biochemistry* **1994**, *33*, 2285-2290.
- 39 Montserat, J.; Chen, L.; Lawrence, D. S.; Zhang, Z-Y. *J. Biol. Chem.* **1996**, 7868-7872.

-
- 40 Wang, Q.; Scheigetz, J.; Gilbert, J.; Snider, J.; Ramachandran, R. *Biochem. Biophys. Acta* **1999**, *1431*, 14-23.
- 41 Huang, Z.; Wang, Q.; Ly, Hoa D.; Gorvindarajan, A.; Scheigetz, J.; Zamboni, R.; Desmarais, S.; Ramachandran, C. *J. Biomol. Screening* **1999**, *4*, 327-334.
- 42 Tonks, N. K.; Diltz, C. D.; Fischer, E. H. *J. Biol. Chem.* **1988**, *263*, 6722-6728.
- 43 Tonks, N. K.; Diltz, C. D.; Fischer, E. H. *J. Biol. Chem.* **1988**, *263*, 6731-6737.
- 44 Barford, D.; Keller, J. C.; Flint, A. J.; Tonks, N. K. *J. Mol. Biol.* **1994**, *239*, 726-730.
- 45 Coordinates obtained from Brookhaven Protein Data bank. Access code PTU. This structure was reported in reference 14.
- 46 Sarmiento, M.; Zhao, Y.; Gordon, S. J.; Zhang, Z-Y. *J. Biol. Chem.* **1998**, *273*, 26368-26374.
- 47 White, M. F.; Kahn, R. *J. Biol. Chem.* **1994**, *269*, 1-4.
- 48 Kennedy, B. P. *Biomed & Pharmacother* **1999**, *53*, 466-470.
- 49 Drake, P. G.; Posner B. I. *Mol. Cell. Biochem.* **1998**, *182*, 79-89.
- 50 Goldstein, B. J.; Ahmad, F.; Ding, W.; Li, P-M.; Zhang, W-R. *Mol. Cell. Biochem.* **1998**, *182*, 91-99.
- 51 Byon, J. C. H.; Kusari, A. B.; Kusari, J. *Mol. Cell. Biochem.* **1998**, *182*, 101-108.
- 52 Kennedy, B.; Ramachandran, C. *Biochem. Pharmacol.* **2000**, *60*, 877-883.
- 53 Liotta, A. S.; Kole, H. K.; Fales, H. M.; Roth, J.; Bernier, M. *J. Biol. Chem.* **1994**, *269*, 22996-23001.

-
- 54 Desmarais, S.; Jia, Z.; Ramachandran, C. *Arch. Biochem. Biophys.* **1998**, *354*, 225-231.
- 55 Burke, T. R.; Kole, H. K.; Roller, P. P. *Biochem. Biophys. Res. Commun.* **1994**, *204*, 129-134.
- 56 Chen, L.; Wu, L.; Otaka, A.; Smyth, M. S.; Roller, P. P.; Burke, T. R.; den Hertog, J.; Zhang, Z-Y. *Biochem. Biophys. Res. Commun.* **1995**, *216*, 976-984.
- 57 Li, Z.; Teo, S-L.; Pallen, C. K.; Ganesan, A. *Bioorg. Med. Chem. Lett.* **1998**, *8*, 2443-2446.
- 58 Kole, H. K.; Akamatsu, M.; Ye B.; Yan, X.; Barford, D.; Roller, P. P.; Burke, T. R. *Biochem. Biophys. Res. Commun.* **1995**, *209*, 817-822.
- 59 Burke, T. R.; Ye, B.; Akamatsu, M.; Ford, H.; Yan, X.; Kole, H. K.; Wolf, G.; Shoelson, S. E.; Roller, P. P. *J. Med. Chem.* **1996**, *39*, 1021-1027.
- 60 Akamatsu, M.; Roller, P. P.; Chen, L.; Zhang, Z-Y.; Ye, B.; Burke, T. R. *Bioorg. Med. Chem.* **1997**, *5*, 157-163.
- 61 Roller, P. P.; Zhang, Z-Y.; Burke, T. R. *Bioorg. Med. Chem. Lett.* **1998**, *8*, 2149-2150.
- 62 Moran, E. J.; Sarshar, S.; Cargill, J. F.; Shahbaz, M. M.; Lio, A.; Mjalli, A. M. M.; Armstrong, R. W. *J. Am. Chem. Soc.* **1995**, *117*, 10787-10788.
- 63 Zheng Huang, personal communication to S. D. Taylor.
- 64 Merggren, M. M.; Burns, L. A.; Abraham, R. T.; Powis, G. *Cancer Res.* **1993**, *53*, 1862-1866.

-
- 65 Huyer, G.; Liu, S.; Kelly, J.; Moffat, J.; Payette, P.; Kennedy, B.; Tsaprailis, G.; Gresser, M.J.; Ramachandran, C. *J. Biol. Chem.* **1997**, *272*, 843-851.
- 66 Posner, B. I.; Faure, R.; Burgess, J. W.; Bevan, A. P.; Lachance, D.; Zhang-Sun, G.; Fantus, G.; Ng, J. B.; Hall, D. A.; Lum, B. S.; Shaver, A. *J. Biol. Chem.* **1994**, *269*, 4596-4604.
- 67 Ham, S. W.; Park H. J.; Lim, S. H. *Bioorg. Chem.* **1997**, *25*, 33-36.
- 68 Ham, S. W.; Park J.; Lee, S-J.; Kim, W.; Kang, K.; Choi, K.H. *Bioorg. Med. Chem. Lett.* **1998**, *8*, 2507-2510.
- 69 Ham, S. W.; Park, J. Lee, S-J.; Yoo, J. S. *Bioorg. Med. Chem. Lett.* **1999**, *9*, 185-186.
- 70 Myers, J. K.; Widlanski, T. S. *Science* **1993**, *262*, 1451-1453.
- 71 Wang, Q.; Dechert, T.; Jirik, F.; Withers, S. G. *Biochem. Biophys. Res. Commun.* **1994**, *200*, 577-583.
- 72 Taylor, W. P.; Zhang, Z-Y.; Widlanski, T. S. *Bioorg. Med. Chem.* **1996**, *4*, 1515-1520.
- 73 Hamaguchi, T.; Sudo, T.; Osada, H. *FEBS Letters* **1995**, *372*, 54-58.
- 74 Sodeoka, M.; Sampe, R.; Kagamizono, T.; Osada, H. *Tetrahedron Lett.* **1996**, *37*, 8775-8778.
- 75 Cebula, R. E.; Blanchard, J. L.; Boisclair, M. D.; Pal, K.; Bockovich, N. J. *Bioorg. Med. Chem. Lett.* **1997**, *7*, 2015-2020.
- 76 Miski, M.; Shen, X.; Cooper, R.; Gillum, A. M.; Fisher, D. K.; Miller, R. W.; Higgins T. J. *Bioorg. Med. Chem. Lett.* **1995**, *5*, 1519-1522.

-
- 77 Imoto, M.; Kakeya, H.; Sawa, T.; Hayashi, C.; Hamada, M.; Takeuchi, T.; Umezawa, K. *J. Antibiot.* **1993**, *46*, 1342-1346.
- 78 Yu, L.; McGill, A.; Ramirez, J.; Wang, P. G.; Z-Y. Zhang *Bioorg. Med. Chem. Lett.* **1995**, *5*, 1003-1006.
- 79 Skorey, K.; Ly, H. D.; Kelly, J.; Hammond, M.; Ramachandran, C.; Huang, Z.; Gresser, M. J.; Wang, Q. *J. Biol. Chem.* **1997**, *272*, 22472-22480.
- 80 Zhang, Y-L.; Keng, Y-F.; Zhao, Y.; Wu, L.; Zhang, Z-Y. *J. Biol. Chem.* **1998**, *273*, 12281-12287.
- 81 Frechette, R. F.; Ackerman, C.; Beers, S.; Look, R.; Moore, J. *Bioorg. Med. Chem. Lett.* **1997**, *7*, 2169-2172.
- 82 Beers, S.; Malloy, E. A.; Wu, W.; Wachter, M. P.; Gunnia, U.; Cavender, D.; Harris, C.; Davis, J.; Brosius, R.; Pellegrino-Gensey, J. L.; Siekierka, J. *Bioorg. Med. Chem.* **1997**, *12*, 2203-2211.
- 83 Kole, H. K.; Smyth, M. S.; Russ, P. L.; Burke, T. R. *Biochem. J.* **1995**, *311*, 1025-1031.
- 84 Burke, T. R.; Ye, B.; Yan, X.; Wang, S.; Jia, Z.; Chen, L.; Zhang, Z-Y.; Barford, D. *Biochemistry* **1996**, *35*, 15989-15996.
- 85 Yao, Z-J.; Ye, B.; Wu, X-W.; Wang, S.; Wu, L.; Zhang, Z-Y.; Burke, T. R. *Bioorg. Med. Chem.* **1998**, *6*, 1799-1810.
- 86 Wang, Q.; Huang, Z.; Ramachandran, C.; Dinaut, A. N.; Taylor, S. D. *Bioorg. Med. Chem. Lett.* **1998**, *8*, 345-350.
- 87 Taylor, S. D.; Kotoris, C. C.; Dinaut, A. N.; Wang, Q.; Ramachandran, C.; Huang, Z. *Bioorg. Med. Chem.* **1998**, *6*, 1457-1468.

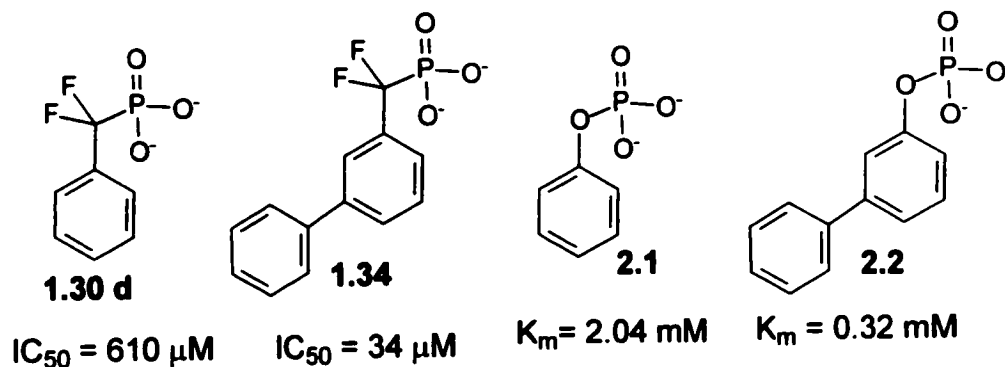
-
- 88 Puius, Y. A.; Zhao, Y.; Sullivan, M.; Lawrence, D. S.; Almo, S. C.; Zhang, Z.-Y. *Proc. Natl. Acad. Sci. USA* **1997**, *94*, 13420-13425.
- 89 Personal communication from S. D. Taylor and Z. Jia.
- 90 Kotoris, C. C.; Chen, M.-J.; Taylor, S. D. *Bioorg. Med. Chem. Lett.* **1998**, *8*, 3275-3280.
- 91 Maclean, D.; Baldwin, J. J.; Ivanov, I. T.; Kato, Y.; Shaw, A.; Schneider, P.; Gordon, E. M. *J. Comb. Chem.* **1999**, *2*, 562-578.
- 92 Balkenhohl, F.; von dem Bussche-Hünnefeld, C.; Lansky, A.; Zechel, C. *Angew. Chem. Int. Ed. Engl.* **1996**, *35*, 2288-2337.
- 93 Terrett, N. K.; Gardner, M.; Gordon, D. W.; Kobylecki, R. J.; Steele, J. *Tetrahedron* **1995**, *51*, 8135-8173.
- 94 Gallop, M. A.; Barrett, R. W.; Dower, W. J.; Fodor, S. P. A.; Gordon, E. M. *J. Med. Chem.* **1994**, *37*, 1233-1251.
- 95 Hsieh- Wilson, L. C.; Xiang, X.-D.; Schultz, P. G. *Acc. Chem. Res.* **1996**, *29*, 164-170.
- 96 Früchtel, J.; Jung, G. *Angew. Chem. Int. Ed. Engl.* **1996**, *35*, 17-42.
- 97 Merrifield, R. B. *J. Am. Chem. Soc.* **1963**, *85*, 2149-2154.
- 98 Winter, M. "Supports for Solid-Phase Organic Synthesis" in "Combinatorial Peptide and Nonpeptide Libraries: A Handbook"; ed. Jung, G.; VCH New York **1996**, 465-510.
- 99 Shemyakin, M. M.; Yu, A.; Ovchinikov, A. A.; Kinyunshkin, A.; Kozhevnikova, I. V. *Tetrahedron. Lett.* **1965**, 2323.

-
- 100 Narita, M.; Itsuno, S.; Hirata, M.; Kusano, K. *Bull. Chem. Soc. Jpn.* **1980**, *53*, 1028-1033.
- 101 Narita, M. *Bull. Chem. Soc. Jpn.* **1978**, *51*, 1477-1480.
- 102 Green, B.; Garson, L. R. *J. Chem. Soc. (C)* **1969**, 401-405.
- 103 Chen, S.; Janda, K. D. *J. Am. Chem. Soc.* **1997**, *119*, 8724-8725.
- 104 Chen, S.; Janda, K. D. *Tetrahedron Lett.* **1998**, *39*, 3943-3946.
- 105 Lee, K. J.; Angulo, A.; Ghazal, P.; Janda, K. D. *Org. Lett.* **1999**, *1*, 1859-1862.
- 106 Gravert, D. J.; Janda, K. D. *Chem. Rev.* **1997**, *97*, 489-509.
- 107 Link, A. *Angew. Chem. Int. Ed. Engl.* **2000**, *39*, 4039-4040.
- 108 Manzotti, R.; Tang, S-Y.; Janda, K. *Tetrahedron* **2000**, *56*, 7885-7892.
- 109 Svensson, A.; Fex, T.; Kihlberg, J. *Tetrahedron Lett.* **1996**, *37*, 7649-7652.
- 110 Svensson, A.; Bergquist, K-E.; Fex, T.; Kihlberg, J. *Tetrahedron Lett.* **1998**, *39*, 7193-7196.
- 111 Drew, M.; Orton, E.; Krowlikowski, P.; Salvino, J. M.; Kumar, N. V. *J. Comb. Chem.* **2000**, *2*, 8-9.
- 112 Salvino, J. M.; Patel, S.; Drew, M.; Krowlikowski, P.; Orton, E.; Kumar, N. K.; Caulfield, T.; Labaudiniere, R. *J. Comb. Chem.* **2001**, *3*, 177-180.

CHAPTER 2 SPSOS SYNTHESIS OF BIARYL DFMP COMPOUNDS VIA A SUZUKI REACTION

2.1 Introduction

As stated in chapter 1, the main objective of our work on PSOS is to develop the chemistry that will allow for the synthesis of aryl DFMP's on NCPS. We began these studies by preparing a series of biaryl DFMP compounds for two principal reasons. Our initial reason was due to the work from within our own group¹ which demonstrated that by substituting the parent compound benzyldifluorophosphonate, **1.30d** with an aryl ring at the *meta* position (**1.34**), the IC_{50} improves from 610 μM to 34 μM , which represents a 17-fold increase in potency. A similar phenomenon has been observed in substrate studies where *meta*-phenyl phenylphosphate (**2.2**) exhibits a K_m value of 0.32 mM which is considerably lower than that of phenylphosphate (**2.1**) ($K_m = 2.04$ mM).^{2,3} There was also evidence that the effect of the *meta*-phenyl ring was due to more than simple non-specific hydrophobic interactions since non-peptidyl substrates *meta*-substituted with aliphatic hydrocarbons (ethyl, isopropyl) exhibited higher K_m 's than *m*-phenyl phenylphosphate (**2.2**).⁴

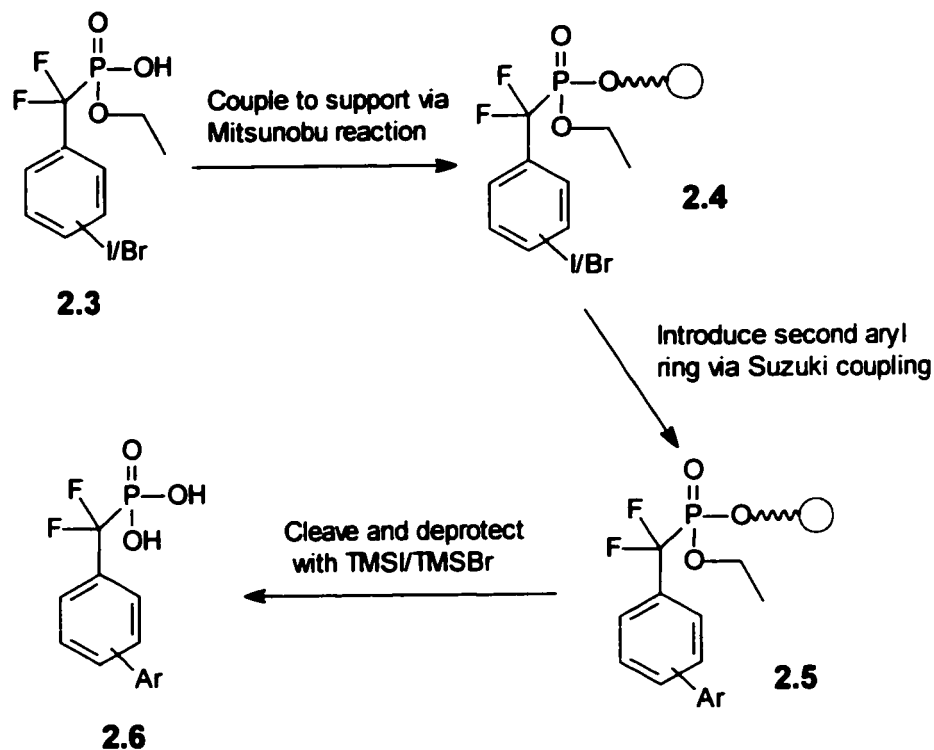


We were also interested in identifying how the addition of the *meta* phenyl ring enhanced inhibitory activity. In order to better understand the effect of the *meta* phenyl ring, we wished to perform molecular dynamics studies of **1.34** docked in the PTP1B active site and compare our results with observations reported by others who also studied PTP1B.

Another motivation for targeting the biaryl series of compounds was the anticipation that such compounds could be prepared by a Suzuki coupling between a polymer-bound aryl bromide or iodide and a series of boronic acids. The Suzuki coupling has been used extensively in PSOS^{5,6} so we felt that this was a good model reaction on which to test our approach to the synthesis of aryl DFMP's on NCPS. Consequently, we envisioned preparing a series of compounds of type **2.5** (Scheme 2.1) with the second aryl ring substituted with a variety of functionalities.

The general strategy towards the biaryl compounds is shown in Scheme 2.1. An aryl phosphonic acid of type **2.3**, bearing an ethyl protecting group, would be attached to NCPS via a phosphonate ester linkage. A Suzuki reaction between polymer-bound **2.4** and a series of boronic acids would produce a collection of polymer-bound biaryls of type **2.5**. ¹⁹F NMR would enable us to monitor the progress of the reactions to ensure a single polymer bound species at each step. Attaching the compounds to the support by a phosphonate ester linkage raises the issue of how to remove the compounds from the support when the synthesis is complete. Ideally, we wished to remove the compounds from the support and deprotect the phosphonate in a single step. Phosphonate diesters

undergo hydrolysis in acid or base to produce the monoesters quite readily, however, further hydrolysis to give the diacids (or salts) requires very harsh conditions which we wished to avoid.



Scheme 2.1. General approach to the synthesis of biaryl DFMP compounds.

Protecting the phosphonates with an acid labile group, such as a *t*-butyl group, and attaching the compounds to the support by an acid-labile linker, such as a Wang linker, would be problematic for two reasons. The *t*-butyl ester analogue of 2.3 would be very difficult to make and would be very unstable. Also, attaching it to the support would be problematic due to steric reasons. Consequently, we chose an ethyl protecting group since phosphonate ethyl esters are easily prepared using an Arbuzov reaction and we anticipated that attaching 2.3 to the support would be relatively straightforward. We also

anticipated that the polymer-bound phosphonates could be deprotected and cleaved from the support in a single step using TMSI or TMSBr, which are commonly used reagents for converting phosphorous esters to the corresponding acids. The resulting phosphonic acids (2.6) would then be converted into easy-to-handle diammonium salts.

2.2 Experimental

General

All modeling studies were performed using the Insight 97.2 software package⁷ run on a Silicon Graphics Octane system with a RISC 10000 processor. Energy minimization and molecular dynamics calculations were performed using the Discover module. Analysis of the results was performed using both the Decipher and Analysis modules.

All reagents for syntheses and biological assays were obtained from commercial suppliers (Sigma-Aldrich, Lancaster, Strem) and used without further purification unless noted otherwise. For silica gel chromatography, certain solvents were distilled prior to use (CHCl_3 , CH_2Cl_2 , hexanes). The silica gel was supplied by Silicycle (230-400 mesh, 60 Å). For reactions requiring anhydrous solvents, the solvents were prepared as described. THF and diethyl ether were distilled over sodium/benzophenone ketyl under an Ar or N_2 atmosphere. Benzene and CH_2Cl_2 were distilled over calcium hydride under an Ar or N_2 atmosphere. DMF was distilled under reduced pressure and stored over 4 Å molecular sieves under Ar. Reactions requiring anhydrous conditions were performed under an N_2 or Ar atmosphere. For these reactions, liquid transfers were performed using oven dried syringes and needles. Melting points were obtained on an Electrothermal capillary melting point apparatus and are uncorrected. ^1H , ^{19}F , ^{13}C , and ^{31}P NMR spectra were recorded on a Varian Gemini 200, or unless noted a Bruker Avance 300 spectrophotometer. For ^1H NMR run in CDCl_3 , chemical shifts (δ) are reported in ppm downfield relative to

the internal TMS standard. For ^1H NMR run in other deuterated solvents lacking an internal TMS standard, chemical shifts are reported relative to solvent residual peaks: D_2O , δ 4.79; $\text{DMSO-}d_6$, δ 2.50 for the central peak of the quintet; acetone- d_6 , δ 2.05 for the central peak of the quintet; and CD_3OD , δ 3.31 for the central peak of the quintet. ^{19}F NMR chemical shifts are reported relative to the external standard trifluoroacetic acid (TFA) (0 ppm). ^{13}C NMR run in CDCl_3 are referenced to solvent peaks (77 ppm for center peak of the triplet). For ^{31}P NMR spectra, chemical shifts are reported in parts per million relative to the external standard 85% phosphoric acid (0 ppm). Abbreviations s, d, t, q, m, and br are used for singlet, doublet, triplet, quadruplet, multiplet, and broad. All NMR couplings are given in Hz. Electron impact (EI) and fast atom bombardment (FAB) mass spectra (MS) were obtained on a Micromass 70-S-250 mass spectrometer. Electrospray mass spectra were obtained using a Micromass Platform mass spectrometer. Analytical HPLC analysis was performed using a Waters LC 4000 System equipped with a Vydac 218TP54 analytical C-18 reverse phase column and a Waters 486 tunable absorbance detector set at 254 nm. The following mobile phase gradient system was used for HPLC analysis of the diammonium salts **2.60-2.73** (solvent A: acetonitrile; solvent B: water with 0.1% TFA modifier): 0 min: 10% A; 6 min: 10% A; 16 min: 100% A; 26 min: 100% A; 36 minutes: 10% A; 51 minutes: 10% A. Enzyme kinetics studies were performed on a Varian Cary 1B spectrophotometer. Ultra-pure water (Millipore[®]) was used for the preparation of all biological samples and buffers. Fluorescein diphosphate (FDP) and PTP1B were kindly provided by Merck-Frosst.

2.2.1 Molecular Modeling

System Preparation The heavy atom coordinates for PTP1B were extracted from the crystal structure of PTP1B complexed with [1,1-difluoro-1-(2-naphthalenyl)-methyl] phosphonic acid (**1.31c**), which was reported by Burke et al.⁸ and available at the Brookhaven Protein Data Bank. Hydrogen atoms were added using the Builder module with the pH set at 7. The active cysteine residue was modeled as the reduced thiolate. The CVFF forcefield and charge templates were used as the parameter set for the minimization and dynamics calculations. For the MD simulations double cutoffs of 20 and 22 Å were employed. The inhibitor (3-phenylphenyl)(difluoro)methylphosphonic acid (**1.34**) was introduced into the active site by superposition on to **1.31c**, followed by deletion of the original inhibitor. Water molecules found in the original crystal structure were retained for the modeling studies. The active site was defined as all residues within 9 Å layer of the inhibitor. The active site was solvated with a 9 Å layer of water, which in turn was covered a 6 Å layer for a total of approximately 900 water molecules.

Energy Minimization In order to prepare the system for MD simulations, the system was first minimized. In order to remove unfavourable contacts, the minimization was performed in a stepwise fashion. In the first stage of minimization, all enzyme residues were kept fixed and the water molecules minimized to 1 kcal/Å convergence using 2500 iterations of steepest descents followed by 2500 steps of conjugate gradient to 0.1 kcal/Å. In the second stage, all water residues were fixed and the protein structure minimized by 2500 steps

of steepest descent to 1 kcal/Å followed by 5000 iterations of conjugate gradient to 0.1 kcal/Å. Finally, a third stage of minimization was performed where the entire system was minimized using 2500 steps of steepest descents to 1 kcal/Å followed by 5000 steps of conjugate gradient to a convergence of 0.1 kcal/Å.

Molecular Dynamics In order to perform the molecular dynamics simulations, the system was divided into three zones. In the first zone, all water molecules and enzyme residues within 6 Å of the inhibitor **1.34** were free to move. Residues and water molecules which fell between 6 and 9 Å of **1.34** had their backbone atoms and oxygen atoms respectively tethered with a force constant of 500 kcal/Å². All residues and water molecules located outside of the 9 Å radius were fixed in their minimized positions. The Verlet leapfrog algorithm was used with a 1 fs time step. The system was warmed slowly from 0 to 300 K and equilibrated for 20 ps and then continued for 100 ps for MD production. During the simulations, trajectories were recorded every 1 ps.

2.2.2 Organic Synthesis

2.2.2.1 Synthesis of Aryl DFMP Compounds

Diethyl difluoro(3-iodophenyl)methylphosphonate (2.11): To 3-iodobenzoic acid (13.14 g, 53 mmol, 1 equiv) in dry CH₂Cl₂ (200 mL) was added oxalyl chloride (13.87 mL, 20.18 g, 159 mmol, 3 equiv) and a catalytic drop of DMF. This reaction was stirred for 3 hrs at room temperature. The solvent and excess oxalyl chloride were removed under reduced pressure. The crude product was placed under high vacuum for 4 hrs. The resulting 3-iodobenzoyl chloride (4.92 g, 18.5 mmol, 1 equiv) was dissolved in dry toluene (9 mL).

Triethyl phosphite (3.20 mL, 3.07 g, 18.46 mmol, 1 equiv) was added. The solution was stirred at room temperature for 3 hrs. The solvent was removed *in vacuo* and the yellow oil was placed under high vacuum overnight. To this intermediate was added DAST (12.20 mL, 14.88 g, 92.3 mmol, 5 equiv) dropwise at $-78\text{ }^{\circ}\text{C}$. After swirling to ensure complete dissolution of the starting material, the reaction was stirred at $0\text{ }^{\circ}\text{C}$ for 2 hrs. The mixture was diluted with CHCl_3 (20 mL) and added to NaHCO_3 (17.06 g, 203.1 mmol, 11 equiv) in ice cold H_2O (40 mL). The crude reaction was extracted with CHCl_3 (3 x 50 mL), dried (MgSO_4), and concentrated leaving a yellow oil. Column chromatography (7:3 hexane/EtOAc, $R_f = 0.5$, followed by CH_2Cl_2 , $R_f = 0.3$) of the crude residue yielded **2.11** as a yellow oil (2.31 g, 40%): ^1H NMR (CDCl_3) δ 7.93 (1H, s), 7.82 (1H, d, $J = 8.8$ Hz), 7.58 (1H, d, $J = 7.3$ Hz), 7.20 (1H, m), 4.19 (4H, m), 1.31 (6H, t, $J = 7.4$ Hz); ^{19}F NMR (CDCl_3) δ -33.29 (d, $J_{\text{FP}} = 112.9$ Hz); ^{31}P NMR (CDCl_3) δ 3.70 (t, $J_{\text{PF}} = 114.5$ Hz); ^{13}C NMR (CDCl_3) δ 139.76, 135.14 (t), 129.98, 125.59 (t), 116.99 (dt, $J_{\text{CF}} = 263.5$ Hz, $J_{\text{CP}} = 218.7$ Hz), 64.79 (d), 16.20 (d); MS m/z (relative intensity) 253 (100), 390 (78), 109 (76); HRMS calcd for $\text{C}_{11}\text{H}_{14}\text{O}_3\text{F}_2\text{PI}$ 389.9693, found 389.9692.

1-(Bromomethyl)-4-iodobenzene (2.17): 4-Iodotoluene (0.750 g, 3.44 mmol, 1 equiv) and *N*-bromosuccinimide (0.612 g, 3.44 mmol, 1 equiv) were dissolved in CCl_4 (6 mL) and refluxed by exposure to an IR lamp for 3 hrs under an Ar atmosphere. The crude reaction was filtered to removed the succinimide precipitate and the filter cake washed with CCl_4 (3 x 18 mL). The solvent was removed *in vacuo* and the product isolated by flash chromatography on silica gel

(hexanes, $R_f = 0.5$) as a white solid (0.276 g, 27%): ^1H NMR (CDCl_3 300 MHz) δ 7.63 (2H, d, $J = 8.3$ Hz), 7.08 (2H, d, $J = 8.3$ Hz), 4.38 (2H, s); ^{13}C NMR (CDCl_3 300 MHz) δ 137.73, 137.17, 130.70, 94.16, 32.53; MS m/z (relative intensity) 217 (100), 90 (42), 89 (23); HRMS calcd for $\text{C}_7\text{H}_6\text{O}_3\text{Br}$ 295.8698, found 295.8703.

Diethyl (4-iodobenzyl)phosphonate (2.18): 1-(Bromomethyl)-4-iodobenzene (2.17) (2.29 g, 7.7 mmol, 1 equiv) was combined with triethyl phosphite (67 mL, 64 g, 38.5 mmol, 5 equiv) in benzene (70 mL). The reaction was refluxed for 12 hrs. The solvent and excess triethyl phosphite were removed under reduced pressure. The product was isolated as a pale yellow oil by flash chromatography on silica gel (EtOAc, $R_f = 0.4$) as a clear thick oil (2.51g, 92%). ^1H NMR (CDCl_3 300 MHz) δ 7.58 (2H, d, $J = 7.8$ Hz), 7.02 (2H, d, $J = 7.8$ Hz), 3.98 (4H, m), 3.05 (2H, d, $J = 22.0$ Hz), 1.24 (6H, t, $J = 6.8$ Hz); ^{31}P NMR (CDCl_3 300 MHz) δ 26.99; ^{13}C NMR (CDCl_3 300 MHz) δ 137.23 (d), 131.52 (d), 131.20 (d), 92.16, 61.96 (d), 32.92 (d, $J_{\text{CP}} = 137.9$ Hz), 16.21 (d); MS m/z (relative intensity) 354 (79), 326 (26), 217 (43), 109 (100), 89 (26); HRMS calcd for $\text{C}_{11}\text{H}_{16}\text{O}_3\text{PI}$ 353.9882, found 353.9893.

Diethyl difluoro(4-iodophenyl)methylphosphonate (2.25): A solution of 2.18 (2 g, 5.6 mmol, 1 equiv) in dry THF (12 mL) was cooled to -78 °C. NaHMDS (1 M in THF, 12.4 mL, 12.4 mmol, 2.2 equiv) was added dropwise over 5 min. The solution was stirred for 1 hr at -78 °C. A solution of NFSi (4.09 g, 13.0 mmol, 2.3 equiv) in dry THF (30 mL) was added dropwise and the reaction stirred at -78 °C for 3 hrs. The reaction was quenched with water (50 mL). The

organic solvent was removed under reduced pressure and the aqueous layer extracted with Et₂O (4 x 50 mL), dried (MgSO₄), and concentrated leaving a yellow oil. Column chromatography (CH₂Cl₂, R_f = 0.5) of the crude residue yielded **2.25** as a yellow oil (1.5 g, 68%): ¹H NMR (CDCl₃ 300 MHz) δ 7.81 (2H, t, J = 8.3 Hz), 7.34 (2H, d, J = 7.8 Hz), 4.21 (4H, m), 1.32 (6H, t, J = 7.3 Hz); ¹⁹F NMR (CDCl₃ 300 MHz) δ -33.53 (d, J_{FP} = 114.5 Hz); ³¹P NMR (CDCl₃ 300 MHz) δ 7.27 (t, J_{PF} = 115.2 Hz); ¹³C NMR (CDCl₃ 300 MHz) δ 137.51, 132.08 (br m), 127.80, 117.59 (dt, J_{CF} = 263.7 Hz, J_{CP} = 218.8 Hz), 97.50 (d, J = 2.5 Hz), 64.78 (d, J = 6.6 Hz), 16.20 (d, J = 5.6 Hz); MS *m/z* (relative intensity) 253 (100), 390 (51), 126 (44), 109 (53); HRMS calcd for C₁₁H₁₄O₃F₂PI 389.9693, found 389.9694.

Diethyl (3-iodobenzyl)phosphonate (2.22): 3-iodobenzyl bromide (2 g, 6.74 mmol, 1 equiv) and triethyl phosphite (5.84 mL, 5.6 g, 33.7 mmol, 5 equiv) were combined in benzene (6 mL). The reaction was refluxed for overnight. The solvent and excess triethyl phosphite was removed by distillation under reduced pressure (30 mm Hg, 70 °C). Column chromatography (EtOAc, R_f = 0.5) of the crude residue yielded **2.22** as a yellow oil (2.31 g, 97%): ¹H NMR (CDCl₃) δ 7.57 (2H, m), 7.25 (1H, d, J = 5.9 Hz), 7.00 (1H, t, J = 8.1 Hz), 4.00 (4H, m), 3.04 (2H, d, J = 21.9 Hz), 1.22 (6H, t, J = 7.4 Hz); ³¹P NMR (CDCl₃) δ 23.36; ¹³C NMR (CDCl₃) δ 138.64 (d), 135.89 (d), 134.22 (d), 130.02 (d), 129.00 (d), 94.05 (d), 62.13 (d), 33.36 (d, J_{CP} = 138.2 Hz), 16.27 (d); MS *m/z* (relative intensity) 354 (100), 217 (97), 227 (50); HRMS calcd for C₁₁H₁₆O₃PI 353.9882, found 353.9879.

Diethyl (3-bromobenzyl)phosphonate (2.23): To a solution of 3-bromobenzyl bromide (25.0 g, 100 mmol, 1 equiv) in benzene (80 mL) was added triethyl phosphite (85.7 mL, 83.1 g, 500 mmol, 5 equiv). The mixture was refluxed overnight. The solvent and excess triethyl phosphite was removed by distillation and **2.23** was obtained as a pure colourless oil by vacuum distillation (29.1 g, 95 %): bp 70 °C, 0.050 mm Hg; ^1H NMR (CDCl_3) δ 7.40 (2H, m, Ar-H), 7.21 (2H, m, Ar-H), 4.04 (4H, m, CH_2), 3.11 (2H, d, $J = 20.5$ Hz, CH_2), 1.26 (6H, t, $J = 7.3$ Hz, CH_3); ^{31}P NMR (CDCl_3) δ 23.28; ^{13}C NMR (CDCl_3) δ 134.31 (d), 132.71 (d), 129.83, 128.35 (d), 122.37, 62.06 (d), 33.55 (d, $J_{\text{CP}} = 139.1$ Hz), 16.18 (d); MS m/z (relative intensity) 109 (100), 169 (73), 306 (49); HRMS calcd for $\text{C}_{11}\text{H}_{16}\text{O}_3\text{PBr}$ 306.0020, found 306.0014.

Diethyl (4-bromobenzyl)phosphonate (2.24): **2.24** was prepared from 4-bromobenzyl bromide using the procedure described for **2.23**. Column chromatography (EtOAc, $R_f = 0.5$) of the crude residue yielded pure **2.24** as a colorless oil in 95% yield: ^1H NMR (CDCl_3) δ 7.43 (2H, d, $J = 8.1$ Hz), 7.17 (2H, t, $J = 8.1$ Hz), 4.00 (4H, m), 3.08 (2H, d, $J = 21.9$ Hz), 1.25 (6H, t, $J = 7.3$ Hz); ^{31}P NMR (CDCl_3) δ 23.19; ^{13}C NMR (CDCl_3) δ 131.56, 131.50, 131.47, 131.34, 130.88 (d), 120.81 (d), 62.10 (d), 33.27 (d, $J_{\text{CP}} = 138.2$ Hz), 16.29 (d); MS m/z (relative intensity) 169 (100), 109 (90), 306 (49); HRMS calcd for $\text{C}_{11}\text{H}_{16}\text{O}_3\text{PBr}$ 306.0020, found 306.0011.

Diethyl difluoro(3-bromophenyl)methylphosphonate (2.26): A solution of **2.23** (5.7 g, 18.6 mmol, 1 equiv) and NFSi (13.4 g, 43.0 mmol, 2.3 equiv) in dry THF (180 mL) was cooled to -78 °C. NaHMDS (1 M in THF, 41.0 mL, 41.0

mmol, 2.2 equiv) was added dropwise over 5 min. The solution was stirred for 1 hr at $-78\text{ }^{\circ}\text{C}$ for 1 h. The reaction was allowed to warm to room temperature and then quenched with water (250 mL). Solvent was removed under reduced pressure and the aqueous layer extracted with Et_2O (4 x 100 mL), dried (MgSO_4), and concentrated leaving a yellow oil. Column chromatography (CH_2Cl_2 , $R_f = 0.5$) of the crude residue yielded pure **2.26** as a yellow oil (4.95 g, 78%): ^1H NMR (CDCl_3) δ 7.74 (1H, s), 7.52 (2H, t, $J = 8.8$ Hz), 7.33 (1H, t, $J = 8.1$ Hz), 4.19 (4H, m), 1.32 (6H, t, $J = 7.3$ Hz); ^{19}F NMR (CDCl_3) δ -33.18 (d, $J_{\text{FP}} = 114.5$ Hz); ^{31}P NMR (CDCl_3) δ 3.68 (t, $J_{\text{PF}} = 113.7$ Hz); ^{13}C NMR (CDCl_3) δ 135.05 (br dt), 133.80, 129.90, 129.37 (br t), 124.99 (br t), 122.41, 117.20 (dt, $J_{\text{CF}} = 264.5$ Hz, $J_{\text{CP}} = 217.8$ Hz), 64.74 (d), 16.16 (d); MS m/z (relative intensity) 109 (100), 205 (54), 342 (25); HRMS calcd for $\text{C}_{11}\text{H}_{14}\text{O}_3\text{F}_2\text{PBr}$ 341.9832, found 341.9846.

Diethyl difluoro(4-bromophenyl)methylphosphonate (2.27): **2.27** was prepared from **2.24** in a same manner as described for **2.26**. Column chromatography (9.5:0.5 $\text{CH}_2\text{Cl}_2/\text{EtOAc}$) of the crude residue yielded pure **2.27** as a yellow oil in 80% yield: ^1H NMR (CDCl_3) δ 7.60 (2H, d, $J = 7.3$ Hz), 7.49 (2H, d, $J = 8.8$ Hz), 4.21 (4H, m), 1.33 (6H, t, $J = 7.4$ Hz); ^{19}F NMR (CDCl_3) δ -32.86 (d, $J_{\text{FP}} = 115.9$ Hz); ^{31}P NMR (CDCl_3) δ 3.58 (t, $J_{\text{PF}} = 115.2$ Hz); ^{13}C NMR (CDCl_3) δ 131.67, 127.96 (br t), 125.41, 117.72 (dt, $J_{\text{CF}} = 263.5$ Hz, $J_{\text{CP}} = 218.7$ Hz), 64.70 (d), 16.19 (d); MS m/z (relative intensity) 205 (100), 109 (71), 342 (39); HRMS calcd for $\text{C}_{11}\text{H}_{14}\text{O}_3\text{F}_2\text{PBr}$ 341.9832, found 341.9828.

Ethyl hydrogen [(3-bromophenyl)(difluoro)methyl]phosphonate (2.28): To a suspension of **2.26** (4.72g, 13.8 mmol, 1 equiv) in H_2O (36 mL) was

added a solution of NaOH (10 M, 2.3 mL, 23.4 mmol, 1.7 equiv). The reaction was stirred at 55 °C for 4 hrs until it became homogeneous. After cooling to room temperature, the crude reaction was washed with ether (2 x 50 mL). The aqueous layer was acidified to pH 0.5-1.0 with 6 M HCl, extracted with CH₂Cl₂ (4 x 100 mL), dried (MgSO₄) and concentrated to give pure **2.28** as a viscous pale yellow oil (4.08 g, 94%): mp 50 °C; ¹H NMR (CDCl₃) δ 10.86 (1H, s), 7.70 (1H, s), 7.62 (1H, d, *J* = 7.3 Hz), 7.50 (1H, d, *J* = 8.7 Hz), 7.33 (1H, t, *J* = 8.1 Hz), 4.16 (2H, m), 1.32 (3H, t, *J* = 7.3 Hz); ¹⁹F NMR (CDCl₃) δ -33.83 (d, *J*_{FP} = 119.1 Hz); ³¹P NMR (CDCl₃) δ 3.75 (t, *J*_{PF} = 118.3 Hz); ¹³C NMR (CDCl₃) δ 134.71 (br dt), 133.89, 129.90, 129.44 (br dt), 125.07 (br dt), 122.42, 116.84 (dt, *J*_{CF} = 262.6 Hz, *J*_{CP} = 224.2 Hz), 65.36 (d), 16.07 (d); MS *m/z* (relative intensity) 205 (100), 314 (37), 109 (20); HRMS calcd for C₉H₁₀O₃F₂PBr 313.9519, found 313.9517.

Ethyl hydrogen [(4-bromophenyl)(difluoro)methyl]phosphonate

(2.29): **2.29** was prepared from **2.27** in a same manner as described for **2.28**. Pure **2.29** was obtained without further purification as a viscous pale yellow oil in a 92% yield: mp. 58 °C; ¹H NMR (CDCl₃) δ 11.61 (1H, s), 7.58 (2H, d, *J* = 8.1 Hz), 7.42 (2H, d, *J* = 8.1 Hz), 4.12 (2H, m), 1.31 (3H, t, *J* = 7.0 Hz); ¹⁹F NMR (CDCl₃) δ -34.38 (d, *J*_{FP} = 119.0 Hz); ³¹P NMR (CDCl₃) δ 3.60 (t, *J*_{PF} = 119.8 Hz); ¹³C NMR (CDCl₃) δ 131.69, 128.03, 125.52, 117.42 (dt, *J*_{CF} = 262.6 Hz, *J*_{CP} = 224.7 Hz), 65.32 (d), 16.13 (d); MS *m/z* (relative intensity) 205 (100), 126 (37), 314 (26); HRMS calcd for C₉H₁₀O₃F₂PBr 313.9519, found 313.9523.

2.2.2.2 Synthesis and Functionalization of NCPS

Chloromethylated NCPS (2.32): Chloromethylated NCPS **2.32** was synthesized using a slightly modified procedure from that reported by Janda *et al.*⁹ VAZO (1.01 g, 4.14 mmol, 0.005 equiv) was added to a solution of styrene (95.45 mL, 86.76 g, 832.8 mmol, 1 equiv) and 4-vinylbenzyl chloride (3.62 mL, 3.92 g, 25.7 mmol, 0.03 equiv) in dry toluene (300 mL). The reaction was deoxygenated by sparging with Ar for 30 min followed by three freeze-pump-thaw cycles. The flask was fitted with a condenser and heated at 110 °C for 40 hrs. The solution was cooled to room temperature and added dropwise (via a separatory funnel) to 2 X 1.5 L of an ice cold solution of HCl in MeOH (10 mL of a 6 N solution in 1.5 L MeOH). The polymer was collected by filtration, washed with 600 mL of MeOH, and dried to give a white solid (79 g). ¹H NMR (CDCl₃): δ 7.5-6.3 (br d), 4.5 (br s), 2.2-1.2 (br d). The chlorine content was determined by NMR methods to be 0.3 mmol/g.

General Procedure for the Determination of Polymer Loading: The extent of polymer functionalization/loading was determined as follows. In the case of the chloromethyl polymer **2.32**, a standard plot was prepared. A series of solutions composed of varying proportions of 4-vinyl benzyl chloride and styrene were prepared ranging from 0.1 mmol Cl/g to 1 mmol/g. The ¹H NMR were recorded for each solution and the integration of the aromatic (Ar) and the benzyl chloride (CH₂-Cl) signals were noted. The ratio of integrations: [CH₂-Cl]/[Ar] was calculated and plotted as a function of mmol Cl/g to produce linear plot. The same ratio was calculated for the ¹H NMR of polymer **2.32**. The value of mmol Cl/g was then obtained by comparison to the standard plot.

Acetylated hydroxymethyl NCPS (2.36): To a solution of **2.32** (20 g, 6 mmol, 1 equiv) in DMF (250 mL) was added potassium acetate (0.94 g, 9.6 mmol, 1.6 equiv). This reaction was heated at 85 °C for 36 hrs. The reaction was cooled to room temperature and added dropwise (via a separatory funnel) to 2 X 1.5 L of an ice cold solution of HCl in MeOH (10 mL of a 6 N solution in 1.5 L MeOH). The product was isolated by vacuum filtration and washed thoroughly with water (2 X 100 mL) and MeOH (2 X 100 mL). The polymer was dried under hi-vacuum and obtained as a powdery white solid (20 g, 95%+ polymer recovery). No other polymer associated species were detected by ^1H NMR. ^1H NMR (CDCl_3): δ 7.4-6.3 (br d), 5.05 (br s), 2.4-1.2 (br d).

***p*-Hydroxymethyl NCPS (2.37):** To **2.36** (75 g, 22.5 mmol, 1 equiv) in THF (480 mL) was added aqueous NaOH (64 mL of a 10 N solution, 640 mmol, 28.4 equiv). The resulting gel like suspension was stirred at 75 °C for 24 hrs. The reaction was cooled and added dropwise (via a separatory funnel) to 2 X 2.0 L of an ice cold. The product was isolated by vacuum filtration and washed thoroughly with water (4 X 100 mL) and MeOH (4 X 100 mL). The polymer was dried under hi-vacuum and obtained as a powdery white solid (75 g, 95%+ polymer recovery). No other polymer associated species were detected by ^1H NMR. ^1H NMR (CDCl_3): δ 7.4-6.3 (br d), 4.60 (br s), 2.4-1.2 (br d).

Benzyl ethyl [(4-bromophenyl)(difluoro)methyl]phosphonate (2.44): **2.29** (1.16 g, 3.7 mmol, 1 equiv.) and triphenyl phosphine (1.46 g, 5.55 mmol, 1.5 equiv) were dissolved in dry THF (25 mL). DIAD (1.09 mL, 1.12 g, 5.55 mmol, 1.5 equiv) was added to the stirred mixture dropwise via syringe. A solution of

benzyl alcohol (575 μ L, 0.60 g, 5.55 mmol, 1.5 equiv) in dry THF (5 mL) was added to the reaction mixture dropwise via syringe and the reaction stirred at room temperature for 2 hrs. The solvent was removed by rotary evaporation and the desired product obtained by silica gel chromatography (9.5:0.5 CH₂Cl₂:EtOAc, R_f = 0.3) as a clear thick oil (0.92 g, 40%): ¹H NMR (CDCl₃) δ 7.48 (2H, d, *J* = 8.3 Hz), 7.39 (2H, d, *J* = 7.8 Hz), 7.24-7.32 (5H, m), 4.51 (2H, m), 4.05 (2H, m), 1.21 (3H, t, *J* = 6.8 Hz); ¹⁹F NMR (CDCl₃) δ -33.86 (d, *J*_{FP} = 117.2 Hz); ³¹P NMR (CDCl₃) δ 6.16 (t, *J*_{PF} = 117.6 Hz); ¹³C NMR (CDCl₃) δ 137.71, 131.44, 128.71 (t, *J* = 8.08 Hz), 128.26, 127.69, 127.57, 127.11, 125.14, 117.49 (dt, *J*_{CF} = 262.2 Hz, *J*_{CP} = 221.8 Hz), 71.78, 65.03 (d, *J* = 7.07 Hz), 16.03 (d, *J* = 5.6 Hz); MS *m/z* (relative intensity) 205 (100), 91 (87), 180 (61), 126 (34); HRMS calcd for C₁₆H₁₆O₃F₂PBr 403.9988, found 403.9995.

1-(2-Tetrahydropyranyloxy)butan-4-ol (2.47): 1,4-butanediol (42.10 mL, 476.0 mmol, 2 equiv) was combined with 3,4-dihydro-2*H*-pyran (21.7 mL, 238.0 mmol, 1 equiv) and a catalytic amount (1 drop) of concentrated HCl (12 M). The reaction was stirred overnight at room temperature. Solid K₂CO₃ was added to quench the reaction. The heterogeneous mixture was stirred for 5 min., diluted with Et₂O (150 mL), washed with brine (3 x 100 mL), dried (MgSO₄), and concentrated *in vacuo*. **2.47** was obtained as a pure colorless oil by vacuum distillation (24.2 g, 56%): bp 85 °C, 0.50 mm; ¹H NMR (CDCl₃) δ 4.61 (1H, s), 3.41-3.87 (6H, br m), 2.23 (1H, s), 1.55-1.81 (10H, br m); ¹³C NMR (CDCl₃) δ 98.78 (d), 67.32 (d), 62.34, 62.12 (d), 30.66, 29.76 (d), 26.48 (d), 25.45 (d),

19.49; MS m/z (relative intensity) 85 (100), 73 (72), 101 (30); HRMS calcd for $C_9H_{19}O_3$ 175.1334, found 175.1328.

1-(2-Tetrahydropyranyloxy)butan-4-ol functionalized NCPS (2.48): To a suspension of sodium hydride (0.48 g, 20 mmol, 5 equiv) in dry DMF (60 mL) was added **2.32** (3.5 g, 20 mmol, 5 equiv) and the mixture was stirred at 0 °C for 2 hrs. 3% chloromethylated non-crosslinked polystyrene (NCPS) (**2.32**) (10 g, 4 mmol, 1 equiv) and $n\text{-Bu}_4\text{NI}$ (0.148 g, 0.40 mmol, 0.10 equiv) were added and the mixture was stirred at room temperature for 12 hrs. The DMF was removed *in vacuo* and the resulting crude polymer was dissolved in CH_2Cl_2 (100 mL), washed with brine (3 x 50 mL), dried (MgSO_4), and concentrated *in vacuo*. The residue was redissolved in CH_2Cl_2 (60 mL) and added dropwise to a solution of cold $\text{H}_2\text{O}/\text{MeOH}$ (600 mL, 1:4). The precipitate was collected by filtration, washed with cold $\text{H}_2\text{O}/\text{MeOH}$ (150 mL, 1:4) and vacuum dried to give **2.48** as a white fluffy solid (9.7 g, 96% polymer recovered). No other polymer-bound species were detected by $^1\text{H-NMR}$. $^1\text{H NMR}$ (CDCl_3) δ 4.65 (1H, br s), 4.45 (2H, br s), 3.85 (2H, br s) 3.5 (4H, br s). Signals in the range of 7.3-6.2 and 2.3-1.2 overlap with that of the NCPS. Consequently, $^1\text{H-NMR}$ assignments were not attempted for any signals which fell in these two regions for this, or any subsequent polymer-bound species described below.

1,4-Butanediol functionalized NCPS (2.49): Polymer **2.48** (4 g, 1.2 mmol) was suspended in a mixture of THF:12 M HCl (30 mL, 4:1) to give a gel like suspension. This mixture was refluxed for 36 h. The reaction mixture was added to cold solution of $\text{H}_2\text{O}/\text{MeOH}$ (250 mL, 1:4). The resulting precipitate was

collected by filtration, washed with cold H₂O/MeOH (100 mL, 1:4), and dried under high vacuum to give polymer **2.49** as a white solid (3.9 g, 95% recovery of polymer): ¹H NMR (CDCl₃) δ 4.47 (2H, br s), 3.68 (2H, br s), 3.51 (2H, br s). The loading of the functionalized polymer was determined to be 0.3 mmole/g using NMR methods by using the general method described above.¹⁰

2.2.2.3 Synthesis of Library of Biaryl DFMP Compounds

Attachment of 2.28 and 2.29 to polymer 2.49 (2.50 and 2.51): To a solution of **2.28** or **2.29** (2 equiv), triphenyl phosphine (2 equiv) and DIAD (2 equiv) in dry THF (5 mL) was added a solution of polymer **2.49** (~ 1 equiv of free hydroxyl group) and triethylamine (5 equiv) in dry THF (25 mL). The mixture was stirred at room temperature for 4 hrs and then added dropwise to a solution of cold H₂O/MeOH (300 mL, 1:4) which resulted in the precipitation of the polymer. The precipitate was collected by filtration, dried under high vacuum which yielded polymer **2.50** or **2.51** as a white powder (96 % recovery of polymer): Polymer **2.50**: ¹H NMR (CDCl₃) δ 4.43 (2H, br s), 4.25 (4H, br m), 3.47 (2H, br s); ¹⁹F NMR (CDCl₃) δ -32.29 (d, *J*_{FP} = 112.9 Hz). Polymer **2.51**: ¹H NMR (CDCl₃) δ 4.45 (2H, br s, Ar-CH₂-O), 4.23 (4H, br m, CH₂-O-P), 3.49 (2H, br s, O-CH₂); ¹⁹F NMR (CDCl₃) δ -32.51 (d, *J*_{FP} = 116 Hz).

General Method for Suzuki Cross Coupling on polymers 2.50 and 2.51 (general structure 2.52 and 2.53): Polymers **2.50** or **2.51** (400-500 g, ~ 1 equiv polymer-bound aryl bromide), arylboronic acid (3 equiv), K₂CO₃ (3 equiv), H₂O (10 equiv), (C₆H₅CN)₂PdCl₂ (0.2 equiv) were placed in a round bottom flask flushed with argon, and dissolved in DMF (3 mL) that had been deoxygenated via

three freeze-pump-thaw cycles. A 400 μL aliquot of each reaction mixture was withdrawn and placed in an argon flushed NMR tube, which was attached to a 180° shaker. The reaction progress was monitored via ^{19}F NMR until 100% conversion was observed. A D_2O insert was used to obtain a lock signal. The reaction mixture was transferred to centrifuge tubes and centrifuged to remove the palladium catalyst. The supernatant was concentrated (3 mL), and added to a solution cold $\text{H}_2\text{O}/\text{MeOH}$ (30 mL, 1:4). The precipitated polymers of type **2.52** and **2.53** were collected by vacuum filtration. Percent recovery of **2.52** and **2.53** varied from 85-95%. Only a single polymer-bound species was evident by ^{19}F NMR. In general, the ^{19}F NMR chemical shift of polymers bearing the biaryl products differed by about 1-2 ppm from that of starting polymers **2.50** and **2.51**.

General method for cleaving the phosphonic acids from polymer 2.52 (2.60-2.73): To a solution of the polymer-bound biaryl derivatives of type **2.52** (~ 400-500 mg, ~1 equiv of polymer-bound phosphonate) in dry CH_2Cl_2 (3 mL) was added TMSI (4 equiv) or TMSBr (10 equiv). The reaction was stirred for 3 hrs (TMSI) or refluxed for 48 hrs (TMSBr). The crude reaction mixture was concentrated *in vacuo* and the residue was subjected to high vacuum for 6 hrs. The residue was dissolved in CH_2Cl_2 (2.5 mL) and added dropwise to a solution of $\text{H}_2\text{O}/\text{MeOH}$ (25 mL, 1:4) and stirred for 12 hrs. The suspension was filtered, and the filtrate was concentrated *in vacuo*. To remove trace amounts of polymer and other organic impurities, the following wash procedure was performed. The crude reaction product was dissolved in a NaOH solution (9 mL, 0.1 M solution) and washed with CH_2Cl_2 (3 x 8 mL). The solution was acidified to pH 0.5-1.0

with 5 N HCl, extracted into Et₂O (5 x 10 mL) and concentrated to give the phosphonic acid products. The phosphonic acids were dissolved in an aqueous solution (2 mL) containing NH₄HCO₃ (2.5 equiv). The solution was frozen and then lyophilized. The lyophilization procedure was repeated until a constant weight was obtained. This yielded the phosphonic acids as white to slightly off-white diammonium salts. See Table 2.2 for yields and purities.

(3-phenylphenyl)(difluoro)methylphosphonic acid, diammonium salt (2.60): Yield: 69.6 (mg/g); ¹H NMR (D₂O) δ 7.38-7.86 (9H, br m); ¹⁹F NMR (D₂O) δ -27.77 (d, *J*_{FP} = 93.1 Hz); ³¹P NMR (D₂O) δ 5.39 (t, *J*_{PF} = 93.9 Hz); ESMS *m/z* (relative intensity) 283 (100). HPLC retention time = 16.4 min. Purity: 97% (HPLC).

(3-(2'-naphthyl)phenyl)(difluoro)methylphosphonic acid (2.61): Yield: 85.2 (mg/g); ¹H NMR (D₂O) δ 7.56-8.27 (11H, br m); ¹⁹F NMR (D₂O) δ -27.90 (d, *J*_{FP} = 97.7 Hz); ³¹P NMR (D₂O) δ 5.32 (t, *J*_{PF} = 95.4 Hz); ESMS *m/z* (relative intensity) 333 (100). HPLC retention time = 17.3 min. Purity: 99% (HPLC).

(3-(4'-fluorophenyl)phenyl)(difluoro)methylphosphonic acid, diammonium salt (2.62): Yield: 75.8 (mg/g); ¹H NMR (D₂O) δ 7.45-7.80 (7H, br m), 7.15 (1H, t, *J* = 8.8 Hz); ¹⁹F NMR (D₂O) δ -27.72 (d, *J*_{FP} = 93.1 Hz), -37.51 (s); ³¹P NMR (D₂O) δ 5.49 (t, *J*_{PF} = 93.1 Hz); ESMS *m/z* (relative intensity) 301 (100). HPLC retention time = 16.4 min. Purity: 96% (HPLC).

(3-(4'-chlorophenyl)phenyl)(difluoro)methylphosphonic acid, diammonium salt (2.63): Yield: 76.2 (mg/g); ¹H NMR (D₂O) δ 7.26-7.74 (8H, br m); ¹⁹F NMR (D₂O) δ -28.95 (d, *J*_{FP} = 100.7 Hz); ³¹P NMR (D₂O) δ 4.86 (t, *J*_{PF} =

99.2 Hz); ESMS m/z (relative intensity) 317 (100). HPLC retention time = 16.9 min. Purity: 99% (HPLC).

(3-(4'-trifluoromethylphenyl)phenyl)(difluoro)methylphosphonic acid, diammonium salt (2.64): Yield: 49.9 (mg/g); ^1H NMR (D_2O) δ 7.58-7.84 (8H, br m); ^{19}F NMR (D_2O) δ 16.29 (s), -28.94 (d, $J_{\text{FP}} = 100.2$ Hz); ^{31}P NMR (D_2O) δ 4.88 (t, $J_{\text{PF}} = 99.2$ Hz); ESMS m/z (relative intensity) 351 (100). HPLC retention time = 17.5 min. Purity: 99% (HPLC).

(3-(4'-ethylphenyl)phenyl)(difluoro)methylphosphonic acid, diammonium salt (2.65): Yield: 74.9 (mg/g); ^1H NMR (D_2O) δ 7.11-7.85 (8H, br m), 2.45 (2H, unres m), 1.03 (3H, t, $J = 7.4$ Hz); ^{19}F NMR (D_2O) δ -28.41 (d, $J_{\text{FP}} = 99.2$ Hz); ^{31}P NMR (D_2O) δ 5.09 (t, $J_{\text{PF}} = 98.4$ Hz); ESMS m/z (relative intensity) 311 (100). HPLC retention time = 17.7 min. Purity: 99% (HPLC).

(3-(3'-chloro-4'-fluorophenyl)phenyl)(difluoro)methylphosphonic acid, diammonium salt (2.66): Yield: 83.5 (mg/g); ^1H NMR (D_2O) δ 7.22-7.74 (6H, br m), 7.18 (1H, t, $J = 8.8$ Hz); ^{19}F NMR (D_2O) δ -28.18 (d, $J_{\text{FP}} = 96.1$ Hz), -40.45 (s); ^{31}P NMR (D_2O) δ 5.22 (t, $J_{\text{PF}} = 94.6$ Hz); ESMS m/z (relative intensity) 335 (100). HPLC retention time = 17.0 min. Purity: 96% (HPLC).

(3-(4'-methylphenyl)phenyl)(difluoro)methylphosphonic acid, diammonium salt (2.67): Yield: 69.9 (mg/g); ^1H NMR (D_2O) δ 7.27-7.84 (8H, br m), 2.31 (3H, s); ^{19}F NMR (D_2O) δ -27.47 (d, $J_{\text{FP}} = 93.1$ Hz); ^{31}P NMR (D_2O) δ 5.54 (t, $J_{\text{PF}} = 92.4$ Hz); ESMS m/z (relative intensity) 297 (100). HPLC retention time = 16.8 min. Purity: 99% (HPLC).

(3-(3'-trifluoromethylphenyl)phenyl)(difluoro)methylphosphonic acid, diammonium salt (2.68): Yield: 78.9 (mg/g); ^1H NMR (D_2O) δ 7.50-7.98 (8H, br m); ^{19}F NMR (D_2O) δ 16.16 (s), -27.74 (d, $J_{\text{FP}} = 93.1$ Hz); ^{31}P NMR (D_2O) δ 5.39 (t, $J_{\text{PF}} = 93.1$ Hz); ESMS m/z (relative intensity) 351 (100). HPLC retention time = 17.4 min. Purity: 100% (HPLC).

(3-(4'-acetylphenyl)phenyl)(difluoro)methylphosphonic acid, diammonium salt (2.69): Yield: 67.3 (mg/g); ^1H NMR (D_2O) δ 7.46-7.80 (8H, br m), 2.45 (3H, s); ^{19}F NMR (D_2O) δ -29.43 (d, $J_{\text{FP}} = 102.3$ Hz); ^{31}P NMR (D_2O) δ 4.54 (t, $J_{\text{PF}} = 102.3$ Hz); ESMS m/z (relative intensity) 325 (100). HPLC retention time = 15.8 min. Purity: 80% (HPLC).

(3-(4'-tert-butylphenyl)phenyl)(difluoro)methylphosphonic acid, diammonium salt (2.70): Yield: 91.1(mg/g); ^1H NMR (D_2O) δ 7.58-7.85 (8H, br m), 1.29 (9H, s); ^{19}F NMR (D_2O) δ -29.41 (d, $J_{\text{FP}} = 102.2$ Hz); ^{31}P NMR (D_2O) δ 4.75 (t, $J_{\text{PF}} = 102.3$ Hz); ESMS m/z (relative intensity) 339 (100). HPLC retention time = 18.1 min. Purity: 99% (HPLC).

(3-(2'-methylphenyl)phenyl)(difluoro)methylphosphonic acid, diammonium salt (2.71): Yield: 70.9 (mg/g); ^1H NMR (D_2O) δ 7.41-7.68 (8H, br m.), 2.32 (3H, s); ^{19}F NMR (D_2O) δ -27.44 (d, $J_{\text{FP}} = 94.7$ Hz); ^{31}P NMR (D_2O) δ 5.39 (t, $J_{\text{PF}} = 93.9$ Hz); ESMS m/z (relative intensity) 297 (100). HPLC retention time = 16.8 min. Purity: 98% (HPLC).

(3-(3'-fluorophenyl)phenyl)(difluoro)methylphosphonic acid, diammonium salt (2.72): Yield: 66.7 (mg/g); ^1H NMR (D_2O) δ 7.83 (1H, s), 7.40-7.67 (6H, br m), 7.08 (1H, t, $J = 5.1$ Hz); ^{19}F NMR (D_2O) δ -27.78 (d, $J_{\text{FP}} =$

93.0 Hz), -35.24 (s); ^{31}P NMR (D_2O) δ 5.41 (t, $J_{\text{PF}} = 93.1$ Hz); ESMS m/z (relative intensity) 301 (100). HPLC retention time = 16.5 min. Purity: 98% (HPLC).

(3-(4'-biphenyl)phenyl)(difluoro)methylphosphonic acid, diammonium salt (2.73): Yield: 98.2 (mg/g); ^1H NMR (D_2O) δ 7.52-7.94 (13H, br m); ^{19}F NMR (D_2O) δ -27.84 (d, $J_{\text{FP}} = 94.6$ Hz); ^{31}P NMR (D_2O) δ 5.32 (t, $J_{\text{PF}} = 94.6$ Hz); ESMS m/z (relative intensity) 359 (100). HPLC retention time = 18.0 min. Purity: 91% (HPLC).

2.2.2.4 Synthesis of 1-hexanol functionalized NCPS

2-(5-hexenyloxy)tetrahydro-2H-pyran (2.89): To a mixture of 5-hexen-1-ol (2.88) (834 μL , 1 g, 10 mmol, 1 equiv) in 3,4-dihydro-2H-pyran (3.63 mL, 3.30 g, 40 mmol, 4 equiv) was added a drop of HCl (12 M). This reaction was stirred for 16 hrs at room temperature. The reaction was quenched by the addition of K_2CO_3 (1 g), and diluted with ether (50 mL). The organic phase was washed with 5% NaHCO_3 (2 X 25 mL), saturated brine (2 x 25 mL), and dried (MgSO_4). The solvent was removed under reduced pressure. The product was purified by distillation at a reduced pressure as a clear oil (1.40 g, 78%): bp 45 $^\circ\text{C}$, 10 mm Hg; ^1H NMR (CDCl_3) δ 5.80 (1H, m), 4.98 (2H, m), 4.58 (1H, s), 3.80 (2H, m), 3.40 (2H m), 2.05 (2H, m), 1.90-1.38 (10H, br m); ^{13}C (CDCl_3) δ 138.67, 114.25, 98.77, 67.31, 62.10, 33.44, 30.81, 29.26, 25.64, 25.58, 19.60. MS m/z (relative intensity) 101 (16), 85 (100), 83 (25), 67 (23), 55 (28); HRMS calcd for $\text{C}_{11}\text{H}_{20}\text{O}_2$ 185.1184, found 185.1184.

2-[6-(4-vinylphenyl)hexyl]oxytetrahydro-2H-pyran (2.91): Alkene (2.89) (300 mg, 1.6 mmol, 1 equiv) was dissolved in dry THF (0.75 mL) and cooled to 0 $^\circ\text{C}$.

A solution of 9-BBN (3.25 mL of a 0.5 M solution in THF, 1.6 mmol, 1 equiv) was added dropwise. The reaction was allowed to warm to room temperature and stirred for 6 hrs. K_2CO_3 (450 mg, 3.2 mmol, 2 equiv), $Pd(dppf)Cl_2$ (40 mg, 0.05 mmol, 0.03 equiv) were added to the reaction mixture. A solution of 4-bromostyrene (213 μ L, 298 mg, 1.6 mmol, 1 equiv) in dry DMF (5 mL) was added dropwise. The reaction was heated under an Ar atmosphere at 50 °C for 16 hrs. The reaction was cooled and diluted with benzene (25 mL) and water (25 mL). The organic layer was separated and the aqueous phase washed with benzene (2 X 25 mL). The combined organic extracts were washed with brine (2 X 25 mL) and dried ($MgSO_4$). Column chromatography (98:2 hexanes:EtOAc, $R_f = 0.2$) of the crude yielded **2.91** as a thick oil (154 mg, 54%): 1H NMR ($CDCl_3$) δ 7.30 (2H, t, $J = 8.8$ Hz), 7.13 (2H, d, $J = 7.3$ Hz), 6.70 (1H, dd, $J_1 = 11.8$ Hz, $J_2 = 17.5$ Hz), 5.70 (1H, d, $J = 17.6$ Hz), 5.18 (1H, d, $J = 10.2$ Hz), 4.56 (1H, s), 3.86-3.67 (2H, br m), 3.55-3.32 (2 H, br m), 2.59 (2H, t, $J = 7.3$ Hz), 1.82-1.21 (14H, br m); ^{13}C ($CDCl_3$) δ 142.51, 136.94, 135.34, 128.52, 126.19, 112.63, 98.84, 67.54, 62.18, 35.65, 31.21, 30.90, 29.79, 29.10, 26.20, 25.68, 19.71; MS m/z (relative intensity) 288 (22), 130 (32), 117 (91), 85 (100); HRMS calcd for $C_{19}H_{28}O_2$ 288.2086, found 288.2086.

THP protected hexanol functionalized polystyrene polymer (2.92):

Polymer **2.92** was prepared by copolymerization with styrene using conditions identical to prepare polymer **2.32**. 1H NMR ($CDCl_3$) δ 4.62 (1H, br s), 3.82 (2H, br m), 3.45 (2H, br m), 2.52 (2H, br m). Signals in the range of 7.3-6.2 and 2.3-1.2

overlap with that of the NCPS. Consequently, $^1\text{H-NMR}$ assignments were not attempted for any signals which fell in these two regions.

Removal of THP group from 2.92 (2.93): Polymer **2.92** was deprotected using the same procedure as for the THP protected polymer **2.48**. $^1\text{H NMR}$ (CDCl_3) δ 3.62 (2H br s), 2.52 (2H br m).

2.2.3 Inhibition Studies

Inhibition Assay of Compounds 2.60-2.73 with PTP1B: Rates of PTP1B catalyzed dephosphorylation in the presence or absence of inhibitors were determined using FDP as substrate in assay buffer containing 50 mM bis-Tris, 2 mM EDTA, 5 mM DTT, and 10 $\mu\text{g/mL}$ BSA at 25 $^\circ\text{C}$. Stock solutions of inhibitors were prepared in assay buffer and found to be stable under these conditions. Assays were carried out in 1 mL cuvettes with total volumes of 700 μL . Reactions were initiated by the addition of PTP1B (final concentration 0.15 $\mu\text{g/mL}$). Rates were obtained by monitoring the production of FMP for 20 min. At 405 nm using a Varian Cary 1 spectrophotometer. The rapid scans were performed in duplicate in the presence of inhibitors using FDP (20 μM) with 150 μM inhibitor at pH 6.5 and 2.5% DMSO.

2.2.4 Synthesis of Biphenyl Phosphine Ligand 2.99

1-(*N,N*-Dimethylamino)-1'-(dicyclohexylphosphino)biphenyl (2.99): Ligand **2.99** was prepared by following the procedure of Buchwald et al.⁴⁸ *N,N*-dimethylamino-2-bromoaniline was prepared by the procedure of Parham.¹¹ In brief, this consisted of suspending 2-bromo-aniline (1 equiv) in water (1 mL/g) and reacting it with dimethyl sulfate (1 equiv) until homogeneous. The reaction

was then neutralized with 25% KOH and additional dimethyl sulfate (1 equiv) was added and the suspension was once again stirred to homogeneity. The crude was made slightly basic with 25% KOH and a third portion of dimethyl sulfate was added and the reaction stirred for 3 hrs at room temperature before being extracted with Et₂O. The ¹H NMR was identical to that reported by Parham *et al.*

In order to prepare the ligand **2.99**, *N,N*-dimethylamino-2-bromoaniline (2 g, 10 mmol, 1.0 equiv) was dissolved in dry THF (10 mL) and cooled to -78°C. *n*-butyllithium (6.5 mL of a 1.6 M solution in hexanes, 10.4 mmol, 1.04 equiv) was added dropwise with stirring. This reaction was stirred at -78 °C for 2 hours and then diluted with an additional aliquot of dry THF (35 mL). In a separate flask, triisopropyl borate (4.6 mL, 3.74 g, 22.2 mmol, 2.22 equiv) was dissolved in dry THF (10 mL) and cooled to -78 °C. The aryl lithium suspension was added dropwise via syringe to the triisopropyl borate solution and the reaction stirred at -78 °C for 1 hr and then warmed to room temperature and stirred for 24 hours. Aqueous HCl (125 mL of a 1 M solution) was added and the reaction stirred for 15 min. The mixture was neutralized to pH 7 using 6 M NaOH and then extracted with 4 x 75 mL Et₂O. The combined organic extracts were concentrated to leave a thick brown oil. The boronic acid was further purified by dissolving it in ether (100 mL) and extracting with aqueous NaOH (3 x 50 mL of a 1 M solution). The combined aqueous extractions were adjusted to pH 7 with HCl (6 M), and then extracted with Et₂O (4 x 50 mL). The combined organic extracts were dried over MgSO₄ and concentrated to yield the crude 2-*N,N*-dimethylaminophenyl boronic acid (1.05 g) as a thick light brown oil. The product

was approximately 55% pure as judged by ^1H NMR. No further purification was performed.

The crude acid was dissolved in a degassed EtOH (2.5 mL) and added to a mixture of $\text{Pd}(\text{PPh}_3)_4$ (350 mg, 0.30 mmol, 10 mol%) and 2-bromoiodobenzene (2.05 g, 7.25 mmol, 2.1 equiv) in degassed DME (50 mL). A solution of Na_2CO_3 (3.07 g, 29 mmol, 8.4 equiv) in degassed water (15 mL) was added to the added to the reaction which was then refluxed for 48 hrs under an Ar atmosphere. The reaction was cooled and the biphasic mixture separated. The aqueous fraction was extracted with Et_2O (3 x 50 mL) and the combined organic fractions were washed with aqueous NaOH (2 x 20 mL). The organic fractions were then extracted with aqueous HCl (4 x 75 mL). The pH of the combined aqueous extracts was adjusted to pH 14 with aqueous NaOH (6 M) and extracted with ether (4 x 75 mL). The organic extracts were dried over MgSO_4 and concentrated and the product, 1-(*N,N*-dimethylamino)-1'-bromobiphenyl, purified by flash chromatography on silica gel (9:1 hexanes:EtOAc, $R_f = 0.3$) to give a white solid (657 mg, 68%): ^1H NMR (CDCl_3) δ 7.68 (1H, d, $J = \text{Hz}$), 6.94-7.38 (7H, m), 2.54 (6H, s).

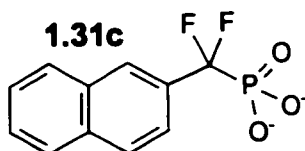
The 1-(*N,N*-dimethylamino)-1'-bromobiphenyl (657 mg, 2.38 mmol, 1 equiv) was dissolved in dry THF (60 mL) and cooled to -78°C . *n*-Butyllithium (1.64 mL of a 1.6 M solution in hexanes, 2.62 mmol, 1 equiv) was added dropwise with stirring. The reaction was stirred at -78°C for 1 hr after which a solution of chlorodicyclohexyl phosphine (776 mg, 3.33 mmol, 1.4 equiv) in dry THF (30 mL) was added dropwise. The reaction was stirred at -78°C for 1 hr,

and then allowed to warm to room temperature over 12 hrs. The reaction was quenched with saturated NH_4Cl (20 mL) and diluted with ether (20 mL). The biphasic mixture was separated and the aqueous portion extracted with ether (2 x 25 mL). The combined organic extracts were dried over Na_2SO_4 , and the solvent removed under reduced pressure. The desired product **2.99** was obtained by recrystallization in degassed, hot EtOH under an Ar atmosphere (487 mg, 52%): ^1H NMR (CDCl_3) δ 7.53 (1H, d, $J = 6.6$ Hz), 7.23-7.38 (4H, m), 7.03 (1H, m), 6.96 (3H, m), 2.42 (6H, s), 1.97-2.07 (1H, m), 1.40-1.85 (11H, m), 0.76-1.41 (10H, m); ^{31}P NMR (CDCl_3) δ -11.91.

2.3 Results and Discussion

2.3.1 Molecular Modeling of 1.34 Bound to PTP1B

Before we began synthesizing the biaryl compounds on NCPS, we first performed some molecular dynamics studies with **1.34** and PTP1B to better understand the mode of recognition of this inhibitor by the enzyme. Among the factors that determine the affinity of an enzyme for an inhibitor are the topographies of both the active site and the ligand. The overall binding event arises due to contributions of countless interactions at the atomic level between the solvent, protein and inhibitor. Though it is impossible to directly observe and measure such interactions at the atomic level, the use of computer modeling techniques does offer insight. Due to the interest in the target enzyme, there have been many modeling studies performed upon PTP1B and its mutants bound to both peptides and small molecules.^{12,13,14,15,16} Many of the previous studies have already established the role of crucial residues for substrate and/or inhibitor recognition within the PTP1B active site. Our goal was to identify which residues interacted with **1.34**, which serves as the parent compound for the biaryl series of inhibitors.



In order to perform our modeling studies, the crystal structure of **1.31c** complexed with PTP1B was used as a starting point due to similarity of **1.34** to **1.31c**. The system was prepared for modeling as described in Section 2.2.1. Equilibration was performed for 20 ps and MD simulation performed for 100 ps.

Within the 20 ps initialization period, the total energy and temperature for the system stabilized which was an indication that the system had reached equilibrium. This was reflected in the 100 ps MD production trajectory which lacked any significant fluctuations in total energy and temperature and is consistent with the time required for equilibration for PTP1B complexed with much larger ligands.¹² In order to verify the results of the 100 ps of MD production, an additional 100 ps was performed which demonstrated very little difference in the dynamic behaviour of the system. This indicated that 100 ps was a suitable time period for simulating the dynamic behaviour of our system.^{12,14} The calculations were also rendered more efficient by fixing and tethering portions of the enzyme remote from the active site in order to reduce the number of interactions that had to be calculated.¹⁷



Figure 2.1. 1.34 (Shown in red) docked with PTP1B. Y46, K120, F182, and C215 are shown as stick renderings coloured purple.

Figure 2.1 is a ribbon representation of PTP1B with inhibitor 1.34 (shown in red) docked in the active site. Some of the key residues involved in the binding of this inhibitor, Y46, K120, F182, and C215 are highlighted. Figure 2.2 shows a more detailed picture of 1.34 bound in the active site.

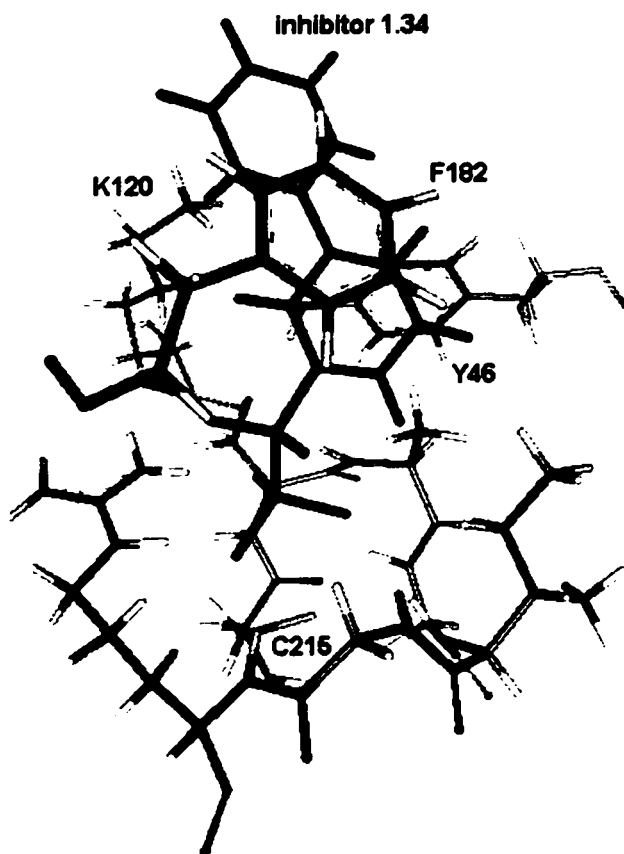


Figure 2.2. 1.34 docked into PTP1B active site.

Inhibitor 1.34 appears to bind to the enzyme in a manner similar to that described for 1.31c. The phosphonate oxygens interact with the backbone amides of residues 215-221 as well as the side chain of R221 via electrostatic attractions. The primary aryl ring of 1.34 is flanked by F182 and Y46 (Figure 2.1 and Figure 2.2) and the fluorine hydrogen bond between one of the fluorines and the N-H backbone amide of F182, described by Burke⁸ and Glover,¹² is also

evident. Hydrophobic interactions with the sidechains V49, A217, and I219 were not quite as evident as reported in other modeling studies.^{12, 13, 14} Due to the relatively small size and simple structure of 1.34, only slight changes were observed in both the structures of PTP1B and the bound inhibitor over the course of the simulation. 'Snapshots' recorded at 25, 50, 75, and 100 ps show little variation when superimposed (Figure 2.3).

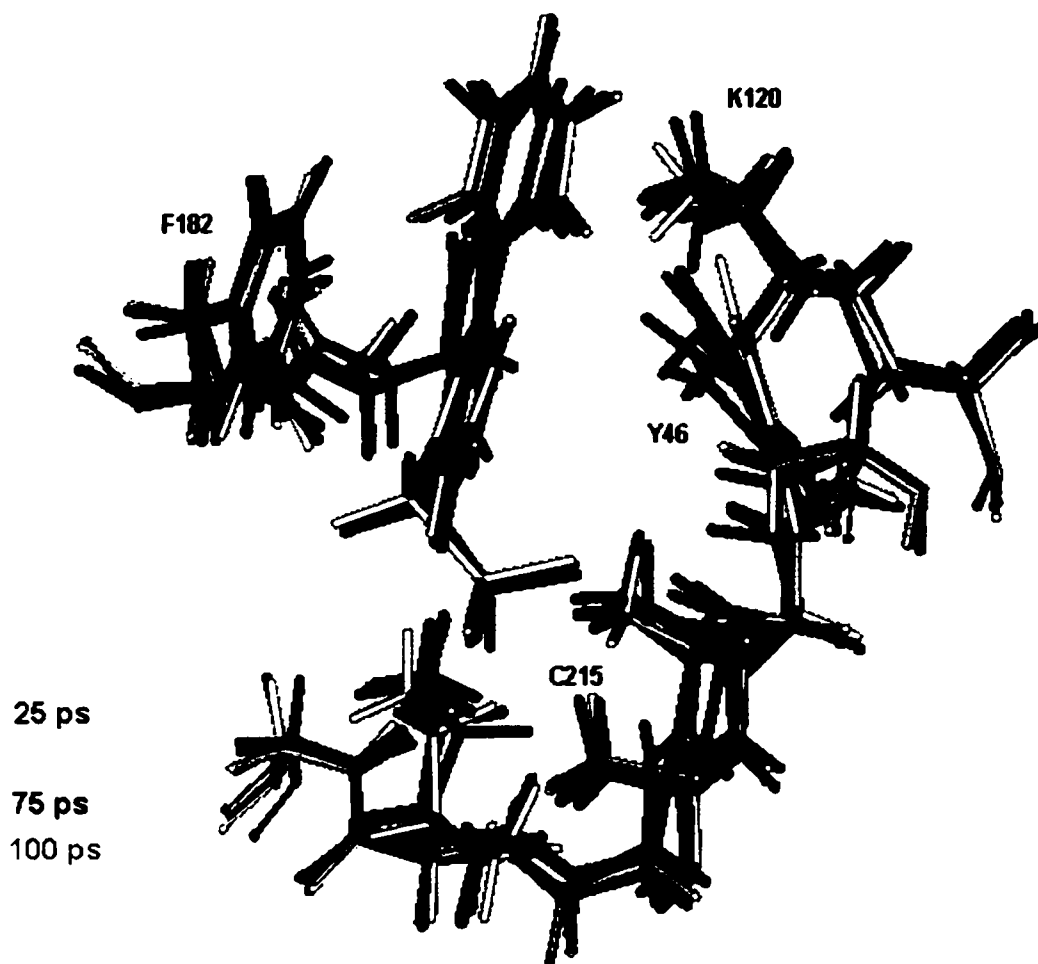


Figure 2.3. Overlay of PTP1B active site and 1.34 at 25, 50, 75, and 100 ps.

In order to identify key residue-inhibitor interactions, fluctuations in crucial distances were recorded as a function of time. We selected distances over

energy values since the latter are much more likely to change with the parameter set used whereas interatomic distances should be more uniform. Furthermore, it is generally agreed that the current generation of molecular forcefields offer calculated interaction energies which are best treated as qualitative indices of binding characteristics.¹⁸

Fortunately, the role of many of the key residues in the active site have been identified.^{12,14} In order to determine if these residues also played a role in binding **1.34**, several key distances were monitored as a function of time as outlined in Figure 2.4. These distances are (a) S atom of C215 to P atom of **1.34**, (b) pro-S fluorine to the N-H of the F182, (c) center to center distance of the aryl ring of F182 to the proximal (ie. proximal to the DFMP group) aryl ring of **1.34**, (d) center to center distance of the aryl ring of Y46 to the proximal aryl ring of **1.34**, (e) center to center distance of aryl ring of Y46 to the distal (distal to the DFMP group) aryl ring of **1.34**, and (f) the distance from the N atom of the K120 sidechain to the center of the distal aryl ring of **1.34**.

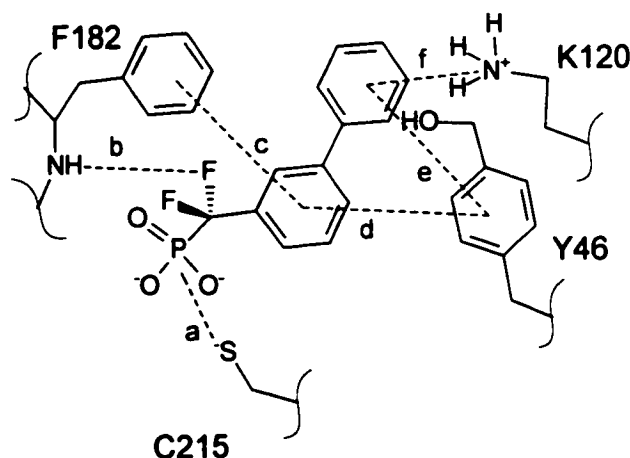


Figure 2.4. Distances monitored during MD run.

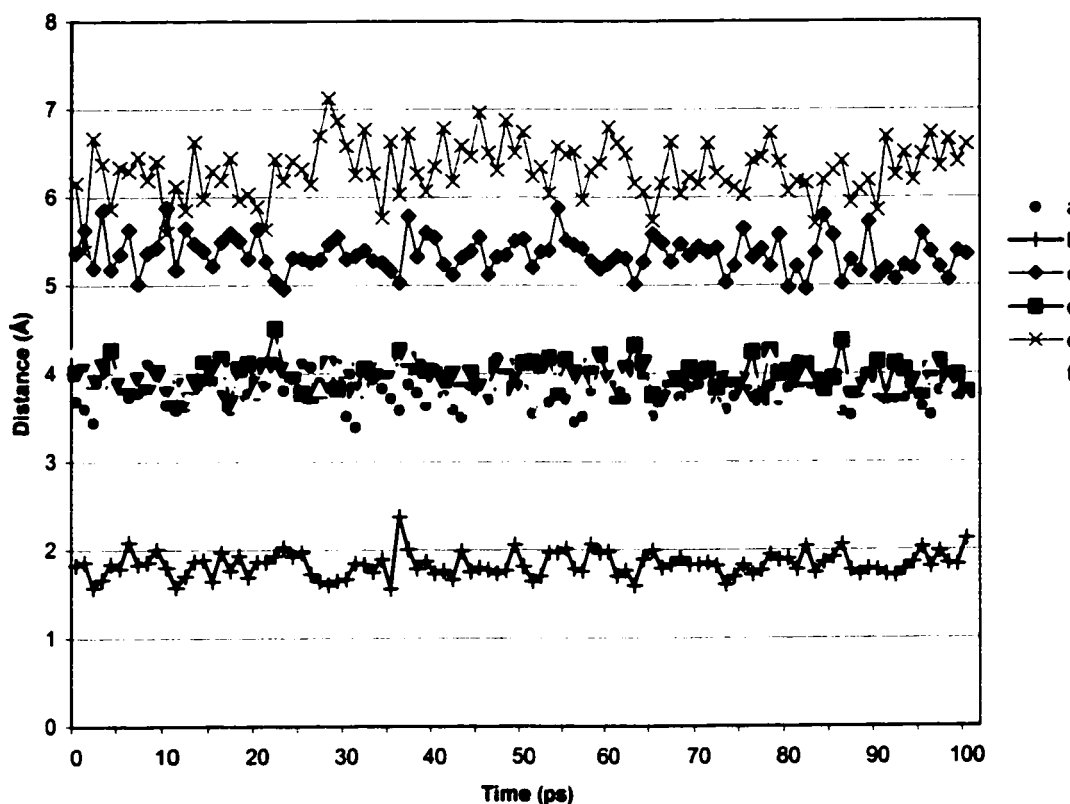


Figure 2.5. Fluctuations in distance over 100 ps for key 1.34-PTP1B interactions.

The results presented in graph of Figure 2.5 offer insight into how 1.34 is bound in the PTP1B active site. The distance between the P atom of 1.34 and the nucleophilic S atom of C215 fluctuated within 0.4 Å about an average value of 3.78 Å. The minor variations in this measurement reflect the strong electrostatic interactions between the phosphonate oxygens and the backbone amides of residues 215-221 and the R221 side chain guanidinium group. The unconventional H-bond originally reported by Burke between the backbone amide hydrogen of F182 and the pro-S α -fluorine atom was approximately 1.9 Å throughout the simulation which offers support for the direct interaction of at least

one of the fluorine atoms with PTP1B. The proximal aryl ring of **1.34** was found to interact more closely with the side chain of F182 than Y46 with average centroid to centroid distances of 4.0 and 5.3 Å respectively, both of which are in close enough contact for π stacking interactions. This same interaction was not as strong for Y46 to the distal aryl ring which showed large fluctuations over the 100 ps trajectory time and averaged \sim 6.3 Å. The distance of the N atom of K120 to the center of the phenyl ring of Y46 fluctuated slightly within 0.6 Å about an average value of 3.91 Å for the duration of the simulation. This distance approximates the typical distance for π -cation interactions (3.6-3.8 Å).¹⁹ More importantly, the lysine side chain presents a perpendicular face to the distal aryl ring which is an ideal geometry for such an interaction (Figure 2.6). This same type of interaction was also observed by Glover and coworker between K120 and the aryl ring of the F₂Pmp group of the DADE(F₂Pmp)L peptide inhibitor which they modeled.¹²

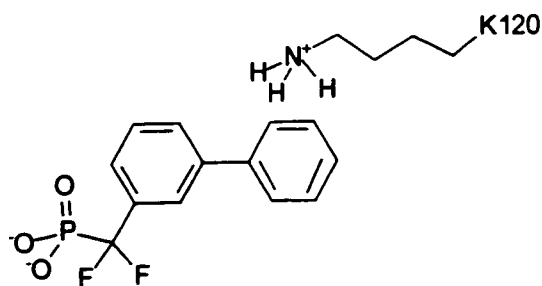


Figure 2.6. Interaction of K120 with distal aryl ring.

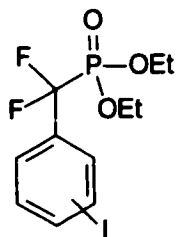
The enhanced potency of **1.34** over **1.31c** (K_i of 17 versus 179 μ M) may be attributed to the additional contacts possible with the more flexible and mobile distal aryl ring. This ring extends slightly further out from the active site and is able to rotate about the C-C bond to maximize additional interactions such as a

possible π -cation interaction with the side chain of K120. These additional interactions reinforce the strong attractive forces between the DFMP and proximal aryl groups of the inhibitor with PTP1B which are also present with **1.31c**. Similar π -cation interactions have been observed in other receptor ligand complexes such as the binding of phosphorylated tyrosine peptides with SH2 domain receptors.¹⁹ The results of these modeling studies strengthen the argument for constructing a biaryl series of inhibitors as a means of exploring what effects various substituents will have upon the inhibitory activity.

2.3.2 Synthesis of Benzylic DFMP Compounds

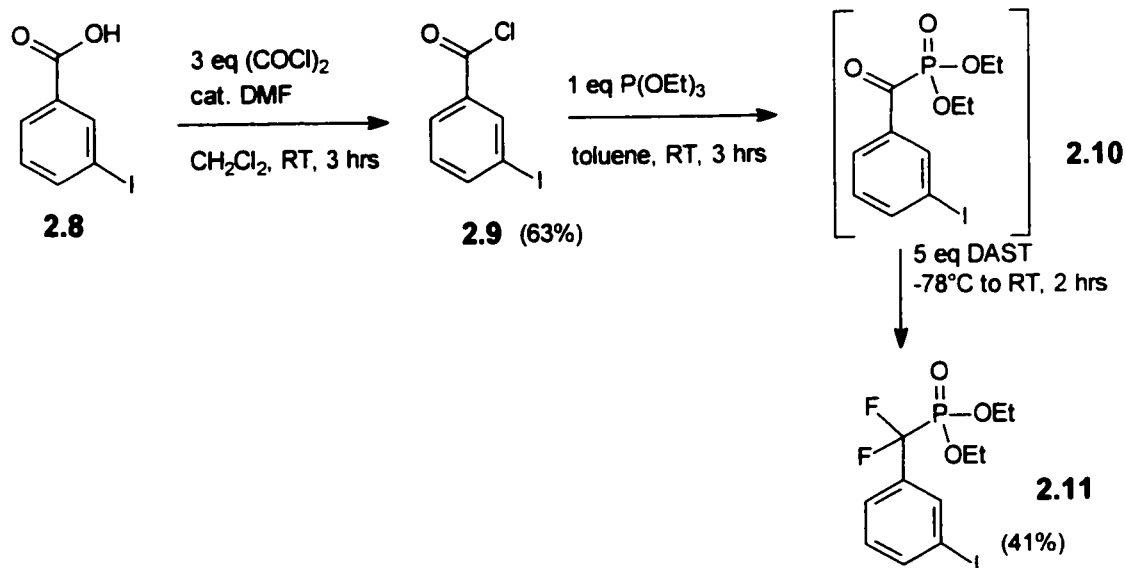
As can be seen in Scheme 2.1, construction of the library begins with the preparation of a benzylic DFMP of type **2.3**. Thus, an efficient and economical synthesis for this class of compound was required. Ideally, the substituent would be either an iodo or bromo group since the reactivity of aryl halides under Suzuki reaction conditions follows the general trend of $I > Br \approx OTf > Cl$.²⁰ There are three general approaches towards the synthesis of aryl DFMP's: (1) conversion of α -keto phosphonates to difluorophosphonates using diethylaminosulfur trifluoride (DAST), (2) coupling of aryl iodides with metallated $BrCF_2P(O)(OEt)_2$ reagents, and (3) electrophilic fluorination of benzyl phosphonates.

2.3.2.1 The DAST Approach



2.7

Since Suzuki couplings proceed more efficiently with aryl iodides, we focused our initial efforts on preparing compounds of type **2.7**. The DAST approach, as reported by Burke,²¹ appeared to be a viable approach towards obtaining the desired compounds. We examined this route with the *meta*-isomer since the starting material was commercially available. The synthesis began with 3-iodobenzoic acid (**2.8**) which was converted to the acid chloride **2.9** using oxalyl chloride/cat. DMF. The use of oxalyl chloride resulted in slightly lower yields (63%) than when thionyl chloride (78%) was employed, but was easier to remove, thus facilitating the purification of **2.9**. An Arbuzov reaction using triethyl phosphite resulted in the α -ketophosphonate intermediate which was not purified. Reaction of crude **2.10** with DAST initially at $-78\text{ }^{\circ}\text{C}$ followed by warming to room temperature gave the desired product **2.11** in a 41% yield.

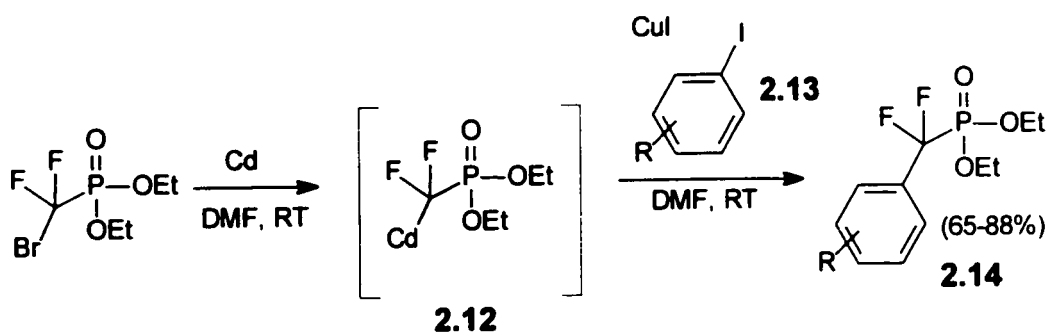


Scheme 2.2. DAST approach to the synthesis of **2.11**.

Although this approach worked, several factors detract from the DAST methodology. The overall yield (26%) of the final product was fairly low. Five equivalents of the expensive DAST reagent was required making this a costly procedure upon scale-up. More alarming was the fact that several groups have reported that the reaction can explode upon scale-up.²² For these reasons, alternative means of accessing the DFMP aryl halides were investigated.

2.3.2.2 Coupling of Aryl Iodides with Br(M)CF₂P(O)(OEt)₂

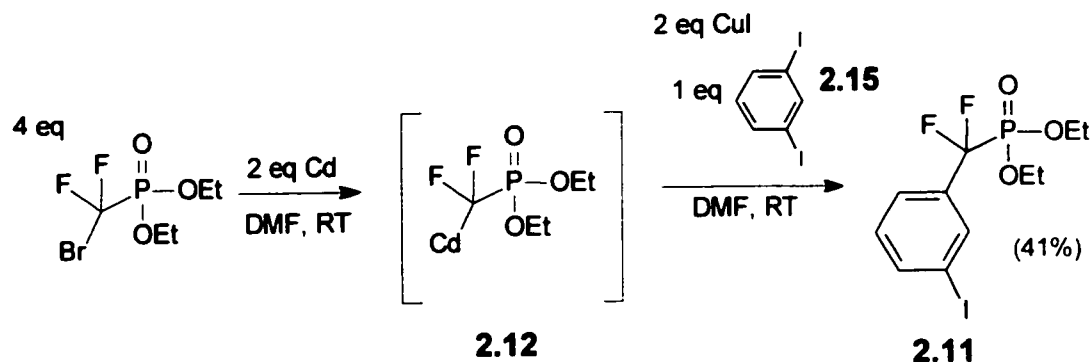
Burton and Qiu reported the preparation of aryl DFMP's by CuCl-promoted coupling of (diethylphosphonyl)difluoromethyl cadmium reagent to aryl iodides (Scheme 2.3).²³ In this procedure, the cadmate **2.12** is prepared by reaction of cadmium metal with the commercially available diethyl bromodifluoromethyl phosphonate. The metallated intermediate is reacted with an aryl iodide in the presence of copper (I) chloride to produce the desired benzylic phosphonate (**2.14**).



Scheme 2.3. Burton and Qiu's approach to the synthesis of aryl DFMP compounds.

The reaction tolerates a variety of functionalities on the aryl ring including nitro, bromo, and ester substituents with yields ranging from 65 to 88%. Shibuya *et al.* reported a similar reaction where zinc is used in the place of cadmium to

form a zincate intermediate which is then reacted with aryl iodides in the presence of copper (I) bromide.²⁴ Attempts at employing both the cadmium and zinc based procedures in our lab were met with very limited success (Scheme 2.4) when 1,3 diiodobenzene was coupled with **2.12**. The reactions suffered from several drawbacks: (1) need for 3 to 5 fold excess of the expensive diethyl bromodifluoromethyl phosphonate reagent, (2) difficulty in the purification of the final products, and (3) low yields (41%) which did not match figures reported by either Burton or Shibuya. Once again, a more efficient and economical method of generating compounds of type **2.11** was required.

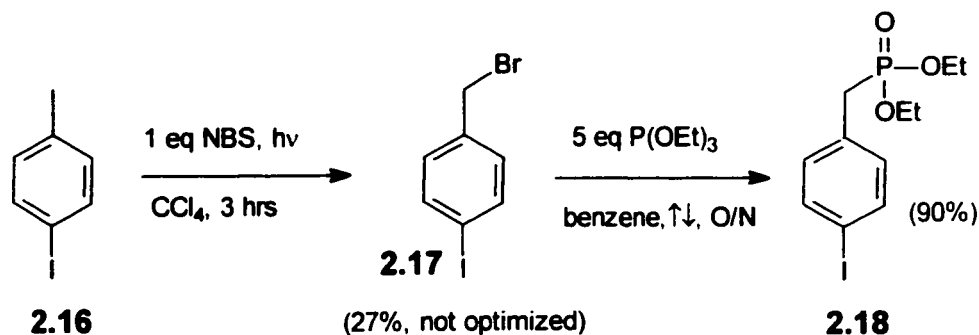


Scheme 2.4. Synthesis of **2.11** using Burton's cadmate procedure.

2.3.2.3 The Electrophilic Fluorination Approach

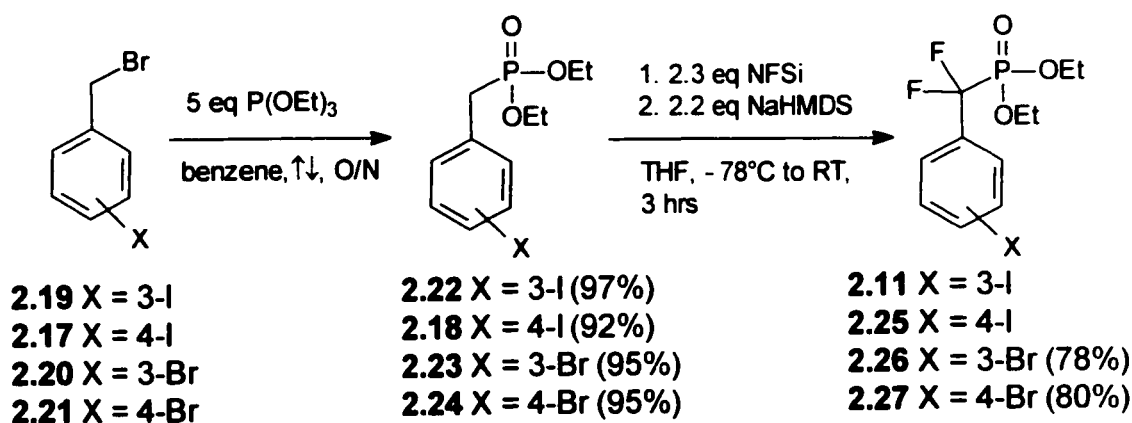
The electrophilic fluorination of benzylic phosphonates as developed within the Taylor group²⁵ was examined. This methodology involves reacting α -carbanions of benzylic phosphonates with N-fluorobenzenesulfonimide (NFSi), a source of electrophilic fluorine. Access to the benzylic phosphonates could be achieved using an Arbuzov reaction between triethyl phosphite and the appropriate benzylic halide. 3-iodobenzyl bromide is commercially available while the 4-iodo compound was prepared by bromination of 4-iodo toluene with

NBS to give 4-iodobenzyl bromide albeit in low yield (Scheme 2.5). The appropriate phosphonate precursors were prepared in excellent yield by an Arbuzov reaction.



Scheme 2.5. Synthesis of iodobenzyl phosphonate **2.18**.

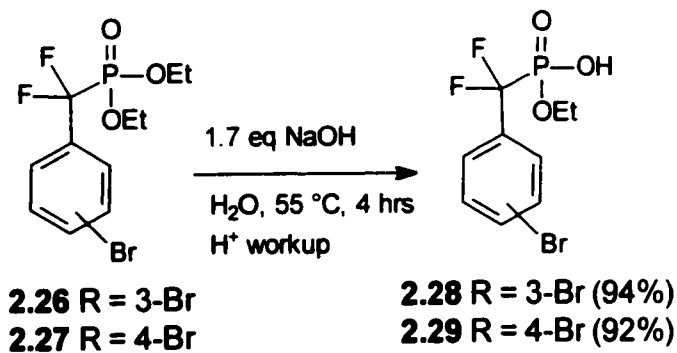
Fluorination of the phosphonates **2.18** and **2.22** was performed using the procedure developed in the Taylor group for the fluorination of benzylic phosphonates.²⁵ This involved reacting **2.18** and **2.22** with 2.1 equivalents of NaHMDS in the presence of 2.3 equivalents of NFSi at -78°C (Scheme 2.6).



Scheme 2.6. Preparation of benzylic phosphonates and DFMP compounds.

Though it was possible to synthesize the aryl iodides **2.11** and **2.25** by electrophilic fluorination, the ^{19}F -NMR revealed the presence of an inseparable contaminant which prevented the isolation of **2.11** and **2.25** in greater than 95%

purity. The impurity may be either an isomer where the position of the iodo group on the aryl ring is different from that of desired product arising from isomers present in the starting material (starting materials are only commercially available 93-97% pure) or may be the result of loss of the iodo group via metallation at the iodine position during the fluorination reaction followed by replacement by a hydrogen atom upon the aqueous work up. Consequently, we examined the aryl bromides for the fluorination reaction (Scheme 2.6). Phosphonates **2.23** and **2.24**, with aryl rings substituted at either the *meta* or *para* position, were prepared in near quantitative yields by an Arbuzov reaction between *para*- or *meta* benzyl bromide and triethyl phosphite. Unlike the aryl iodides, phosphonates, **2.23** and **2.24**, underwent the fluorination reactions quite cleanly and the desired products, **2.26** and **2.27**, were obtained in 78-80% yield. Despite the fact that the aryl iodides undergo the Suzuki reaction more readily, the easy access to the aryl bromides compounds made them a more attractive substrate when issues such as the availability, cost of starting materials and purity of the products were considered. As a result, the aryl bromides were chosen as the fundamental unit upon which the biaryl series of inhibitors were constructed.

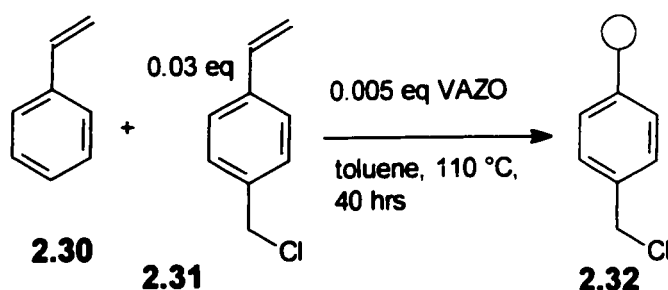


Scheme 2.7. Synthesis of monoacids **2.28** and **2.29**.

In order to prepare the phosphonates **2.26** and **2.27** for attachment to the NCPS support, the phosphonates were hydrolyzed in base then acidified to give phosphonic acids **2.28** and **2.29** (Scheme 2.7).

2.3.3 Synthesis of Chloromethylated NCPS

Functionalized NCPS is not commercially available, but can be easily prepared via free radical polymerization. The work reported by Janda *et al.* served as the basis for our polymer synthesis and functionalization.⁹ Synthesis of 3% chloromethylated NCPS was performed using a slightly modified procedure where VAZO²⁶ was employed as the initiator rather than AIBN (Scheme 2.8). The polymer was prepared by copolymerizing styrene with 0.03 equivalents of 4-vinyl benzyl chloride (**2.31**) with 0.005 equivalents of the free radical initiator VAZO in toluene at 110 °C for 40 hours. Purification of the polymer, and all subsequent polymer bound intermediates was a simple procedure of adding the polymer solution to a stirred 4:1 mixture of methanol and water. The polymer precipitated as a fluffy solid which could then be manipulated as would an insoluble polymer support. Isolation of the polymer was achieved by vacuum filtration followed by any necessary wash and rinse steps.



Scheme 2.8. Synthesis of 3% chloromethylated NCPS (**2.32**).

The functionalization of the polymer was kept low in order to ensure that the solubility properties of the polymer did not change upon covalent attachment of the aryl bromide. The Cl content, or loading capacity, of the polymer was evaluated by ^1H NMR methods. This required the preparation of a standardized curve correlating integration ratio to Cl content. In order to plot the curve, solutions of **2.30** and **2.31** ranging from 0.1 mmol/g Cl content to 1.0 mmol/g, were prepared and the ratio of the integration of $-\text{CH}_2\text{Cl}$ signals to the aromatic region were measured. This permitted the plot of integration ratio as a function of Cl content. Measurement of the same ratio in the synthesized polymer allowed us to conclude that our loading was approximately 0.3 mmol/g.

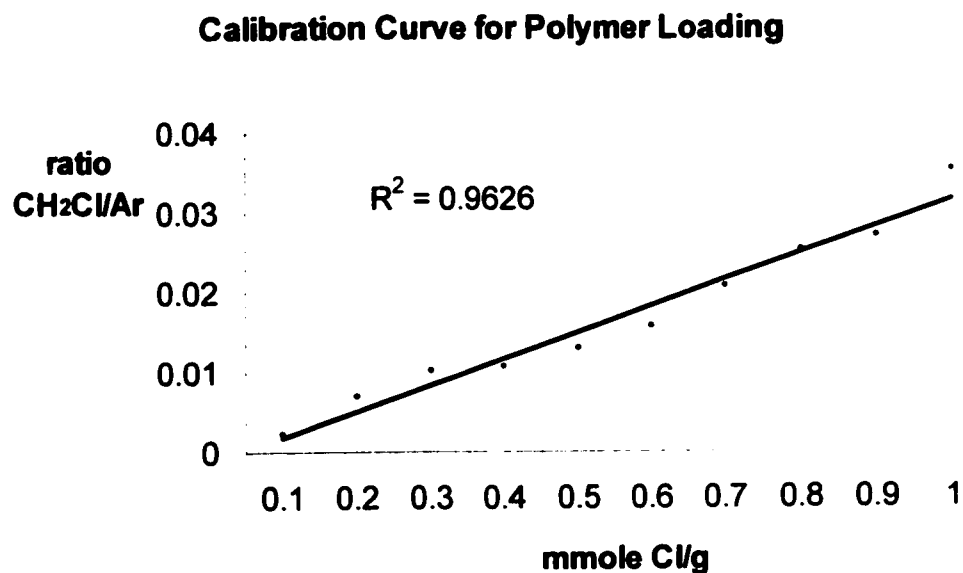
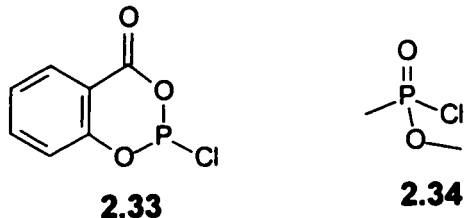


Figure 2.7 Calibration curve for determination of Cl content.

2.3.4 Attachment of Phosphonates to NCPS

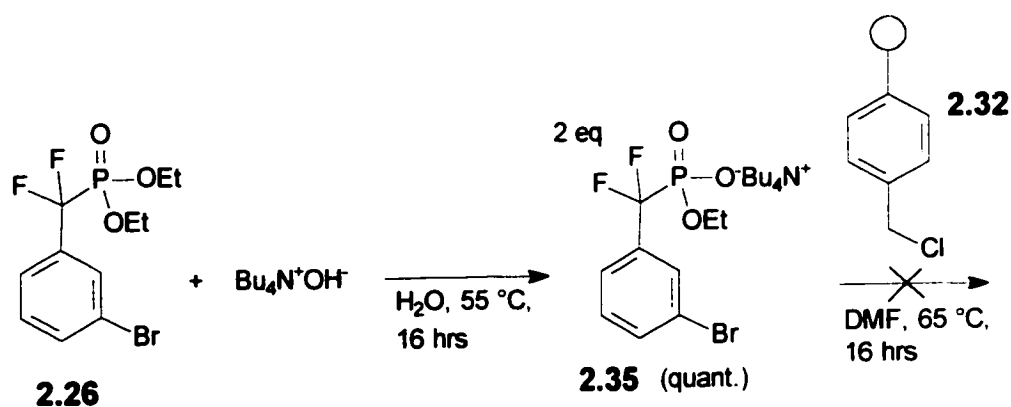
There are very few examples of the attachment and release of small molecules to and from a polymer support involving a phosphate or phosphonate

linkage.²⁷ Mjalli et al. employed Wang resin and attached a phosphate functionality by reaction with 2-chloro-4*H*-1,3,2-benzodioxaphosphorino-4-one (**2.33**) which was then hydrolyzed to the phosphate salt.²⁸ This route was obviously not compatible with the DFMP functionality. Nicolaou *et al.* attached a methyl phosphonate methyl ester to a support by reacting the acid chloride **2.34** with an alcohol functionalized polymer.²⁹ These two reports serve as the only precedents where either a phosphate or phosphonate ester bond was used to attach a small molecule to a polymer support. Neither strategy addressed the issue of simultaneous product cleavage and deprotection. It was essential to our strategy that the conditions used to form the linkage be compatible with the DFMP functionality and that the linkage be stable enough to withstand our reaction conditions yet labile under the deprotection conditions.



Our initial efforts to attach the phosphonates to NCPS involved first converting them to their tetrabutyl ammonium salts and then reacting these with the chloromethylated NCPS. However, attempts to react 2 equivalents of **2.35** with the chloromethylated polymer **2.32** in DMF at 65 °C for 18 hours (Scheme 2.9) were not successful. The ¹⁹F NMR showed multiple signals in addition to the expected bound and unbound substrates. ¹H NMR revealed that the reaction did not go to completion as indicated by the presence of both the –CH₂Cl and –CH₂-O-P peaks which differ by 0.4-0.5 ppm. The excess tetrabutyl ammonium salt

also posed a problem since it was difficult to separate from the polymer. It was possible that although the coupling did proceed quantitatively, the use of the elevated temperatures hydrolyzed the resulting benzylic phosphonate ester linkage due to the presence of residual water in the DMF solvent and base. As a result, the peaks observed in the ^1H NMR were possibly due to the CH_2OH signals which overlap with the CH_2Cl peaks.³⁰

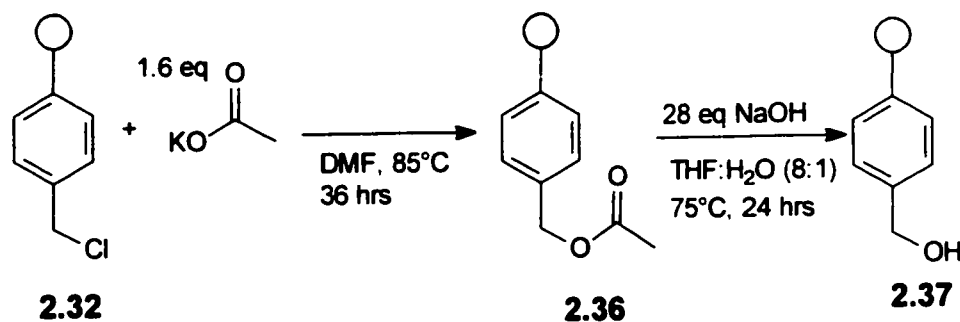


Scheme 2.9. Attempt to attach **2.26** to 3% chloromethylated NCPS using the tetrabutyl ammonium salt.

Two alternatives remained for attachment of the aryl bromides **2.26** and **2.27** to NCPS. The first possibility was the converse of Scheme 2.9 in that the phosphonic acids would be converted to the corresponding acid chlorides and then reacted with hydroxymethylated polymer as Nicolaou *et al.* reported. An alternative was to use the procedure of Campbell *et al.* who employed Mitsunobu conditions to construct peptidyl phosphonates on a solid support by reacting phosphonic acids with polymer-bound alcohols.³¹ This approach was attractive since it avoided the extra step of forming the acid chloride.

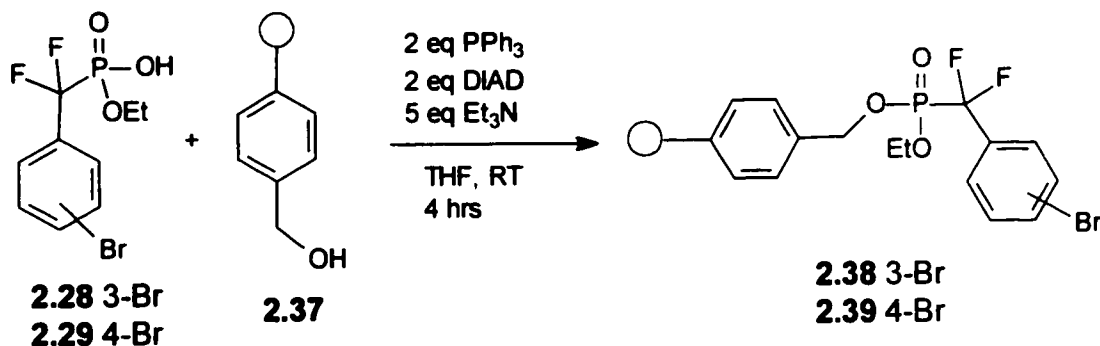
Initial efforts to replace the chloromethyl group on the NCPS with an hydroxymethyl functionality consisted of reacting **2.32** with an excess of NaOH in

a THF/water solvent system. However, due to the similarity in the $-\text{CH}_2\text{-Cl}$ and $-\text{CH}_2\text{-OH}$ chemical shifts, we were unable to ascertain whether or not the reaction went to completion, or even if it proceeded at all. To circumvent this problem, we converted **2.32** to ester **2.36** using 1.6 equivalents of potassium acetate in DMF at 85 °C for 36 hours (Scheme 2.10). The chemical shifts of the $-\text{CH}_2\text{-Cl}$ and $-\text{CH}_2\text{-OAc}$ signals differ by 0.5 ppm and allowed for the verification of complete conversion to the acetylated hydroxymethyl polymer. Initial attempts to convert the ester to the free alcohol employed LiAlH_4 to reduce the ester. The precipitation and purification of the polymer was hampered by the presence of the aluminum salts. Hydrolysis of the ester functionalized polymer proved to be a more efficient route. The addition of 28 equivalents of NaOH as a 10 M aqueous solution to a solution of polymer in THF resulted in a gel like suspension which was heated at 75 °C for 24 hours. Upon cooling and precipitation of the polymer in methanol, ^1H NMR indicated that the complete removal of the acetate group had occurred to result in the hydroxymethyl polymer **2.37**. Polymer recovery was typically greater than 96% for these modification reactions.



Scheme 2.10. Conversion of chloromethylated NCPS to hydroxymethyl NCPS.

In Campbell's solid phase Mitsunobu reactions,³¹ the coupling was found to proceed more readily using tris(4-chlorophenyl) phosphine instead of triphenyl phosphine, which is usually used for solution phase Mitsunobu couplings. We viewed the use of tris(4-chlorophenyl) phosphine as a drawback due to its cost. Since our reactions were being performed on a soluble polymer under homogeneous conditions, we felt that the original solution phase conditions,^{32,33} which employed triphenylphosphine, would suffice for quantitative coupling of all free hydroxyl sites. This was indeed the case as we found that complete loading could be achieved, as verified by ¹H NMR, by adding a solution of the polymer **2.37** and 5 equivalents of triethyl amine to a mixture composed of 2 equivalents of each of the phosphonic acid **2.28** or **2.29**, triphenyl phosphine and DIAD (Scheme 2.11) and stirring at room temperature for 4 hours.



Scheme 2.11. Mitsunobu coupling of phosphonic acids **2.28** and **2.29** to polymer **2.37**.

The order of addition and combination of the reagents was found to be crucial for quantitative loading of the phosphonic acids. Deviation from the described procedure resulted in incomplete polymer loading. Purification was achieved by adding the crude reaction mixture to a 4:1 methanol/water solution followed by filtration. ¹H and ¹⁹F NMR indicated that no other polymer bound

species were present. During the course of the loading, the polymer was consistently recovered in yields exceeding 97%.

2.3.5 Room Temperature Suzuki Couplings

We first attempted to couple phenyl boronic acid to polymer-bound phosphonates **2.38** and **2.39** using classic Suzuki conditions^{34,35,36,37} which involved heating these reactants in the presence of a base and Pd catalyst. Although the coupling took place, a considerable amount of hydrolysis of the phosphonate from the polymer occurred as indicated in the ¹H NMR. In order to minimize the problem of hydrolysis, we decided to use room temperature Suzuki coupling conditions.

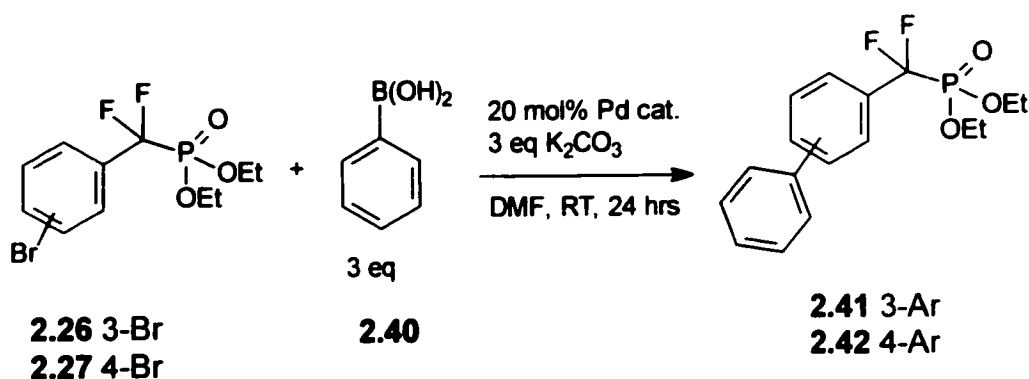
Two criteria which we wished to adhere to for the room temperature Suzuki reaction were: (1) for the reaction to proceed cleanly without the formation of by-products originating from the DFMP bearing substrates (ie. avoid the production of DFMP bearing side-products) and (2) for the reaction to proceed to completion. These requirements were selected to ensure that when conducted upon the polymer bound aryl bromides, the Suzuki reaction would yield exclusively the desired intermediates thus ensuring the purity of the final products. The task of developing the reaction conditions was made slightly more challenging since we opted to employ the more readily accessible aryl bromides **2.38** and **2.39**, rather than the more reactive iodo compounds.

At the time we began these studies there were already numerous reports of the Suzuki reaction performed upon insoluble polymer supports, but these reactions were all performed at elevated temperatures and usually on aryl

iodides.^{34,35,38,39,40} There were also numerous examples of solution phase Suzuki reactions performed upon aryl bromides at elevated temperatures.²⁰ However, at the time that we began our studies, there were only a handful of examples of room temperature Suzuki reactions in solution. There were no examples of room temperature Suzuki cross coupling being performed upon polymer bound aryl bromides. It became evident that we would have to develop our own unique conditions based upon the available precedents.

At the time we began our studies, three reports describing room temperature Suzuki couplings on aryl bromides had appeared in the literature. Anderson and coworkers had performed such couplings using 5 mol% Pd(PPh₃)₄, TlOH in DMA or DMF.^{41,42} The use of Tl(OH), an expensive and toxic compound, was a reagent we wished to avoid. Most interestingly, Campi *et al.* had shown that room temperature Suzuki couplings could be accomplished using 5 mol% Pd(OAc)₂, aqueous Na₂CO₃ or solid Ba(OH)₂ in degassed ethanol.⁴³ Unfortunately, NCPS is insoluble in ethanol. Thus, we began our studies by using a combination of the Anderson and Campi procedures using Pd(OAc)₂ as catalyst but conducting the reaction in DMF, a polar aprotic solvent in which NCPS is soluble. Aryl bromides **2.26** and/or **2.27** and phenyl boronic acid were used as model reactants (Scheme 2.12). The reactions were followed by ¹⁹F NMR where an approximately 0.75 ppm shift between the aryl bromide and the biaryl product could be observed. After some experimentation, we found that we could get this reaction to proceed to 92% completion within 24 hours at room temperature by increasing the amount of catalyst to 20 mol% and using 3

equivalents of phenyl boronic acid and potassium carbonate as base (Scheme 2.12).



Scheme 2.12. Model Suzuki reaction.

Although the reaction worked, the catalyst loading was quite high. In an attempt to find more efficient catalysts, several commercially available palladium catalysts were screened starting at 20 mol% loading. Though this catalyst loading was not ideal, we focused upon identifying effective catalysts first and optimizing catalyst loading at a later stage. As presented in Table 2.1, $Pd(PhCN)_2Cl_2$ and $PdCl_2$ were the most effective followed by $Pd(OAc)_2$ and $Pd_2(dba)_3$. A common trait shared by these three reagents is the absence of strong coordinating phosphine ligands.

In an effort to increase the lifetime of the catalyst, the effect of adding various coordinating phosphine ligands, such as PPh_3 and dppe, was studied with the most active Pd catalysts from Table 2.1. The rationale was that in prolonging the life of the catalyst, by preventing its conversion to Pd black, we would be able to increase the turnover number and thus lower the amount of catalyst required for the reaction. However, none of the catalyst/ligand combinations were able to match or surpass the efficiency of the $Pd(PhCN)_2Cl_2$

or PdCl₂ system. Since Pd(PhCN)₂Cl₂ was less expensive than PdCl₂, all subsequent studies were carried out using Pd(PhCN)₂Cl₂.

Table 2.1. Evaluation of Pd catalysts for the Suzuki coupling

Catalyst	% Conversion after 24 hours ^c
Pd(OAc) ₂	92
PdCl ₂ ^b	100
Pd(PhCN) ₂ Cl ₂	100
Pd ₂ (dba) ₃	92
Pd(dppf)Cl ₂	80
Pd(dppe) ₂ Cl ₂ ^b	48
Pd(dppe) ₂ ^b	39
Pd(PPh ₃) ₄	38
Pd(PPh ₃) ₂ Cl ₂	7
Pd(PEt ₃) ₂ Cl ₂	6
Pd(acac) ^b	3

^a1 equiv **2.30/2.31**, 3 equiv. PhB(OH)₂, 3 equiv. K₂CO₃, 20 mol% catalyst in DMF for 24 hrs at room temperature. ^bDetermined by Justyna Grzyb
^cPercent conversion of **2.47/2.48** into biaryl product after 24 hrs as determined by ¹⁹F NMR.

A serendipitous event led us to investigate the rate enhancing effects of water upon the rate of the Pd(PhCN)₂Cl₂ reaction. It was found that the inclusion of minute amounts of water enhanced the rate of the reaction. A possible role of the water is to quaternize the boronic acid to enhance its reactivity in the transmetalation step. It was found that by adding in 10 equivalents of water, the model reactions were complete within 18 hours. This amount was found to be sufficient to accelerate the reaction in model studies using **2.26** and **2.27** but low enough as to avoid precipitation of the polymer when **2.38** and **2.39** were used. The Suzuki reactions were characterized by fairly rapid conversion in the early stages which slowed dramatically as the reaction progressed as well as the

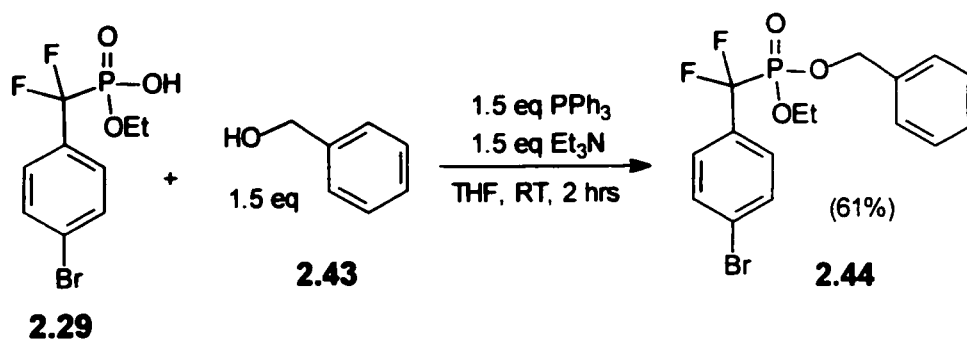
formation of Pd black precipitate. Decreasing the catalyst loading to below 20 mol% resulted in incomplete conversion after 24 hours as did reducing the amount of boronic acid from 3 equivalents.

Further studies by Justyna Grzyb, an undergraduate and later an M.Sc. student in the Taylor group, with the Pd(PhCN)₂Cl₂/H₂O system, indicated that other solvents that are compatible with NCPS (benzene, toluene, THF, DME) were less effective than DMF and organic bases, such as Et₃N, were less effective than K₂CO₃. The final Suzuki reaction conditions which we utilized for the preparation of the library employed 1 equivalent of the polymer bound aryl bromide, 3 equivalents of boronic acid and K₂CO₃ in the presence of 20 mol% Pd(PhCN)₂Cl₂ and 10 equivalents of water in DMF for the Suzuki reaction on the polymer.

2.3.6 Attaching a Linker Chain to Polymer 2.32

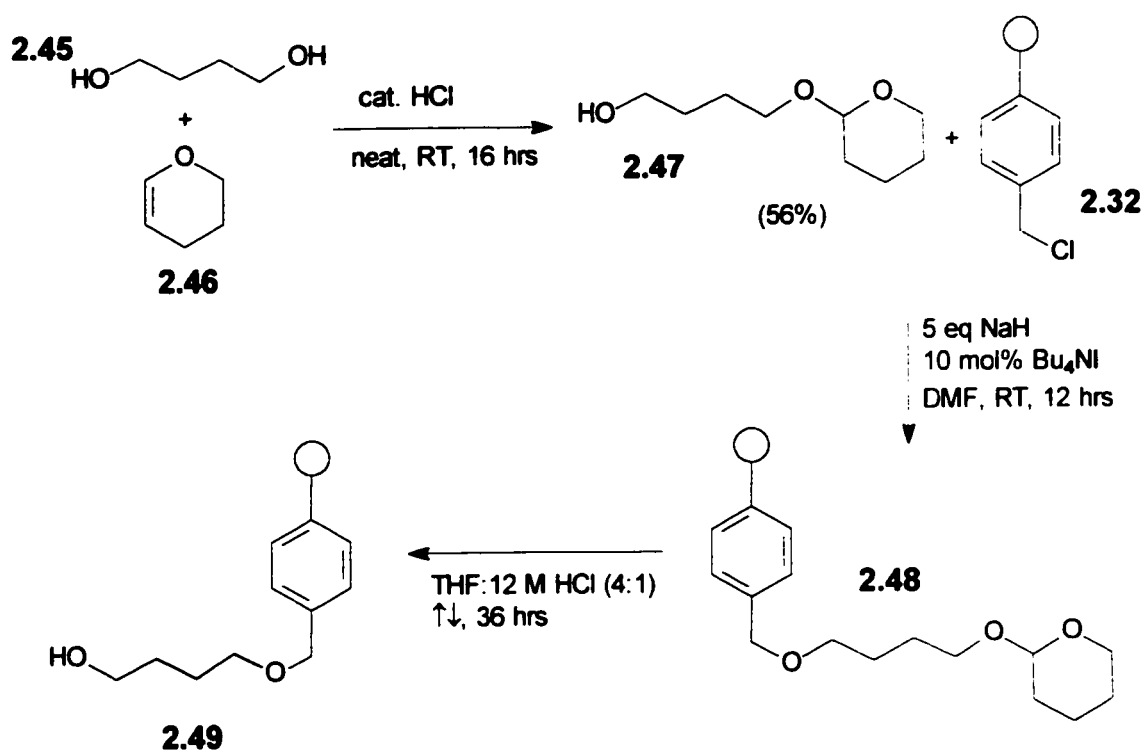
Our room temperature Suzuki reaction conditions were examined using polymer bound phosphonate **2.38**. To our dismay, we still observed some hydrolysis (by ¹H NMR) even under these mild reaction conditions. Since this was not a problem with phosphonates **2.26** and **2.27**, studied in solution above, we concluded that the benzyl ester linkage of the phosphonate to the polymer was more susceptible to hydrolysis than the ethyl esters of the model phosphonates **2.26** and **2.27**. In order to verify this, **2.44** was synthesized as seen in Scheme 2.13 and subjected to our Suzuki reaction conditions. The extent of hydrolysis was determined to be approximately 40% over a 24 hour period as determined by ¹⁹F NMR when **2.44** was subjected to our Suzuki

coupling conditions. In order to avoid the hydrolysis problem, it was necessary to substitute the benzylic ester linkage with a more stable bond.



Scheme 2.13. Synthesis of benzyl phosphonate ester **2.44**.

We chose to replace the benzylic phosphonate ester linkage by introducing a 1,4-butanediol linker arm on to the NCPS support. Nicolaou and coworkers have attached 1,4-butanediol to Merrifield resin using NaH/ⁿBu₄NI in DMF.²⁹ We chose not to use this approach since we were concerned that some cross-linking, between chloromethyl sites, would take place which would alter the solubility properties of the polymer and result in the loss of sites to which the phosphonic acid may be attached. We therefore chose to protect one alcohol moiety of the diol as a THP ether (**2.47**) by reaction with 0.5 equivalent of 3,4-dihydro-2*H*-pyran in the presence of a catalytic amount of HCl. The remaining free alcohol was reacted with polymer **2.32** in the presence of 5 equivalents of sodium hydride and 10 mol% tetrabutyl ammonium iodide in DMF at room temperature. The THP protecting group of **2.48** was removed under reflux conditions in a 4:1 THF:12 M HCl solvent system to yield the desired polymer **2.49** (Scheme 2.14).



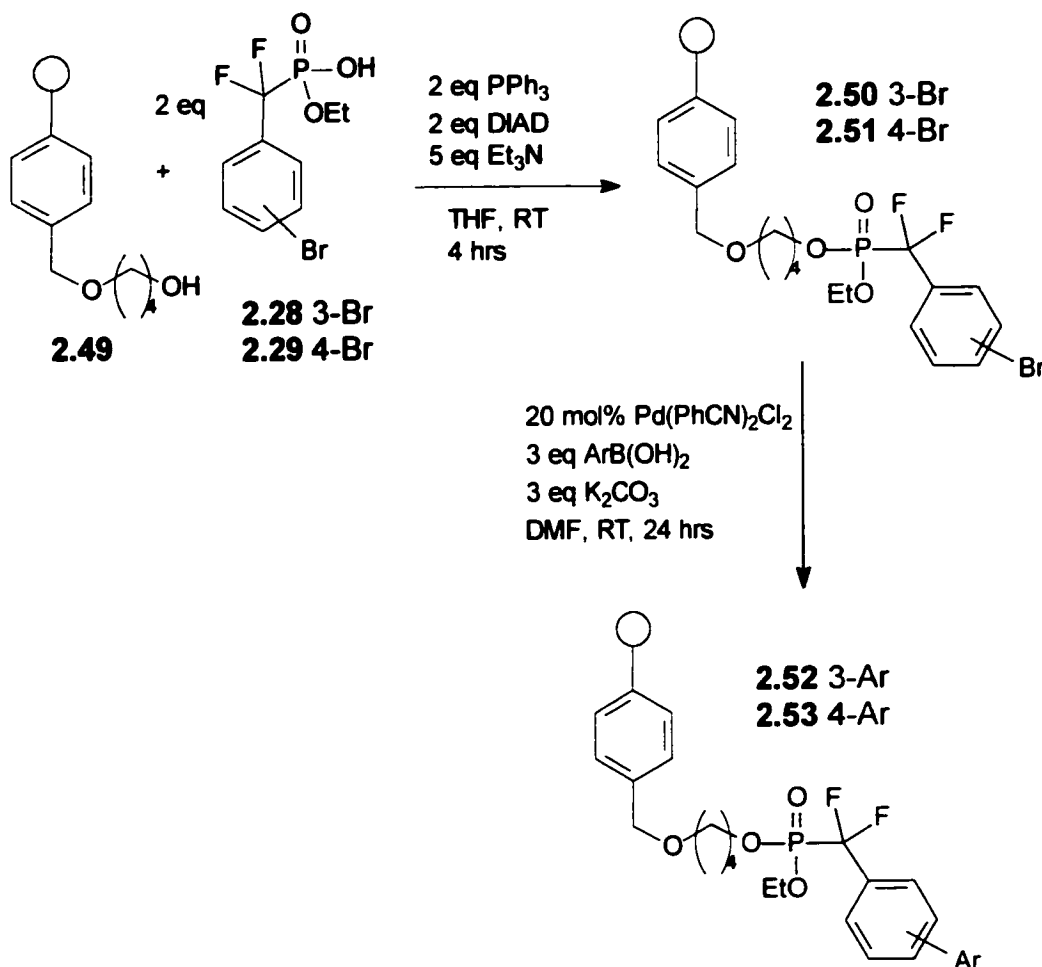
Scheme 2.14. Functionalization of NCPS with 1,4-butanediol linker.

The introduction of the 1,4-butanediol linker arm did not alter the solubility properties of the bulk polymer. The loading capacity of polymer 2.49 could be determined by NMR methods by preparing a calibration curve in a manner analogous to polymer 2.32. It was hoped that the linker arm would not only provide a stronger phosphonate ester linkage, but also improve the accessibility of the reactant by distancing the aryl bromide away from the hydrophobic polymer backbone. Recovery of the polymer in each functionalization step was always greater than 97%.

2.3.7 Reaction Sequence for Library Synthesis

Polymer 2.49 was loaded with both the *meta* and *para* bromo phosphonic acids 2.28 and 2.29 in separate batch reactions utilizing the same Mitsunobu

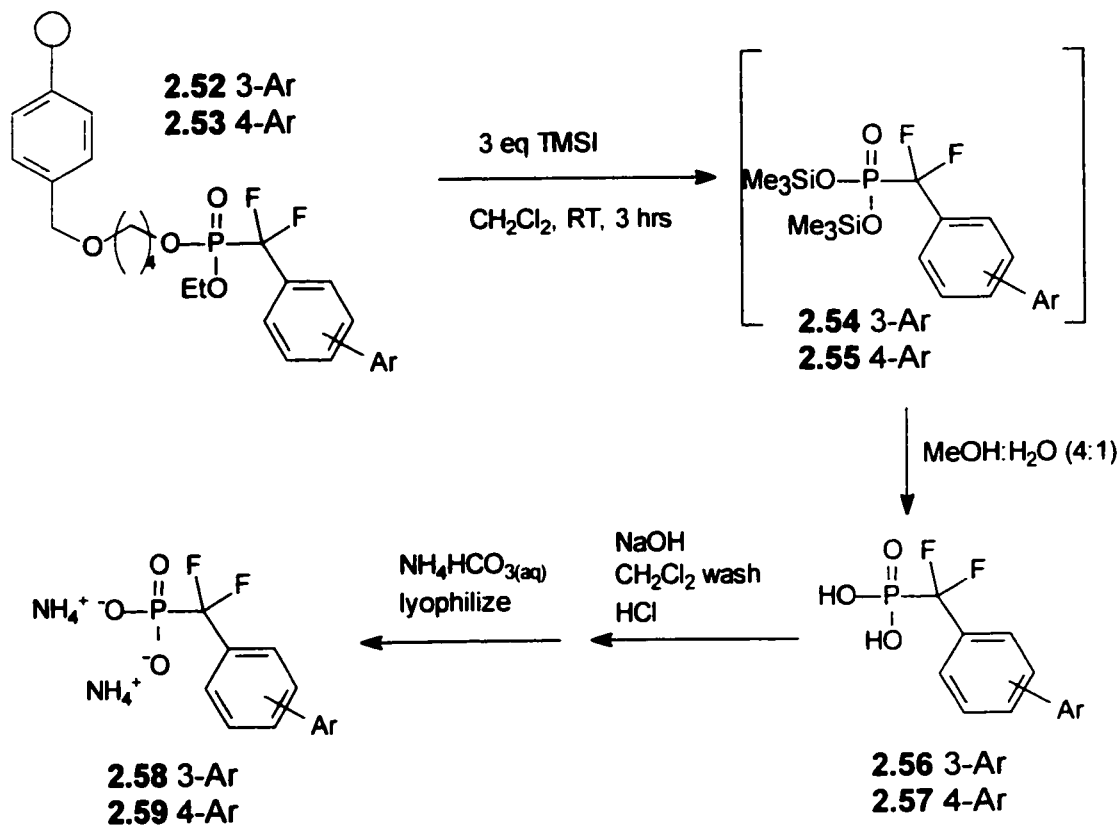
conditions developed for polymer **2.37**, to give the polymer bound aryl bromides **2.50** and **2.51** as seen in Scheme 2.15. No differences in reactivity were observable between the alkyl and benzyl alcohol groups of **2.49** and **2.37** respectively. A Suzuki reaction was performed on **2.50** and **2.51** using our room temperature conditions and phenyl boronic acid. No hydrolysis from the support was detected (by ^1H and ^{19}F NMR). This chemistry was therefore expanded using the *meta*-substituted aryl bromide **2.50** and 13 other commercially available boronic acids to give a "meta library" of 14 polymer-bound biaryls. Completion of each reaction was verified by ^{19}F -NMR. Aryl boronic acids which bore electron withdrawing substituents such as CF_3 , and acetyl groups exhibited faster reaction rates than those bearing electron donating groups. All of the coupling reactions were complete within 24 hours. No systematic study was conducted to better characterize the trends observed in the relative reaction rates. The Pd black precipitate was removed by centrifugation and the polymer bound intermediates purified by precipitation of the crude reaction into a methanol:water solution followed by filtration. ^1H and ^{19}F NMR indicated that no other polymer bound species were present. On the smaller scale of the individual Suzuki couplings, the loss of polymer material due to transfer errors was inevitable and recoveries ranged from 80 to 95%. As a result, even though we were able to achieve complete conversion of the aryl bromides to the biaryl products, the loss of polymer meant a less than quantitative yield. We were never able to consistently obtain 97-99% recovery of polymer, which is what Janda and coworkers reported for their prostanoid syntheses.⁹



Scheme 2.15. Mitsunobu and Suzuki couplings on NCPS.

The final step for synthesizing the library was cleavage of the biaryl DFMP compounds from the support and deprotection of the ethyl group as shown in Scheme 2.16. The use of 4 equivalents of iodo trimethylsilane (TMSI) at room temperature over 3 hours resulted in simultaneous cleavage and deprotection of the phosphonate ester. The crude reactions were precipitated and stirred in a 4:1 methanol:water solution in order to hydrolyze the silyl ester intermediates to the

free acids. The polymer was removed by filtration, and the products collected in the filtrate and then concentrated. However, NMR analysis revealed that, in addition to cleaving the ester bonds, the ether linkage between the polymer and linker arm was also cleaved.



Scheme 2.16. Cleavage and deprotection of phosphonic acids from the support.

We attempted to minimize this problem using TMSBr, a milder reagent (10 equivalents, reflux, 2 days), however, ether cleavage still occurred. The slight traces of polymer and linker chain cleavage byproducts that did remain were removed by addition of an aqueous sodium hydroxide solution to the crude product, followed by washing the aqueous solution with dichloromethane, acidification of the aqueous layer to less than pH 1 and then extraction of the

phosphonic acid products into diethyl ether which was then concentrated. The phosphonic acids were dissolved in an aqueous ammonium bicarbonate solution and lyophilized. The lyophilization was repeated until a constant weight was obtained. This yielded a series of *meta* biaryl phosphonic acids as their ammonium salts (2.60-2.73). The analogous "para library" (2.74-2.87) was prepared in an identical manner by Justyna Grzyb. The yields of the products ranged from 46 to 89%. The range of yields may have been due to the final extraction step into ether since the solubility of these compounds in ether varies dramatically from compound to compound. All of the compounds were characterized by ^1H , ^{31}P , and ^{19}F NMR. HPLC was also used to determine purity. Of the twenty-eight compounds obtained, twenty-two were obtained in 95% purity or better and only three compounds were less than 90% pure. All of the compounds could be assayed against PTP1B without the need for further purification. It is interesting to note that the purity obtained by HPLC did not always coincide with that obtained by ^{19}F -NMR. HPLC is often used as the sole means of determining the purity of compounds obtained by PSOS. Our results underscore the importance of using other methods in addition to HPLC to determine purity.

Table 2.2 Yields and Purities of *meta* Compounds 2.60-2.73.

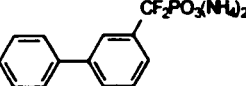
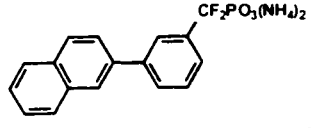
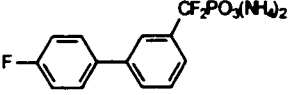
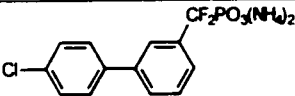
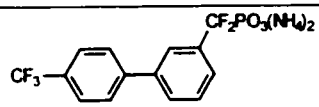
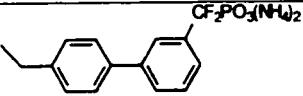
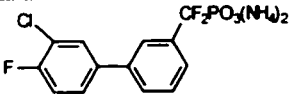
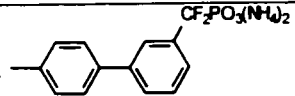
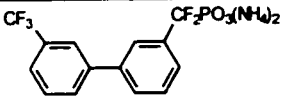
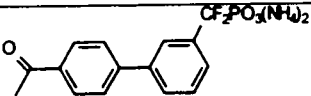
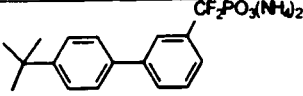
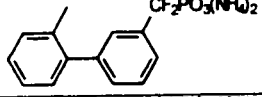
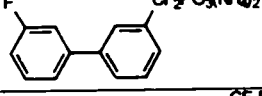
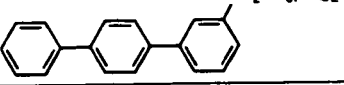
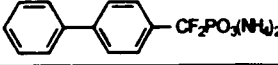
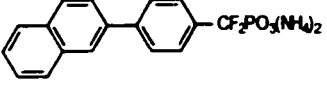
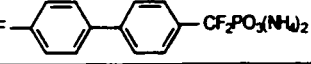

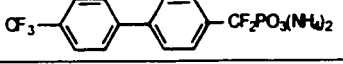
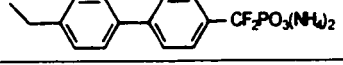
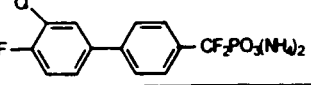
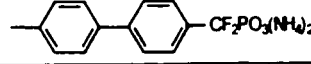
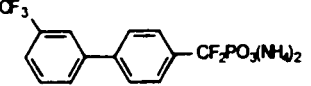
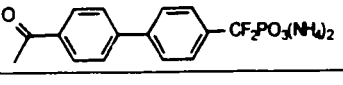
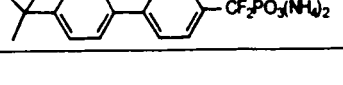
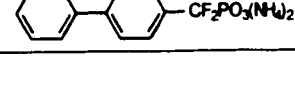
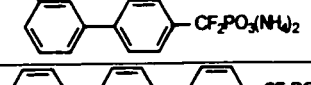

Product	% Yield	Purity	
		¹⁹ F NMR	HPLC
2.60 	70	100	100
2.61 	46	99	90
2.62 	82	100	100
2.63 	75	100	92
2.64 	61	100	96
2.65 	55	100	94
2.66 	56	99	96
2.67 	59	100	97
2.68 	60	100	99
2.69 	58	75	95
2.70 	64	99	87
2.71 	82	100	97
2.72 	71	100	97
2.73 	57	70	100

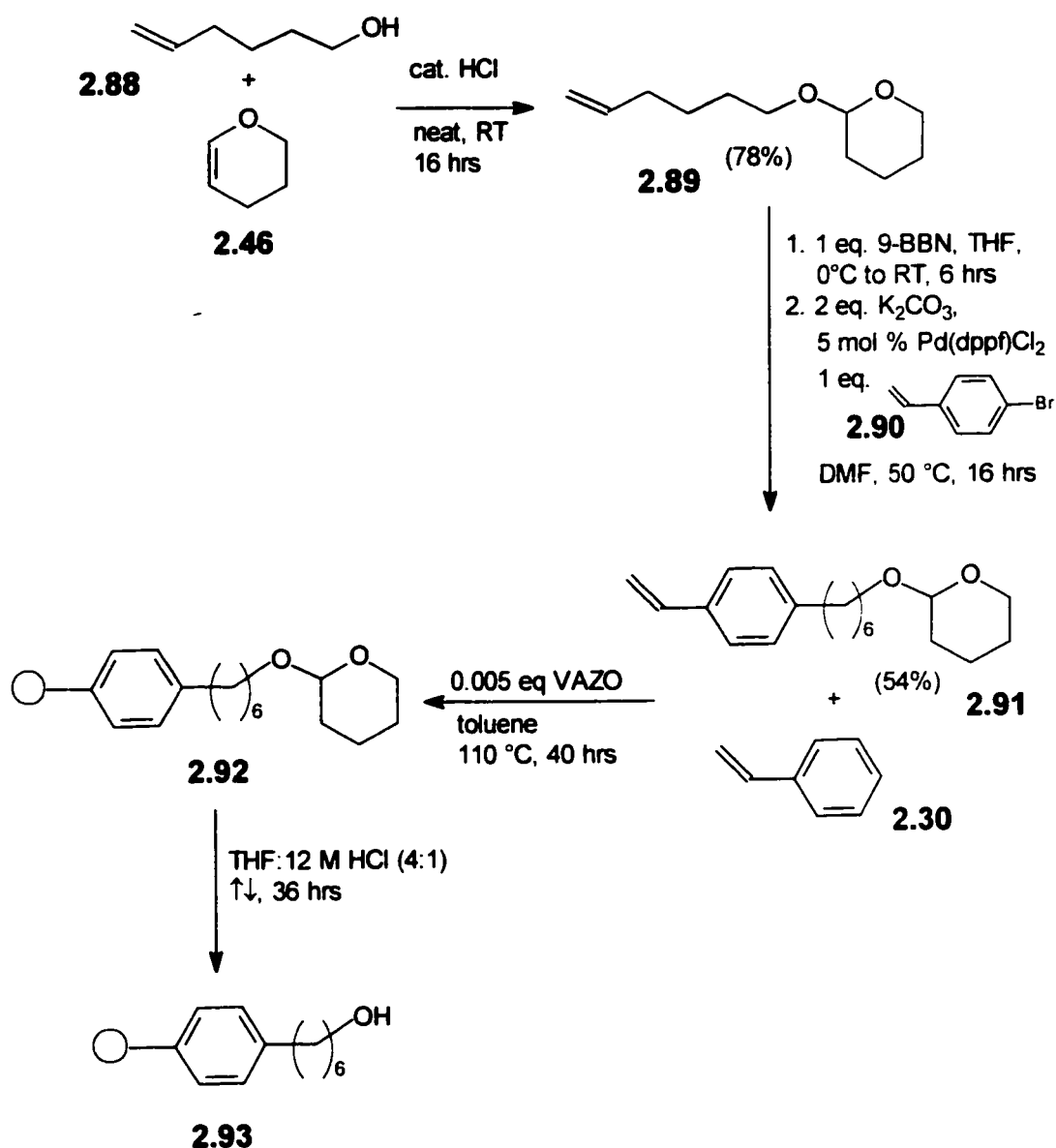
Table 2.3 Yields and Purities of *para* series of compounds 2.74-2.86.⁴⁴

Product	% Yield	Purity	
		¹⁹ F NMR	HPLC
2.74 	89	98	99
2.75 	64	97	97
2.76 	75	100	99
2.77 	68	100	100
2.78 	67	97	100
2.79 	75	96	100
2.80 	70	98	98
2.81 	66	100	100
2.82 	54	98	97
2.83 	90	100	91
2.84 	64	100	96
2.85 	67	99	98
2.86 	81	100	99
2.87 	61	96	96

2.3.8 Library Construction Using a C-C Linker Arm

Due to the presence of linker chain derived contaminants in the crude product resulting from cleavage of the benzyl alkyl ether by TMSI or TMSBr we investigated the possibility of replacing the C-O ether linkage with a more chemically resistant C-C bond. Functionalization of the bulk polymer in the same manner as was performed for the conversion of **2.32** to **2.49** did not appear to be a feasible route. Instead, we chose to synthesize the functionalized monomer **2.91** which could be copolymerized with styrene (Scheme 2.17). Synthesis of polymer **2.93** began with 5-hexen-1-ol (**2.88**) which was protected with the THP group in a 78% yield by reaction with 3,4-dihydro-2H-pyran with a catalytic amount of HCl. A Suzuki reaction was then performed by first forming the 9-BBN derivative of **2.89** *in situ* and coupling it with 4-bromostyrene in the presence of K₂CO₃ and Pd(dppf)Cl₂ to give monomer **2.91** in a 54% yield.^{45, 46}

The monomer **2.91** was copolymerized with styrene in a 1:0.03 ratio using 0.005 equivalents of VAZO as an initiator to yield the protected polymer **2.92**. Removal of the THP group was achieved as described for polymer **2.48** to result in the C-C linker arm polymer **2.93**. This polymer had the same solubility properties as polymer **2.49**. Polymer **2.93** was examined as a support for library construction by attaching phosphonic acid **2.28** to it using the Mitsunobu reaction followed by reaction with the boronic acids. Removal of the compounds from the support was achieved using TMSI as described above. NMR analysis of the crude reaction products indicated that none of them were contaminated with byproducts resulting from cleavage of the linker.



Scheme 2.17. Synthesis of polymer **2.93**.

Nevertheless, it was apparent that there were some drawbacks compared to using the C-O linker approach. More steps were required using the C-C linker approach. Also, the Suzuki coupling of **2.89** to **2.90** proceeded in only modest

yield and the product **2.91** was very difficult to purify. Even though the purities of the crude phosphonic acids were considerably better using the C-C linker approach, the crude material was still contaminated with trace amounts of polymer, therefore, necessitating a washing step. Consequently, the final yields and purity of the final products was almost identical using the two approaches.

2.3.9 Inhibition Studies with Biaryl Phosphonates and PTP1B

The *meta* (**2.60-2.73**) and *para* (**2.74-2.87**) series of compounds were initially assayed for PTP1B inhibition at a concentration of 150 μM , using 20 μM fluorescein diphosphate (FDP) as the substrate in 50 mM Bis-Tris buffer containing 2 mM EDTA, 5 mM DTT, 10 $\mu\text{g/mL}$ BSA and a final DMSO concentration of 2.5%. The assays were monitored at 450 nm over a course of 20 minutes. The results of the initial screens are given in Table 2.4. The *meta* series of phosphonic acids (**2.60-2.73**) were consistently more potent than the *para* series (**2.74-2.87**). Though **2.75** and **2.87** of the *para* series displayed inhibitory activity at the 150 μM rapid screen, it was quite clear that the *meta* analogs were more potent. The entire *meta* series was reassayed at 50 μM in order to identify the best inhibitors. The most potent inhibitors were found to be **2.61**, **2.69**, and **2.73** which bear the *p*-naphthyl, *p*-acetyl and *p*-phenyl substituents respectively on the second aryl ring.

Table 2.4 Results from Rapid Screen of 2.60-2.87 for PTP1B inhibition.^a

Phosphonic Acid	% Inhibition ^a	
	150 μ M	50 μ M
2.60	84 ^b	65 ^b
2.61	100 ^b	71 ^b
2.62	88 ^b	74 ^b
2.63	92 ^b	65 ^b
2.64	91 ^b	75 ^b
2.65	90 ^b	74 ^b
2.66	88 ^b	70 ^b
2.67	87 ^b	70 ^b
2.68	60 ^b	ND
2.69	94 ^b	80 ^b
2.70	85 ^b	59 ^b
2.71	24 ^b	ND
2.72	89 ^b	74 ^b
2.73	98 ^b	87 ^b
2.74	43	ND
2.75	80	ND
2.76	38	ND
2.77	50	ND
2.78	43	ND
2.79	49	ND
2.80	54	ND
2.81	38	ND
2.82	56	ND
2.83	50	ND
2.84	41	ND
2.85	29	ND
2.86	61	ND
2.87	80	ND

^a See Experimental for procedure. ^b Performed by J. Grzyb.

These compounds were resynthesized by solution phase methods, and reevaluated for inhibition using the same buffer system employed in the rapid screen assays with the exception of the DMSO concentration which was increased to 5% in order to avoid solubility problems.⁴⁴ The results of these

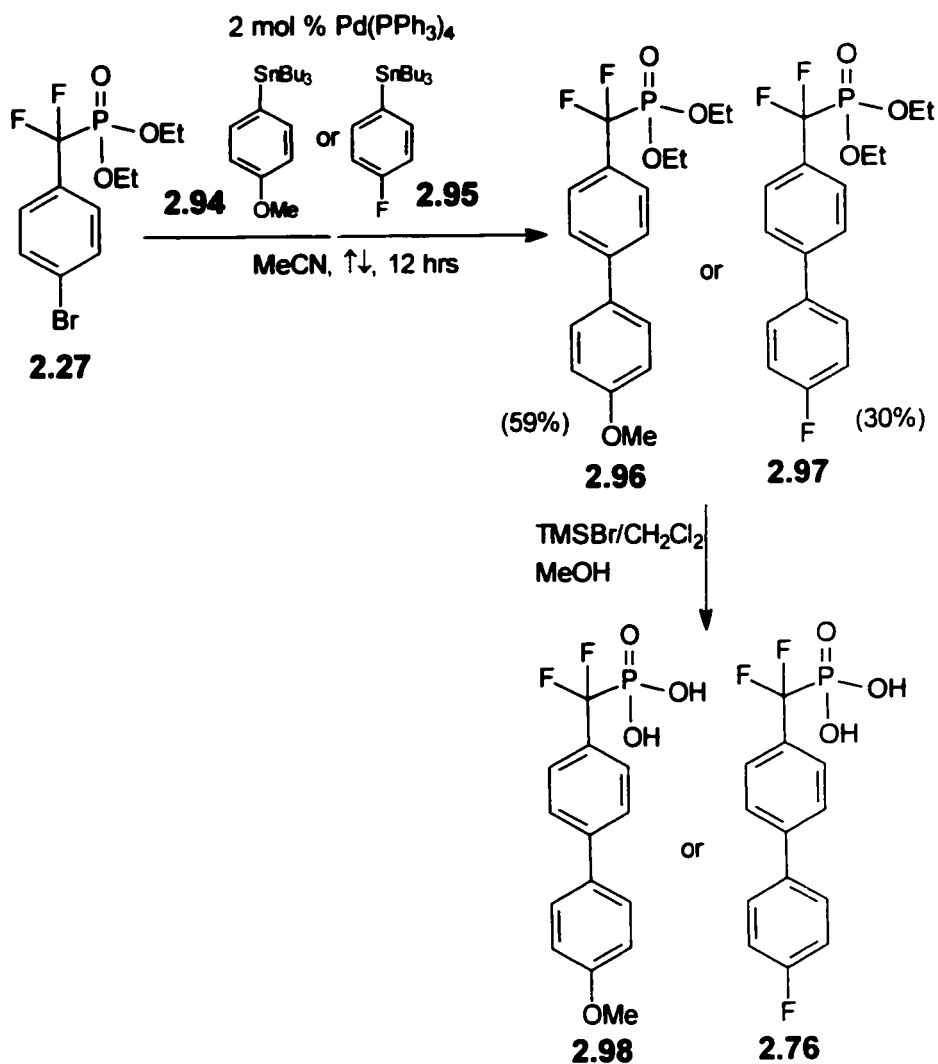
assays are presented in Table 2.5. For compounds **2.73** and **2.61**, there was good agreement between the results obtained with the “solution phase” and “polymer phase” compounds. The value obtained for **2.69** made via solution chemistry is slightly lower than that obtained using the liquid phase methodology which is most likely a result of an impurity being present (70% pure by ^{19}F -NMR) in the compound obtained from SPSOS.

Table 2.5. Inhibition of PTP1B with **2.61**, **2.69**, and **2.73** constructed using conventional solution phase chemistry.^a

Compound	% Inhibition from solution ^b	% Inhibition from SPSOS ^c	IC ₅₀ (μM) ^d
2.61	71	71	24
2.69	69	80	21
2.73	89	87	8.6

^aAssays were performed by Justyna Grzyb using 20 μM fluorescein diphosphate (FDP) as the substrate in 50 mM Bis-Tris buffer (pH 6.3) containing 2 mM EDTA, 5 mM DTT, 10 μg/mL BSA and a final DMSO concentration of 5.0%. The assays were monitored at 450 nm.^bResults obtained using compounds prepared using conventional solution phase chemistry. ^cResults obtained using compounds prepared by SPSOS.

The IC₅₀ values for **2.61**, **2.69**, and **2.73** were determined (Table 2.5). Compound **2.73** was clearly the best inhibitor with an IC₅₀ of 8.6 μM. Its K_i was determined to be 1.7 μM.⁴⁴ and exhibited mixed competitive-non-competitive inhibition. This was not totally unexpected considering the rather hydrophobic nature of the inhibitor which may allow it to partake in non-specific, hydrophobic interactions with the enzyme. Nevertheless, at the time we completed these studies, this was one of the most potent small molecule inhibitors of PTP1B.



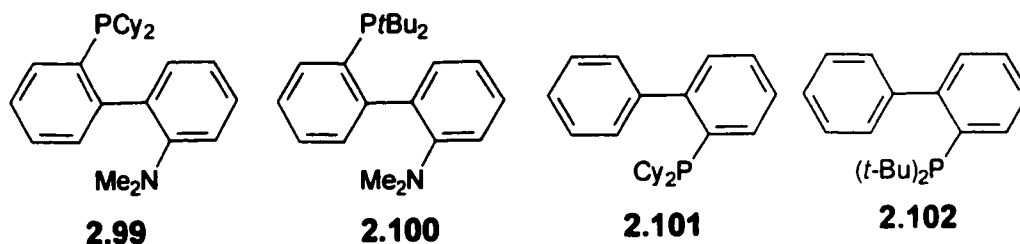
Scheme 2.18. Synthesis of biaryl DFMP compounds via a Stille coupling.

While our work was in progress, Shibuya and workers reported the synthesis of compounds **2.98** and **2.76** in solution by a Stille coupling between aryl bromide **2.27** and stannanes **2.94** and **2.95** (Scheme 2.18).⁴⁷ The yields of the Stille couplings was 59% (for **2.96**) and 30% (for **2.97**). Our yield for compound **2.76** using the SPSOS approach was 75% (see Table 2.3). Thus, we believe our Suzuki chemistry, whether performed in solution or on NCPS, is superior to Shibuya's Stille coupling approach for preparing this class of biaryl

compounds. Shibuya also reported that compound **2.98** exhibited an IC_{50} of 451 μM with PTP1B. Unfortunately, no inhibition data for **2.76** was reported. We found compound **2.76** to be a poor inhibitor of PTP1B exhibiting only 38% inhibition at 150 μM (see Table 2.4).

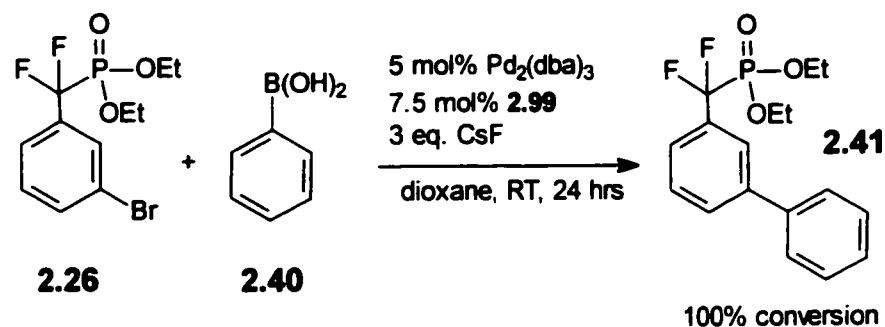
2.3.10 Suzuki Couplings with Novel Phosphine Ligands

During the course of our work, Buchwald and coworkers reported several papers describing novel biaryl phosphine ligands for room temperature Suzuki coupling reactions.^{48,49,50} When employed in conjunction with an appropriate palladium catalyst, these new catalyst systems exhibited high turnover and remarkable reactivity. Catalyst systems involving ligand **2.99** were among the first to be reported and were able to catalyze the cross coupling of aryl chlorides with various boronic acids while using Pd catalyst loadings as



low as 0.5-2%. Since we were interested in decreasing the catalyst loading for our Suzuki reactions, we synthesized **2.99** (not commercially available) and evaluated Buchwald's chemistry on our model system (Scheme 2.19) in solution using the conditions reported by Buchwald.⁴⁸ We found, that 5 mol% of Pd₂(dba)₃ in conjunction with 7.5 mol% **2.99** was sufficient to catalyze the quantitative coupling of phenyl boronic acid **2.40** to the *meta*-bromo compound **2.26** at room temperature over 24 hours (Scheme 2.19). Although the reaction

worked, these conditions are not a significant improvement over the ones that we developed here. Although our catalyst loading is higher, our conditions do not require an additional ligand. Also, we found the synthesis of this ligand very tedious and low yielding.



Scheme 2.19. Buchwald's Suzuki coupling conditions.

In a later paper, Buchwald and coworkers reported that phosphines **2.100**-**2.102** could similarly be employed in catalyst systems with the advantage that at least **2.102** is commercially available.⁵⁰ Buchwald reports that the use of these ligands in Suzuki couplings offer the advantage of high turnover numbers, which translates into lower catalyst loadings, and the ability to promote the cross coupling of normally unreactive aryl chlorides under extremely mild conditions. Buchwald has recently demonstrated that the biphenyl phosphine ligands can function as polymer supported reagents.⁵¹ When ligands **2.101** and **2.102** were attached to Merrifield resin and preincubated with a Pd source, these systems catalyzed C-C and C-N bond formation at elevated temperatures (65-80°C). We have not yet evaluated these ligands for performing our chemistry. This work is in progress in the Taylor group. We should also point out that other groups besides Buchwald's have also recently developed conditions for performing room

temperature Suzuki reactions.^{52,53} A full evaluation of these new conditions with our systems will be performed in the Taylor group in due course.

2.4 Summary

In summary, the polymer supported syntheses of a series of biaryl derivatives bearing the α,α -difluoromethylenephosphonic acid group was reported. NCPS was used as the support which enabled the reactions to be carried out under homogeneous conditions and reactions to be followed using conventional ^{19}F NMR. Synthesis of the biaryl phosphonic acids was initiated by attaching mono-ethyl esters of α,α -difluorophosphonic acids to 3% alkylhydroxy-modified NCPS via a phosphate ester linkage. Suzuki reaction conditions were developed which allowed for the formation of a series of polymer-bound biaryl phosphonates at ambient temperature. Removal of phosphonic acids from the support and cleavage of the ethyl protecting group was achieved in a single step using TMSI or TMSBr. Yields of the phosphonic acids ranged from 46-90% and, in most cases, were obtained in purities (96-99%) after cleavage from the support, that was sufficient for biological screening. One of the compounds exhibited an K_i of 1.7 μM .

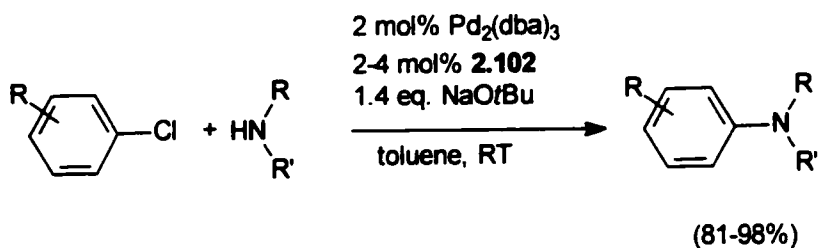
The work presented in this chapter demonstrated that our SPSOS approach is a viable tactic for preparing biaryl DFMP's and as means of discovering inhibitors of PTP1B. In the next chapter, we expand on our SPSOS approach and present another, perhaps more challenging example, of this chemistry. Our conclusions concerning the general applicability of this approach to the synthesis of aryl DFMP's, as well as our opinions concerning the use of

NCPS for small molecule library construction in general, are given at the end of chapter 3.

2.5 Future Directions for Preparing DFMP Compounds on SPSOS Using Palladium Chemistry

The aryl bromide substrates employed in this study may potentially participate in other palladium catalyzed coupling reactions. A survey of the recent literature reveals numerous reactions which may serve to expand the repertoire of reactions compatible with NCPS as well lead towards new DFMP bearing PTP inhibitors. Some of the reactions that we are considering for our SPSOS methodology are discussed below.

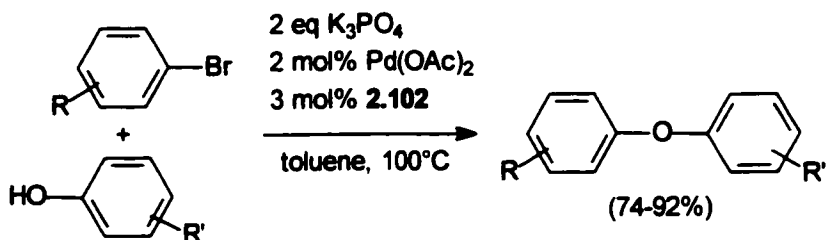
Additional reports from Buchwald's lab describe the use of ligands **2.99-2.102** for additional palladium catalyzed reactions involving aryl halides. The palladium catalyzed amination of aryl halides and triflates as shown in Scheme 2.20 was found to proceed even with aryl chlorides under fairly mild conditions with a low catalyst loading.^{48,54}



Scheme 2.20. Pd catalyzed amination of aryl chlorides.

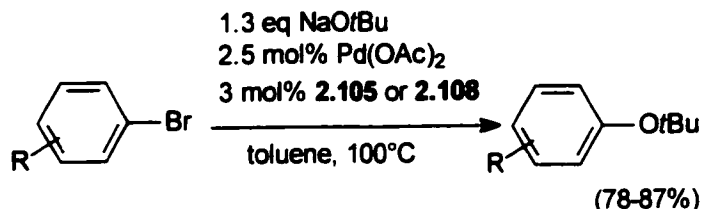
The use of ligand **2.102** in the preparation of ethers from aryl halides was also reported.⁵⁵ The reaction of phenols with aryl bromides in the presence of

$\text{Pd}(\text{OAc})_2$ and **2.102** resulted in the formation of biaryl ethers as outlined in Scheme 2.21.



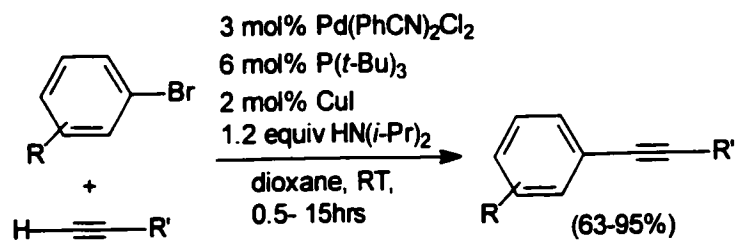
Scheme 2.21. Pd catalyzed biaryl ether formation.

Ligands **2.99** and **2.102** were also useful for the conversion of aryl bromides and chlorides to aryl *t*-butyl ethers as outlined in Scheme 2.22.



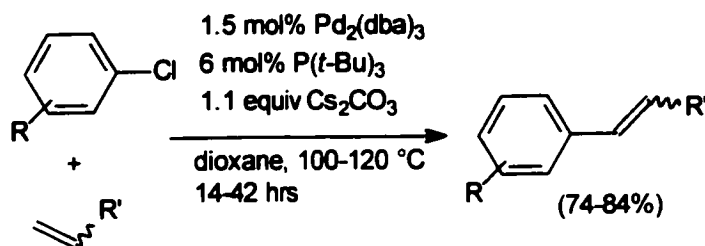
Scheme 2.22. Pd catalyzed aryl *t*-butyl ether formation.

Mild Sonogashira coupling reaction conditions were reported by Fu *et al.*⁵⁶ and Thorand *et al.*⁵⁷ for the formation of aryl alkynes from aryl bromides. The conditions reported by Fu and coworkers are outlined in Scheme 2.23.



Scheme 2.23. Room temperature Sonogashira coupling conditions.

Heck coupling conditions shown in Scheme 2.24, which were reported by Hartwig *et al.*⁵⁸ which employed aryl chlorides as substrates may also potentially be adapted to the DFMP bearing aryl bromides used in our own work.

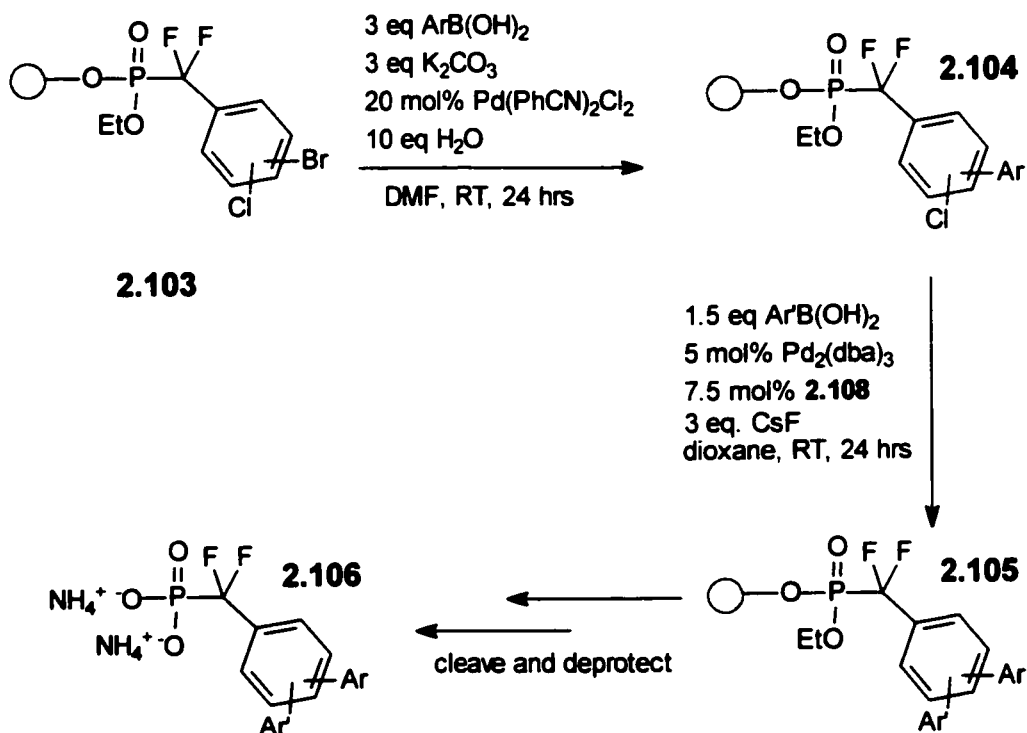


Scheme 2.24. Heck coupling conditions with aryl chlorides.

The reactions outlined above represent a sampling of what new avenues may be pursued in order to diversify the types of reactions compatible with the NCPS support while also preparing novel compounds which may potentially inhibit PTPases. While some of the reaction conditions described do require elevated temperatures, it is possible that room temperature variants may be found.

An example of how we envision using the new Pd catalyst systems for increasing the diversity of our libraries is shown in Scheme 2.25. By combining the Suzuki reaction conditions which we developed with the aryl chloride coupling conditions reported by Buchwald *et al.* it may be possible to build a large library of novel DFMP-bearing compounds. The fundamental building block of the library would be an aryl compound attached to the support by a phosphonate ester linkage of the DFMP group (2.103). The aryl ring itself would bear both chloro and bromo substituents. Utilizing the room temperature Suzuki coupling conditions developed and described in this work, an aryl ring would be introduced selectively at the bromo position since these conditions do not permit the

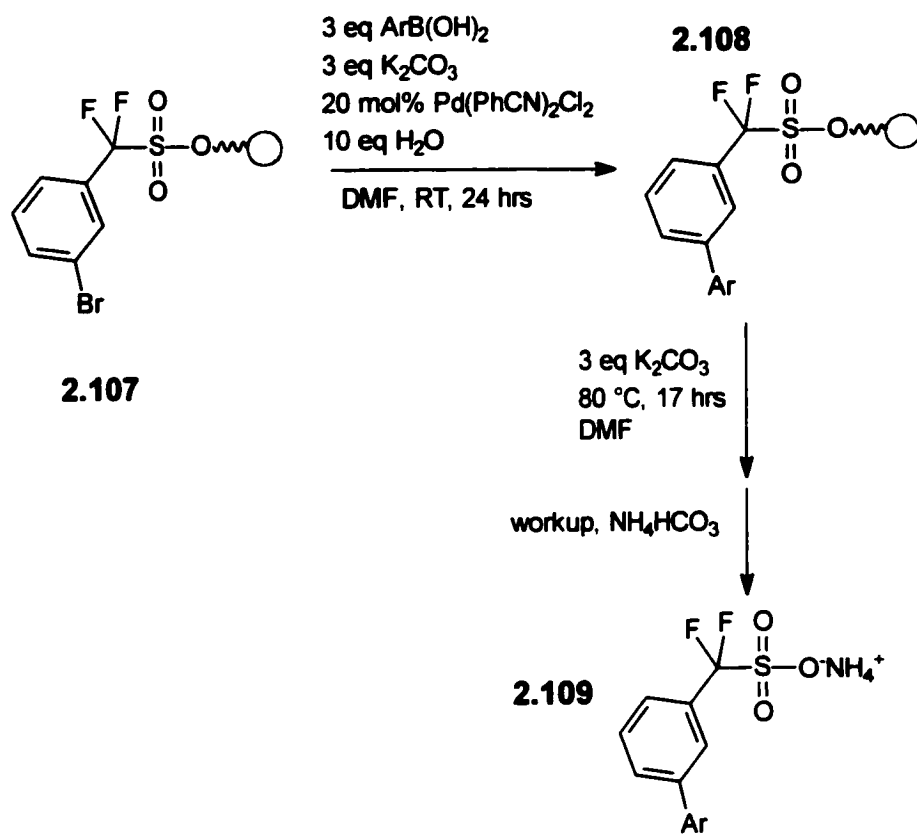
coupling of aryl chlorides. The polymer bound intermediate **2.104** can be purified via the precipitation and filtration protocol, before being reacted with a second aryl boronic acid to give the polymer bound triaryl intermediate **2.105**. The final products (**2.106**) would be obtained using the deprotection/cleavage and workup sequence utilized for the biaryl library. If only the 14 boronic acids employed in this study were used in such a sequence, a minimum library size of 196 compounds would be possible, assuming only one substitution pattern on the core aryl ring (ie. 3,4 or 3,5). Also, there are many more boronic acids commercially available and so this procedure has the potential for preparing a library containing several thousand compounds.



Scheme 2.25. Route towards a library of triaryl DFMP bearing inhibitors.

2.6 Synthesis of a Biaryl DFMS Library

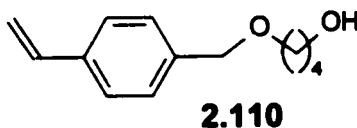
The methodology we described here to synthesize the biaryl series of DFMP bearing inhibitors has recently been applied to the synthesis of a series of biaryl compounds bearing the difluoromethylenesulfonate (DFMS) functionality. The DFMS group is a mono anionic phosphotyrosine mimetic.⁵⁹ Although the DFMS group is not as effective as the DFMP group as a phosphomimetic (in terms of PTP1B inhibition), it has the advantage of being monoanionic and, therefore, compounds bearing this moiety may exhibit superior cell permeability compared to DFMP-bearing compounds. Carmen Leung, a MSc. graduate in the Taylor group has successfully prepared a series of *meta* biaryl DFMS compounds on NCPS. The general approach towards this library is outlined in Scheme 2.26 and begins with the polymer bound aryl bromide **2.107** which is attached to the NCPS support via a sulfonate ester linkage. Diversity is achieved by performing a series of parallel Suzuki reactions with a variety of boronic acids utilizing the conditions developed in section 2.3.5. The sulfonate ester can be cleaved under mild conditions (ie. 3 equivalents of K_2CO_3 at 80 °C in DMF) which allows for a broader range of functionalities on the second aryl ring (25 aryl and heteroaryl boronic acids were used in this study). Further studies on the preparation of this class of compounds on NCPS are in progress in the Taylor group.



Scheme 2.26. Synthesis of *meta* biaryl DFMS library.

2.7 References

- 1 Taylor, S. D.; Kotoris, C. C.; Dinaut, A. N.; Wang, Q.; Ramachandran, C.; Huang, Z. *Bioorg. Med. Chem.* **1998**, *6*, 1457-1468.
- 2 Montserat, J.; Chen, L.; Lawrence, D. S.; Zhang, Z-Y. *J. Biol. Chem.* **1996**, *7868-7872*.
- 3 Zhang, Z-Y. *J. Biol. Chem.* **1995**, *270*, 11199-11204.
- 4 Chen, L.; Montserat, J.; Lawrence, D. S.; Zhang, Z-Y. *Biochemistry* **1996**, *35*, 9348-9354.
- 5 Hermkens, P. H. H.; Ottenheijm, H. C. J.; Rees, D. *Tetrahedron* **1996**, *52*, 4527-4554.
- 6 Wendeborn, S.; De Mesmaeker, A.; Brill, W. K-D.; Berteina, S. *Acc. Chem. Res.* **2000**, *33*, 215-224.
- 7 Molecular Simulations Inc., San Diego, CA.
- 8 Burke, T. R.; Ye, B.; Yan, X.; Wang, S.; Jia, Z.; Chen, L.; Zhang, Z-Y.; Barford, D., *Biochemistry* **1996**, *35*, 15989-15996.
- 9 Chen, S.; Janda, K. D., *J. Am. Chem. Soc.* **1997**, *119*, 8724-8725.
- 10 For polymer **2.49** compound **2.110** was used to prepare the calibration plot. Compound **2.110** was prepared and kindly provided by J. Grzyb of the Taylor group.



- 11 Parham, W. E.; Piccirilli, R. M. *J. Org. Chem.* **1977**, *42*, 257-260.

-
- 12 Glover, N. R.; Tracey, A. S. *Biochemistry* **1999**, *38*, 5256-5271.
- 13 Yao, Z-J.; Ye, B.; Wu, X-W.; Wang, S.; Wu, L.; Zhang, Z-Y.; Burke, T. R.,
Bioorg. Med. Chem. **1998**, *6*, 1799-1810.
- 14 Glover, N. R.; Tracey, A. S. *Biochem. Cell Biol.* **1999**, *77*, 469-486.
- 15 Peters, G. H.; Frimurer, T. M.; Andersen, J. N.; Olsen O. H. *Biophysical Journal* **1999**, *77*, 505-515.
- 16 Glover, N. R.; Tracey, A. S. *J. Am. Chem. Soc* **1999**, *121*, 3579-3589.
- 17 Karplus, M.; Petsko, G. A. *Nature* **1990**, *347*, 631-639.
- 18 Kollman, P. A. *Curr. Opin. Struct. Biol.* **1994**, *4*, 240-245.
- 19 Ma, J. C.; Dougherty, D. A. *Chem. Rev.* **1997**, *97*, 1303-1324.
- 20 Miyaura, N.; Suzuki, A. *Chem. Rev.* **1995**, *95*, 2457-2483.
- 21 Smyth, M. S.; Burke, T. R. *Org. Prep. Proced. Int.* **1996**, *28*, 77-81.
- 22 Merck-Frosst Co., personal communication to S. D. Taylor.
- 23 Qiu, W.; Burton, D. J. *Tetrahedron Lett.* **1996**, *37*, 2745-2748.
- 24 Yokomatsu, T.; Murano, T.; Suemune, K.; Shibuya, S. *Tetrahedron.* **1997**, *53*,
815-822.
- 25 Taylor, S. D.; Kotoris, C. C.; Dinaut, A. N.; Chen, M-J. *Tetrahedron.* **1998**, *54*,
1691-1714.
- 26 VAZO was employed on the advice of Prof. M. Winnik of the Department of
Chemistry, University of Toronto. AIBN is considered a regulated substance
and its export from the U.S. is sporadic.
- 27 James, I. W. *Tetrahedron* **1999**, *55*, 4855-4946.
- 28 Cao, X.; Mjalli, A. M. M. *Terahedron Lett.* **1996**, *34*, 6073-6076.

-
- 29 Nicolaou, K. C.; Pastor, J.; Winssinger, N.; Murphy, F. J. *Am. Chem. Soc.* **1997**, *120*, 5132-5133.
- 30 J. Lee of the Taylor group has recently demonstrated that the di-tetrabutyl ammonium salt can displace the chloride groups of chloromethylated polystyrene at room temperature within 24 hours. No hydrolysis occurs due to the excellent stability of the phosphonate monoester linkage.
- 31 Campbell, D. A.; Bermak, J. C.; Burkoth, T. S.; Patel, D. *J. Am. Chem. Soc.* **1995** *117*, 5381-5382.
- 32 Campbell, D. A. *J. Org. Chem.* **1992**, *57*, 6331-6335.
- 33 Campbell, D. A.; Bermak, J. C. *J. Org. Chem.* **1994**, *59*, 658-660.
- 34 Miyaura, N.; Yanagi, T.; Suzuki, A. *Synthetic Communications*. **1981**, *11*, 513-519.
- 35 Frenette, R.; Friesen, R. W. *Tetrahedron Lett.* **1994**, *35*, 9177-9180.
- 36 Piettre, S. R.; Baltzer, S. *Tetrahedron Lett.* **1997**, *38*, 1197-1200.
- 37 Watanabe, T.; Miyaura, N.; Suzuki, A. *Synlett.* **1992**, *3*, 207-210.
- 38 Larhed, M.; Linderberg, G.; Hallberg, A. *Tetrahedron Lett.* **1996**, *37*, 8219-8222.
- 39 Guiles, J. W.; Johnson, S. G.; Murray, W.V. *J. Org. Chem.* **1996**, *61*, 5169-5171.
- 40 Wenderborn, S.; Berteina, S.; Brill, W. K-D.; Des Mesmaeker *Synlett* **1998**, 671-675.
- 41 Anderson, J. C.; Namli, H. *Synlett.* **1995**, 756-758.
- 42 Anderson, J. C.; Namli, H. Roberts, C. A. *Tetrahedron*, **1997**, 15123-15134.

-
- 43 Campi, E. M.; Jackson, W. R.; Marcuccio, S. M.; Naeslund, C. G. M. *J. Chem. Soc. Chem. Commun.* **1994**, 20, 2395-2396.
- 44 Prepared or performed by J. Grzyb.
- 45 Ishiyama, T.; Abe, S.; Miyaura, N.; Suzuki, A. *Chem. Lett.* **1992**, 691-694.
- 46 Johnson, C.; Braun, M. P. *J. Am. Chem. Soc.* **1993**, 115, 11014-11015.
- 47 Yokomatsu, T.; Murano, T.; Umesue, I.; Soeda, S.; Shimeno, H.; Shibuya, S. *Bioorg. Med. Chem. Lett.* **1999**, 9, 529-532.
- 48 Old, D. W.; Wolfe, J. P.; Buchwald, S. L. *J. Am. Chem. Soc.* **1998**, 120, 9722-9723.
- 49 Wolfe, J. P.; Buchwald, S. L. *Angew. Chem. Int. Ed.* **1999**, 38, 2413-2416.
- 50 Wolfe, J. P.; Singer, R. A.; Yang, B. H.; Buchwald, S. L. *J. Am. Chem. Soc.* **1999**, 121, 9550-9561.
- 51 Parrish, C. A.; Buchwald, S. L. *J. Org. Chem.* **2001**, 66, 3820-3827.
- 52 Zim, D.; Monteiro, A. L.; Dupont, J. *Tetrahedron Lett.* **2000**, 41, 8199-8202.
- 53 Zim, D.; Gruber, A. S.; Ebeling, G.; Dupont, J.; Monteiro, A. L. *Org. Letters* **2000**, 2, 2881-2884.
- 54 Wolfe, J. P.; Tomori, H.; Sadighi, J. P.; Yun, J.; Buchwald, S. L. *J. Org. Chem.* **2000**, 65, 1158-1174.
- 55 Aranyos, A.; Old, D. W.; Kiyomori, A.; Wolfe, J. P.; Sadighi, J. P.; Buchwald, S. L. *J. Am. Chem. Soc.* **1999**, 121, 4369-4378.
- 56 Hundertmark, T.; Littke, A. F.; Buchwald, S. L.; Fu, G. C. *Org. Letters* **2000**, 2, 1729-1731.
- 57 Thorand, S.; Krause, N. *J. Org. Chem.* **1998**, 63, 8551-8553.

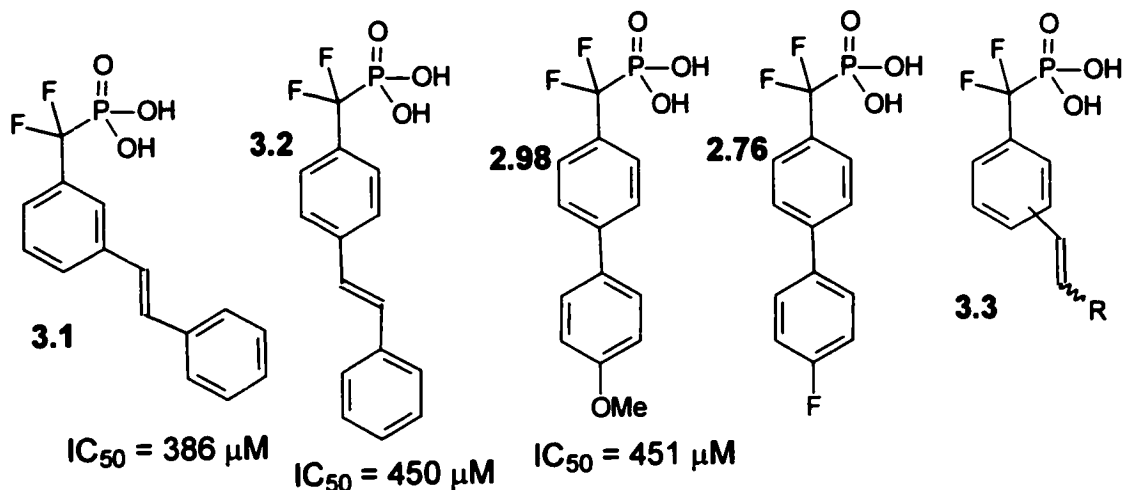
58 Littke, A. F.; Hartwig, J. F. *J. Org. Chem.* **1999**, *64*, 10-11.

59 Kotoris, C. C.; Chen, M-J.; Taylor, S. D. *Bioorg. Med. Chem. Lett.* **1998**, *8*,
3275-3280.

CHAPTER 3 SYNTHESIS OF STYRL BASED PTP1B INHIBITORS

3.1 Introduction

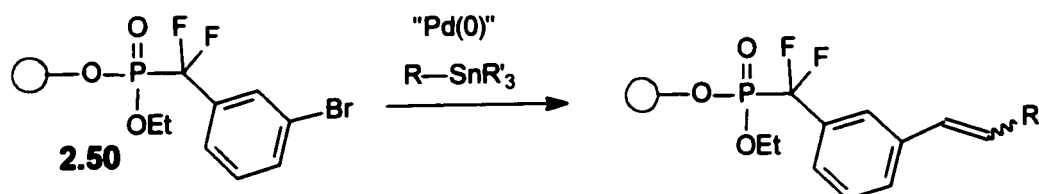
Our success in applying NCPS for synthesizing biaryl inhibitors of PTP1B prompted us to explore other reactions that would allow us to obtain an additional series of potential inhibitors. As mentioned in Section 2.3.9 while our NCPS/Suzuki studies were in progress, Shibuya and co-workers reported a series of aryl DFMP's substituted with various hydrophobic groups.¹ Among this series of compounds were *E*-stilbene derivatives **3.1** and **3.2**, which exhibited IC₅₀'s of 386 μM and 450 μM respectively. Shibuya also reported the *para*-substituted biphenyl derivatives **2.76** and **2.98**, both of which were less potent inhibitors than **3.1** and **3.2**. We therefore decided to construct a series of compounds of styrene-like DFMPs of type **3.3**.



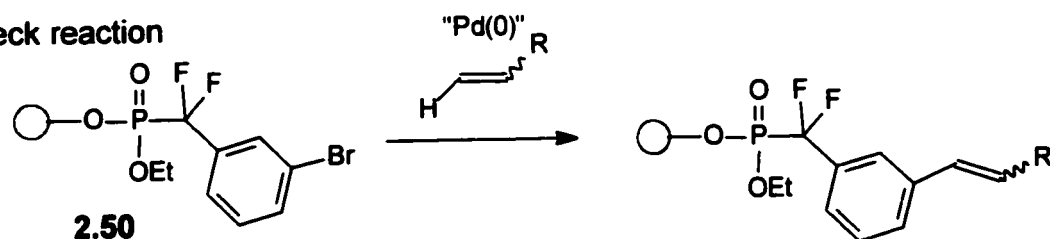
We considered three routes for a combinatorial approach to compounds of type **3.3**: A Stille coupling of various substituted stannanes with polymer-bound aryl bromides of type **2.50** (see Section 2.3.6) (Scheme 3.1), a Heck reaction (Scheme 3.1) between **2.50** and a variety of alkenes, and a Wittig reaction in

which a polymer-bound aldehyde or phosphonate is coupled with a variety of Wittig reagents (phosphonium salts), Horner-Emmons reagents (phosphonates) or aldehydes (Scheme 3.2). All three of these reactions have been used for the preparation of compound libraries using insoluble supports.²

Stille coupling

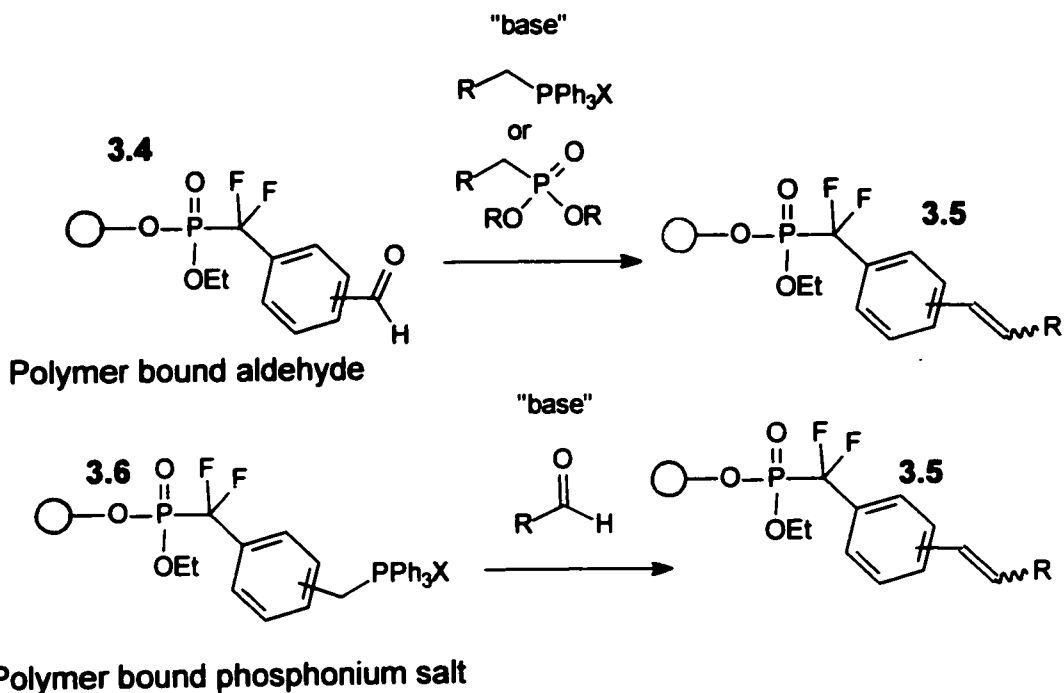


Heck reaction



Scheme 3.1. Stille and Heck approaches towards library construction.

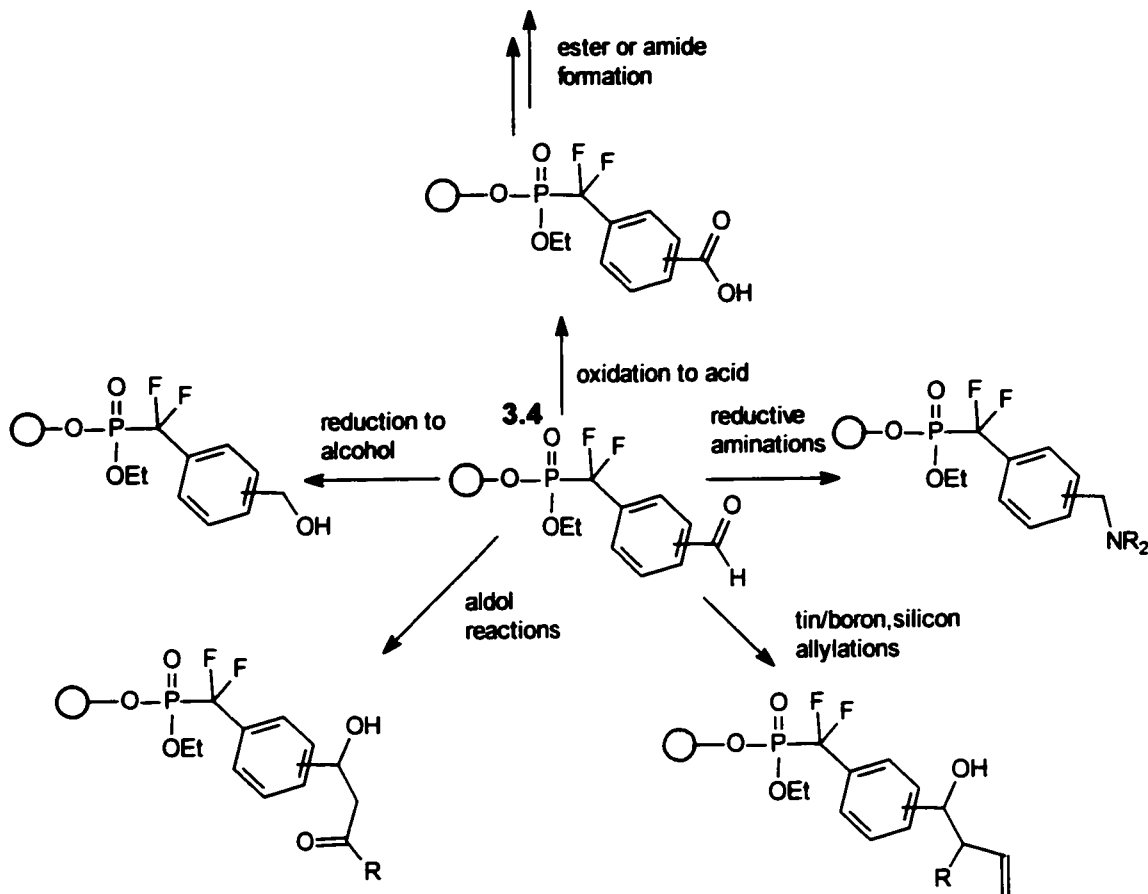
We chose to use a Wittig or Horner-Emmons approach to the desired compounds for a number of reasons. Although Shibuya and coworkers used the Stille reaction to prepare **3.1** and **3.2** in solution in reasonable yields (68 and 69%) using aryl bromides, the reactions required heating which we wished to avoid.¹ The Stille route would also require the preparation of a wide variety of stannanes which we also wished to avoid. The Heck reaction is performed at elevated temperatures in the presence of base which we thought would be problematic with our compounds as discussed in section 2.3.6. We felt that the development of room temperature Heck reaction conditions on aryl bromides would be quite challenging due to the lack of literature precedents.



Scheme 3.2. Wittig approaches towards library construction.

At the time we began these studies, there were already several examples of solid phase Wittig or Horner-Emmons reactions including variations where the phosphonium salt/phosphonate is attached to the support^{3,4,5,6,7} and others where the aldehyde is immobilized.^{8,9,10,11} We chose to use polymer-bound aldehydes since a large number of Wittig or Horner-Emmons reagents are commercially available and, at the time we began these studies, we did not anticipate problems in constructing the polymer-bound aldehyde. We also decided to employ a Wittig reaction instead of the Horner-Emmons approach since there are many more Wittig reagents commercially available than Horner-Emmons reagents. In preparing the library of stilbene-like compounds, we did not wish to target a specific isomer. The formation of a mixture of *E* and *Z* isomers in the Wittig reaction would add an additional element of diversity. Finally, it did not escape our attention that the polymer-bound aldehyde could

also be used as an intermediate to a number of other polymer-bound species which could also be used to prepare other classes of aryl DFMP's using other types of reactions (Scheme 3.3).



Scheme 3.3. Alternative reactions with a polymer bound aldehyde.

3.2 Experimental

General

The general details for the preparation, purification, and characterization of compounds is as described in section 2.2 with a few minor changes. ^1H , ^{19}F , ^{13}C , and ^{31}P NMR spectra were recorded on a Bruker Avance 200, 300 or 500 as indicated. References for NMR spectra are as described in Section 2.2. Mass spectra were obtained as described in Section 2.2. The prepacked LC-NH₂ columns used for the purification of the phosphonic acids were provided by Supelco. Analytical HPLC analysis was performed using a Waters 600 system equipped with a Vydac 218TP54 analytical C-18 reverse phase column and a Waters 2487 dual wavelength absorbance detector set at 254 nM. HPLC analysis was conducted using the solvent gradient described in Section 2.2.

3.2.1 Synthesis of Protected Aryl Aldehyde DFMP Compounds

4-(bromomethyl) benzaldehyde (3.11). Method A: To a solution of 4-(bromomethyl) benzoic acid (3.10) (1 g, 4.65 mmol, 1 equiv) in dry THF (10 mL), was added borane-dimethyl sulfide (2.32 mL of a 2 M solution in toluene, 4.65 mmol, 1 equiv). This reaction was heated at 60 °C for 1 hr. The reaction was cooled and the THF removed under reduced pressure. The solid was dissolved in dry CH₂Cl₂ (5 mL) and added to a suspension of pyridinium chlorochromate (1 g, 4.65 mmol, 1 equiv) in dry CH₂Cl₂ (5 mL). This reaction was refluxed for 1 hr then cooled, diluted with Et₂O (20 mL) and filtered through Celite. The Celite was rinsed thoroughly with Et₂O (5 X 20 mL). The combined organic washings were dried (MgSO₄) and the solvent removed under reduced pressure. Flash

column chromatography on silica gel (4:1 hexanes:EtOAc, $R_f = 0.5$) yielded the product as crystalline needles (626 mg, 68%). **Method B:** 4-(hydroxymethyl) benzaldehyde (**3.13**) (3.5 g, 26 mmol) was dissolved in toluene (20 mL). To this was added 48% HBr (8 mL). The reaction was refluxed for 18 hrs. The reaction was quenched by pouring it onto ice. The resulting biphasic mixture was extracted with EtOAc (4 x 25 mL), and the combined organic extracts washed with 5% NaHCO₃ (2 x 25 mL), brine (2 x 25 mL), and dried over MgSO₄. The solvent was removed under reduced pressure and the product obtained by recrystallization in hexanes (4.5 g, 87 %): ¹H NMR (CDCl₃, 300 MHz) δ 10.2 (1H, s), 7.87 (2H, d, $J = 8.3$ Hz), 7.56 (2H, d, $J = 7.9$ Hz), 4.52 (2H, s). ¹³C NMR (CDCl₃, 300 MHz) δ 191.34, 144.04, 135.88, 129.95, 129.50, 31.93; MS m/z (relative intensity) 119 (96), 91 (100), 90 (33), 63 (12); HRMS calcd for C₈H₇OBr 197.9674, found 197.9674.

4-(hydroxymethyl) benzaldehyde (3.13): **3.13** was prepared by the procedure of Endo.¹⁵ Terephthalaldehyde (12.5 g, 93 mmol) was dissolved in a 4:1 mixture of ethanol:water (50 mL). 5% Pd/C was added (150 mg) to the mixture. The reaction was stirred under a H₂ balloon for 18 hrs. The crude reaction was filtered to remove the catalyst and extracted with EtOAc (3 X 50 mL). The product was obtained as a white solid by silica gel chromatography (3:2 hexanes:EtOAc, $R_f = 0.25$) (6 g, 48% yield): ¹H NMR (CDCl₃, 200 MHz) δ 9.99 (1H, s), 7.87 (2H, d, $J = 7.9$ Hz), 7.53 (2H, d, $J = 7.9$ Hz), 4.80 (2H, s), 2.19 (1H, br s); ¹³C NMR (CDCl₃, 300 MHz) δ 192.29, 148.04, 135.22, 129.84, 126.78,

64.08; MS m/z (relative intensity) 136 (68), 107 (100), 89 (38), 77 (72); HRMS calcd for $C_8H_8O_2$ 136.0524, found 136.0525.

2-[4-(bromomethyl)phenyl]-1,3-dioxolane (3.14): **3.11** (0.5 g, 2.51 mmol, 1 equiv) and 1,2-ethanediol (750 μ L, 0.842 g, 13.6 mmol, 5.1 equiv) were dissolved in benzene (6 mL) with a catalytic amount of *para*-toluene sulfonic acid monohydrate. The reaction was refluxed under a Dean-Stark apparatus for 8 hrs. The reaction was cooled and the crude washed with 5% $NaHCO_3$. The aqueous phase was further extracted with Et_2O (4 X 10 mL) and the organic phases combined. The combined organic extracts were washed with brine (2 x 25 mL) and dried over $MgSO_4$. The solvent was removed *in vacuo*. Flash chromatography on silica gel (4:1 hexanes:EtOAc, $R_f = 0.3$) yielded the product as a white solid (426 mg, 70%): 1H NMR ($CDCl_3$, 200 MHz) δ 7.43 (2H, d, $J = 8.2$ Hz), 7.38 (2H, d, $J = 8.8$ Hz), 5.78 (1H, s), 4.45 (2H, s), 4.02 (4H, m); ^{13}C NMR ($CDCl_3$, 300 MHz) δ 144.18, 135.98, 130.08, 129.59, 103.15, 65.23, 31.94; ; MS m/z (relative intensity) 223 (22), 119 (100), 91 (80), 73 (19); HRMS calcd for $C_{10}H_{11}O_2Br$ 240.9864, found 240.9876.

diethyl [4-(1,3-dioxolan-2-yl)benzyl]phosphonate (3.15): **3.14** (2 g, 8.22 mmol, 1 equiv) was dissolved in benzene (7 mL) with triethyl phosphite (7.05 mL, 6.83 g, 41.1 mmol, 5 equiv). The reaction was refluxed for 16 hrs. The solvent and excess phosphite were removed by vacuum distillation. Column chromatography on silica gel (EtOAc, $R_f=0.3$) yielded **3.15** as a clear colourless oil (2.10 g, 85%): 1H NMR ($CDCl_3$, 200 MHz) δ 7.43 (2H, d, $J = 7.8$ Hz), 7.32 (2H, d, $J = 7.8$ Hz), 5.79 (1H, s), 4.04 (8H, m), 3.16 (2H, d, $J = 21.5$ Hz), 1.24

(6H, t, $J = 7.0$ Hz) ^{13}C NMR (CDCl_3 , 300 MHz) δ 136.43, 130.34 (d, $J = 6.02$ Hz), 129.76, 126.56, 103.38, 65.15, 62.21, 33.36 (d, $J_{\text{CP}} = 138.6$ Hz), 16.25; ; MS m/z (relative intensity) 299 (67), 256 (58), 200 (54), 146 (58), 120 (70), 91 (100); HRMS calcd for $\text{C}_{14}\text{H}_{21}\text{O}_5\text{P}$ 299.1048, found 299.1062.

diethyl [[4-(1,3-dioxolan-2-yl)phenyl](difluoro)methyl]phosphonate

(3.16): A solution of **3.15** (1.74 g, 5.8 mmol, 1 equiv) and NFSi (4.16 g, 13.32 mmol, 2.3 equiv) in dry THF (15 mL) was cooled to -78 °C. To this was added NaHMDS (12.75 mL of a 1 M solution in THF, 12.75 mmol, 2.2 equiv) dropwise. The bath was removed and the reaction allowed to warm to room temperature over 3 hrs. The reaction was quenched with saturated NH_4Cl (5 mL) and diluted with water (20 mL). The THF was removed under reduced pressure and the remaining aqueous suspension extracted with Et_2O (3 x 25 mL). The combined organic extracts were dried over MgSO_4 , and the solvent removed by rotary evaporator. The product was obtained by silica gel chromatography (3:2 hexanes:EtOAc, $R_f = 0.3$) as a yellow oil (1.48 g, 76% yield): ^1H NMR (CDCl_3 , 300 MHz) δ 7.86 (2H, d, $J = 8.2$ Hz), 7.78 (2H, d, $J = 8.5$ Hz), 6.07 (1H, s), 4.26-4.50 (8H, m), 1.53 (6H, t, $J = 7.0$ Hz); ^{19}F NMR (CDCl_3 , 300 MHz) δ -31.32 (d, $J_{\text{F-P}} = 112.7$ Hz); ^{31}P NMR (CDCl_3 , 300 MHz) δ 7.57 (d, $J_{\text{F-P}} = 115.2$ Hz); ^{13}C NMR (CDCl_3 , 300 MHz) δ 140.92, 133.27 (m), 126.58, 126.26, 117.94 (dt, $J_{\text{CF}} = 263.2$ Hz, $J_{\text{CP}} = 218.3$ Hz), 102.86, 65.28, 64.81 (d, $J = 7.13$ Hz), 16.21(d, $J = 5.6$ Hz).

diethyl difluoro(4-formylphenyl)methylphosphonate (3.7): **3.16** (0.5 g, 1.49 mmol) was dissolved in a solution of THF: 5% HCl (10 mL of a 7:3 solution) and stirred for 12 hrs. The reaction was extracted with Et_2O (3 x 15

mL). The organic layers were combined and dried over MgSO_4 . The solvent was removed, and the product obtained by silica gel chromatography (3:2 hexanes:EtOAc, $R_f = 0.4$) as a clear colourless oil (0.39 g, 90% yield): ^1H NMR (CDCl_3 , 300 MHz) δ 10.09 (1H, s), 7.98 (2H, d, $J = 8.2$ Hz), 7.80 (2H, d, $J = 7.8$ Hz), 4.23 (4H, m), 1.33 (6H, t, $J = 7.0$ Hz); ^{19}F NMR (CDCl_3 , 300 MHz) δ -31.45 (d, $J_{\text{F-P}} = 112.7$ Hz); ^{31}P NMR (CDCl_3 , 300 MHz) δ 7.89 (d, $J_{\text{F-P}} = 116.2$ Hz).

ethyl hydrogen difluoro(4-formylphenyl)methylphosphonate (3.17):

3.16 (200 mg, 0.6 mmol, 1 equiv) was suspended in water (1.5 mL) containing NaOH (120 μL of a 10 M solution, 1.2 mmol, 2 equiv). The reaction was heated at 55 $^\circ\text{C}$ for 4 hrs until it became homogeneous. The reaction was cooled to 4 $^\circ\text{C}$ and washed with Et_2O (1 x 5 mL) and then acidified to $\text{pH} < 1$. The reaction was stirred for 12 hrs at room temperature. The product was extracted into CH_2Cl_2 (3 x 5 mL). The solvent was removed by reduced pressure and the product obtained as a thick clear oil (125 mg, 79% yield): ^1H NMR (CDCl_3 , 300 MHz) δ 10.06 (1H, s), 7.95 (2H, d, $J = 7.6$ Hz), 7.72 (2H, d, $J = 7.9$ Hz), 4.15 (2H, m), 1.29 (3H, t, $J = 7.0$ Hz); ^{19}F NMR (CDCl_3 , 300 MHz) δ -34.79 (d, $J_{\text{F-P}} = 117.4$ Hz); ^{31}P NMR (CDCl_3 , 300 MHz) δ 5.48 (d, $J_{\text{F-P}} = 116.8$ Hz).

3.2.2 Synthesis of Sulfamide Mitsunobu Reagent

3,3-dimethyl 1,2,5-thiadiazolidine 1,1-dioxide (3.21):²¹ Sulfamide (5 g, 52 mmol, 1 equiv) was dissolved in dry pyridine (50 mL) and refluxed under a N_2 atmosphere. The diamine **3.20** (5.59 mL, 4.70 g, 53 mmol, 1.02 equiv) was added dropwise via syringe over 1 hr. The mixture was refluxed for 20 hrs. The reaction was cooled and the solvent removed under reduced

pressure. The crude solid was dissolved in hot EtOAc (50 mL) and filtered to remove any insoluble impurities. The EtOAc was removed *in vacuo*. The product was obtained by recrystallization in EtOAc-hexanes as a white solid (3.65 g, 48% yield): ^1H NMR (CD_3OD , 200 MHz) δ 4.89 (2H, br s), 3.18 (2H, s), 1.33 (6H, s).

3,3-dimethyl 1,2,5-thiadiazolidine 1,1-dioxide triphenyl phosphine adduct (3.22):²⁰ Triphenyl phosphine (5.24 g, 20 mmol, 1 equiv) and the cyclic sulfamide **3.21** (3 g, 20 mmol, 1 equiv) were dissolved in dry THF (60 mL). DEAD (3.14 mL, 3.48 g, 20 mmol, 1 equiv) was added dropwise via syringe over 10 min. The reaction was stirred at room temperature for 3 hrs during which a white precipitate formed. The precipitate was filtered by suction, rinsed with dry Et_2O (3 x 50 mL), and dried under vacuum (7.48 g, 90% yield): ^1H NMR ($\text{DMSO}-d_6$, 200 MHz) δ 7.60 (15H, br m), 3.74 (2H, s), 1.33 (6H, s).

3.2.3 Synthesis of Protected Aryl Alcohol DFMP Compounds

[4-(bromomethyl)phenyl]methanol (3.29): Benzyl triethyl ammonium borohydride (10.10 g, 46 mmol, 2 equiv) was dissolved in dry CH_2Cl_2 (70 mL) and cooled to 0 °C. A solution of chloro trimethylsilane (5.90 mL, 5.05 g, 46 mmol, 2 equiv) in dry CH_2Cl_2 (24 mL) was added dropwise. The reaction was stirred for 15 min at which point a suspension of 4-(bromomethyl) benzoic acid (**3.10**) (5 g, 23 mmol, 1 equiv) was added dropwise via syringe. The ice bath was removed and the reaction allowed to warm to room temperature to stir for 5.25 hrs. The reaction was quenched by the addition of 10% NaHCO_3 (85 mL). The biphasic mixture was extracted with CH_2Cl_2 (4 x 125 mL). The combined organic

extracts were washed with 5% NaHCO₃ (3 x 100 mL), brine (2 x 100 mL), and dried (MgSO₄). The solvent was removed *in vacuo* and the product obtained by silica gel chromatography (7:3 hexanes:EtOAc, R_f = 0.4) as a white solid (1.98 g, 43% yield): ¹H NMR (CDCl₃, 300 MHz) δ 7.35 (4H, br s), 4.66 (2H, s), 4.57 (2H, s), 2.00 (1H, br s); ¹³C NMR (CDCl₃, 300 MHz) δ 140.92, 136.44, 128.56, 127.02, 64.17, 45.90;

4-(bromomethyl)benzyl [1-(*tert*-butyl)-1,1-diphenylsilyl] ether (3.30): Imidazole (1.5 g, 22 mmol, 2.2 equiv) was dissolved in dry DMF (2 mL) with *tert*-butyl-diphenyl silyl chloride (3.64 mL, 3.85 g, 14 mmol, 1.4 equiv). To this mixture was added, via syringe, a solution of alcohol **3.29** (2.01 g, 10 mmol, 1 equiv) in dry DMF (2 mL). The reaction was stirred for 20 min. The reaction was diluted with water (10 mL), and extracted with Et₂O (4 x 15 mL). The combined organic extracts were washed with brine (2 x 20 mL) and dried over MgSO₄. The solvent was removed *in vacuo* and the product isolated by silica gel chromatography (4:1 hexanes:EtOAc, R_f = 0.3) as a thick clear oil (4.49 g, quantitative): ¹H NMR (CDCl₃, 200 MHz) δ 7.66 (4H, m), 7.35 (10H, br m), 4.76 (2H, s), 4.56 (2H, s), 1.09 (9H, s).

diethyl [4-([1-(*tert*-butyl)-1,1-diphenylsilyl] oxymethyl)benzyl] phosphonate (3.31): The benzyl bromide **3.30** (1 g, 2.4 mmol, 1 equiv) was dissolved in triethyl phosphite (4 mL, 3.88 g, 23 mmol, 10 equiv). The reaction was refluxed for 18 hrs. The triethyl phosphite was removed *in vacuo* and the product obtained as a white solid by silica gel chromatography (EtOAc, R_f = 0.4) (1.12 g, 98% yield): ¹H NMR (CDCl₃, 300 MHz) δ 7.69 (4H, m), 7.40 (6H, m),

7.29 (4H, m), 4.76 (2H, s), 4.02 (4H, m), 3.16 (2H, d, $J = 21.7$ Hz), 1.25 (6H, t, $J = 7.0$ Hz), 1.09 (9H, s); ^{31}P NMR (CDCl_3 , 300 MHz) δ 28.28; ^{13}C NMR (CDCl_3 , 300 MHz) δ 139.73 (d, $J = 3.3$ Hz), 136.09 (d, $J = 4.2$ Hz), 135.58, 133.46, 129.86, 129.72, 127.86, 126.26 (d, $J = 3$ Hz), 65.38, 62.18 (d, $J = 6.4$ Hz), 33.44 (d, $J_{\text{CP}} = 137.7$), 26.96, 19.37, 16.42; ; MS m/z (relative intensity) 439 (100), 305 (24), 199 (44), 104 (38); HRMS calcd for $\text{C}_{28}\text{H}_{37}\text{O}_4\text{Si}$ ($-\text{C}_4\text{H}_9$) 439.1494, found 439.1494.

Diethyl [[4-([1-(*tert*-butyl)-1,1-diphenylsilyl]oxymethyl)phenyl] (difluoro) methyl] phosphonate (3.32): Phosphonate 3.31 (600 mg, 1.2 mmol, 1 equiv) and NFSi (830 mg, 2.66 mmol, 2.3 equiv) were dissolved in dry THF (50 mL) and cooled to -78 °C. NaHMDS (2.65 ml of a 1 M solution, 2.65 mmol, 2.2 equiv) was added dropwise to the solution. The mixture was stirred at -78 °C for 2 hrs and then stirred at room temperature for 16 hrs. The reaction was quenched by adding water (25 mL). The THF was removed under reduced pressure and the aqueous phase extracted with Et_2O (3 x 20 mL). The combined organic extracts were washed with brine (2 x 25 mL) and dried over MgSO_4 . The solvent was removed by rotary evaporation and the product obtained by silica gel chromatography (7:3 hexane:EtOAc, $R_f = 0.4$) as a white solid (328 mg, 51% yield): ^1H NMR (CDCl_3 , 300 MHz) δ 7.67 (6H, br m), 7.43 (8H, br m), 4.82 (2H, s), 4.21(4H, m), 1.34 (6H, t, $J = 7.04$), 1.13 (9H, s); ^{19}F NMR (CDCl_3 , 300 MHz) δ -31.97 (d, $J_{\text{F-P}} = 117.4$ Hz); ^{31}P NMR (CDCl_3 , 300 MHz) δ 8.09 (t, $J = 117.6$ Hz); ^{13}C NMR (CDCl_3 , 300 MHz) δ 144.16, 136.04 (m), 135.63, 133.29, 129.98, 127.99, 126.30, 125.98, 118.31 (dt, $J_{\text{CF}} = 263.2$ Hz, $J_{\text{CP}} = 218.8$ Hz), 65.80,

64.84, 26.96, 19.42, 16.42; ; MS m/z (relative intensity) 491 (52), 475 (100), 263 (41), 199 (67); HRMS calcd for $C_{28}H_{35}O_4Si$ ($-C_4H_9$) 475.1306, found 475.1293.

3-(Bromomethyl)benzyl (2-nitrobenzyl) ether (3.35): α,α' -Dibromo-*m*-xylene (2 g, 7.52 mmol, 1 equiv) and 2-nitrobenzyl alcohol (1.16 g, 7.52 mmol, 1 equiv) were dissolved in CH_2Cl_2 (40 mL). Silver (I) oxide (2.63 g, 11.10 mmol, 1.5 equiv) was added. The reaction was refluxed for 18 hrs and then cooled and the solvent removed *in vacuo*. The product was obtained by flash chromatography on silica gel (1:1 hexanes: CH_2Cl_2 , $R_f = 0.4$) as an off white solid (0.87 g, 34% yield): 1H NMR ($CDCl_3$, 300 MHz) δ 8.06 (1H, d, $J = 7.9$ Hz), 7.84 (1H, d, $J = 8.2$ Hz), 7.64 (1H, d, $J = 7.6$ Hz), 7.37 (5H, br m), 4.95 (2H, s), 4.65 (2H, s), 4.5 (2H, s); ^{13}C NMR ($CDCl_3$, 300 MHz) δ 146.80, 138.16, 137.64, 134.40, 133.30, 128.57, 128.36, 128.12, 127.79, 127.68, 127.22, 124.24, 72.28, 68.68, 33.24; MS m/z (relative intensity) 256 (26), 183 (48), 120 (84), 105 (100); HRMS calcd for $C_{15}H_{14}O_3NBr$ 336.0235, found 336.0244.

diethyl (3-[(2-nitrobenzyl)oxy]methylbenzyl)phosphonate (3.36): The dibenzyl ether **3.35** (865 mg, 2.57 mmol, 1 equiv) was dissolved in benzene (2 mL) and triethyl phosphite (2.2 mL, 2.14 g, 12.83 mmol, 5 equiv). The reaction was refluxed for 16 hrs. The benzene and excess phosphite were removed under reduced pressure. The product **3.36** was obtained by flash chromatography on silica gel (EtOAc, $R_f=0.4$) as a white solid (550 mg, 54% yield): 1H NMR ($CDCl_3$, 300 MHz) δ 8.08 (1H, d, $J = 8.2$ Hz), 7.87 (1H, d, $J = 8.2$ Hz), 7.66 (1H, t, $J = 7.6$ Hz), 7.45 (1H, t, $J = 7.6$ Hz), 7.30 (4H, m), 4.95 (2H, s), 4.66 (2H, s), 4.02 (4H, m), 3.17 (2H, d, $J = 21.7$ Hz), 1.24 (6H, t, $J = 7.0$ Hz); ^{31}P

NMR (CDCl₃, 300 MHz) δ 27.80; ¹³C NMR (CDCl₃, 300 MHz) δ 147.22, 138.04, 134.93, 133.68, 131.92 (d, *J* = 9.1 Hz), 129.29 (d, *J* = 6.0 Hz), 129.07 (d, *J* = 6.5 Hz), 128.75, 128.69 (d, *J* = 3.0 Hz), 128.02, 126.24, 124.61, 72.91, 62.20, 62.11, 33.62 (d, *J*_{CP} = 137.9 Hz), 16.34 (d, *J* = 5.6 Hz); MS *m/z* (relative intensity) 394 (45), 257 (74), 242 (66), 105 (100); HRMS calcd for C₁₉H₂₄O₆NP 394.1420, found 394.1437.

Diethyl difluoro(3-[(2-nitrobenzyl) oxy] methyl phenyl) methyl phosphonate (3.37): Phosphonate **3.36** (200 mg, 0.51 mmol, 1 equiv) and NFSi (349 mg, 1.12 mmol, 2.2 equiv) were dissolved in dry THF (7 mL). The mixture was cooled to -78 °C and NaHMDS (1.12 mL of a 1 M solution, 1.12 mmol, 2.2 equiv) was added dropwise. The reaction was stirred at -78 °C for 2 hrs followed by an additional 6 hrs at room temperature. The reaction was quenched with water (10 mL) and the THF removed under vacuum. The aqueous phase was extracted with Et₂O (3 x 15 mL). The combined organic extracts were washed with brine (2 x 30 mL) and dried over MgSO₄. After removal of the solvent under reduced pressure, the product was isolated, by silica gel chromatography (1:1 hexanes:EtOAc, *R_f* = 0.4) as an off white solid (142 mg, 68% yield): ¹H NMR (CDCl₃, 300 MHz) δ 8.09 (1H, d, *J* = 8.2 Hz), 7.86 (1H, d, *J* = 7.6 Hz), 7.42-7.71 (6H, br m), 4.98 (2H, s), 4.72 (2H, s), 4.20 (4H, m), 1.31 (6H, t, 7.0 Hz). ¹⁹F NMR (CDCl₃, 300 MHz) δ -32.52 (d, *J*_{F-P} = 117.4 Hz); ³¹P NMR (CDCl₃, 300 MHz) δ 7.79 (t, *J* = 116.0 Hz); ¹³C NMR (CDCl₃, 300 MHz) δ 147.14, 138.20, 134.63, 137.76 (m), 129.81, 128.62, 127.99, 126.19, 125.64 (m), 125.14 (m), 124.59, 117.88 (dt, *J*_{CF} = 263.2 Hz, *J*_{CP} = 217.8 Hz), 72.51, 68.99, 64.73 (d, *J* = 6.7 Hz),

16.20 (d, $J = 5.6$ Hz); MS m/z (relative intensity) 293 (70), 277 (58), 237 (20), 141 (100), 91 (26); HRMS calcd for $C_{19}H_{22}O_6F_2NP$ 430.1231, found 430.1210.

Diethyl 3-[(allyloxy)methyl]benzylphosphonate (3.41): To a suspension of sodium hydride (5.68 g of a 60% dispersion in mineral oil, 142 mmol, 1.5 equiv) in dry THF (750 mL) was added allyl alcohol (7.08 ml, 104 mmol, 1.1 equiv) and 15-Crown-5 (1.88 ml, 9.47 mmol, 0.10 equiv). This suspension was stirred for 15 min after which α,α' -dibromo-*m*-xylene (25 g, 94.7 mmol, 1.0 equiv) was added portionwise. This reaction was refluxed for 18 hrs under a N_2 atmosphere. The reaction was cooled to room temperature and then quenched by adding 25 mL of a saturated NH_4Cl solution. An additional 250 mL of water was added to dissolve any solids present. The THF was then removed under reduced pressure. The aqueous layer was extracted with Et_2O (3 X 250 mL). The combined organic extracts were dried ($MgSO_4$) and concentrated to leave an orange oil. Hi-vacuum distillation (75 °C, 50 μ) provided the desired intermediate which was contaminated with the starting material and the di-allyl substituted side product. The mixture was dissolved in benzene (75 mL) and reacted with triethyl phosphite (75ml, 441 mmol, 4.7 equiv) under reflux conditions for 12 hrs. The reaction was cooled and the benzene and triethyl phosphite removed under reduced pressure. The desired product was obtained by silica gel chromatography ($EtOAc$, $R_f=0.4$) as a clear oil (15.4 g, 54%): 1H NMR ($CDCl_3$) δ 7.21-7.31 (4H, m), 5.95 (1H, m), 5.26 (1H, $J = 33.2$ Hz), 5.22 (1H, d, $J = 26.4$ Hz), 4.50 (2H, s), 3.95-4.05 (6H, m), 3.15 (2H, d, $J = 21.5$ Hz), 1.24 (6H, t, $J = 6.8$ Hz); ^{31}P NMR ($CDCl_3$) δ 27.72; ^{13}C NMR ($CDCl_3$) δ 138.58 (d, $J =$ Hz),

134.67, 131.66 (d, $J = 9.1$ Hz), 128.99 (d, $J = 13.6$ Hz), 128.99, 128.47 (d, $J = 3.0$ Hz), 126.12 (d, $J = 3.5$ Hz), 116.90 (d, $J = 2.0$ Hz), 71.80, 71.02, 61.97 (d, $J = 7.1$ Hz), 33.60 (d, $J_{CP} = 137.9$ Hz), 16.30 (d, $J = 5.6$ Hz).

Diethyl [3-[(allyloxy)methyl]phenyl(difluoro)methyl]phosphonate (3.42): NFSi (9.34 g, 29.9 mmol, 2.1 equiv) and **3.41** (4.25 g, 14.2 mmol, 1 equiv) were combined and dissolved in dry THF (235 mL). The mixture was cooled to -78 °C. NaHMDS (29.2 mL of a 1 M solution in THF, 29.2 mmol, 2.05 equiv) was added dropwise over 15 min after which the cold bath was removed and the reaction allowed to warm to room temperature over 2 hrs. The reaction was quenched by the addition of water (75 mL) and the THF removed under reduced pressure. The aqueous layer was extracted with Et₂O (5 X 60 mL). The combined organic extracts were dried (MgSO₄) and concentrated to leave an orange oil. Column chromatography (CH₂Cl₂:EtOAc (95:5), $R_f = 0.3$) yielded the desired product as a pale yellow oil (3.83 g, 80%): ¹H NMR (CDCl₃) δ 7.40-7.60 (4H, m), 5.88-6.01 (1H, m), 5.28 (1H, d, $J = 33.2$ Hz), 5.24 (1H, d, $J = 26.4$ Hz), 4.56 (2H, s), 4.18 (4H, m), 4.04 (2H, m), 1.31 (6H, t, $J = 6.4$ Hz); ¹⁹F NMR (CDCl₃) δ -32.72 (d, $J_{FP} = 115.5$ Hz); ³¹P NMR (CDCl₃) δ 7.84 (t, $J_{PF} = 116.0$ Hz); ¹³C NMR (CDCl₃) δ 138.89 (d, $J = 1.5$ Hz), 134.50, 132.71 (dt, $J_{CF} = 30.3$ Hz, $J_{CP} = 13.6$ Hz), 129.84 (q, $J = 2.0$ Hz), 128.45 (d, $J = 1.0$ Hz), 125.25 (m), 118.04 (dt, $J_{CF} = 308.2$ Hz, $J_{CP} = 218.3$ Hz), 117.10, 71.43, 71.24, 64.70 (d, $J = 7.1$ Hz), 16.25 (d, $J = 5.0$ Hz)

Ethyl hydrogen [3-[(allyloxy)methyl] phenyl (difluoro) methyl] phosphonate (3.43): To a suspension of **3.42** (3.66 g, 10.96 mmol, 1 equiv) in

water (18.3 mL) was added an aqueous solution of sodium hydroxide (1.64 mL of a 10 M solution, 16.4 mmol, 1.5 equiv). This reaction was heated at 55 °C for 3 hrs until it became homogeneous. The reaction was cooled to 4 °C and washed with Et₂O (1 X 25 mL). The aqueous phase was then acidified to pH < 1 with a solution of 6 M hydrochloric acid. The resulting cloudy suspension was extracted with CH₂Cl₂ (5 x 25 mL). The combined organic washings were dried (MgSO₄) and concentrated under reduced pressure to give **3.43** as a thick orange oil (3.26 g, 97%): ¹H NMR (CDCl₃) δ 7.38-7.54 (4H, br m), 5.87-6.05 (1H, m), 5.27 (1H, d, *J* = 31.8 Hz), 5.23 (1H, d, *J* = 24.9 Hz), 4.55 Hz (2H, d), 4.05-4.14 (4H, m), 1.27 (3H, t, *J* = 6.8 Hz); ¹⁹F NMR (CDCl₃) δ -34.16 (d, *J*_{FP} = 118.1 Hz); ³¹P NMR (CDCl₃) δ 7.59 (t, *J*_{PF} = 120.3 Hz); ¹³C NMR (CDCl₃) δ 138.69 (d, *J* = 1.5 Hz), 134.28, 132.31 (dt, *J*_{CF} = 29.8 Hz, *J*_{CP} = 14.1 Hz), 129.55 (d, *J* = 2.0 Hz), 128.35 (d, *J* = 1.5 Hz), 125.25 (m), 117.55 (dt, *J*_{CF} = 299.6 Hz, *J*_{CP} = 224.3 Hz), 117.12, 71.27, 71.07, 65.09 (d, *J* = 7.1 Hz), 15.97, (d, *J* = 5.6 Hz);

Diethyl difluoro[3-(hydroxymethyl)phenyl]methylphosphonate (3.38):

The protected alcohol **3.42** (4 g, 12.0 mmol, 1 equiv), *p*-toluene sulfinic acid (2.43 g, 15.6 mmol, 1.3 equiv), and Pd(PPh₃)₄ (2.76 g, 2.4 mmol, 0.2 equiv) were dissolved in CH₂Cl₂ (320 mL) and refluxed for 18 hrs under a N₂ atmosphere. The reaction was cooled and the solvent removed *in vacuo*. The product was obtained via silica gel chromatography (3:1 EtOAc:hexanes, R_f = 0.25) as a thick orange-red oil (3.0 g, 85%): ¹H NMR (CDCl₃, 300 MHz) δ 7.58 (1H, s), 7.42 (4H, m), 4.68 (1H, br s), 4.61 (2H, s), 4.11 (4H, m), 1.26 (6H, t, *J* = 6.9 Hz); ¹⁹F NMR (CDCl₃, 300 MHz) δ -33.00 (d, *J*_{FP} = 117.2 Hz); ³¹P NMR (CDCl₃, 300 MHz) δ

7.54 (t, $J_{PF} = 117.4$ Hz); ^{13}C NMR (CDCl_3 , 300 MHz) δ 141.89, 131.83 (m), 128.78, 128.02, 124.35 (m), 123.87 (m), 117.63 (dt, $J_{CF} = 263.2$ Hz, $J_{CP} = 218.8$ Hz), 64.58 (d, $J = 7.1$ Hz), 63.38, 15.75 (d, $J = 5.6$ Hz), 117.12, 71.27, 71.07, 65.09 (d, $J = 7.1$ Hz), 15.97, (d, $J = 5.6$ Hz); MS m/z (relative intensity) 294 (23), 157 (100), 140 (52), 109 (39); HRMS calcd for $\text{C}_{12}\text{H}_{17}\text{O}_4\text{F}_2\text{P}$ 294.0832, found 294.0832.

3.2.4 Synthesis of Dess-Martin Reagent^{42,43}

1, 1, 1-triacetoxy-1,1-dihydro-1,2-benz-iodoxol-3(1H)-one (Dess-Martin periodinane: 2-iodo-benzoic acid (4.26 g, 17.20 mmol, 1 equiv) was suspended in H_2SO_4 (40 mL of a 0.730 M solution). KBrO_3 (3.80 g, 22.8 mmol, 1.3 equiv) was portionwise over 30 min as the reaction was heated to 65 °C. The reaction was stirred at 65 °C for 4 hrs. The reaction was cooled to 0 °C and filtered under suction. The filtrate was washed with water, (2 x 40 mL), ethanol (2 x 40 mL), and Et_2O (2 x 40 mL). The solid was then dissolved in acetic anhydride (15 mL) and acetic acid (13 mL). This reaction was heated at 95 °C for 2 hrs. The reaction was cooled, sealed, covered, and allowed to sit for 1 week. The product precipitated out of solution as a white solid, which was isolated by filtration under and Ar atmosphere. The product was washed with dry Et_2O (3 x 40 mL) and dried under a stream of Ar gas (4.48 g, 62% yield): ^1H NMR (CDCl_3) δ 8.29 (2H, d, $J = 8.0$ Hz), 8.10 (1H, t, $J = 8.0$ Hz), 7.90 (1H, t, $J = 7.5$ Hz), 2.31 (3H, s), 1.99 (6H, s).

3.2.5 On Polymer Reactions - Synthesis of Wittig Library

Attachment of 3.43 to the polymer: The functionalized polymer **2.49** (8.65 g at 0.4 mmol/g, 3.5 mmol, 1 equiv) was dissolved in 30 mL of dry THF. To this was added triethylamine (2.41 mL, 1.75 g, 17.3 mmol, 5 equiv). In a separate round bottom flask, **3.43** (3.18 g, 10.4 mmol, 3 equiv) and triphenyl phosphine (2.72 g, 10.4 mmol, 3 equiv) were dissolved in dry THF (16 mL). DIAD (diisopropylazidodicarboxylate, 2.04 mL, 2.10 g, 10.4 mmol, 3 equiv) was added dropwise to the solution of **3.43** and triphenylphosphine. The polymer solution was then transferred via syringe to the solution of **3.43**, triphenylphosphine, and DIAD. The reaction was stirred for 18 hrs at room temperature. The reaction was terminated by precipitation of the polymer in a stirred solution of MeOH-water (9:1). The polymer was filtered under suction and dried under hi-vacuum. Recovery of the polymer was 96%+: $^1\text{H NMR}$ (CDCl_3) δ 7.38-7.62 (4H, br m), 5.95 (1H, m), 5.27 (1H, d, $J = 33.7$ Hz), 5.22 (1H, d, $J = 26.9$ Hz), 4.54 (2H, br s), 4.38 (2 H, br m), 4.18 (4 H, br m), 4.02 (2H, d, $J = 5.4$ Hz), 3.40 (2 H, br s); $^{19}\text{F NMR}$ (CDCl_3) δ -32.41 (d, $J_{\text{F-P}} = 115.5$ Hz); $^{31}\text{P NMR}$ (CDCl_3) δ 7.86 (t, $J_{\text{PF}} = 119.3$ Hz)

Removal of the allyl group from 3.44 (3.45): The loaded polymer **3.44** (5.94 g at 0.4 mmol/g, 2.38 mmol, 1 equiv), *p*-toluene sulfinic acid (484 mg, 3.10 mmol, 1.3 equiv), and $\text{Pd}(\text{PPh}_3)_4$ (549 mg, 0.48 mmol, 0.2 equiv) were dissolved in CH_2Cl_2 (60 mL). The reaction was gently refluxed for 18 hrs. Recovery of the polymer was achieved by cooling of the reaction and precipitation in a stirred solution of MeOH-water (9:1). The polymer was filtered under suction and dried under hi-vac. Recovery of the polymer was greater than 96%: $^1\text{H NMR}$ (CDCl_3)

δ 7.40-7.85 (4H, br m), 4.62 (2H, s), 4.38 (2 H, br m), 4.18 (4 H, br m), 3.40 (2 H, s); ^{19}F NMR (CDCl_3) δ -32.54 (d, $J_{\text{FP}} = 117.2$ Hz), -32.74 (d, $J_{\text{FP}} = 108.6$ Hz); ^{31}P NMR (CDCl_3) δ 7.94 (t, $J_{\text{PF}} = 117.3$ Hz).

On Polymer Oxidation of Benzylic Alcohol of 3.45 (3.46): A solution of polymer 3.45 (3 g at 0.4 mmol/g, 1.2 mmol, 1.0 equiv) in dry CH_2Cl_2 (15 mL) was added to a solution of the Dess-Martin reagent (891 mg, 2.1 mmol, 1.75 equiv) in dry CH_2Cl_2 (6.75 mL). This reaction was stirred at room temperature for 2 hrs after which the polymer was precipitated by the dropwise addition of the reaction to a stirred solution of MeOH-water (9:1). The polymer was filtered under suction and dried under hi-vac. Recovery of the polymer was in excess of 96%: ^1H NMR (CDCl_3) δ 10.02 (1H, s), 8.13 (1H, s), 7.98 (1H, d, $J = 7.8$ Hz), 7.88 (1H, d, $J = 7.3$ Hz), 7.60 (1H, t, $J = 8.3$ Hz), 4.38 (2 H, br m), 4.18 (4 H, br m), 3.40 (2 H, br s); ^{19}F NMR (CDCl_3) δ -33.20 (d, $J_{\text{FP}} = 113.8$ Hz); ^{31}P NMR (CDCl_3) δ 8.01 (t, $J_{\text{PF}} = 115.8$ Hz).

General procedure for Wittig reaction on the polymer: KH (64 mg of a 30% suspension, 0.48 mmol, 4 equiv) was weighed into a dry round bottom flask and rinsed with hexanes (2 x 5 mL) and suspended in dry THF (1.5 mL). Phosphonium salt (0.54 mmol, 4.5 equiv) and 18-crown-6 (6.3 mg, 0.024 mmol, 0.2 equiv) were added to the flask, and the reaction stirred under N_2 for 1 hr. A THF solution of polymer 3.46 (400 mg at 0.3 mmol/g, 0.12 mmol, 1 equiv, in 1 mL of THF) was added dropwise to the mixture. The flask was sealed with a Teflon cap and stirred for 24 hrs. The reaction was quenched by adding it dropwise to a stirred mixture of MeOH:water (9:1). The polymer was filtered under suction and

dried under hi vacuum. Polymer recovery was greater than 90% for all reactions. General procedure for cleavage/deprotection of Wittig reaction products. The polymer from the Wittig reaction (400 mg at 0.3 mmol/g, 0.12 mmol, 1 equiv) was dissolved in dry CH_2Cl_2 (1.5 mL). TMSBr (158 μL , 183 mg, 1.2 mmol, 10 equiv) was added dropwise via syringe. The reactions were sealed and allowed to stir for 3 days at room temperature. The solvent and excess TMSBr were removed under reduced pressure. Three additional rinse cycles were performed where the crude was redissolved in CH_2Cl_2 (3 mL) and dried on a rotary evaporator in order to remove all traces of TMSBr. The polymer was redissolved in CH_2Cl_2 (2 mL) and precipitated in a stirred MeOH-water mixture (9:1). The precipitated reactions were stirred for 18 hrs after which the polymer was removed by filtration under vacuum and the filtrate concentrated.

General procedure for the purification of the phosphonic acids on Supelco LC-NH₂ columns: Purification of phosphonic acids **3.61-3.82** was accomplished using 3 mL columns prepacked with 500 mg of LC-NH₂ adsorbent (Supelco). The columns were rinsed with THF (6mL) prior to use. The crude material, following filtration of the polymer and removal of the solvent, from a deprotection reaction was dissolved in THF (0.5 mL) and applied to the column. The solution of crude was allowed to settle into the column bed by gravity after which the column was rinsed, under pressure supplied by a syringe, with THF (10 mL), MeOH (8 mL), and water (8 mL). Elution was performed using passing a solution of ammonium hydroxide (6 mL of a 0.5 M solution) under pressure.

The solution was lyophilized until a constant weight was obtained to remove the solvent and excess NH_4OH .

Difluoro 3-[(E)-2-phenyl-1-ethenyl]phenylmethylphosphonic acid, diammonium salt (3.61): Yield: 33 mg (77.5 mg/g); ^1H NMR (D_2O) δ 7.64 (1H, s), 7.44 (1H, d, $J = 8.3$ Hz), 7.33 (1H, s), 7.09-7.23 (7H, m), 6.54 (1H, s); ^{19}F NMR (D_2O) δ -31.94 (d, $J_{\text{FP}} = 101.7$ Hz), -31.12 (d, $J_{\text{FP}} = 106.1$ Hz); ^{31}P NMR (D_2O) δ 6.04 (t, $J_{\text{PF}} = 101.2$ Hz), 5.94 (t, $J_{\text{PF}} = 101.2$ Hz); FAB m/z 309. HPLC retention time = 15.78 min, 15.88 min. Purity: 100% (HPLC).

Difluoro 3-[(E/Z)-2-(4-methylphenyl)-1-ethenyl] phenylmethyl phosphonic acid, diammonium salt (3.62): Yield: 24 mg (60 mg/g); ^1H NMR (D_2O) δ 7.71 (1H, s), 7.55 (1H, d, $J = 7.7$ Hz), 7.43 (2H, m), 7.37 (1H, m), 7.18 (2H, m), 7.09 (1H, d, $J = \text{Hz}$), 7.10 (1H, d, $J = \text{Hz}$), 6.59 (1H, s), 2.24 (2H, s), 2.18 (1H, s); ^{19}F NMR (D_2O) δ -29.58 (d, $J_{\text{FP}} = 93.3$ Hz), -29.66 (d, $J_{\text{FP}} = 93.3$ Hz); ^{31}P NMR (D_2O) δ 2.70 (t, $J_{\text{PF}} = 94.3$ Hz), 2.68 (t, $J_{\text{PF}} = 94.3$ Hz); FAB m/z 323. HPLC retention time = 16.16 min, 16.29 min. Purity: 90% (HPLC).

Difluoro 3-[(E/Z)-2-(2-methylphenyl)-1-ethenyl] phenyl methyl phosphonic acid, diammonium salt (3.63): Yield: 26 mg (65 mg/g); ^1H NMR (D_2O) δ 7.86 (1H, s), 7.71 (2H, m), 7.50 (2H, m), 7.29 (2H, s), 7.16 (2H, m), 6.80 (1H, m), 2.44 (2H, s), 2.28 (1H, s); ^{19}F NMR (D_2O) δ -29.88 (d, $J_{\text{FP}} = 93.3$ Hz); ^{31}P NMR (D_2O) δ 2.62 (t, $J_{\text{PF}} = 94.3$ Hz), 2.53 (t, $J_{\text{PF}} = 94.3$ Hz); FAB m/z 323. HPLC retention time = 16.20 min. Purity: 100% (HPLC).

3-[(E/Z)-2-(4-bromophenyl)-1-ethenyl] phenyl (difluoro) methyl phosphonic acid, diammonium salt (3.64): Yield: 31 (77.5 mg/g); ^1H NMR

(D₂O) δ 7.84 (1H, s), 7.67 (1H, d, J = 7.9 Hz), 7.54 (3H, m), 7.43 (1H, d, J = 8.3 Hz), 7.28 (1H, s), 7.19 (1H, d, J = 8.3 Hz), 6.78 (1H, d, J = 12.4 Hz), 6.67 (1H, d, J = 12.4 Hz); ¹⁹F NMR (D₂O) δ -29.68 (d, J_{FP} = 93.3 Hz), -29.71 (d, J_{FP} = 93.3 Hz); ³¹P NMR (D₂O) δ 2.75 (t, J_{PF} = 89.3 Hz); FAB m/z 389. HPLC retention time = 16.38 min, 16.62 min. Purity: 99% (HPLC).

3-[(E/Z)-2-(4-chlorophenyl)-1-ethenyl] phenyl(difluoro) methyl phosphonic acid, diammonium salt (3.65): Yield: 28 mg (70 mg/g); ¹H NMR (D₂O) δ 7.82 (1H, s), 7.65 (1H, d, J = 8.7 Hz), 7.58 (1H, d, J = 8.1 Hz), 7.54 (1H, m), 7.47 (1H, m), 7.41 (1H, d, J = 8.1 Hz), 7.26 (2H, m), 6.75 (1H, d, J = 12.2 Hz), 6.68 (1H, d, J = 12.2 Hz); ¹⁹F NMR (D₂O) δ -29.61 (d, J_{FP} = 93.3 Hz), -29.66 (d, J_{FP} = 93.3 Hz); ³¹P NMR (D₂O) δ 2.69 (t, J_{PF} = 91.8 Hz); FAB m/z 343. HPLC retention time = 16.26 min, 16.47 min. Purity: 99% (HPLC).

Difluoro 3-[(E/Z)-2-(4-fluorophenyl)-1-ethenyl] phenyl methyl phosphonic acid, diammonium salt (3.66): Yield: 27 (67.5 mg/g); ¹H NMR (D₂O) δ 7.83 (1H, m), 7.65 (2H, m), 7.48-7.55 (2H, m), 7.40 (2H, m), 7.17 (1H, t, J = 8.8 Hz), 7.01 (1H, t, J = 9.0 Hz), 6.73 (1H, d, J = 3.4 Hz); ¹⁹F NMR (D₂O) δ -29.93 (d, J_{FP} = 93.3 Hz), -38.06 (s), -38.66(s); ³¹P NMR (D₂O) δ 2.54 (t, J_{PF} = 96.8 Hz); FAB m/z 327. HPLC retention time = 15.89, 16.01 min. Purity: 97% (HPLC).

Difluoro 3-[(E)-2-(4-nitrophenyl)-1-ethenyl]phenylmethylphosphonic acid, diammonium salt (3.67): Yield: 32 mg (80 mg/g); ¹H NMR (D₂O) δ 8.07 (1H, d, J = 6.8 Hz), 7.96 (2H, d, J = 7.7 Hz), 7.72 (1H, s), 7.60 (1H, d, J = 7.7 Hz), 7.41 (1H, m), 7.32 (1H, d, J = 8.1 Hz), 7.18 (1H, m), 6.81 (1H, d, J = 12.0

Hz), 6.67 (1H, d, $J = 12.0$ Hz); ^{19}F NMR (D_2O) δ -30.36 (d, $J_{\text{FP}} = 96.9$ Hz), -30.40 (d, $J_{\text{FP}} = 96.9$ Hz); ^{31}P NMR (D_2O) δ 2.35 (t, $J_{\text{PF}} = 94.3$ Hz); FAB m/z 354. HPLC retention time = 15.72 min, 15.92 min. Purity: 95% (HPLC).

Difluoro 3-[(1E/Z)-4-methyl-1,3-pentadienyl]phenylmethylphosphonic acid, diammonium salt (3.68): Yield: 25 mg (62.5 mg/g); ^1H NMR (D_2O) δ 7.73 (1H, s), 7.55 (1H, d, $J = 7.5$ Hz), 7.45 (2H, m), 7.23 (1H, m), 6.58 (1H, d, $J = 15.8$ Hz), 6.11 (1H, d, $J = 11.3$ Hz), 1.90 (3H, s), 1.86 (3H, s); ^{19}F NMR (D_2O) δ -29.83 (d, $J_{\text{FP}} = 93.3$ Hz); ^{31}P NMR (D_2O) δ 2.64 (t, $J_{\text{PF}} = 94.3$ Hz); FAB m/z 287. HPLC retention time = 15.82 min. Purity: 95% (HPLC).

Difluoro 3-[(1E/Z,3E/Z)-4-phenyl-1,3-butadienyl] phenylmethyl phosphonic acid, diammonium salt (3.69): Yield: 19.8 (49.5 mg/g); ^1H NMR (D_2O) δ 6.99-7.73 (10H, m), 6.72 (3H, m); ^{19}F NMR (D_2O) δ -9.73 (d, $J_{\text{FP}} = 86.2$ Hz); ^{31}P NMR (D_2O) δ 2.57 (t, $J_{\text{PF}} = 94.3$ Hz); FAB m/z 335. HPLC retention time = 16.51 min, 16.85. Purity: 95% (HPLC).

3-[(E/Z)-1-butenyl]phenyl(difluoro)methylphosphonic acid, diammonium salt (3.70): Yield: 9.8 mg (24.5 mg/g); ^1H NMR (D_2O) δ 7.34-7.45 (4H, m), 6.39 (1H, d, $J = 6.39$), 5.71 (1H, m), 2.25 (2H, m), 0.94 (3H, t, $J = 7.5$ Hz); ^{19}F NMR (D_2O) δ -29.52 (d, $J_{\text{FP}} = 93.3$ Hz); ^{31}P NMR (D_2O) δ 2.80 (t, $J_{\text{PF}} = 91.8\text{Hz}$); FAB m/z 261. HPLC retention time = 15.20 min. Purity: 100% (HPLC).

Difluoro 3-[(E/Z)-4-phenyl-1-butenyl]phenylmethylphosphonic acid, diammonium salt (3.71): Yield: 17 mg (42.5 mg/g); ^1H NMR (D_2O) δ 7.24-7.52 (9H, m), 6.53 (1H, d, $J = 12.2$ Hz), 5.82 (1H, m), 2.82 (2H, t, $J = 7.7$ Hz), 2.79 (2H, q, $J = 7.1$ Hz); ^{19}F NMR (D_2O) δ -29.30 (d, $J_{\text{FP}} = 89.8$ Hz); ^{31}P NMR (D_2O) δ

2.78 (t, $J_{PF} = 89.3$ Hz); FAB m/z 337. HPLC retention time = 16.35 min. Purity: 100% (HPLC).

3-[(*E/Z*)-2-cyano-1-ethenyl]phenyl(difluoro)methylphosphonic acid, diammonium salt (3.72): Yield: 29 mg (72.5 mg/g); ^1H NMR (D_2O) δ 7.70 (1H, s), 7.59 (1H, d, $J = 7.0$ Hz), 7.52 (2H, m), 7.42 (1H, t, $J = 7.7$ Hz), 6.10 (1H, d, $J = 16.7$); ^{19}F NMR (D_2O) δ -30.45 (d, $J_{FP} = 93.3$ Hz); ^{31}P NMR (D_2O) δ 2.33 (t, $J_{PF} = 94.3$ Hz); FAB m/z 258. HPLC retention time = 9.40 min, 10.07 min. Purity: 91% (HPLC).

3-[(*E/Z*)-3-ethoxy-3-oxo-1-propenyl] phenyl(difluoro) methyl phosphonic acid, diammonium salt (3.73): Yield: 21 mg (52.5 mg/g); ^1H NMR (D_2O) δ 7.67-7.86 (4H, m), 7.54 (1H, t, $J = 7.5$ Hz), 6.63 (1H, d, $J = 16.0$ Hz), 4.28 (2H, q, $J = 6.8$ Hz), 1.33 (3H, t, $J = 7.3$ Hz); ^{19}F NMR (D_2O) δ -30.85 (d, $J_{FP} = 96.9$ Hz), -30.93 (d, $J_{FP} = 96.9$ Hz); ^{31}P NMR (D_2O) δ 2.14 (t, $J_{PF} = 96.8$ Hz); FAB m/z 305. HPLC retention time = 14.66 min. Purity: 97% (HPLC).

3-[(*E/Z*)-3-(allyloxy)-3-oxo-1-propenyl] phenyl (difluoro) methyl phosphonic acid, diammonium salt (3.74): Yield: 35 mg (87.5 mg/g); ^1H NMR (D_2O) δ 7.87 (1H, s), 7.81 (1H, d, $J = 15.8$ Hz), 7.71 (2H, m), 7.53 (1H, t, $J = 7.7$ Hz), 6.65 (1H, d, $J = 16.0$ Hz), 6.04 (1H, m), 5.41 (1H, d, $J = 17.5$ Hz), 5.32 (1H, d, $J = 10.5$ Hz), 4.75 (2H, d, $J = 4.1$ Hz); ^{19}F NMR (D_2O) δ -30.28 (d, $J_{FP} = 93.3$ Hz); ^{31}P NMR (D_2O) δ 2.42 (t, $J_{PF} = 91.8$ Hz); FAB m/z 317. HPLC retention time = 15.00 min. Purity: 100% (HPLC).

3-[(*E/Z*)-3-(benzyloxy)-3-oxo-1-propenyl] phenyl(difluoro) methyl phosphonic acid, diammonium salt (3.75): Yield: 31 mg (77.5 mg/g); ^1H NMR

(D₂O) δ 7.82 (1H, s), 7.75 (1H, d, J = 16.0 Hz), 7.67 (2H, m), 7.41-7.52 (6H, m), 6.59 (1H, d, J = 16.2 Hz), 5.25 (2H, s); ¹⁹F NMR (D₂O) δ -31.09 (d, J_{FP} = 96.9 Hz); ³¹P NMR (D₂O) δ 2.03 (t, J_{PF} = 96.8 Hz); FAB m/z 367. HPLC retention time = 15.84 min. Purity: 92% (HPLC).

Difluoro 3-[(E/Z)-2-(1-naphthyl)-1-ethenyl]phenylmethylphosphonic acid, diammonium salt (3.76): Yield: 33 mg (82.5 mg/g); ¹H NMR (D₂O) δ 7.11-7.92 (11H, m), 6.86 (1H, m), 6.72 (1H, m); ¹⁹F NMR (D₂O) δ -29.82 (d, J_{FP} = 93.3 Hz), -29.92 (d, J_{FP} = 93.3 Hz); ³¹P NMR (D₂O) δ 2.54 (t, J_{PF} = 94.3 Hz); FAB m/z 359. HPLC retention time = 16.47 min, 16.59 min. Purity: 93% (HPLC).

3-[(E/Z)-2-(4-ethoxyphenyl)-1-ethenyl] phenyl (difluoro) methyl phosphonic acid, diammonium salt (3.77): Yield: 33 mg (82.5 mg/g); ¹H NMR (D₂O) δ 7.82 (1H, s), 7.67 (1H, d, J = 8.5 Hz), 7.61, (2H, d, J = 8.8 Hz), 7.53 (1H, m), 7.49 (2H, m), 7.29 (1H, m), 7.21 (1H, m), 7.04 (1H, d, J = 8.5 Hz), 4.16 (2H, q, J = 7.7 Hz), 1.40 (3H, t, J = 7.5 Hz); ¹⁹F NMR (D₂O) δ -29.78 (d, J_{FP} = 93.3 Hz); ³¹P NMR (D₂O) δ 2.67 (t, J_{PF} = 94.3 Hz); FAB m/z 353. HPLC retention time = 16.25 min. Purity: 98% (HPLC).

Difluoro 3-[(E/Z)-3-methoxy-3-oxo-1-propenyl]phenylmethyl phosphonic acid, diammonium salt (3.78): Yield: 32 mg (80 mg/g); ¹H NMR (D₂O) δ 7.84 (1H, s), 7.66-7.77 (3H, m), 7.53 (1H, t, J = 7.9 Hz), 6.62 (1H, d, J = 16.0), 3.82 (3H, s); ¹⁹F NMR (D₂O) δ -30.74 (d, J_{FP} = 96.9 Hz); ³¹P NMR (D₂O) δ 2.24 (t, J_{PF} = 96.8 Hz); FAB m/z 291. HPLC retention time = 13.93 min. Purity: 80% (HPLC).

3-[(E)-3-(dimethylamino)-1-propenyl] phenyl(difluoro) methyl phosphonic acid, diammonium salt (3.79): Yield: 12 mg (30 mg/g); ^1H NMR (D_2O) δ 7.62 (1H, d, $J = 7.5$ Hz), 7.53 (2H, m), 7.36 (1H, d, $J = 7.7$ Hz), 7.10 (1H, d, $J = 11.5$ Hz), 7.59 (1H, m), 4.06 (2H, d, $J = 7.0$ Hz), 2.84 (6H, s); ^{19}F NMR (D_2O) δ -29.77 (d, $J_{\text{FP}} =$ Hz); ^{31}P NMR (D_2O) δ 2.68 (t, $J_{\text{PF}} = 91.8$ Hz); FAB m/z 290. HPLC retention time = 4.24 min. Purity: 72% (HPLC).

3-[(E/Z)-2-chloro-1-ethenyl]phenyl(difluoro)methylphosphonic acid, diammonium salt (3.80): Yield: 30 mg (75 mg/g); ^1H NMR (D_2O) δ 7.87 (1H, m), 7.44-7.64 (2H, m), 6.96 (1H, q, $J = 13.7$ Hz), 6.85 (1H, d, $J = 7.9$ Hz), 6.46 (1H, d, $J = 8.1$ Hz); ^{19}F NMR (D_2O) δ -29.92 (d, $J_{\text{FP}} = 93.3$ Hz), -29.95 (d, $J_{\text{FP}} = 93.3$ Hz); ^{31}P NMR (D_2O) δ 2.62 (t, $J_{\text{PF}} = 91.8$ Hz), 2.58 (t, $J_{\text{PF}} = 94.3$ Hz); FAB m/z 267. HPLC retention time = 14.42 min, 14.65 min. Purity: 99% (HPLC).

Difluoro-3-[(E/Z)-2-(4-methoxyphenyl)-1-ethenyl] phenylmethyl phosphonic acid, diammonium salt (3.81): Yield: 27 mg (67.5 mg/g); ^1H NMR (D_2O) δ 7.82 (1H, s), 7.66 (1H, d, $J = 8.1$ Hz), 7.62 (2H, d, $J = 8.5$ Hz), 7.53 (1H, d, $J =$), 7.49 (1H, m), 7.31 (1H, d, $J =$), 7.20 (1H, d, $J =$), 7.05 (2H, d, $J =$), 3.87 (3H, s); ^{19}F NMR (D_2O) δ -29.47 (d, $J_{\text{FP}} = 93.3$ Hz); ^{31}P NMR (D_2O) δ 2.80 (t, $J_{\text{PF}} = 91.8$ Hz); FAB m/z 339. HPLC retention time = 15.85 min. Purity: 87% (HPLC).

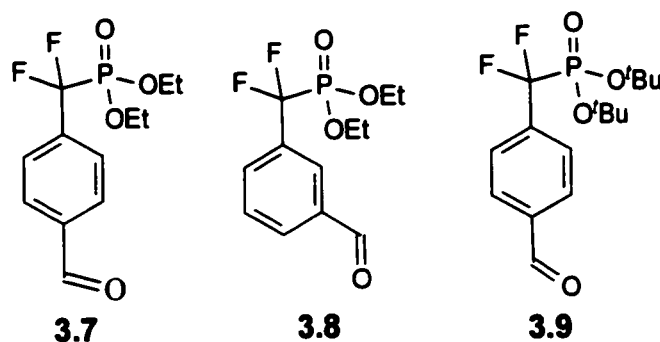
3-[(E/Z)-2-(4-butoxyphenyl)-1-ethenyl] phenyl (difluoro) methyl phosphonic acid, diammonium salt (3.82): Yield: 22 mg (55 mg/g); ^1H NMR (D_2O) δ 7.82 (1H, m), 7.63 (3H, m), 7.48 (3H, m), 7.31 (1H, m), 7.20 (1H, m), 7.07 (1H, m), 4.12 (2H, m), 1.76 (2H, m), 1.47 (2H, m), 0.96 (3H, m); ^{19}F NMR

(D₂O) δ -29.49 (d, $J_{FP} = 93.3$ Hz); ³¹P NMR (D₂O) δ 2.75 (t, $J_{PF} = 91.8$ Hz); FAB m/z 381. HPLC retention time = 17.52 min. Purity: 100% (HPLC).

3.3 Results and Discussion

3.3.1 Studies on Model Compounds in Solution.

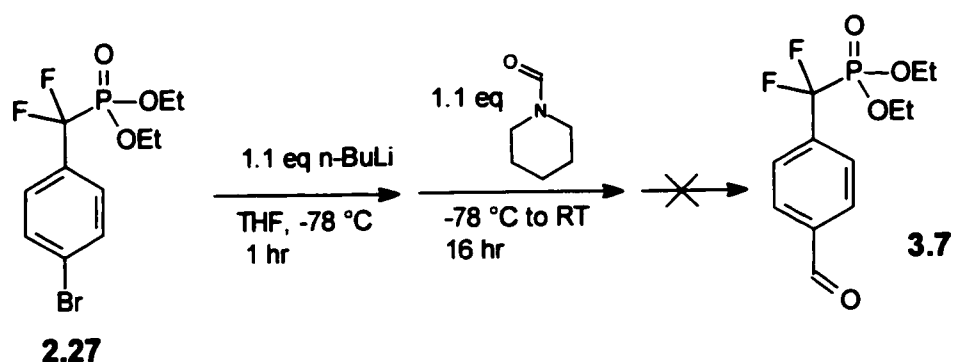
Before trying Wittig reactions on the polymer, we had to develop the conditions in solution. The first step was to develop a method for readily constructing aldehydes **3.7** and **3.8**. Even though we were more interested in the *meta* substituted aldehyde, for many of our studies, the *para*-aldehyde **3.7** served as our model substrate since many of the starting materials were already available in the Taylor lab. There was no reason to believe that the position of the aldehyde group relative to the DFMP group would affect its reactivity in the Wittig reaction.



Aldehyde **3.9** had been prepared before by Burke and coworkers by a Bouveault reaction by reacting *t*-butyl protected DFMP aryl bromide with *n*-butyl lithium followed by the addition of ethyl formate. Unfortunately, the yield was very low (35%). We attempted the Bouveault reaction on the *para*-substituted aryl bromide **2.27** using a modified version of Burke's procedure (Scheme 3.4).¹²

The *para* bromo DFMP compound **2.27** was reacted with *n*-butyl lithium at -78 °C after which 1.1 equivalent of *N*-formyl piperidine, which is a common reagent used for Bouveault reaction,^{13,14} was added and the reaction allowed to

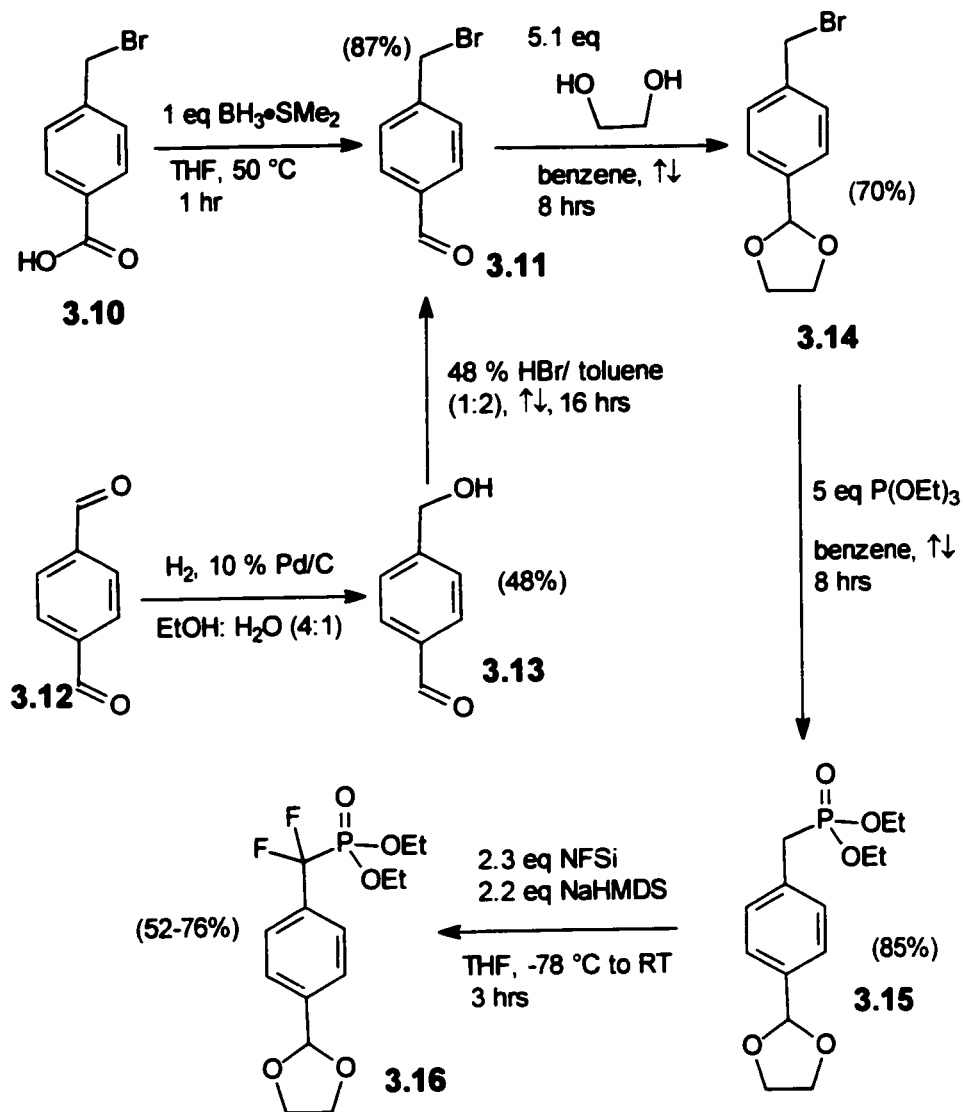
warm to room temperature over 16 hours. The crude ^{19}F NMR of the reaction showed a series of singlets as opposed to the expected doublets of both the starting material and product, indicating decomposition of the DFMP functionality. The ability of Burke to obtain the desired compound using the Bouveault reaction, albeit in low yield, was probably due to the greater stability of the *t*-butyl esters to the reaction conditions than the ethyl esters. It was apparent that an alternative approach to **3.7** was required.



Scheme 3.4. Attempted Bouveault reaction on aryl bromide **2.27**.

To prepare **3.7**, we began with 4-(bromomethyl) benzoic acid (**3.10**) which was reduced by reaction with 1 equivalent of borane-dimethyl sulfide complex in THF (Scheme 3.5). Oxidation of the borane adduct with 1 equivalent of pyridinium chlorochromate in CH_2Cl_2 yielded the 4-(bromomethyl) benzaldehyde intermediate in a 72% yield. Due to the high cost of **3.10**, a less expensive preparation of 4-(bromomethyl) benzaldehyde (**3.11**) was also examined. This alternate route began with inexpensive terephthalaldehyde (**3.12**) which was reduced to 4-(hydroxymethyl) benzaldehyde (**3.13**) in 48% yield using the procedure of Endo et al.¹⁵ Conversion of **3.13** to **3.11** was achieved in 87% yield by refluxing **3.13** in a biphasic solvent system of 2:1 toluene:48% HBr. The

aldehyde moiety of **3.11** was protected as the acetal by refluxing with 5.1 equivalents of 1,2-ethanediol in benzene for 8 hours under a Dean-Stark apparatus to obtain **3.14** in yields ranging from 48 to 70%.

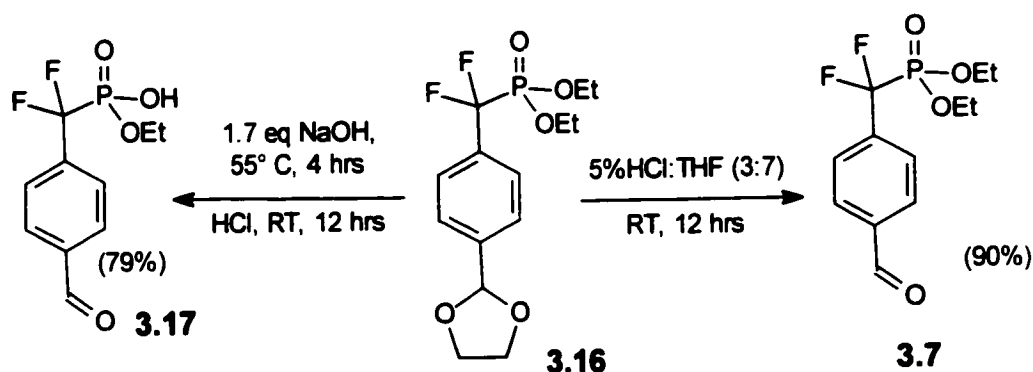


Scheme 3.5. Synthesis of phosphonate **3.16**.

The phosphonate functionality was introduced using an Arbuzov reaction between benzyl bromide **3.14** and triethyl phosphite to obtain phosphonate **3.15** in an 85% yield. The acetal group of **3.15** was found to be extremely labile as

partial degradation was observed upon silica gel. Fluorination of **3.15** began with deprotonation with 2.2 equivalents of NaHMDS in the presence of 2.3 equivalents of NFSi. The difluorinated product **3.16** could be obtained in a 52-76% yield.

The protected precursor **3.16** could be deprotected to the desired aldehyde **3.7** with HCl in THF as shown in Scheme 3.6 in a 90% yield. This aldehyde served as the initial model substrate for the development of Wittig reaction conditions. Alternatively, basic hydrolysis of phosphonate **3.16** followed by acid workup gave the monophosphonic acid **3.17**, with the acetal protecting group removed, in an overall 79% yield (Scheme 3.6). We intended to load this material on to the polymer support using Mitsunobu conditions. The aryl aldehyde **3.7** was found to be extremely susceptible to oxidation and had to be stored under argon or vacuum. Conversion to the carboxylic acid was observable upon standing on the bench top and at 4 °C within 5 days.

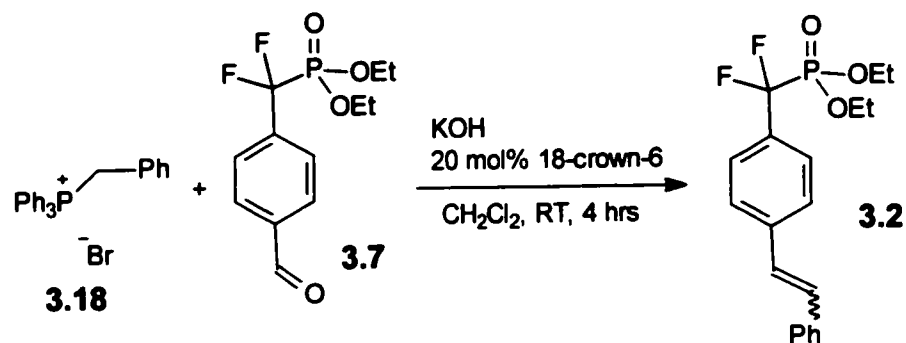


Scheme 3.6. Deprotection of **3.16**.

3.3.2 Model Wittig Reactions

As mentioned earlier, there are several examples of solid phase Wittig reactions including variations where the phosphonium salt is attached to the

support^{3,4} and others where the aldehyde is immobilized.^{8,9,10} Many of these reactions employed bases which were potentially problematic with the DFMP group (eg. $\text{CH}_3\text{O}^-\text{Na}^+$ or *n*-butyllithium)^{8,10} or required elevated temperatures for reaction to proceed.⁹ We sought to develop room temperature Wittig reaction conditions in order to facilitate performing multiple parallel reactions and avoid the risk of cleaving the phosphonate ester bond. The conditions employed would also have to be compatible with the sensitive DFMP functionality as well as the solubility requirements of the NCPS support. Due to the solubility properties of the NCPS support, we did not limit our literature investigations exclusively to reports describing solid phase Wittig reaction conditions.

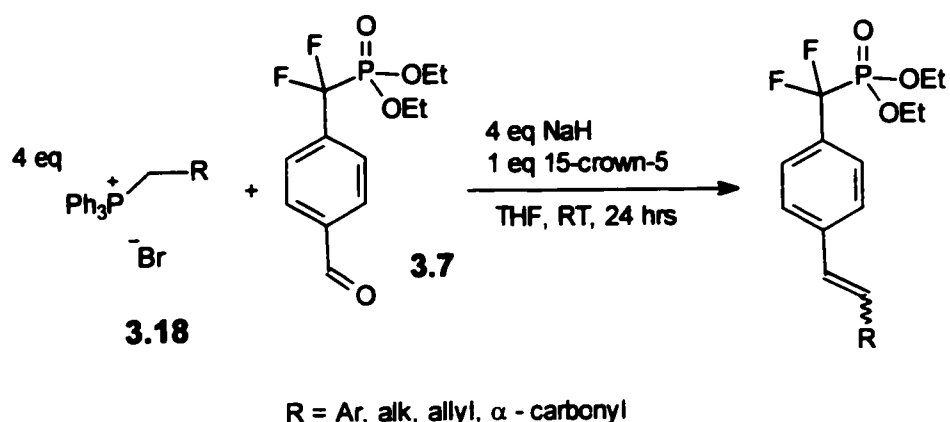


Scheme 3.7. Synthesis of 3.2 using Bellucci's Wittig conditions.

Bellucci *et al.*¹⁶ reported an extremely simple and efficient method of conducting solution phase Wittig reactions with benzyltriphenylphosphonium salts. Their conditions employed 1 equivalent of both the phosphonium reagent and the aryl aldehyde with 2 equivalents of potassium hydroxide in the presence of 5 to 10 mol% of 18-crown-6 in CH_2Cl_2 . The geometry of the resulting stilbene compounds could be controlled by performing the reaction at either $-70\text{ }^\circ\text{C}$, or $25\text{ }^\circ\text{C}$. When these conditions were used with model aldehyde substrate 3.7

employing phosphonium salt **3.18**, the reaction was complete within 4 hours. Hydrolysis of the DFMP group, which was initially a cause for concern, was less than 5%. These conditions appeared extremely promising since inexpensive and easy to handle reagents were employed. Also, the reactions did not require anhydrous conditions. Unfortunately, we found that the reaction was not applicable to a diverse range of phosphonium salts. When allylic and alkyl Wittig reagents were evaluated, the reactions failed to go to completion with no further progress observed past 60-80% after 24 hours. The addition of more base and phosphonium salt failed to increase the yields. These observations are most likely due to the higher pK_a values of the α protons of the unstabilized phosphonium salts. The use of more base led to an increased amount of hydrolysis.

In order to avoid the hydrolysis problem, we tried the reaction using sodium hydride as base in the presence of 15-crown-5. NaH is a stronger base than KOH and is non nucleophilic and is therefore capable of deprotonating even the alkyl phosphonium salts without the fear of nucleophilic attack at the phosphonate group. With the benzylic phosphonium salts, quantitative conversion was achieved within 24 hours using 4 equivalents of NaH and 20 mol% 15-crown-5, whereas the less acidic alkyl phosphonium reagents required a full equivalent of 15-crown-5 (Scheme 3.8). The formation of both the *E* and *Z* isomers could be observed in the ^{19}F NMR as a set of overlapping doublets. Although these conditions required a significant amount of crown ether, we decided to attempt them on the polymer-bound aldehyde.



Scheme 3.8. Wittig reaction using NaH and 15-crown-5.

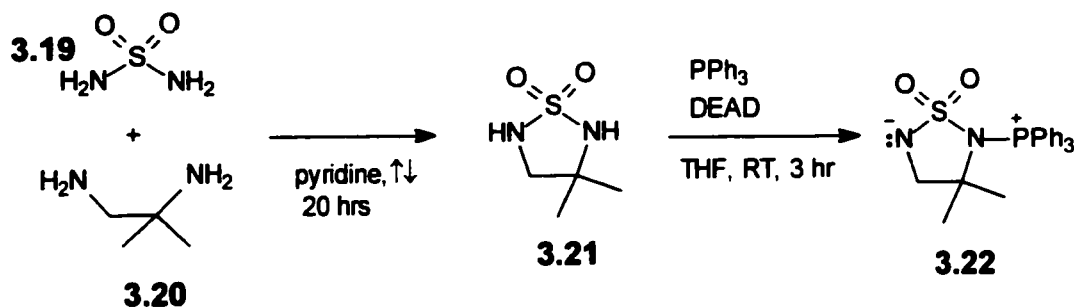
3.3.3 Attachment of 3.7 to the Polymer Support

Our initial attempts at attaching the aldehyde **3.17** to the polymer support consisted of employing the same Mitsunobu conditions (2 equivalents of the phosphonic acid **3.17**, DIAD, and PPh₃, and 5 equivalents of triethyl amine) used for the aryl bromide substrates in the preparation of the biaryl series of inhibitors. We had reason to be optimistic that our reaction conditions would also be successful in this instance based upon the work of Devraj¹⁷ and Hamper¹⁸ who have both reported the successful coupling of hydroxybenzaldehydes to solid supports using Mitsunobu conditions. Both groups employed typical Mitsunobu conditions employing DEAD or DIAD to activate PPh₃ with a phenolic group acting as a nucleophile to form an ether linkage to the support. When we applied our Mitsunobu conditions to the coupling of aldehyde **3.17** to polymer **2.49**, NMR analysis revealed that although partial loading may have occurred as indicated by signal changes at 3.5-4.0 ppm, no aldehyde signal was observable. Attempts to perform the reaction with DEAD and TMAD in the place of DIAD were similarly unsuccessful. We concluded that the problem was most likely due to the

aldehyde functionality which could affect the outcome of the coupling reaction in two possible ways. The presence of the highly electron withdrawing aldehyde functionality may lower the pK_a of the phosphonic acid therefore deactivating it as a nucleophile in the Mitsunobu reaction. An attempt to perform the reaction using the more reactive tris-4-chlorophenyl phosphine reagent was also unsuccessful. A more likely effect is the reaction of Mitsunobu reagents, or their byproducts with the aldehyde group thus accounting for the lack of signals in the 9-10 ppm range in the 1H NMR.

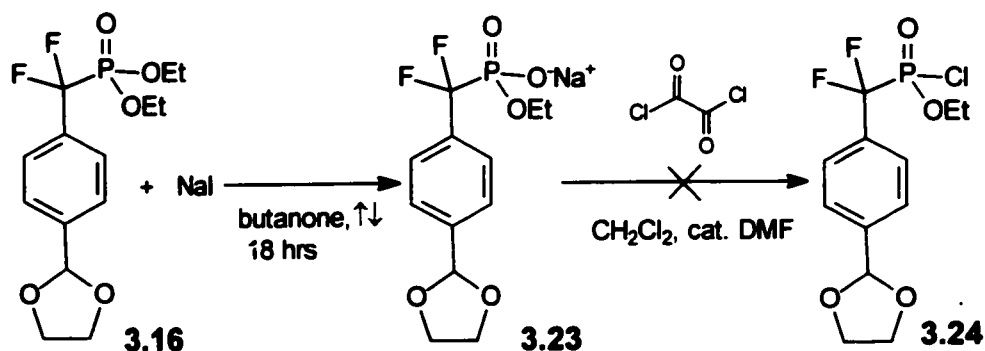
A recent report by Swayze¹⁹ appeared to offer a solution towards the coupling of **3.17** to the polymer. Swayze was able to couple 4-hydroxy benzaldehyde to ArgoGel using Mitsunobu conditions, but rather than use standard reagents such as DIAD or DEAD, Swayze employed a novel sulfonamide betaine, **3.22**, first reported by Castro *et al.*²⁰ Swayze's attempts to use both DIAD and DEAD to activate the phosphine resulted in contamination of the polymer bound aldehyde, presumably due to reaction of the DIAD/DEAD byproducts with the aldehyde functionality. Betaine **3.22** serves as a source of $[PPh_3]^+$ and is potentially useful due to the lack of the reactive diazido functionality. Though not commercially available, **3.22**, is easily prepared in two steps. Sulfamide (**3.19**) is reacted with 1 equivalent of the diamine **3.20** to produce the cyclic sulfamide **3.21**.²¹ Triphenylphosphine is reacted with **3.21** and DEAD to produce the adduct **3.22** (Scheme 3.9). The novel triphenylphosphine cyclic sulfamide betaine is a solid which can be stored for several months without significant decomposition. Unfortunately, when the coupling of aldehyde **3.17**

was attempted with betaine **3.22**, the results were mixed. Only partial loading was observed by ^1H NMR. An aldehyde signal was observable but the ^{19}F NMR showed multiple signals. Under these conditions, the coupling could not be achieved quantitatively or cleanly.



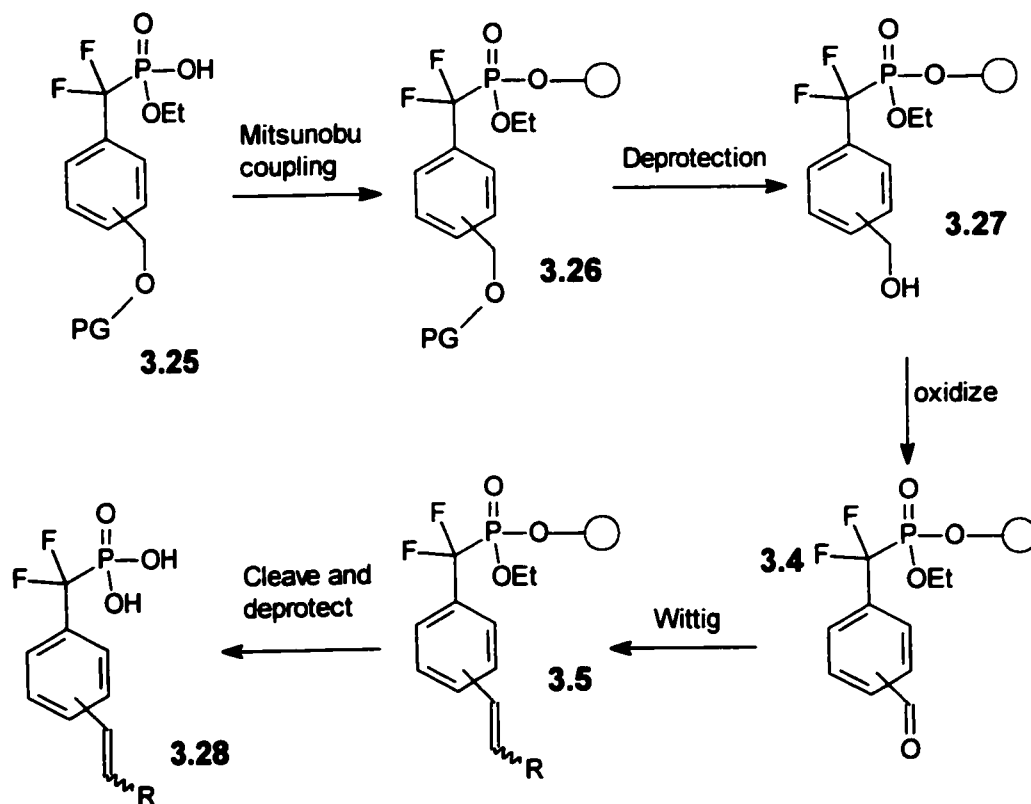
Scheme 3.9. Synthesis of betaine **3.22**.

An alternative approach towards loading **3.17** on to the polymer was to couple the acetal **3.16** followed by on polymer deprotection to the aldehyde. This involved conversion of the phosphonate to the acid chloride followed by attack of the hydroxyl function of the polymer **2.49**. Due to the acid sensitive nature of the acetal group, a mild method of converting the diethyl ester to the acid chloride was required. We found that the **3.16** could easily be converted to the sodium salt (**3.23**) by refluxing with sodium iodide in butanone as shown in Scheme 3.10. Using a procedure reported by Patel,²² we attempted to convert the sodium salt to the acid chloride using oxalyl chloride and a catalytic amount of DMF. Unfortunately, the ^{19}F NMR of **3.24** showed multiple signals. Nevertheless, we attempted to react polymer **2.49** with the crude acid chloride. However, the results were consistently unsuccessful at achieving a quantitative formation of the phosphonate ester linkage.



Scheme 3.10. Attempt at converting 3.16 to the acid chloride.

Based upon the results of these experiments, it was concluded that loading the aldehyde onto the polymer was fraught with too many difficulties and that an alternative approach would have to be taken. Two options were now available.



Scheme 3.11. Revised approach towards library construction.

One was to attach the phosphonic acid to the support with the aldehyde group protected. However, a survey of the literature revealed that most aldehyde protecting groups will not endure the strongly acidic conditions required to obtain the phosphonic acid or cannot be removed under conditions compatible with the solubility requirements of NCPS.²³ The other option was to construct the phosphonate with a protected alcohol moiety on the aryl ring and then load this onto the support. Once loaded, the alcohol could be deprotected and oxidized to the aldehyde (Scheme 3.11). We felt that the latter was the more feasible of the two approaches.

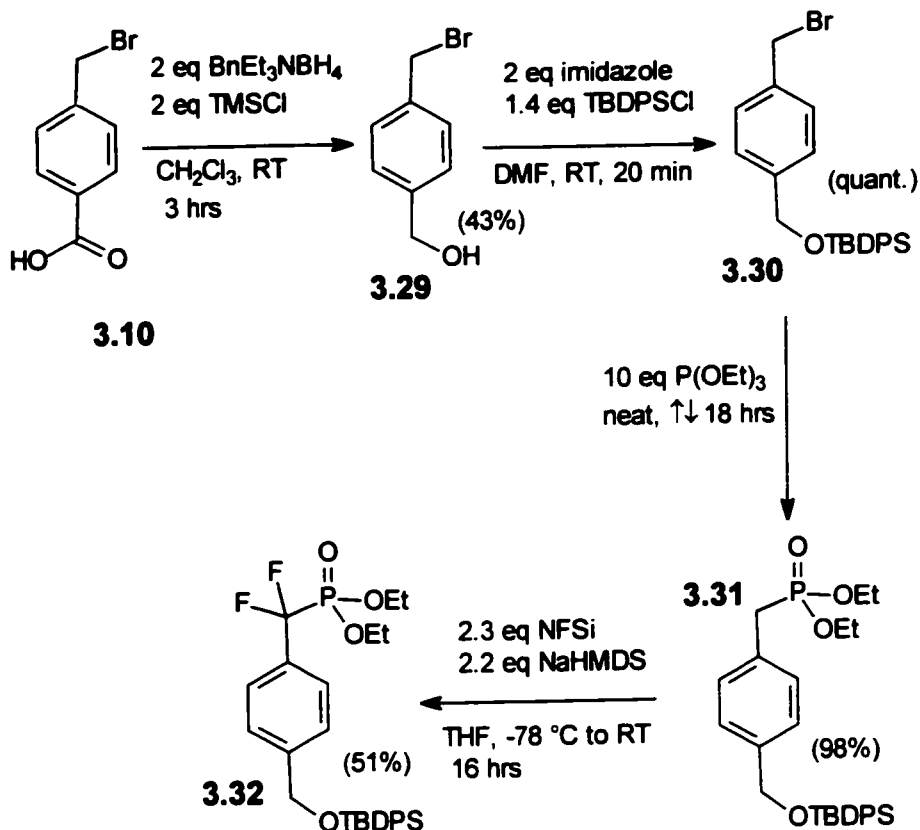
3.3.4 Synthesis of Phosphonates Bearing a Protected Alcohol Moiety on the Aryl Ring

Any group used to protect the alcohol group (as outlined in Scheme 3.11) would have to be stable towards the basic conditions used to hydrolyze the phosphonate diester as well as the strongly acidic conditions required to isolate the resulting monoacid. In addition, the group would have to be removed cleanly under relatively mild conditions in a quantitative yield.

Our initial approach towards a *para* substituted benzyl alcohol bearing the DFMP functionality was to utilize a silyl ether. Silyl groups can be selectively removed in high yield by employing a source of fluoride anion. Base and acid stability increases with steric bulk about the Si atom. The *tert*-butyl-diphenyl silyl (TBDPS) group potentially met the requirements of our reaction sequence.

The synthesis of **3.32**, as outlined in Scheme 3.11, began with [4-(bromomethyl)phenyl] methanol (**3.29**) which was obtained by reduction of 4-

(bromomethyl)benzoic acid (**3.10**) in a 43% yield using benzyltriethylammonium borohydride and chloro trimethylsilane as described in a procedure reported by Das *et al.*²⁴



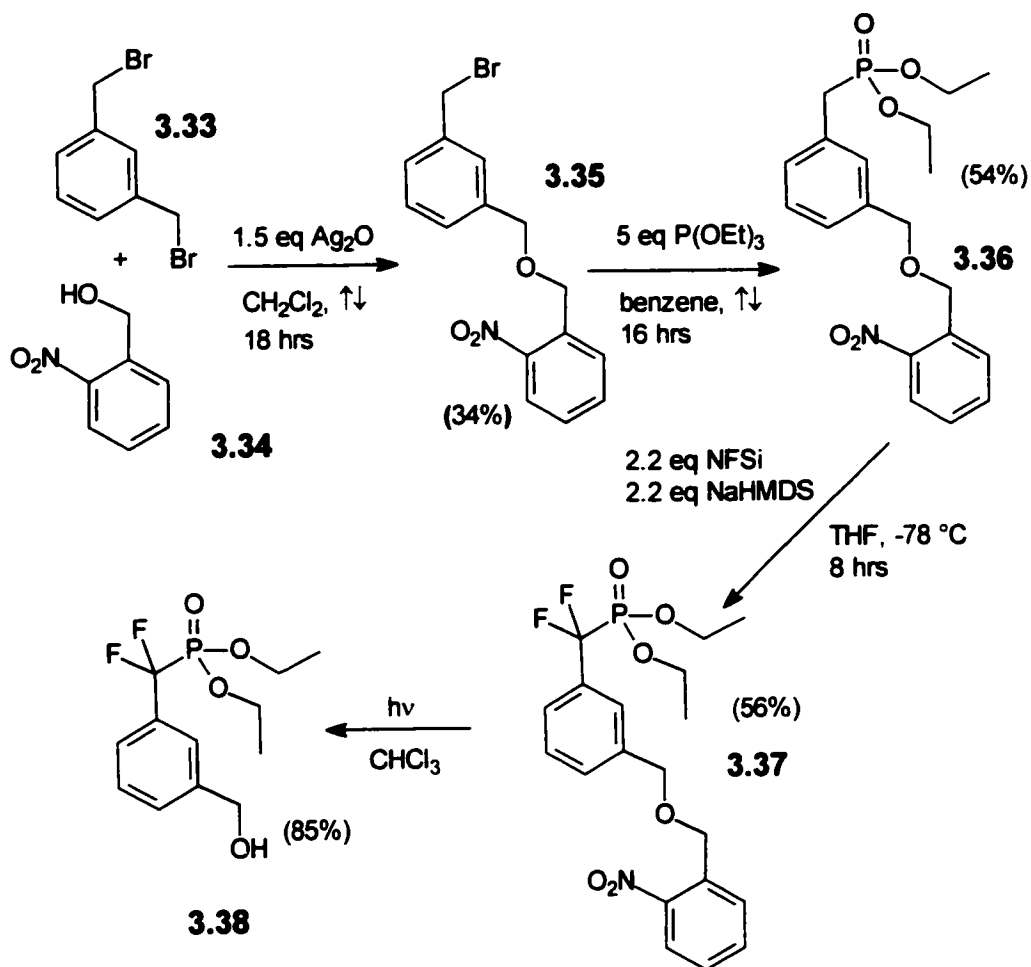
Scheme 3.12. Synthesis of TBDPS protected alcohol **3.32**.

The alcohol functionality was protected by reaction with 1.4 equivalents of TBDPS chloride in the presence of imidazole in dry DMF in quantitative yields. The phosphonate group was introduced in near quantitative yields by an Arbuzov reaction with triethyl phosphite. In order to get a good yield in this reaction, we found that it had to be run in neat triethylphosphite under refluxing conditions. This is in contrast to the usual Arbuzov conditions which are performed under milder conditions (in refluxing benzene). It appears that the large TBDPS group

imposes some steric hindrance to the reaction. Using our usual NFSi/NaHMDS protocol, fluorophosphonate **3.32** was produced in only a 51% yield. Steric interference by the TBDPS group may have also been a factor in this reaction. We found that the TBDPS group could be removed cleanly using ammonium fluoride in DMF at 80 °C which gave us polymer compatible deprotection conditions. Unfortunately, the conversion of the phosphonate diester to the mono acid did not proceed as smoothly. Hydrolysis of the diester had to be performed at 75 °C for 18 hours, presumably due to the presence of the bulky TBDPS group which hindered attack at the phosphonate group. Upon acidification and isolation of the monoacid, the ^{19}F NMR showed multiple signals which was indicative of the formation of side products. As determined by ^1H NMR, these additional signals arose from the presence of starting material and hydrolysis of the TBDPS protecting group. The instability of the TBDPS group, and the low yields obtained in the fluorination required that we investigate other protecting groups. These studies also indicated that steric factors influence the chemistry with the *para*-substituted compounds and these steric factors may be even more pronounced with the *meta*-substituted compounds. Consequently, all further model studies were performed using *meta*-substituted compounds since we were more interested in the *meta* series of compounds.

The next protecting groups we chose to evaluate were the *o*-nitrobenzyl and allyl groups since they can be removed under very mild conditions.²³ The *o*-nitrobenzyl group is removed by UV light of approximately 280 nm. Though the nitroso aldehyde byproduct is potentially reactive, the reaction proceeds

selectively and fairly cleanly with few side reactions.²⁵ The *o*-nitrobenzyl group has been applied in PSOS previously.^{26,27} The allyl group can be removed in the presence of a nucleophile and a Pd catalyst and has also been previously used in PSOS.²⁸



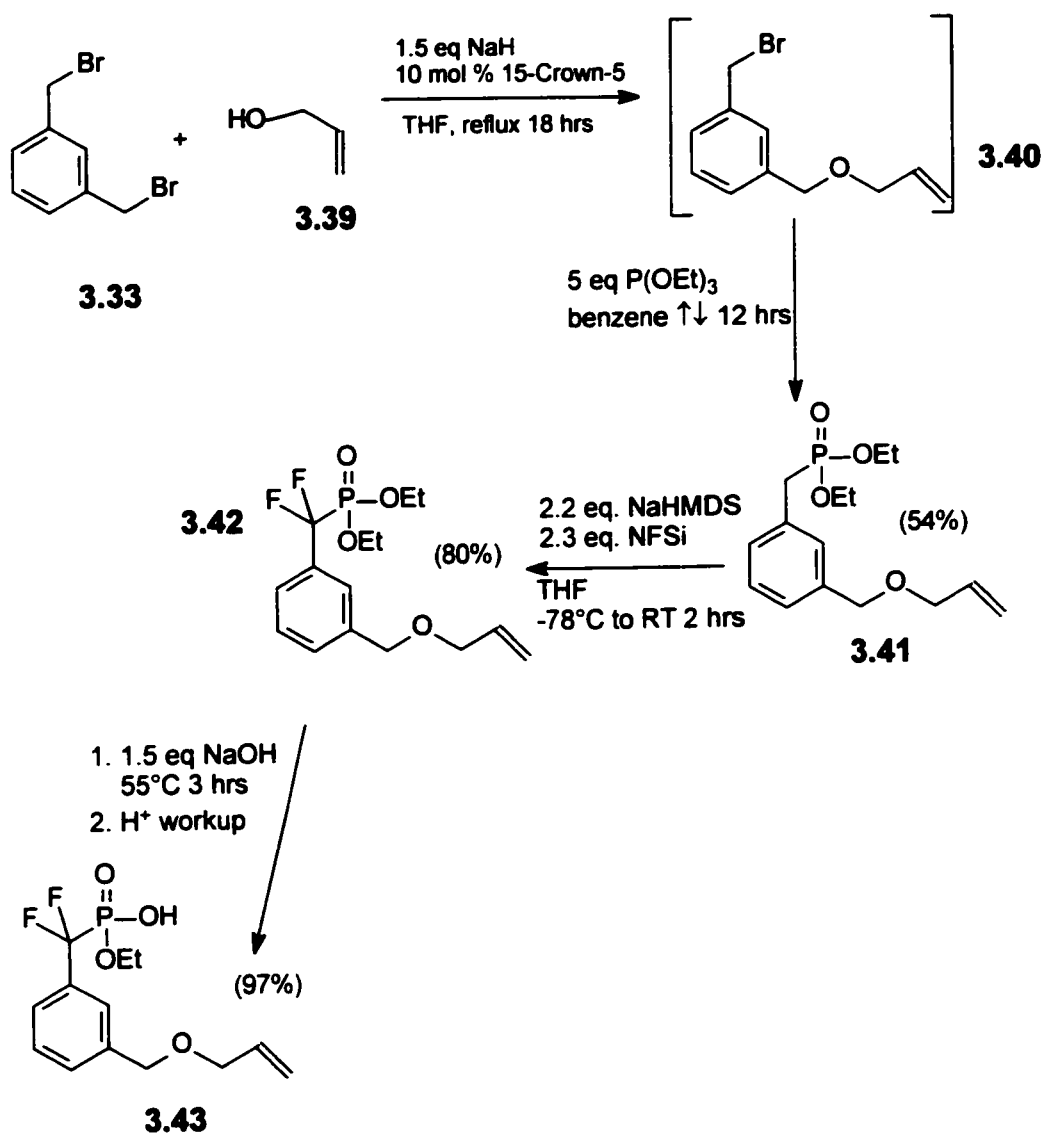
Scheme 3.13. Synthesis of *o*-nitrobenzyl protected alcohol **3.37**.

Synthesis of the appropriate *o*-nitrobenzyl protected precursor, as outlined in Scheme 3.13, began with α,α' -dibromo-*meta*-xylene which was reacted with *o*-nitrobenzyl alcohol in the presence of Ag_2O to produce the dibenzyl ether **3.35** in a 34% yield. The yield of **3.35** was similarly low when other base and solvent

combinations such as NaH/DMF/THF, K₂CO₃/DMF, imidazole/DMF, and K₂CO₃/benzene were employed. An Arbuzov reaction with triethyl phosphite in refluxing benzene produced the phosphonate precursor **3.36** in a disappointing 54% yield. When the reaction was performed by refluxing in neat triethyl phosphite, the yield dropped significantly, presumably due to decomposition of the *o*-nitrobenzyl group at higher temperatures. The fluorination of **3.36** also proceeded in a disappointing yield (56% yield). Deprotection experiments of **3.37** using a Rayonet UV reactor demonstrated that the *o*-nitrobenzyl group could be removed quantitatively in 8 hours as judged by ¹⁹F NMR, where a single signal attributable to the deprotected compound **3.38**, was observed. The product was isolated in a 85% yield upon scale up. Though the deprotection results were encouraging, the low yields encountered in the reactions used to produce the precursors were a definite drawback to the use of this protecting group.

Synthesis of the allyl protected precursor **3.42** also began with α,α' -dibromo-*meta*-xylene which was reacted with 1.1 equivalents of allyl alcohol in the presence of 1.5 equivalents of NaH and 10 mol% of 15-crown-5 under refluxing conditions in THF. The resulting allyl-benzyl ether **3.40** was not isolated but rather reacted in the Arbuzov reaction to produce the diethyl phosphonate **3.41** in an overall 54% yield for two consecutive steps. Although the overall yield of these two steps was not outstanding, the materials were inexpensive and readily available. Electrophilic fluorination of **3.41** using the usual conditions proceeded in an 80% yield. The allyl group proved to be stable to both the basic conditions required to remove an ethyl group from **3.42** and the strongly acidic

conditions required to isolate the phosphonic acid **3.43**, which was obtained in a 97% yield.



Scheme 3.14. Synthesis of allyl protected alcohol **3.42**.

The stability of the allyl group to our reaction sequences and the ease by which phosphonic acid **3.43** was prepared was very promising as far as library construction was concerned. In order to be able to construct the library, we required conditions to selectively and quantitatively remove the allyl protecting

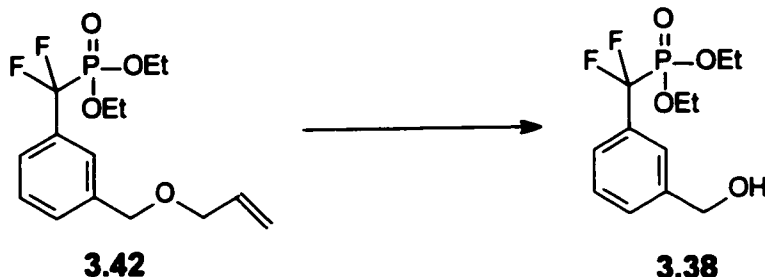
group to liberate the benzylic alcohol under mild conditions. The precursor **3.42** was used as the model substrate to investigate allyl deprotection conditions. There are many different methods which have been developed to remove allyl groups from alcohols.²³ We focused on methods that we felt would be compatible with the phosphonate group and the solubility properties of NCPS. The results of these studies are outlined in Table 3.1. The reactions were performed on a small scale and monitored using ¹⁹F NMR. Since the site of cleavage was quite removed from the DFMP group, only changes of 0.05 to 0.1 ppm were observed in the ¹⁹F NMR upon conversion to product. Nevertheless, this small shift was sufficient to allow us to follow the reaction.

The best conditions involved using a Pd catalyst and *p*-toluenesulfonic acid since a near quantitative conversion was observed by ¹⁹F NMR after 18 hours at room temperature. Upon scale up of the reaction to 100 mg, the desired product **3.38** was isolated in a 85% yield.

With the reactive aldehyde functionality replaced with the far more stable allyl ether group, the Mitsunobu conditions employed for coupling the aryl bromo phosphonic acids **2.28** and **2.29** to the support were found to be applicable to **3.43**. However, the procedure required a few changes in order to achieve quantitative loading of all free hydroxyl sites as shown in Scheme 3.15. The number of equivalents of the phosphonic acid **3.43**, triphenyl phosphine, and DIAD were all increased to three. The reaction was also considerably slower requiring 18 hours to go to completion. These modifications presumably arose

due to the steric hindrance imposed by the presence of the *meta* allyl ether group.

Table 3.1. Allyl deprotection conditions.



Entry	Reaction Conditions	% Conversion by ¹⁹ F NMR	Comments
1	1.5 eq NaBH ₄ 0.75 eq I ₂ (THF, RT, 24 hrs) ^a	< 50%	Multiple signals observed.
2	1.2 eq DDQ (CH ₂ Cl ₂ , RT, 48 hrs) ^b	< 5%	No reaction after 48 hours.
3	10 mol% Pd(PPh ₃) ₄ 1.5 eq NaBH ₄ (THF, RT, 24 hrs) ^c	< 10%	Multiple signals observed.
4	10 mol% Pd(PPh ₃) ₄ 2 eq dimedone (THF, RT, 24 hrs) ^d	0%	No reaction after 48 hours.
5	20 mol% Pd(PPh ₃) ₄ 1.4 eq <i>p</i> -toluene sulfinic acid (CH ₂ Cl ₂ , RT, 18 hrs) ^e	> 90%	¹⁹ F NMR showed only desired product formed.

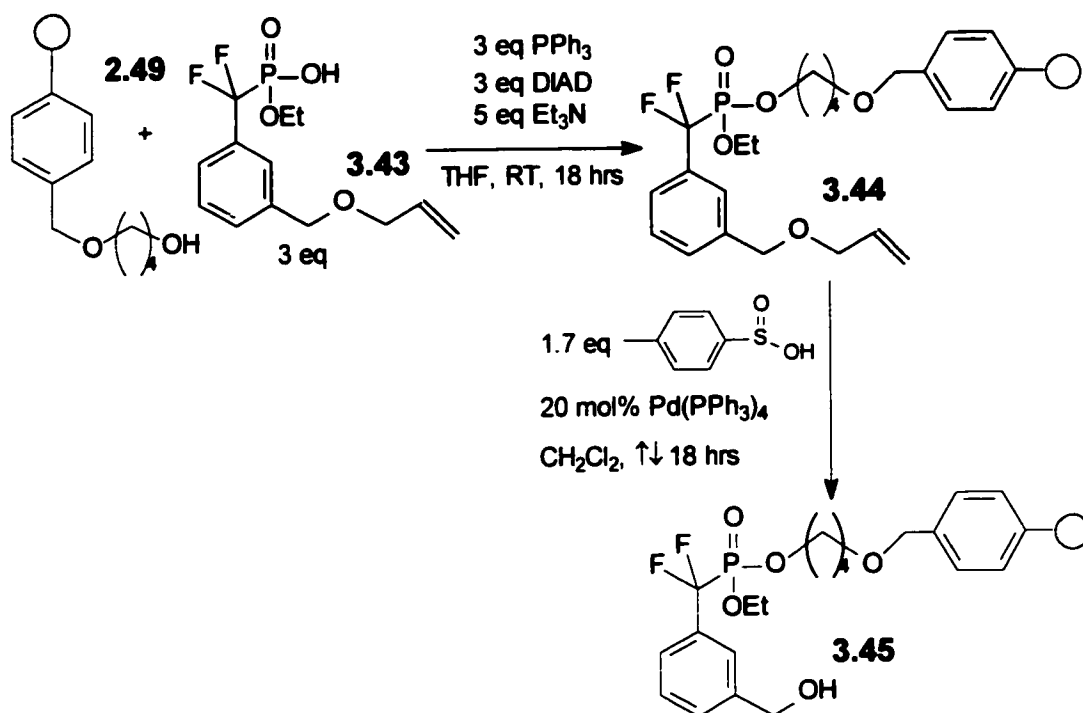
^a Thomas, R. M.; Mohan, G. H.; Iyengar, D. S. *Tetrahedron. Lett.* **1997**, *38*, 4721-4723.

^b Yadav, J. S.; Chandrasekhar, S.; Sumithra, S.; Kache, R. *Tetrahedron. Lett.* **1996**, 6603-6606.

^c Beugelmans, R.; Bourdet, S.; Bigot, A.; Zhu, J. *Tetrahedron. Lett.* **1994**, *35*, 4349-4350.

^d Zhang, H. X.; Guibe, F.; Balavoine, G. *Tetrahedron Lett.* **1988**, *29*, 623-626.

^e Honda, M.; Morita, H.; Nagakura, I. *J. Org. Chem.* **1997**, *62*, 8932-8936.



Scheme 3.15. Coupling of **3.43** to functionalized NCPS and removal of allyl group.

When we attempted to remove the allyl group on polymer bound phosphonate **3.44** using the conditions developed for model compound **3.42** ($\text{Pd}(\text{PPh}_3)_4$ /*p*-toluenesulfonic acid, CH_2Cl_2 , room temperature, 18 hours) the reaction progressed to 90% conversion as judged by both ^{19}F and ^1H NMR. We found that complete conversion could be achieved by increasing the amount of *p*-toluene sulfonic acid to 1.7 equivalents and refluxing in CH_2Cl_2 for 18 hours to produce the polymer bound benzylic alcohol **3.44**. No other polymer bound species were observed in either the ^1H or ^{19}F NMR and no evidence of cleavage of the phosphonate ester bond was detected. Soon after we had adapted these conditions to the soluble polymer support, Opatz *et al.*²⁹ reported similar results. Using DME or dioxane as a solvent, 5 equivalents of *p*-toluene sulfonic acid, and

25 mol% Pd(PPh₃)₄, these workers were able to cleave allyl ethers bound to either Tentagel or insoluble polystyrene based resins in yields greater than 98% at room temperature.

3.3.5 Model and on Polymer Oxidation Reactions

Our requirements for the oxidation of the benzyl alcohol in polymer-bound **3.45** to the aldehyde were no different from those for the other reactions we were developing. Ideally, the reaction conditions needed be fairly mild and proceed quantitatively and cleanly with little or no side reactions. The conditions had to be compatible with the solubility requirement of NCPS, and ideally, the reagents would be readily available and inexpensive. In exploring our options for performing the oxidation, we employed both **3.42** and polymer bound **3.45** as substrates. Once again, we examined reports of both solution and solid phase oxidations.

Our solution phase studies with **3.38** began with examining the use of MnO₂ as an oxidant. Several groups have reported that MnO₂ is an effective oxidizing agent for benzylic alcohols.^{30,31,32} There are also examples of MnO₂ being used in *in situ* oxidation-Wittig reactions.^{33,34,35} The use of this reagent was attractive since it is inexpensive, readily available, and operates at room temperature. Initial experiments demonstrated that the oxidation of **3.38** to the aldehyde could be effected using 5 equivalents of MnO₂ in CH₂Cl₂ in a reaction time of 36 hours. We also found that by employing the Wittig reaction conditions outlined in Scheme 3.7, which were adapted from Belluci *et al.*,¹⁶ we were able to carry out the *in situ* oxidation-Wittig reaction sequence by using 15 equivalents of

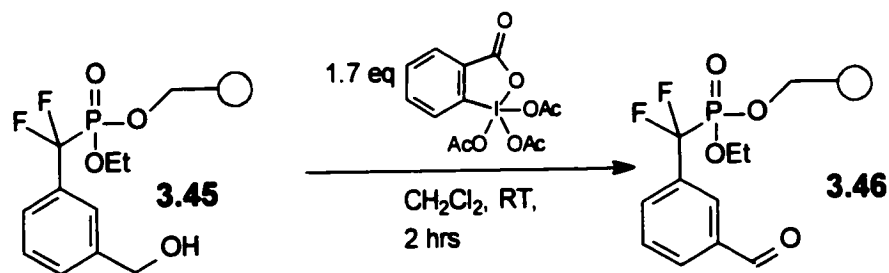
oxidant added in three separate portions. The ^{19}F NMR revealed that only the desired products were present after 48 hours. Unfortunately, MnO_2 is a heterogeneous oxidant and is not soluble in CH_2Cl_2 . When oxidation of the polymer bound alcohol **3.45** was attempted, no reaction occurred. This presumably arises from the inability of the tethered alcohol to access the MnO_2 surface due to the extremely hydrophobic nature of the NCPS backbone. From these results, we concluded that solution phase reactions that involve heterogeneous reactants would generally translate poorly to soluble polymer supported systems.

The Swern oxidation is a commonly used oxidation reaction which employs common inexpensive reagents and utilizes DMSO as an oxidant. When **3.38** was subjected to the Swern oxidation conditions, the resulting ^{19}F NMR revealed multiple signals in addition to the expected product and starting material. These results, and the fact that the reaction must be carried out at low temperatures, which detracts from its convenience, prompted us to pursue other avenues.

Bolm et al.³⁶ reported the development of a mild catalytic TEMPO/Oxone based system for the synthesis of aldehydes and ketones. These conditions consisted of 2 mol% TEMPO, 4 mol% tetrabutyl ammonium bromide, and 2.2 equivalents of OXONE in CH_2Cl_2 at room temperature. When applied to **3.38**, the reaction was very sluggish and only 30% conversion was observed in the ^{19}F NMR after 24 hours.

A potential solution to our problem was the use of the tetra-*n*-propylammonium perruthenate (TPAP)/*N*-methylmorpholine-*N*-oxide (NMO) oxidant systems pioneered by Ley and coworkers.^{37,38} The oxidation of primary and secondary alcohols bound to Wang resin using TPAP/NMO has been reported³⁹ as well as the development of polymer supported perruthenate reagents.^{40,41} When the TPAP/NMO system was applied to the polymer bound substrate **3.45** in CH₂Cl₂, the reaction mixture turned into a gel. It appears that the combination of TPAP and NMO is not compatible with the solubility requirements of NCPS therefore causing the support to precipitate out of solution.

Dess-Martin periodinane is also reputed to be a mild and efficient oxidant. When purchased from commercial suppliers, the reagent is fairly expensive, however, it can be readily prepared from inexpensive starting materials.^{42,43,44} Oxidation of the polymer bound **3.45** was attempted with 1.7 equivalents of Dess-Martin periodinane in CH₂Cl₂ at room temperature as shown in Scheme 3.16.



Scheme 3.16. Dess-Martin oxidation of polymer-bound **3.45**.

The reaction was found to be complete within 2 hours as judged by ¹⁹F-NMR. The ¹⁹F NMR of the precipitated polymer revealed a single set of doublets and the ¹H NMR displayed an aldehyde signal and was free of any polymer

bound contaminants. In effect, the Dess-Martin oxidation fulfilled all of our requirements for an on polymer oxidation.

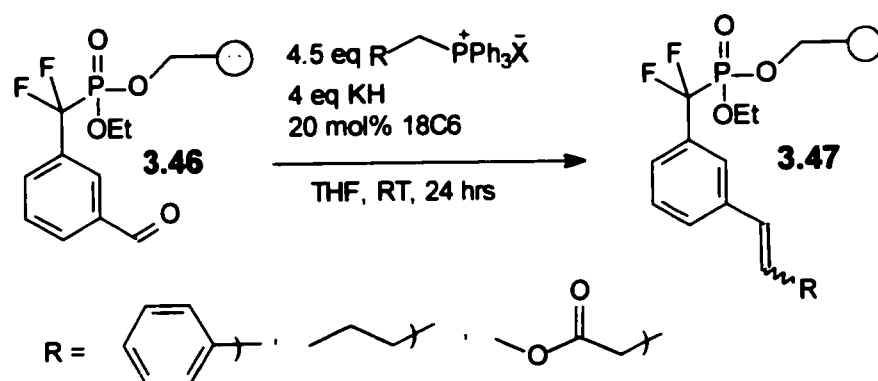
3.3.6 On Polymer Wittig Reactions

The Wittig reaction conditions outlined in Scheme 3.8 (4 equivalents NaH, 1 equivalent 15-crown-5, 4 equivalents phosphonium salt, THF, room temperature) were performed upon the polymer bound aldehyde **3.46** using benzylphosphonium salt **3.18**. Upon precipitation of the polymer, the ^{19}F NMR exhibited exclusively the signals from the desired alkene products. Verification by ^1H NMR showed the disappearance of the characteristic aldehyde signal at about 10 ppm. However, also present in the ^1H NMR was a signal due to the presence of 15-crown-5. Even after multiple precipitations, some 15-crown-5 still remained. Due to the amount of catalyst employed, and its hydrophobic nature, precipitation of the polymer inevitably resulted in occlusion of the catalyst within the polymer. The presence of the polyether catalysts would undoubtedly affect the following TMSBr/TMSI deprotection reaction so elimination of the contaminant appeared to be essential. Lowering the amount of 15-crown-5 used was not an option since our earlier studies revealed that complete conversion was not possible in the case of less acidic phosphonium salts.

We also evaluated NaHMDS as a base. It is a sufficiently strong base to provide uniform deprotonation among a diverse range of phosphonium salts. NaHMDS is also a homogeneous reagent which would obviate the need for a phase transfer catalyst. However, when we tried this base using polymer bound **3.46** and phosphonium salt **3.18**, some cleavage of the phosphonate from the

support occurred. This may be a result of the NaHMDS or even the amine byproduct (HMDS) acting as a nucleophile to cleave the phosphonate ester bond.

The next base we examined was KH. In theory, the base component of KH is the same as NaH. However, the larger K cation results in a much more exposed, and therefore more reactive, hydride. Using KH as a base, we found that the on-polymer Wittig reaction could be achieved with 100% conversion to the desired alkene products when only 20 mol% of 18-crown-6 was present and using three very different (benzyl, alkyl and α -carbonyl) types of phosphonium salts (Scheme 3.17).



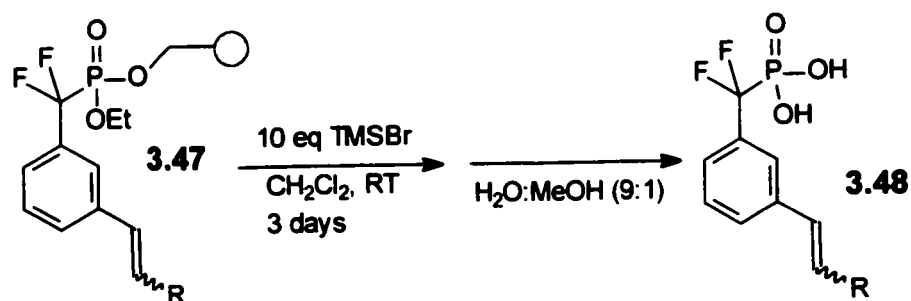
Scheme 3.17. On-polymer Wittig reaction using KH/18-crown-6.

In order to verify completion, the reactions were run for 24 hours prior to being precipitated in a 9:1 MeOH:water mixture. The filtered polymer from each reaction was analyzed by ^1H NMR, to verify the disappearance of the aldehyde signal, and by ^{19}F to ensure that no undesired side reactions had occurred. We also examined the ^1H spectra to ensure that the phosphonate ester linkage remained intact. In using this method to evaluate our reaction conditions, it

appeared as if we were achieving quantitative conversion of the aldehyde to desired alkene products.

3.3.7 Cleavage and Deprotection of Wittig Products

The conditions that we developed for cleaving the biaryl series of compounds from the polymer (see Section 2.3.6) were examined using the polymer-bound Wittig products shown in Scheme 3.17 above as model compounds. This involved the use of 10 equivalents of TMSBr in CH₂Cl₂ at room temperature over 3 days, as shown in Scheme 3.18. The use of TMSI was avoided since we anticipated that some of the library would contain TMSI-sensitive ether and ester functionalities. Though the reactions could have been accelerated by refluxing for two days, it was found to be more convenient to perform multiple parallel reactions at room temperature. The free acids were then obtained by precipitating and stirring the reactions in a 9:1 solution of MeOH and water. ¹H NMR revealed that the crude products were contaminated with varying amounts of polymer, phosphonium salt, and triphenyl phosphine oxide, and as in the case of the biaryl library, required further purification.



Scheme 3.18. Cleavage and deprotection of products from the support.

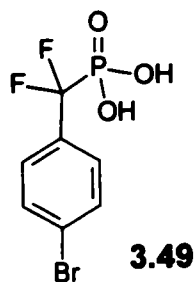
3.3.8 Purification of Phosphonic Acids by Ion Exchange

Before constructing the full library, one of the things we wished to change was the manner in which the final products were purified. The extraction/wash/extraction procedure which was used to purify the biaryl phosphonic acids was a route we wished to avoid for purifying the alkenes. We felt that the strongly acidic conditions required for the extraction of the acids into an organic phase would isomerize all the compounds to the more stable *E* isomer as well as compromise the various ester groups we wished to incorporate into the library. In order to avoid the acidification procedure, we wished to use the phosphonic acid functionality, which we hoped would be unique to our compounds of interest, as a means temporarily immobilizing our compounds onto an ion exchange resin. In principle, when the crude filtrate from the cleavage/deprotection reaction is applied to an anion exchange resin, our negatively charged anions would interact with the cationic sites of the support and be temporarily immobilized by electrostatic interactions. Since any major impurities, such as triphenyl phosphine oxide or excess phosphonium salt, would lack an acid functionality, they could be separated from the desired products by simply washing with the appropriate solvents. Our products could then be eluted from the resin in a pure form by using an appropriate volatile base. Success in purifying our compounds is based upon the assumption that only our desired products contained an acidic functionality.

There are examples in the literature where groups have reported the use of ion exchange resins as scavengers^{45,46} in parallel reactions and also as a means of rapid parallel purification.^{47,48,49} None of these reports dealt with the

purification of phosphoric or phosphonic acids. Work reported by Holy *et al.*⁵⁰ serves as one of the few examples of phosphonic purification using an ion exchange resin. In this instance, Dowex 1X2 resin was used to purify adenine phosphonic acid analogues which were eluted from the resin using glacial acetic acid.

In order to investigate potential ion exchange media, we utilized the model compound **3.49**.⁵¹ We considered **3.49** to be a suitable test compound since it contained the difluoromethylene phosphonic acid functionality which was common to all of our compounds and serves as the 'handle' by which temporary immobilization would occur.



Due to the acidic nature of our compounds, we required an anion exchange resin but due to the lack of literature precedents, were unsure of whether a strong or weak ion exchanger would best suit our application. The success reported by Bookser *et al.*⁴⁹ in using a Dowex resin for the parallel purification of carbon acids prompted us to investigate the use of the strong anion exchanger Dowex 1x8-400. This resin is polystyrene based with a gel type consistency and is functionalized with Ph-CH₂-N⁺Me₃ cationic sites. A column consisting of 1 mL of the OH⁻ counterion form of Dowex 1x8-400 resin was assembled. This corresponded to approximately 10 equivalents of functionalized

sites with respect to the test compound **3.49** which was loaded onto the resin as a THF solution. The column was washed with 5 bed volumes of water, THF, and MeOH. These washings were concentrated and checked by ^{19}F NMR to ensure the absence of any 'product.' In order to successfully remove **3.49** from the resin, we had to protonate the phosphonic acid thereby rendering it neutral and thus unable to interact electrostatically with the resin. However, the pK_a 's of our α -fluorophosphonic acids were very low, which meant that we required a very strong acid to remove the products from the resin. We chose TFA since its pK_a (0.3)⁴⁹ is approximately the same as that of the first ionization constant of our fluorophosphonic acids and the TFA could be readily removed by rotary evaporation. However, even when we used a vast excess of 95% TFA in CH_2Cl_2 , we were unable to recover any of the desired product from the column.

Weak anion exchangers are functionalized with free amine groups, which can form salt linkages with acids. In order to remove the product from the support, a base is used to deprotonate the immobilized amine which then becomes neutral and therefore unable to bind the anion of interest. The cations in solution serve as the counterions for the acid which is then eluted as a salt.

The first weak anion exchanger we examined was Amberlyst A21 which is a polystyrene based macroreticular resin with alkyl amine functionalities.⁵² Compound **3.49** was loaded, as a THF solution, onto a volume of Amberlyst A21 which provided approximately a 10 fold excess of functional sites. The resin was then washed with 4 bed volumes of water, MeOH, and THF. None of the compound **3.49** was present in these washes as determined by ^{19}F -NMR. In

order to isolate our compound, we employed solutions of NH_4HCO_3 and NH_4OH since these basic salts could be removed from the final product by lyophilization. Varying concentrations of these bases were examined in order to determine optimal elution conditions (Table 2).

Table 3.2. Recovery of **3.49** from Amberlyst A21 using varying amounts of NH_4HCO_3 and NH_4OH .

Base	Equiv of base ^a	% recovery of phosphonic acid 3.49
NH_4HCO_3	4	24
"	8	34
"	16	33
NH_4OH	4	32
"	8	37
"	16	38

^a relative to functional sites on Amberlyst A21

As seen in Table 3.2, we were unable to recover the diammonium salt of **3.49** in greater than a 38% yield. These results were surprising since we employed a sufficient amount of base to deprotonate all of the functional amine sites several times over. A possible explanation is that interactions other than salt linkages contributed to binding to the resin. Due to the hydrophobic nature of the aryl ring of **3.49**, it is possible that **3.49** interacted with the polystyrene matrix via hydrophobic interactions which therefore limited our ability to isolate it.⁵³

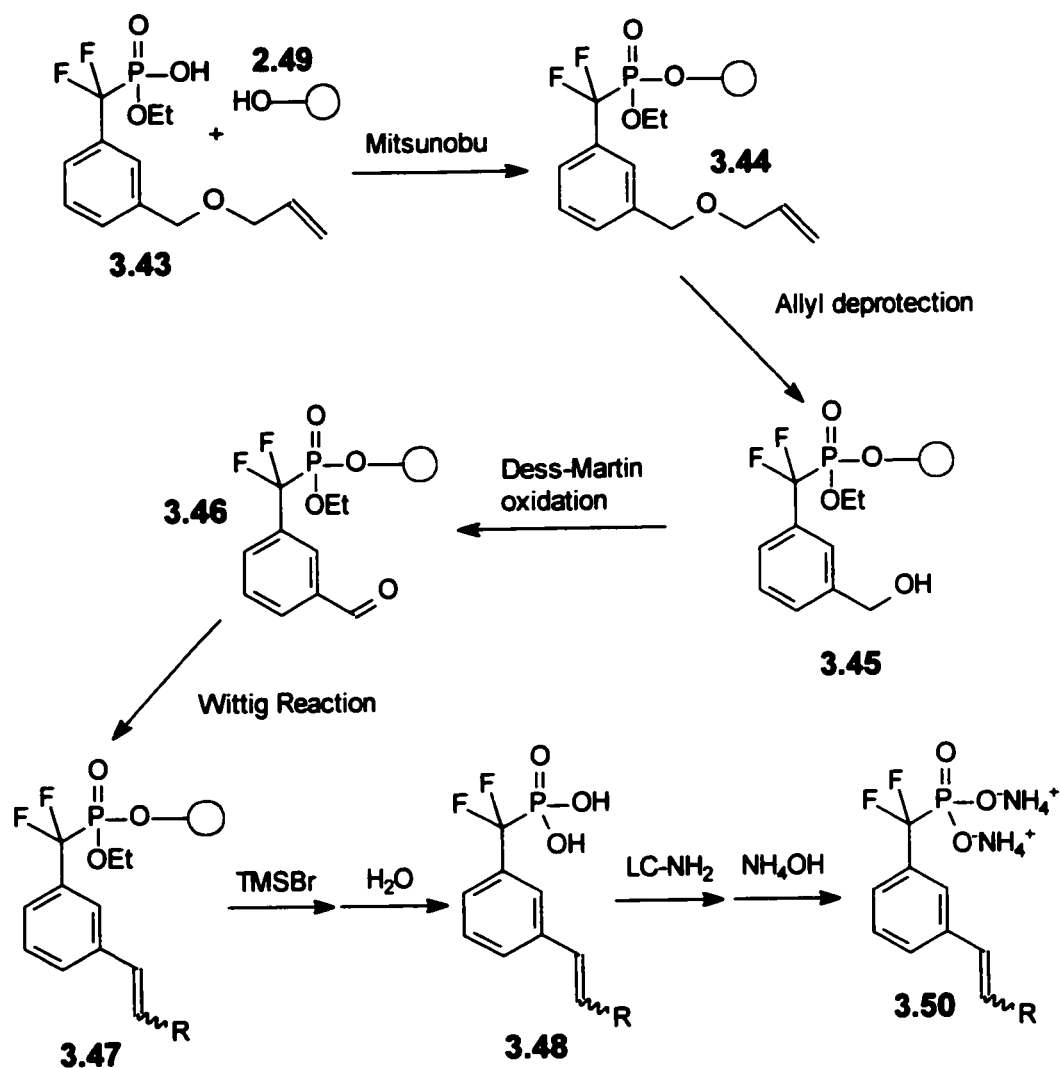
In order to prevent potential hydrophobic interactions with the backbone matrix of the ion exchange media, we chose to avoid polystyrene based resins. Fortunately, alternative ion exchange media do exist. LC-NH₂ weak anion exchange media is a product offered by Supelco that is intended for use as a solid phase extraction tool. It is comprised of a silica matrix functionalized with

propylamine groups and is available as the free packing, or prepacked in columns. We evaluated the use of the 3 mL columns prepacked with 500 mg of sorbent, for our application. Compound **3.49** was applied to the column as a THF solution. Extensive washing with 10 mL THF, 8 mL MeOH, and 8 mL water demonstrated that **3.49** was immobilized on the resin since no trace of the compound was found upon concentration of the washings. Quantitative recovery of **3.49** as its diammonium salt could be achieved by elution with 6 mL of 0.5 M NH_4OH , which was a 25 fold excess of base relative to **3.49**. Isolation of the product as its diammonium salt was performed by lyophilizing the elutions several times which removed both the water and excess NH_4OH . We found that these results were highly reproducible and were confident that the LC- NH_2 prepacked columns were the most efficient means of parallel purification for our phosphonic acids. The use of these columns should be widely applicable for the purification of a wide range of organic acids regardless of whether they are carbon, phosphorous, or sulfur based and are particularly useful when hydrophobic interactions with the backbone matrix may interfere with product recovery.

3.3.9 Library Synthesis

In order to synthesize the library, the coupling of **3.43** to the polymer **2.49** was performed in a batch procedure as were the deprotection and oxidation reactions. For the synthesis of the individual compounds, up to six reactions were run in parallel in separate vessels. The KH, 18-crown-6, and phosphonium salts were premixed in dry THF for 1 hour in order to generate the anion. A

single batch of polymer bound aldehyde solution was made up in a separate vessel and partitioned equally among the parallel reactions using a syringe. Reactions were performed with approximately 400 mg of polymer for each reaction with a loading of 0.3 mmol/g of polymer. The reactions were then stirred for 24 hours at room temperature before being quenched by addition to a stirred 9:1 MeOH-water solution.



Scheme 3.19. Reaction sequence for library synthesis.

As with the biaryl library, recovery of the polymer was not quantitative, and ranged from 80-95%. Following filtration and drying of the polymer from each reaction, the cleavage and deprotections steps were performed in parallel. The deprotection reactions were run for 3 days. Excess TMSBr reagent was removed *in vacuo* followed by repeated cycles of redissolving the polymer and drying by rotary evaporation. The polymer was precipitated in a solution of MeOH-water (9:1) and the crude stirred for 18 hours in order to hydrolyze the silyl ester intermediates. Following hydrolysis of the silyl esters the polymer was removed by vacuum filtration and the filtrate concentrated to give the crude phosphonic acid products. The crude acids were applied to the LC-NH₂ columns and eluted with 0.5 M NH₄OH to obtain our products as their diammonium salts. This reaction and purification sequence is summarized in Scheme 3.19.

We attempted the Wittig reaction on polymer-bound **3.46** with 31 phosphonium salts. The phosphonium salts that failed to yield the desired products are shown in Figure 3.1. Phosphonium salts which yielded highly stabilized anions (**3.51-3.53**) were very slow to react and proceeded to only 40-60% completion after 24 hours. Other phosphonium salts (**3.54-3.56**) simply failed to react at all which was most likely due to steric reasons. Salt **3.59**, which bears an unprotected carboxylic acid group also did not react even when additional base was added. With phosphonium salts **3.57-3.58**, the ³¹P-NMR and ¹⁹F-NMR of the products from these reactions displayed multiple signals which could not be attributed to the desired products. We are unable to find an explanation as to why this was the case for these two compounds.

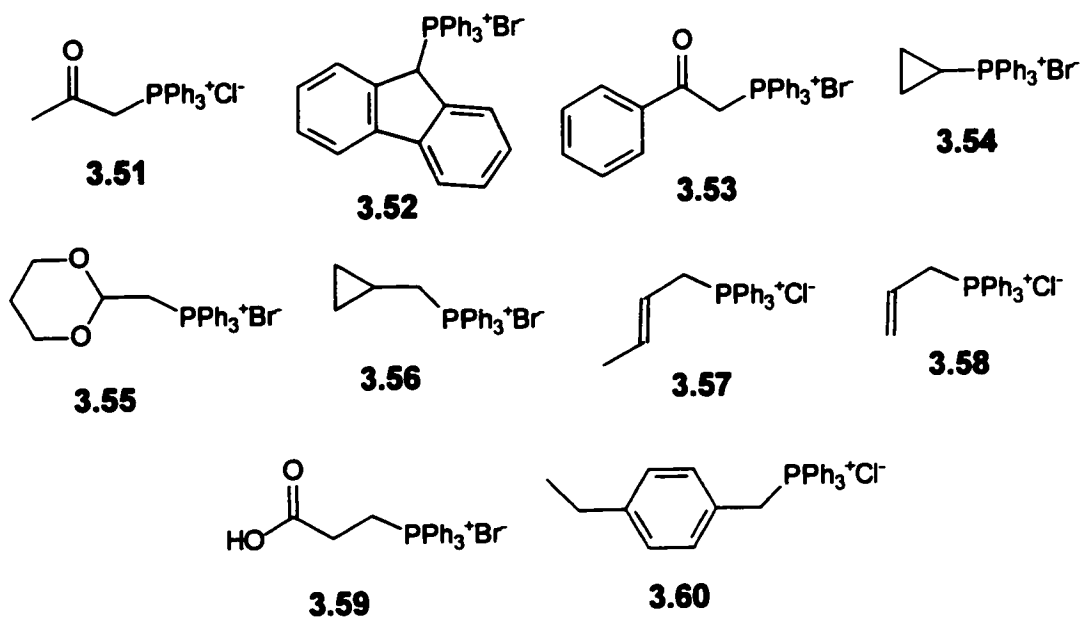
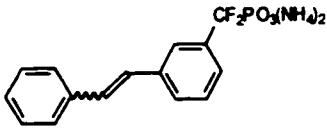
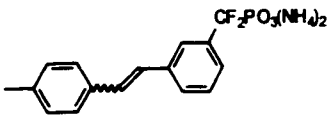
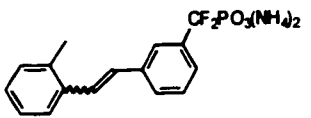
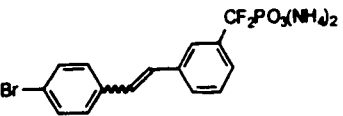
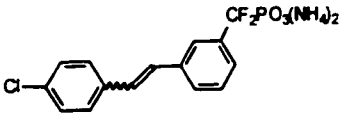
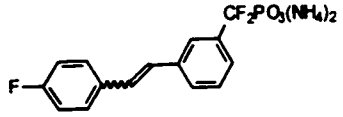
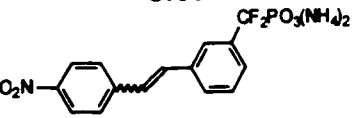
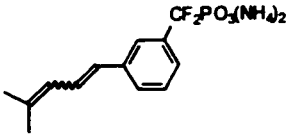
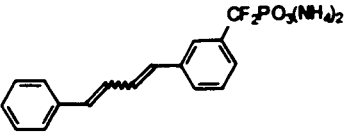
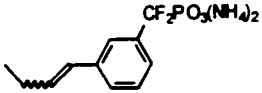
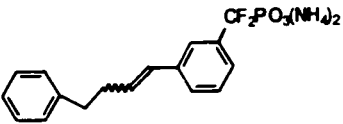
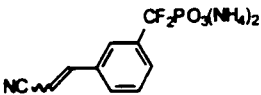
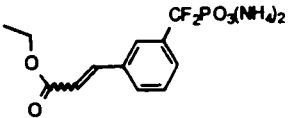
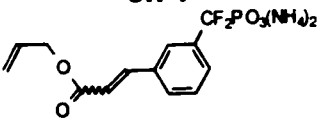
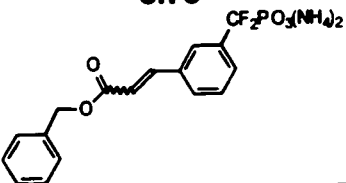


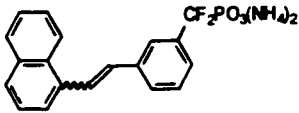
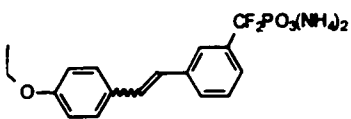
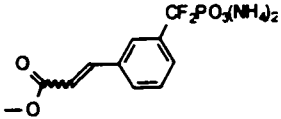
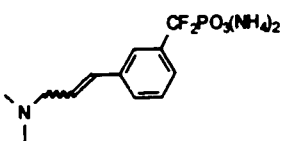
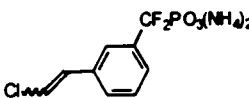
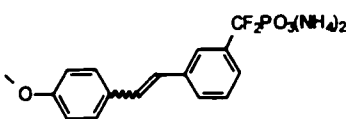
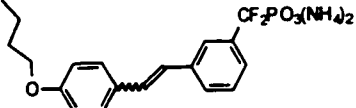
Figure 3.1. Phosphonium salts which failed to give desired products.

Twenty-two phosphonium salts gave the desired products, as judged by ^1H , ^{19}F , and ^{31}P NMR, in various states of purity. These compounds, the yields and the purities, are listed in Table 3.3. The Wittig conditions are compatible with some benzylic, allylic, α -carbonyl, alkyl, and α -substituted phosphonium salts. Yields ranged from 28 to 82%. A survey of the results in Table 3.3 offers no pattern to either the yields or purities that were obtained. No attempt was made to identify which geometric isomers were formed for each reaction. In some instances, sets of overlapping doublets were clearly present in the ^{19}F NMR which clearly indicates the presence of both *E* and *Z* isomers whereas other compounds displayed only a single signal which may mean that a single compound was obtained or both isomers were obtained but their ^{19}F NMR signals overlap.

Table 3.3. Product yields and purities from the 'Wittig library.'

Compound	% Yield	HPLC	Purity	
			¹⁹ F	³¹ P
3.61 	82	100	100	100
3.62 	56	90	98	98
3.63 	60	100	99	93
3.64 	61	99	98	97
3.65 	62	99	99	98
3.66 	62	97	96	100
3.67 	68	95	98	100

3.68 	65	95	92	98
3.69 	44	95	90	97
3.70 	28	100	100	98
3.71 	38	100	100	98
3.72 	82	91	95	99
3.73 	41	97	97	98
3.74 	83	100	96	100
3.75 	64	92	88	100

<p style="text-align: center;">3.76</p> 	70	93	88	97
<p style="text-align: center;">3.77</p> 	71	98	85	88
<p style="text-align: center;">3.78</p> 	82	80	96	100
<p style="text-align: center;">3.79</p> 	31	72	97	85
<p style="text-align: center;">3.80</p> 	83	65	98	95
<p style="text-align: center;">3.81</p> 	60	87	83	56
<p style="text-align: center;">3.82</p> 	49	100	92	43

The purity of each compound was assessed by ^{19}F NMR, ^{31}P NMR, and HPLC. ^1H -NMR was of little use for determining purity for most of the compounds since the protons in most of the compounds were in the aromatic

region. For a given compound, variations among the three measurements was not uncommon, which emphasizes the importance of verifying product purity by as many means as possible. Of the twenty-two compounds in Table 3.3, fourteen were obtained in greater than 90% purity (3.61-3.74). Of the eight that were obtained in less than 90% purity (3.75-3.82), 4 were obtained in 80% purity or better (3.75-3.78). Two of the four (3.79-3.82) that were obtained in the lowest purity had a phenolic ether group on the distal (distal from the phosphonate group) aryl ring (3.81 and 3.82). This may have been due to some reaction of the ether moiety with TMSBr. However, compound 3.77, which also bears a phenolic ether group was obtained in much better purity than 3.81 and 3.82.

^{31}P -NMR and MS analysis revealed that the primary contaminant for most of the compounds was inorganic phosphate (P_i). This was very surprising since it was not present in all of the compounds and was not evident when we worked out the Wittig reaction conditions on our test compounds (see Scheme 3.17). Nevertheless, in some instances such as with compounds 3.81 and 3.82, the amount of P_i was quite significant accounting for over 40% of the entire product as determined by ^{31}P NMR.⁵⁴ P_i was not present in polymer-bound aldehyde 3.46 which indicated that it must have been produced during the Wittig reaction. It is very unlikely that the P_i from the phosphonium salt or triphenylphosphine oxide (a byproduct of the reaction). The most likely source of this contaminant is by cleavage of the P-CF_2 bond during the Wittig reaction, although there is no literature precedent for this reaction. The severing of the $\text{CF}_2\text{-P}$ bond accounts

for the relatively clean ^{19}F signals we observed for the polymer bound alkenes as well as the appearance of an intact phosphonate linkage in the ^1H NMR. Upon cleavage of the $\text{CF}_2\text{-P}$ bond, the fluorine containing byproducts are released from the support and collected in the filtrate while the phosphonate ester bond to the polymer remains intact. As a result of this unwanted reaction, the ^1H NMR would appear to indicate that the Wittig reaction proceeded as desired since no aldehyde proton is observed and no change occurs for the $\text{CH}_2\text{-O-P}$ signal. The TMSBr deprotection reactions would remove both our desired compounds and the phosphate contaminant from the support as inorganic phosphate. Like the desired phosphonic acids, P_i would be temporarily immobilized on the LC-NH_2 columns and be co-eluted as the ammonium salt. We do not know why some of the compounds had significant quantities of P_i (such as **3.79**, **3.81** and **3.82**) and why others had none since there does not appear to be any pattern. Fortunately, the amount of P_i can be semi-quantitated by ^{31}P -NMR and the P_i will not affect the PTP1B inhibition studies as P_i does not inhibit PTP1B, at least at the concentrations that the compounds were screened.

3.3.10 Inhibition Studies

Jason Lee, an undergraduate in the Taylor group, has recently performed inhibition studies with the compounds listed in Table 3.3. A rapid screen of these compounds was performed using approximately $50\ \mu\text{M}$ of each compound. From this screen, compound **3.74**, bearing an allyl ester moiety, was identified as the most potent. None of the stilbene-like compounds exhibited any significant inhibition at this concentration. The IC_{50} of **3.74** was determined to be $11\ \mu\text{M}$

while that of the methyl (**3.78**) ester was approximately 40 μM and that of the ethyl (**3.73**) was greater than 50 μM . It appears that the allyl group is more effective than a simple alkyl group. Molecular modeling studies will have to be performed to determine why this is so. The allyl group may be capable of π -stacking interactions with Y46 or π -cation interactions with K120. A more careful analysis of **3.74** revealed that it is a reversible competitive inhibitor with a K_i of 5 μM , which is quite remarkable considering the simplicity of the compound.

3.4 Summary of the Wittig Library

The Wittig library demonstrated that we can expand the type of chemistry for preparing aryl DFMP's on NCPS beyond a simple Suzuki coupling. The synthesis of the alkenes involved a total of five reactions on the polymer which consisted of coupling, deprotection, oxidation, Wittig reaction, and deprotection/cleavage steps. We were able to prepare 22 novel compounds in states ready for rapid screen assays against PTP1B. A competitive inhibitor exhibiting a K_i of 5 μM was identified. The limitations of our Wittig reaction conditions seems to arise from the sensitive nature of the DFMP group. We were also successful in applying a novel technique for the purification of the phosphonic acids using LC-NH₂ solid phase extraction columns. This purification technique can potentially be used for purifying a diverse range of organic acids.

3.5 Conclusions Concerning the Use of Soluble Polymers as Supports for PSOS

Now that we have some experience constructing compounds on NCPS, we feel that we are now qualified to make some conclusions concerning the use

of NCPS in PSOS. There are definite advantages in using soluble support such as NCPS. We found that being able to follow the reactions on the support by conventional solution NMR to be particularly useful. We also found that conditions developed in solution were usually (but not always) transferable to the support with a few minor adjustments. We would say that these two issues are perhaps the greatest advantages to using a soluble polymer versus an insoluble polymer where working out the conditions on the support can often be very time consuming. Nevertheless, in spite of these advantages, it is clear that there are some disadvantages to using a soluble polymer. Perhaps the greatest disadvantage is that, at least with NCPS, recovery of the polymer is not quantitative after precipitation and filtration. We found this to be a major problem when working with less than 500 mg of polymer. One way of improving polymer recovery is to use centrifugation instead of filtration. This approach is currently under investigation in the Taylor group. Also, with NCPS, a considerable amount of solvent is required for the precipitation step. The occlusion of contaminants within NCPS during the precipitation step is also a potential problem. Finally, to our knowledge, SPSOS has not yet been automated. Due to the above listed disadvantages, we believe that the SPSOS using NCPS is not well suited to the synthesis of libraries requiring many synthetic steps or the parallel synthesis of large libraries, at least not until the problem of polymer recovery is solved. Centrifugation may be the key towards more efficient polymer recovery between reactions. Until this problem is solved, we believe that the SPSOS using NCPS is useful only when a lead compound is available and libraries consisting of 10-

100 analogues each are required and the number of steps in the synthesis does not exceed four or five on the support.

3.5.1 Conclusions Concerning the Synthesis of DFMP's on Polymer Supports

Is it more convenient to prepare aryl DFMP's on a polymer support in the manner we described here or is standard solution phase methodology better? The answer depends upon the amount of time required to work out the conditions on the support. When conducting reactions on the support, it is preferable to use conditions that allows one to drive the reactions to 100% completion so that products are not contaminated with large quantities of incomplete material. This is not a requirement in solution since materials are purified by chromatography at the end of each step. If such conditions are available or can be *rapidly* developed, then we believe the polymer-supported route is probably the more convenient approach when preparing more than ten compounds.

We should point out that the hydrolytic lability of the DFMP group is a problem whether the reactions are performed on the support or in solution. The only DFMP compounds that can be prepared on a support or in solution in good yield are those that can be made under relatively mild conditions. To get around the problem of hydrolytic lability of the phosphonate ester linkage during PSOS, one could react polymer-bound aryl iodides with $\text{BrCdCF}_2\text{PO}(\text{OEt})_2$ in the presence of CuCl (Burton's chemistry, see Section 2.3.2.2), as the last step of the synthesis. However, we found that attaching the compounds to the support by the DFMP group was very convenient in terms of following the reactions using

^{19}F NMR. The ability to do this would be lost if addition of the DFMP group was the last step of the reaction sequence. Also, we have found that Burton's chemistry requires a considerable excess of the cadmate reagent to proceed in reasonable yields⁵⁵ even in solution, which would make this a very expensive procedure on a support especially if one wishes to drive the reactions to completion.

The use of TMSI or TMSBr to remove the compounds from the support and deprotect the ethyl group in a single step was very convenient but also had the draw back in that the high reactivity of these reagents limits the type of functional groups which can be incorporated on the polymer-bound aryl phosphonate. However, we should note that this would also be a problem whether one made DFMP compounds in solution or on the support unless one used the DAST procedure to prepare the DFMP compounds in solution since this is the only procedure that allows one to use *t*-butyl protecting groups which does not require TMSBr or TMSI for removal. However, as mentioned earlier (see section 2.3.2.1), DAST is expensive and there are certain health risks when using this procedure.

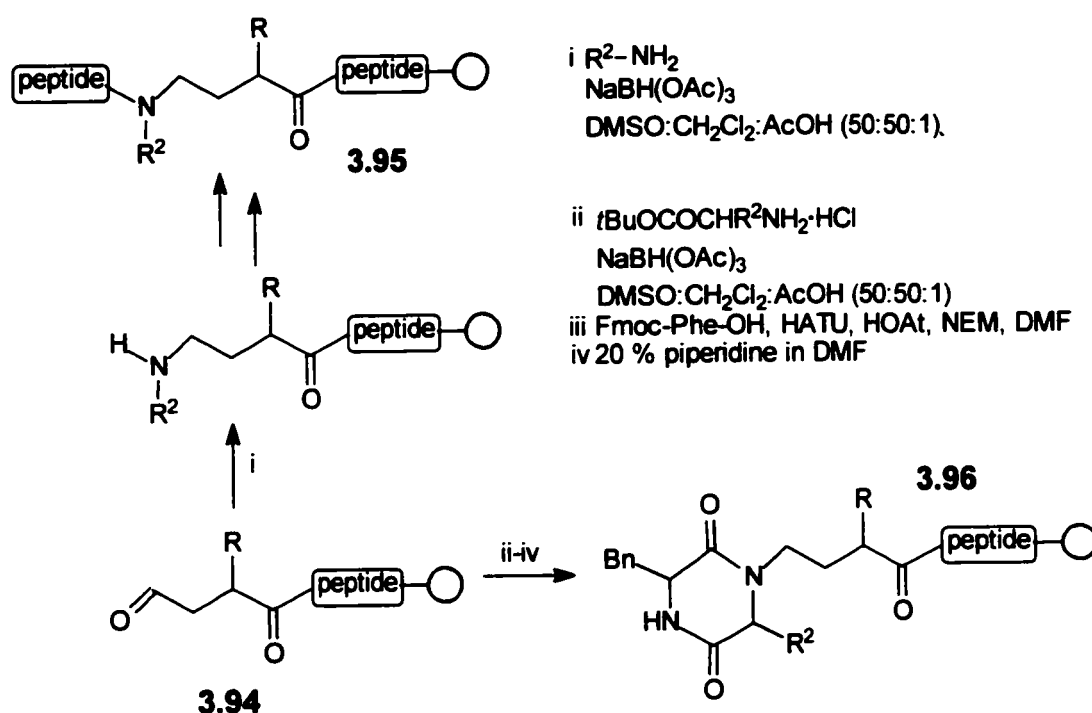
3.6 Future Directions

3.6.1 Future Work With Aryl Aldehyde DFMP Compounds on NCPS

As in the case of the polymer bound aryl bromide compounds (2.50 and 2.51), the polymer bound aldehyde 3.46 may also serve as a versatile building block for the purpose of expanding the diversity of aryl DFMP compounds. Some potential routes were outlined in Scheme 3.3. A survey of the recent literature

offers a few other examples of reactions which may be adopted to NCPS in order to build libraries based upon the aldehyde core.

Groth and coworker reported a diverse range of reactions on a polymer bound N-terminal peptide aldehydes for the synthesis of novel peptide isosteres.⁵⁶ A total of four reactions were evaluated: (a) reductive amination with amines, (b) reductive amination with amino esters, (c) Horner-Wadsworth-Emmons olefinations, and (d) Pictet-Spengler condensations. Examples of reductive aminations are presented in Scheme 3.20.

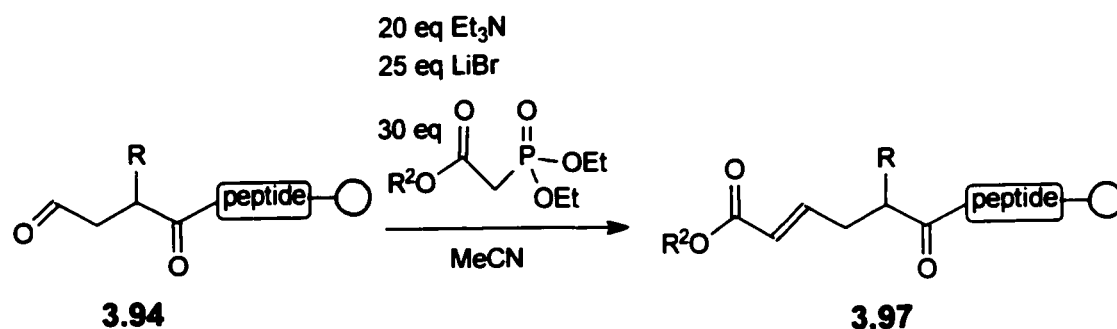


Scheme 3.20. Reductive amination as a route to diversity.

Starting from polymer bound aldehyde **3.94**, reductive amination followed by peptide coupling to the resulting amine led to the synthesis of compounds of the type **3.95** where the N-alkyl-4-amino butyric peptide isostere is positioned centrally in a peptide. Alternatively a reaction sequence composed of a reductive

amination with an amino ester, followed by the coupling of a Fmoc protected amino acid to the free amine and finally the removal of the Fmoc group led to a series of 2,5-diketopiperazine peptides with the general structure of **3.96**.

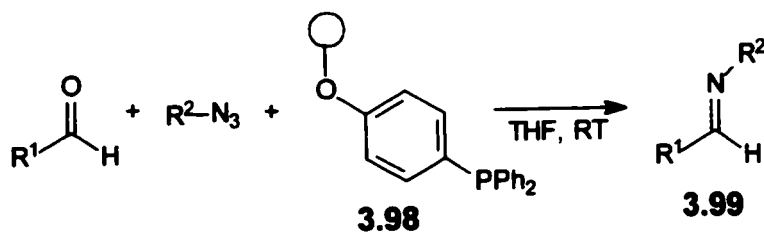
Mild Horner-Emmons-Wadsworth conditions as outlined in Scheme 3.21 were also reported. In these reactions diethyl phosphonoacetates with various protecting groups on the carbon ester were reacted with the polymer bound aldehyde in the presence of triethyl amine and lithium bromide in acetonitrile. The resulting olefin-esters could be deprotected for further elongation with various protected amino acids.



Scheme 3.21. HWE reactions with polymer bound aldehydes.

Charette *et al.* employed NCPS as a support for reagents in the Staudinger/Aza-Wittig reaction.⁵⁷ This is a slight variation in strategy where triphenyl phosphine was immobilized on NCPS (**3.98**) and used as a reagent in the reaction between an aldehyde and an azide. This was a solution to the problem of separating the desired products from the triphenyl phosphine oxide byproduct. In Charette's approach, the triphenyl phosphine is retained on the NCPS which is precipitated and filtered. The conditions are obviously compatible

with NCPS, and should be easily adapted to our system with the polymer bound aldehyde and triphenyl phosphine free in solution.



Scheme 3.22. Staudinger/Aza-Wittig reaction with polymer supported triphenylphosphine.

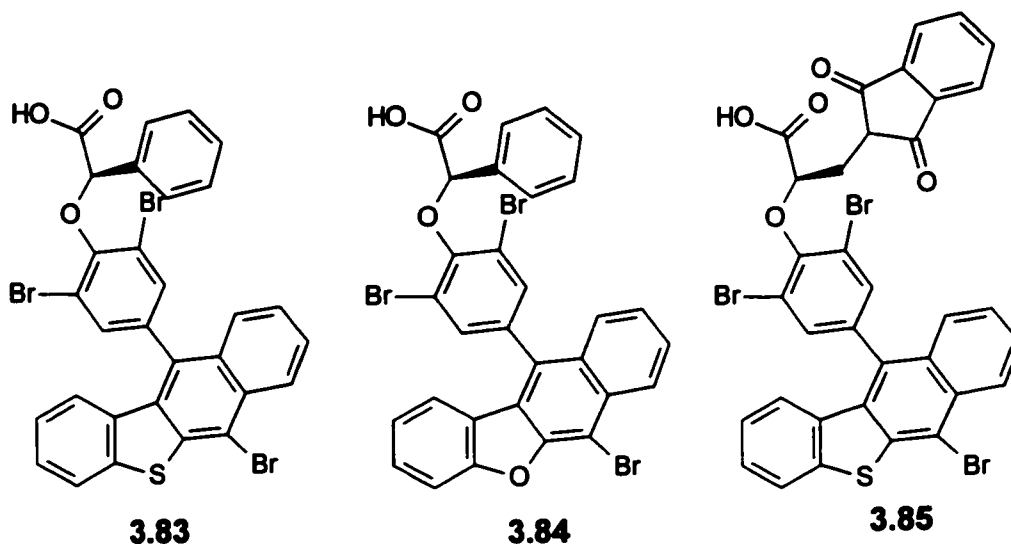
The polymer bound aldehyde functionality offers much flexibility in the number and types of reactions which may be used in order to prepare additional series of novel compounds for screening against PTP1B. The number and types of compounds can be increased even further if the polymer bound DFMP compound is reacted as either the alcohol and/or acid. The potential reactions in this route are too numerous to mention here, but it is evident that a wide range of reactions may potentially be adapted to the NCPS support.

3.6.2 Alternative Applications of Aryl DFMP Compounds

Though we synthesized our compounds with PTP1B as the biological target, the compounds described herein and in Chapter 2 may also be screened against other PTPases. As outlined in Section 1.3, the family of PTPases comprises a fairly diverse group of enzymes. In many instances, the function of these enzymes has yet to be determined. Many of the compounds described in this work may be useful tools in elucidating the biological role of other PTPases even if they show little or no activity against PTP1B.

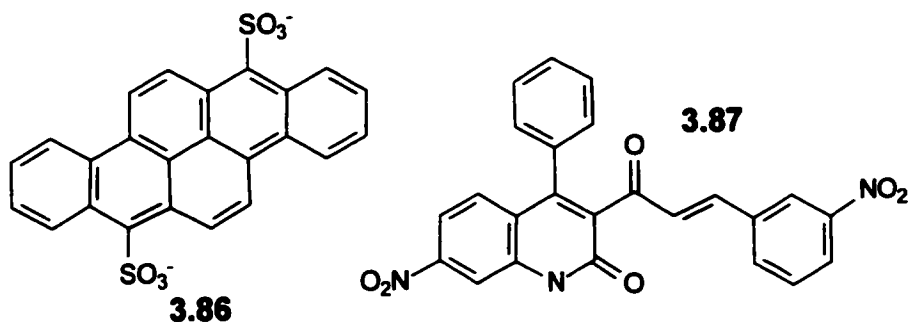
3.7 Recent Advances in PTP1B Inhibitor Design

While our studies on constructing the biaryl and styryl DFMP libraries were in progress, several other groups reported their progress in the discovery of novel PTP1B inhibitors.

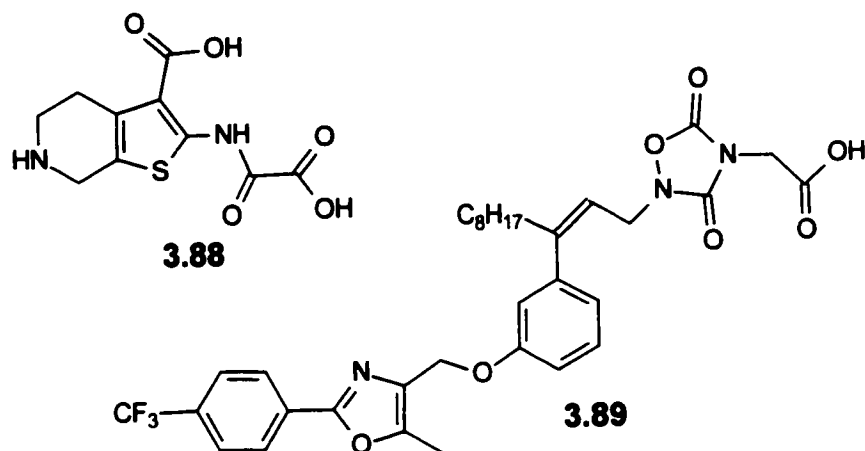


Wrobel *et al.* described several compounds with sub micromolar IC_{50} values.⁵⁸ Compounds **3.83-3.85** had IC_{50} values of 61, 83, and 11 nM respectively. Compounds **3.83** and **3.84** were effective in lowering glucose levels when administered orally to diabetic test mice. However, these compounds were not successful in clinical trials.⁵⁹

Sarmiento *et al.* used DOCK methodology to investigate potential PTP1B inhibitors and discovered compounds **3.86** and **3.87** with K_i values of 39 and 54 μ M respectively against PTP1B.⁶⁰ These compounds also displayed some selectivity since the K_i values for PTP α , LAR, and VHR were over 100 μ M.

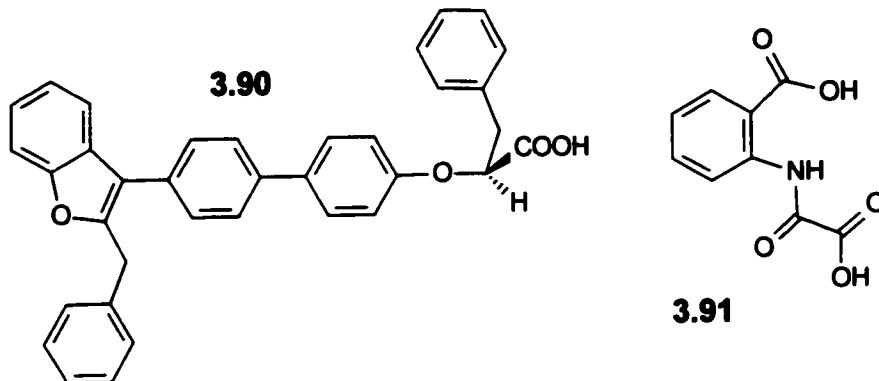


Using structure based design guided by PTP1B mutants and X-ray crystal structures, Iversen *et al.* prepared **3.88** which was found to have a K_i of 5.1 μM against PTP1B.⁶¹ Remarkable selectivity was exhibited by **3.88** since of the 7 PTPase enzymes evaluated, the K_i of **3.88** against CD45 ranked a distant second at 840 μM .

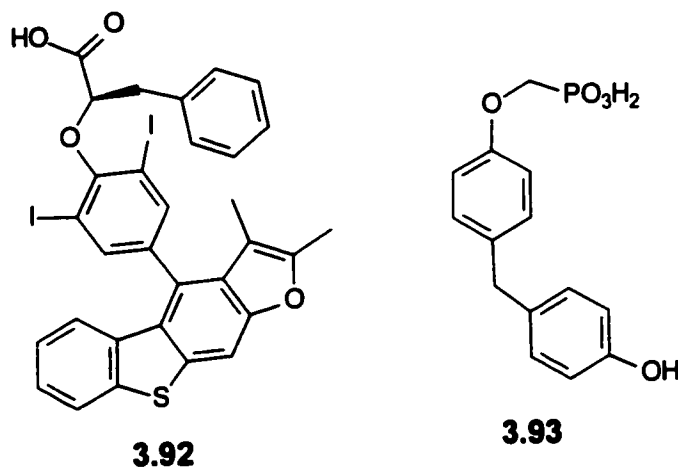


Malamas and coworkers prepared a series of compounds based upon a azolidinedione scaffold.⁶² The most effective compound against PTP1B was **3.89** which had an IC_{50} value of 120 nM. Malamas also reported an even more potent series of inhibitors based upon benzofuran and benzothiophene biphenyl scaffolds. Though other analogues exhibited better *in vitro* potency against PTP1B, **3.90** had a IC_{50} of 320 nM and from the more than 80 compounds tested, was the most effective in reducing glucose levels in test mice in *in vivo* tests.

Compound **3.90** also exhibited at least a 10 fold selectivity over other PTPases such as LAR, PTP α , VHR and He-PTP.⁶³ We are not aware of any clinical studies being done with these compounds.



Andersen and coworkers found that **3.91** was an effective inhibitor of PTP1B with a K_i of 8 μM .⁶⁴ The 2-(oxalylamino)-benzoic acid group is among the most effective phenyl phosphate mimetics identified to date.



On the basis of modeling and X-ray crystallography data, Wrobel and coworkers modified the scaffold of **3.83-3.85** obtain the thiacyclopenta(*b*) fluorine system of **3.92**. Compound **3.92** had an IC_{50} of 74 nM against PTP1B.⁶⁵ The aryloxyposphonate moiety was found to be a suitable surrogate for the

phosphate group. Compound **3.93** was found to have a K_i of 47 μM against PTP1B by Ibrahimi *et al.*⁶⁶

The work described in this section represents the major advances in the development of small molecule inhibitors of PTP1B which were reported during the course of our work. The interest in PTP1B has yet to subside due to its attractiveness as a biological target for the treatment of type 2 diabetes. Though it is obvious that much progress has been made in finding novel inhibitors of PTP1B, other factors must be considered. The potency of small molecule PTP1B inhibitors is continually being improved, but the issue of selectivity must also be addressed due to the widespread presence of PTPases throughout the body. Due to the similarity between many other PTPases and PTP1B, selectivity may prove to be the most crucial consideration in obtaining an actual viable therapeutic candidate.

3.8 REFERENCES

- 1 Yokomatsu, T.; Murano, T.; Umesue, I.; Soeda, S.; Shimeno, H.; Shibuya, S. *Bioorg. Med. Chem. Lett.* **1999**, *9*, 529-532.
- 2 Lorsbach, B. A.; Kurth, M. J. *Chem. Rev.* **1999**, *99*, 1549-1581.
- 3 Hughes, I. *Tetrahedron. Lett.* **1996**, *37*, 7595-7598.
- 4 Bolli, M. H.; Ley, S. V. *J. Chem. Soc. Perkin Trans. 1* **1998**, 2243-2246.
- 5 Salvino, J. M.; Kiesow, T. J.; Dambrough, S.; Labaudiniere R. *J. Comb. Chem.* **1999**, *1*, 134-139.
- 6 Barret, A. G. M.; Cramp, S. M.; Roberts, R. S.; Zecri, F. *J. Org. Lett.* **1999**, *1*, 579-582.
- 7 Wipf, P. Henninger, T. C. *J. Org. Chem.* **1997**, *62*, 1586-1587.
- 8 Leznoff, C. C.; Sywanyk, W. *J. Org. Chem.* **1977**, *42*, 3203-3205.
- 9 Vagner, J.; Krchnak, V.; Lebl, M.; Barany, G. *Collect. Czech. Chem. Commun.* **1996**, *61*, 1697-1702.
- 10 Peters, J-U.; Blechert, S. *Synlett* **1997**, 348-350.
- 11 Johnson, C. R.; Zhang, B. *Tetrahedron Lett.* **1995**, *36*, 9253-9256.
- 12 Burke Jr., T. R.; Smyth, M. S.; Nomizu, M.; Otaka, A.; Roller, P. P. *J. Org. Chem.* **1993**, *58*, 1336-1340.
- 13 Hartman, G. D.; Phillips, B. T.; Halczenko, W. *J. Org. Chem.* **1985**, *50*, 2423-2427.
- 14 Hartman, G. D.; Halczenko, W.; Phillips, B. T. *J. Org. Chem.* **1986**, *51*, 142-148.

-
- 15 Endo, Y.; Ohno, M.; Hirano, M.; Itai, A.; Shudo, K. *J. Am. Chem. Soc.* **1996**, *118*, 1841-1855.
- 16 Bellucci, G.; Chiappe, C.; Lo Moro, G. *Tetrahedron Lett.* **1996**, *37*, 4225-4228.
- 17 Devraj, R.; Cushman, M. J. *J. Org. Chem.* **1996**, *61*, 9368-9373.
- 18 Hamper, B. C.; Dukesherer, D. R.; South, M. S. *Tetrahedron. Lett.* **1996**, *37*, 3671-3674
- 19 Swayze, E. E. *Tetrahedron. Lett.* **1997**, *38*, 8465-8468.
- 20 Castro, J. L.; Matassa, V. G. *J. Org. Chem.* **1994**, *59*, 2289-2291.
- 21 Personal communication from Y. Han, Merck Frosst.
- 22 Patel, D. V.; Rielly-Gavin, K.; Ryono, D. E. *Tetrahedron. Lett.* **1990**, *31*, 5591-5594.
- 23 Greene, T. W.; Wuts, P. G. M. "Protective Groups in Organic Synthesis" 3rd Ed., John Wiley & Sons Inc. **1999**.
- 24 Das, J.; Chandrasekaran, S. *Syn. Commun.* **1990**, *20*, 907-912.
- 25 Rajasekharan Pillai, V. N. *Synthesis* **1980**, 1-26.
- 26 Holmes, C. P.; Jones, D. G. *J. Org. Chem.* **1995**, *60*, 2318-2319.
- 27 Holmes, C. P. *J. Org. Chem.* **1997**, *62*, 2370-2380.
- 28 Gomez-Martinez, P.; Dessolin, M.; Guibe, F.; Albericio, F. *J. Chem. Soc., Perkin Trans. 1* **1999**, 2871-2874.
- 29 Opatz, T.; Kunz, H. *Tetrahedron. Lett.* **2000**, *41*, 10185-10188.
- 30 Aoyama, T.; Sonoda, N.; Yamauchi, M.; Toriyama, K.; Anzai, M.; Ando, A.; Shioiri, T. *Synlett* **1998**, 35-36.

-
- 31 Hirano, M.; Yakabe, S.; Chikamori, H.; Clark, J. H.; Morimoto, T. *J. Chem. Res. (S)* **1998**, 308-309.
- 32 Hirano, M.; Yakabe, S.; Chikamori, H.; Clark, J. H.; Morimoto, T. *J. Chem. Res. (S)* **1998**, 770-771.
- 33 Wei, X.; Taylor, R. J. K. *Tetrahedron. Lett.* **1998**, 3815-3818.
- 34 Blackburn, L.; Wei, X.; Taylor, R. J. K. *Chem. Commun.* **1999**, 1337-1338.
- 35 Wei, X.; Taylor, R. J. K. *J. Org. Chem.* **2000**, *65*, 616-620.
- 36 Bolm, C.; Magnus, A. S.; Hildebrand, J. P. *Org. Lett.* **2000**, *2*, 1173-1175.
- 37 Griffith, W. P.; Ley, S. V.; Whitcombe, G. P.; White, A. D. *J. Chem. Soc. Chem. Commun.* **1987**, 1625-1627.
- 38 Ley, S. V.; Norman, J.; Griffith, W. P.; Marsden, S. P. *Synthesis* **1994**, 639-666.
- 39 Yan, B.; Sun, Q.; Wareing, J. R.; Jewell, C. F. *J. Org. Chem.* **1996**, *61*, 8765-8770.
- 40 Hinzen, B.; Ley, S. V. *J. Chem. Soc., Perkin Trans 1* **1997**, 1907-1908.
- 41 Haurert, F.; Bolli, M. H.; Hinzen, B.; Ley, S. V. *J. Chem. Soc., Perkin Trans 1* **1998**, 2235-2237.
- 42 Dess, D. B.; Martin, J. C. *J. Org. Chem.* **1983**, *48*, 4156-4158.
- 43 Ireland, R. E.; Liu, L. *J. Org. Chem.* **1993**, *58*, 2899.
- 44 Stevenson, P. J.; Treacy, A. B.; Nieuwenhuyzen, M. J. *J. Chem. Soc., Perkin Trans. 2* **1997**, 589-591.
- 45 Gayo, L. M.; Suto, M. J. *Tetrahedron. Lett.* **1997**, *38*, 513-516.

-
- 46 Suto, M. J.; Gayo-Fung, L. M.; Palanky, M. S. S.; Sullivan, R. *Tetrahedron* **1998**, *54*, 4141-4150.
- 47 Siegel, M. G.; Hahn, P. J.; Dressman, B. A.; Fritz, J. E.; Grunwell, J. R.; Kaldor, S. W. *Tetrahedron. Lett.* **1997**, *38*, 3357-3360.
- 48 Organ, M. G.; Mayhew, D.; Cooper, J. T.; Dixon, C. E.; Lavorato, D. J.; Kaldor, S. W.; Siegel, M. G. *J. Comb. Chem.* **2001**, *3*, 64-67.
- 49 Bookser, B. C.; Zhu, S. *J. Comb. Chem.* **2001**, *3*, 205-215.
- 50 Holy, A.; Rosenberg, I. *Collect. Czech. Chem. Commun.* **1987**, *52*, 2801-2809.
- 51 Compound **3.49** was generously provided by J. Lee of the Taylor group.
- 52 The exact nature of the alkyl amine functionality is proprietary information which belongs to the manufacturer Rohm and Haas.
- 53 Personal communication from B. Vogler, Supelco Technical Support.
- 54 Maniara, G.; Rajamoorthi, K.; Rajan, S.; Stockton, G. W. *Anal. Chem.* **1998**, *70*, 4921-4928.
- 55 Qabar, M. N.; Urban, J.; Kahn, M. *Tetrahedron* **1997**, *53*, 11171-11178.
- 56 Groth, T.; Meldal, M. *J. Comb. Chem.* **2001**, *3*, 45-63.
- 57 Charette, A. B.; Boezio, A. A.; Janes, M. K. *Org. Lett.* **2000**, *2*, 3777-3779.
- 58 Wrobel, J.; Sredy, J.; Moxham, C.; Dietrich, A.; Li, Z.; Sawicki, D. R.; Seestaller, L.; Wu, L.; Katz, A.; Sullivan, D.; Tio, C.; Zhang, Z-Y. *J. Med. Chem.* **1999**, *42*, 3199-3202.
- 59 S . D. Taylor, personal communication.

-
- 60 Sarmiento, M.; Wu, L.; Keng, Y-F.; Song, L.; Luo, Z.; Huang, Z.; Wu, G-Z.; Yuan, A. K.; Zhang, Z-Y. *J. Med. Chem.* **2000**, *46*, 146-155.
- 61 Iversen, L. F.; Andersen, H. S.; Branner, S.; Mortensen, S. B.; Peters, G. H.; Norris, K.; Olsen, O. H.; Jeppesen, C. B.; Lundt, B. F.; Ripka, W.; Moller, K. B.; Moller, N. P. H. *J. Biol. Chem.* **2000**, *275*, 10300-10307.
- 62 Malamas, M. S.; Sredy, J.; Gunawan, I.; Mihan, B.; Sawicki, D. R.; Seestaller, L.; Sullivan, D.; Flam, B. R. *J. Med. Chem.* **2000**, *43*, 995-1010.
- 63 Malamas, M. S.; Sredy, J.; Moxham, C.; Katz, A.; Xu, W.; McDevitt, R.; Adebayo, F. O.; Sawicki, D. R.; Seestaller, L.; Sullivan, D.; Taylor, J. R. *J. Med. Chem.* **2000**, *43*, 1293-1310.
- 64 Andersen, H. S.; Iversen, L. F.; Jeppesen, C. B.; Branner, S.; Norris, K.; Rasmussen, H. B.; Moller, K. B.; Moller, N. P. H. *J. Biol. Chem.* **2000**, *275*, 7101-7108.
- 65 Wrobel, J.; Li, Z.; Sredy, J.; Sawicki, D. R.; Seestaller, L.; Sullivan, D. *Bioorg. Med. Chem. Lett.* **2000**, *10*, 1535-1538.
- 66 Ibrahimi, O. A.; Wu, L.; Zhao, K.; Zhang, Z-Y. *Bioorg. Med. Chem. Lett.* **2000**, *10*, 457-460.

CHAPTER 4 ANTIBODY CATALYZED HYDROLYSIS OF PHOSPHOTRIESTERS

4.1 Introduction

4.1.1 Overview and Global Objectives

In chapters 1-3 our work focused on naturally occurring phosphatases and methods for preparing inhibitors of these enzymes. In this chapter, the focus of our work shifts from naturally occurring phosphatases to artificial phosphatases or what we call phosphohydrolases. More specifically, this chapter deals with our efforts to obtain catalytic antibodies capable of catalyzing the hydrolysis of phosphate triesters or phosphonate diesters.

Phosphate esters are found throughout biological systems and, therefore, their hydrolysis represents a reaction of fundamental importance. The development of catalytic antibodies, or abzymes, capable of hydrolyzing phosphate esters has been an area of interest since the first examples of these artificial catalysts were first reported.^{1,2} In addition to perhaps shedding some light on how proteinaceous systems catalyze phosphate ester hydrolysis, such abzymes may perhaps find use as artificial restriction enzymes and as detoxification agents of organophosphorus poisons. An integral part of obtaining an abzyme is the design and synthesis of a transition state analogue (TSA) of the reaction in question. The objective of the work described in this chapter is to examine the use of cyclic five-membered phosphinate esters as TSA's for obtaining phosphohydrolase abzymes. Here we report the synthesis of such compounds bearing nitrophenyl groups at the 2- and 5-position on the five

membered ring, their conjugation to carrier proteins, and our attempts to obtain phosphohydrolase abzymes using these TSA's.

4.1.2 Antibodies

The mammalian immune system represents an incredibly diverse source of antibodies, or immunoglobulins, which are the protein based agents responsible for recognizing and binding to entities that are foreign to an organism. There are several classes of antibodies only one of which, the IgG class, is of practical use when developing abzymes. A typical IgG antibody has a molecular weight of 150 000 daltons. It is composed of two polypeptide chains called the light and heavy chains which are connected by disulfide bonds, as shown in Figure 4.1. Both the heavy and light chains contain variable regions (V_H and V_L) which are highly polymorphic. Most of the variation in amino acid sequence is concentrated into three short hypervariable sequences. The hypervariable sequences line the antibody's antigen-binding site and determine the binding properties of the antibody. Proteolysis by the enzyme papain cleaves the antibody molecule at the hinge portion of the molecule and produces two Fab fragments (antigen binding fragments) and one Fc fragment (named in this way because it is easily crystallized). The Fab retains all the binding specificity of the entire antibody molecule, since this segment of the immunoglobulin contains the hypervariable sequences.

Figure 4.2 is a ribbon representation of the X-ray crystal structure of a monoclonal IgG antibody. The two heavy chains are in blue and green and the

two light chains are in red. The antigen binding sites are located at the termini of 'arms' of the Y formed by the Fab portion.

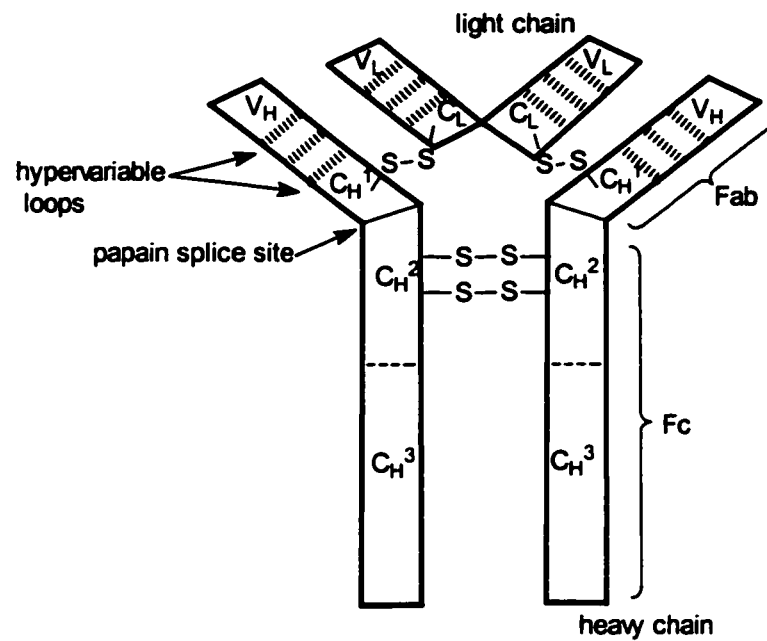


Figure 4.1. A schematic representation of a IgG class antibody.



Figure 4.2. A ribbon representation of an IgG class antibody.³

By varying the sequence of the V_L and V_H segments, up to 10^8 different antibody molecules are possible.^{4,5} This represents a significant pool of molecules which are able to display a wide array of binding properties. Antibodies can exhibit both remarkable specificity and affinity in binding to their antigens with association constants ranging from 10^4 to 10^{14} . A significant advance in the field of immunology was the work of Köhler and Milstein⁶ who devised a method of obtaining monoclonal antibodies from immortalized immune cell hybrids. This hybridoma technology makes it possible to generate large amounts of antibodies with specific and distinct binding properties. Hybridoma techniques are a solution to the problem of polyclonal antibody preparations which are composed of a variety of antibodies which differ in their specificity and affinity for a ligand and, are therefore difficult to characterize and utilize in diagnostic type applications.

In brief, to obtain monoclonal antibodies using hybridomas techniques, the antigen of interest is conjugated to a carrier protein. A mouse is immunized with the protein conjugate, or hapten, whose immune system responds by generating antibodies against the hapten. After an incubation period ranging from weeks to months, the mouse is sacrificed and the spleen harvested for the antibody producing lymphocytes. The lymphocytes are unable to grow continuously in cultures and are thus fused with myeloma cells. The resulting myeloma hybrids, or hybridomas, retain the favourable characteristic of both the myeloma and lymphocytes in that they can be grown continuously in culture and produce the antibodies of interest. The resulting hybrids are separated and the antibodies

that they produce are evaluated for the binding property of interest. When cell lines expressing the antibody of interest are identified, the hybridomas can then be reintroduced into a host animal in order to produce the antibodies on a larger scale. The ability to use hybridoma cells in order obtain large amounts of monoclonal antibodies was an important development which was almost essential for the field of catalytic antibodies.

A more recent development has led to an alternative to using animal immunizations and hybridomas techniques. The Fab fragments of antibodies can be encoded in phage vector systems, and the actual Fab fragments expressed on the viral coat. The random combination of the Fab coding gene sequences leads to a library of Fab fragments which rivals that produced by the mammalian immune system in terms of diversity. Once Fab segments which bind the antigen of interest are found, the phages can be introduced into bacterial systems for production of the antibody Fab fragments on a larger scale.⁷

4.1.3 Catalytic Antibodies

Antibodies and enzymes are alike in that they are both protein based macromolecules which bind their target ligands. The fundamental difference is in their respective functions. As a result of evolution, enzymes are catalysts in that they bind to their substrates and exert a chemical change upon them whereas the traditional notion of antibodies is that of binding to an antigen for the purpose of 'labelling' it for neutralization and/or destruction by other elements of the immune response. Pauling⁸ originated the idea that enzymes catalyze reactions by preferential binding of the transition state over the ground state of the

substrates. Using this principle, Jencks⁹ was the first to propose the idea of employing antibodies as catalysts by raising antibodies against transition state-like haptens since the antibodies cannot be raised against the transition states themselves, since by definition, transition states have a negligible lifetime. However, it is possible to mimic a transition state for a reaction using a transition state analogue (TSA). TSA's have been applied as potent enzyme inhibitors.¹⁰ Abzymes raised against a TSA would, in theory, have the ability to bind to and stabilize the transition state (TS) for a reaction in order to lower its activation free energy and therefore catalyze the reaction.

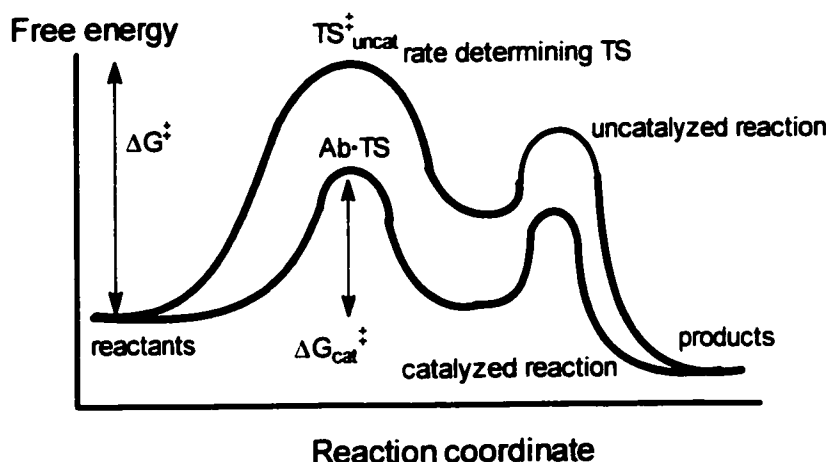


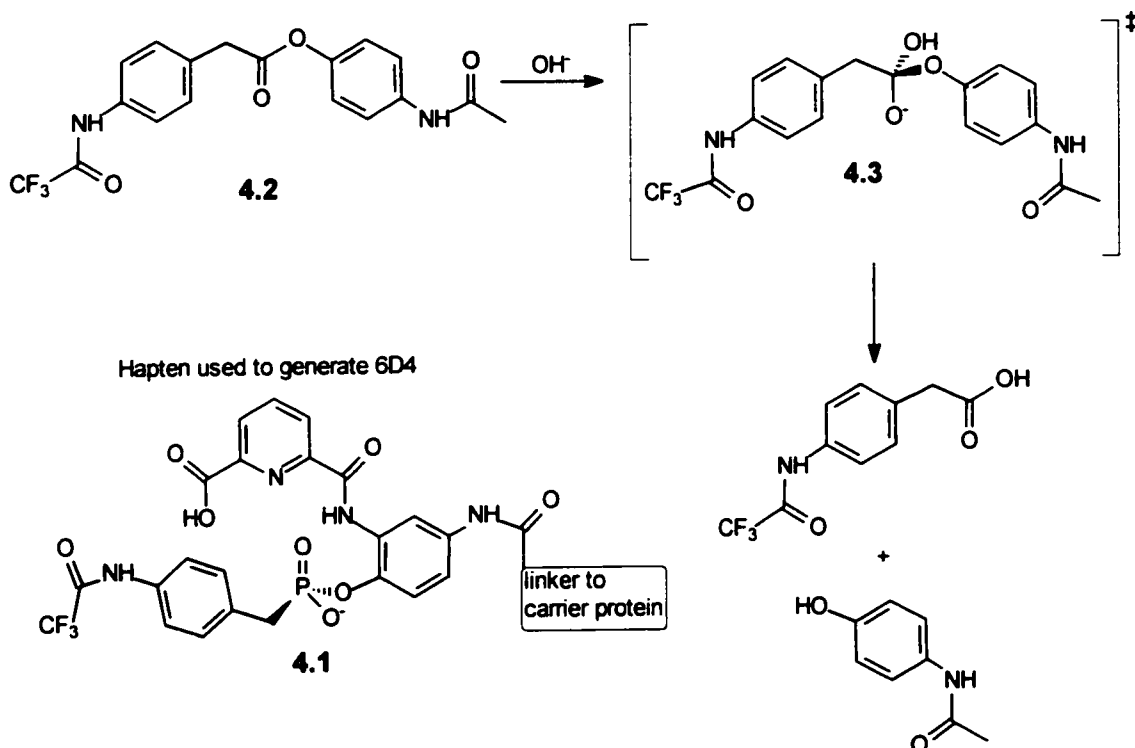
Figure 4.3. Abzymes catalyze reactions by lowering the energy of the transition state.

Figure 4.3 demonstrates this principle. The rate of the reaction is dictated by how readily the reactants are able to reach the transition state. Formation of the transition state is inevitably associated with a high energy barrier (ΔG^{\ddagger}). Since the antibodies would be raised against haptens which mimic the transition state of the reaction, they would similarly bind to and stabilize the actual

transition state thereby lowering its energy ($\Delta G_{\text{cat}}^\ddagger$). As long as the value of ΔG^\ddagger is greater than $\Delta G_{\text{cat}}^\ddagger$ the action of the antibody is catalytic.

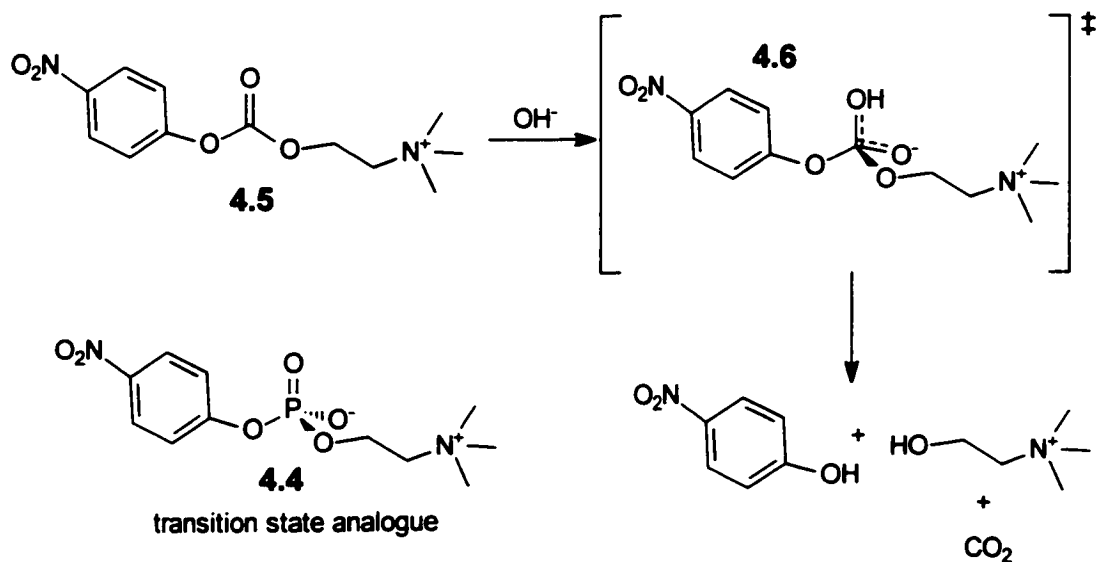
The earliest attempt to test the Jencks' idea in the lab by Raso *et al.* failed to produce any novel catalysts^{11,12} and it is believed that this is at least partially due to the difficulties that arose in the purification and isolation of the polyclonal antibody preparations. This work predated the accomplishments of Köhler and Milstein⁶ and was thus were unable to take advantage of hybridoma technology.

In 1986, two separate groups reported their success in obtaining catalytic antibodies capable of hydrolyzing ester and carbonate substrates.^{1,2} These reports are considered the seminal papers in the field and mark the transition of Jencks' concept from theory to practice.



Scheme 4.1. Ester hydrolysis by abzyme 6D4.

Lerner *et al.* found that antibody 6D4, which was raised against **4.1**, was capable of hydrolyzing **4.2** with a k_{cat} of 0.027 s^{-1} which represents a 960 fold enhancement over the uncatalyzed reaction (Scheme 4.1).¹ The substrate **4.2** bound to 6D4 with a K_m of $1.9 \mu\text{M}$. Antibody 6D4 was inhibited by the TSA **4.1** with a K_i of $1.6 \times 10^{-7} \text{ M}$. Though the 2,6-dicarboxylate pyridine functionality was intended to incorporate a metal coordination site, **4.1** was used as a non-chelated hapten for obtaining 6D4 which acted as a catalyst in the absence of metal cofactors. Hydrolysis of **4.2** proceeds through the tetrahedral transition state **4.3** which is mimicked in geometry and charge distribution by the phosphonate **4.1** which acts as a TSA for the reaction. Since 6D4 binds the TSA, it presumably also binds to and stabilizes the actual transition state for the reaction in order to lower its energy for catalysis.



Scheme 4.2. Carbonate hydrolysis by MOPC167.

Schultz *et al.* found that antibody MOPC167, which bound **4.4** with high affinity ($K_d = 1.4 \times 10^{-6} \text{ M}$), was able to catalyze the hydrolysis of carbonate **4.5**

with a k_{cat} of 0.4 min^{-1} which represented a 770 fold increase over the uncatalyzed reaction.² The abzyme demonstrated Michaelis-Menten kinetics and substrate specificity. Phosphate **4.4** serves as an analogue to **4.6**, which is the proposed tetrahedral transition state for the reaction and catalysis is achieved by stabilization of the transition state.

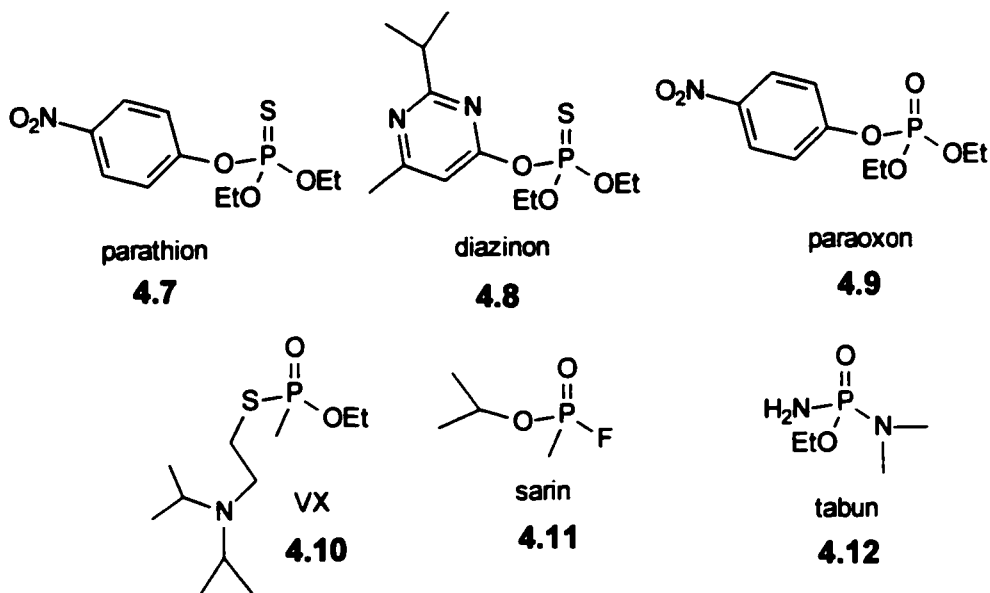
Since the publication of these papers, the field has progressed significantly with many novel catalysts having been reported elicited by a diverse range of hapten design strategies. The enormity of the field precludes an adequate summary here but several excellent reviews on the topic of catalytic antibodies are available.^{13,14,15} The interest in catalytic antibodies still continues due to the potential applications which include the development of novel catalysts, the evaluation of proposed catalytic mechanisms, and use as novel therapeutic agents.

4.1.4 Phosphatase Catalytic Antibodies

Phosphate esters are present throughout biological systems and certain examples of phosphates ester bonds are among the most stable linkages in living systems. The interest in developing phosphatase abzymes stems mainly from the potential practical and therapeutic applications. The development of artificial restriction abzymes with preprogrammed specificities not found in nature is often cited as an example of a practical application of phosphatase antibodies.

Many toxic agents contain a phosphorous ester functionality. Examples of organophosphorous insecticides include parathion (**4.7**), diazinon (**4.8**), and paraoxon (**4.9**). Paraoxon is used in many developing countries and has been

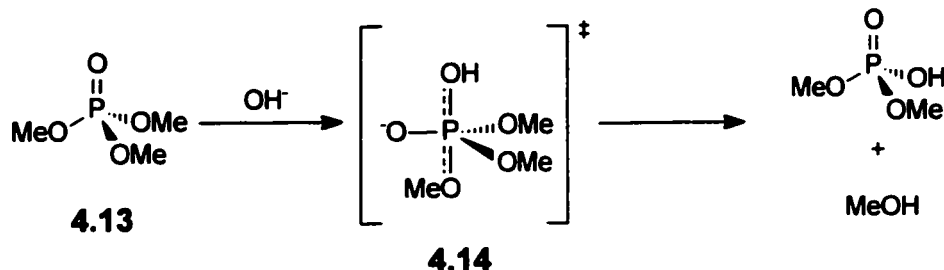
linked to the poisoning of agricultural workers. A few examples of phosphorous based chemical warfare agents are VX (4.10), sarin, (4.11), and tabun (4.12).



One can envision using catalytic antibodies as a novel therapeutic agent to treat victims of organophosphorous based toxins. In this application, victims and/or potential patients would be immunized with an appropriate antigen and the resulting immune response would generate antibodies capable of hydrolyzing the toxins before they can have their deleterious effects. The catalytic destruction of toxins *in homo* would be a radical departure from convention where antibodies neutralize toxins by simply immobilizing them by virtue of their recognition and binding.

Besides the inherent stability of certain phosphate esters, perhaps the greatest challenge in obtaining a phosphatase abzyme is the lack of suitable transition state analogues. As an example, the hydrolysis of trimethyl phosphate (4.13) proceeds through a trigonal bipyramidal transition state (TBP) (4.14) as shown in Scheme 4.3. There are few chemical species which are able to both

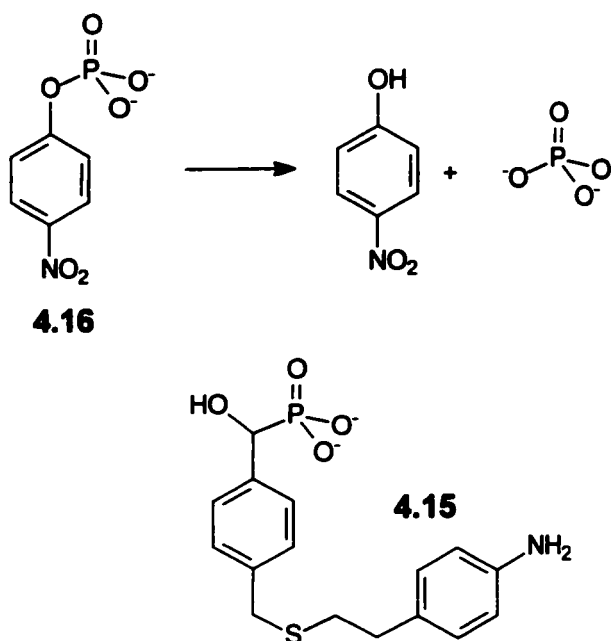
mimic the TBP geometry and charge distribution found of **4.14** and serve as immunogens for eliciting antibodies. Such compounds are often toxic or hydrolytically labile which prevents their use in immunization procedures.



Scheme 4.3. Phosphate ester hydrolysis proceeds through a trigonal bipyramidal transition state.

When we began our own investigations into developing phosphatase abzymes, there were only a few examples of the hydrolysis of phosphate esters by catalytic antibodies. There were also additional reports of hapten design and syntheses for the purpose of eliciting phosphatase abzymes where researchers outlined their strategy for developing novel catalysts.

Scanlan *et al.* raised antibodies against **4.15** and found five antibodies which were capable of hydrolyzing *p*-nitrophenyl phosphate (**4.16**) at rates appreciably greater than the uncatalyzed reaction (Scheme 4.4).¹⁶ One antibody, 38E1, was characterized in greater detail and found to have a k_{cat} of 0.0012 min^{-1} and a K_m of $155 \mu\text{M}$. 38E1 was also capable of multiple turnovers. The report by Scanlan does not offer a mechanistic explanation for the basis of the catalysis and no subsequent investigations into 38E1 have been reported. The workers do however suggest that **4.15** may mimic a species involving attack of a water molecule on the phosphate monoester.



Scheme 4.4. Antibody catalyzed phosphate monoester hydrolysis.

Rosenblum and coworkers reported a more rational strategy for inhibitor design when they immunized mice with **4.17**.¹⁷ The charged amine oxide group is intended to elicit complementary opposite charges in the side chains of the antibody binding site as seen in Figure 4.4. The placement of the charged residues would stabilize the developing charges in the transition state for the hydrolysis of **4.19** and **4.20** which results in the release of *p*-nitrophenol. The strategy in using **4.17** was to address the electrostatic characteristics of the transition state without an attempt to mimic its TBP geometry. Several catalysts were elicited, but one in particular, Tx1-4C6, proved to be more efficient than the others. Tx1-4C6 catalyzed the hydrolysis of **4.19** and **4.20** with k_{cat} values of 1.01×10^{-2} and 1.85×10^{-3} respectively which represents rate enhancements of 360 and 21 fold over the uncatalyzed reactions. This work demonstrated that it is

possible to obtain catalysts by addressing only the electrostatic features of the transition state.

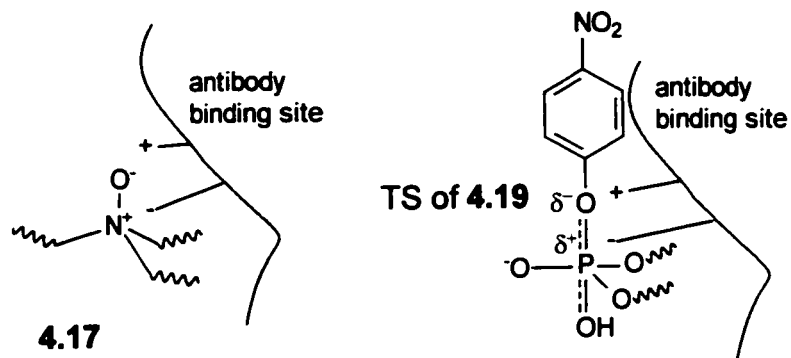
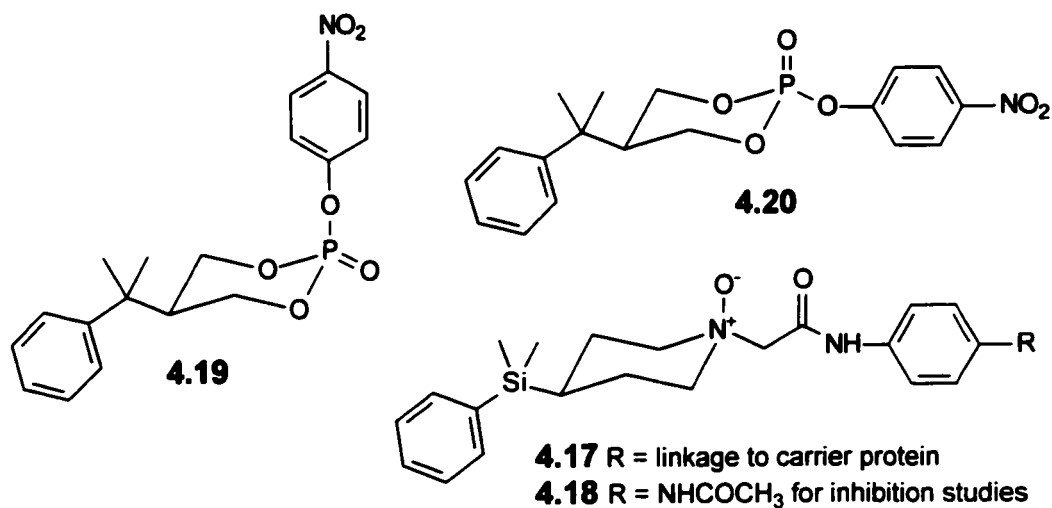
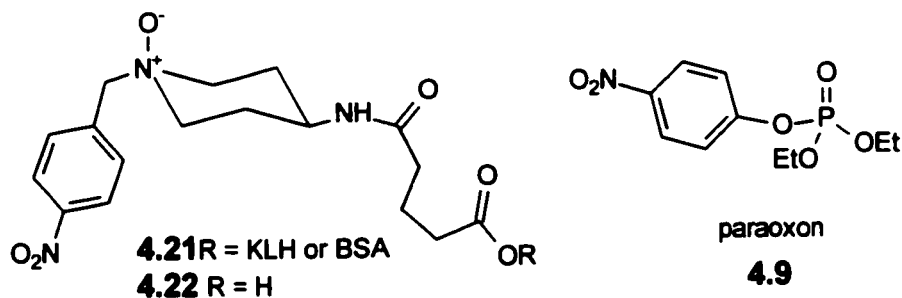


Figure 4.4. Development of complementary charges in antibody active site and their role in stabilizing charges in the TS of **4.19**.



Using the same principles to obtain Tx1-4C6, Lavey *et al.* immunized mice with **4.21** in order to produce antibodies capable of hydrolyzing the insecticide

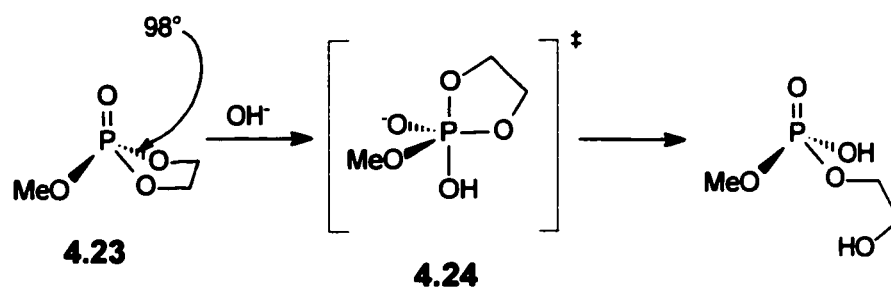
paraoxon (**4.9**).^{18,19} Hapten **4.21** incorporates the *p*-nitrobenzyl group which is used to evoke a strong immune response and allow the abzyme to recognize the *p*-nitrophenol group of **4.9**. Of the 25 monoclonal antibodies which were found to bind **4.21**, only one, 3H5, was found to act as a catalyst. The k_{cat} of 3H5 for paraoxon hydrolysis varied with pH. The maximum rate enhancement over the uncatalyzed reaction was found to occur at pH 8.51 where a 516 fold increase was observed. Catalyst 3H5 had an optimal K_m of 1.6 mM at pH 7.8 and was competitively inhibited by the unconjugated hapten **4.22**. Though the observed rate enhancement was not useful for clinical applications, 3H5 successfully demonstrates the potential use of abzymes for the treatment of organophosphorus poisoning.

4.1.5 Specific Objectives

It is very apparent that the hydrolysis of phosphate esters by catalytic antibodies represents a significant chemical challenge and that there is room for improvement in this area. Whereas other groups have addressed the electrostatic requirements of the transition state, our hapten design focuses on geometric considerations.

It has been known for many years that cyclic five-membered phosphate esters hydrolyze much faster than their acyclic analogues. For example, methylethylenephosphate (MEP, **4.23**, Scheme 4.5) hydrolyzes 10^6 times faster than its acyclic analogue **4.13** and results almost exclusively in the ring opening product under basic conditions.^{20,21,22,23}

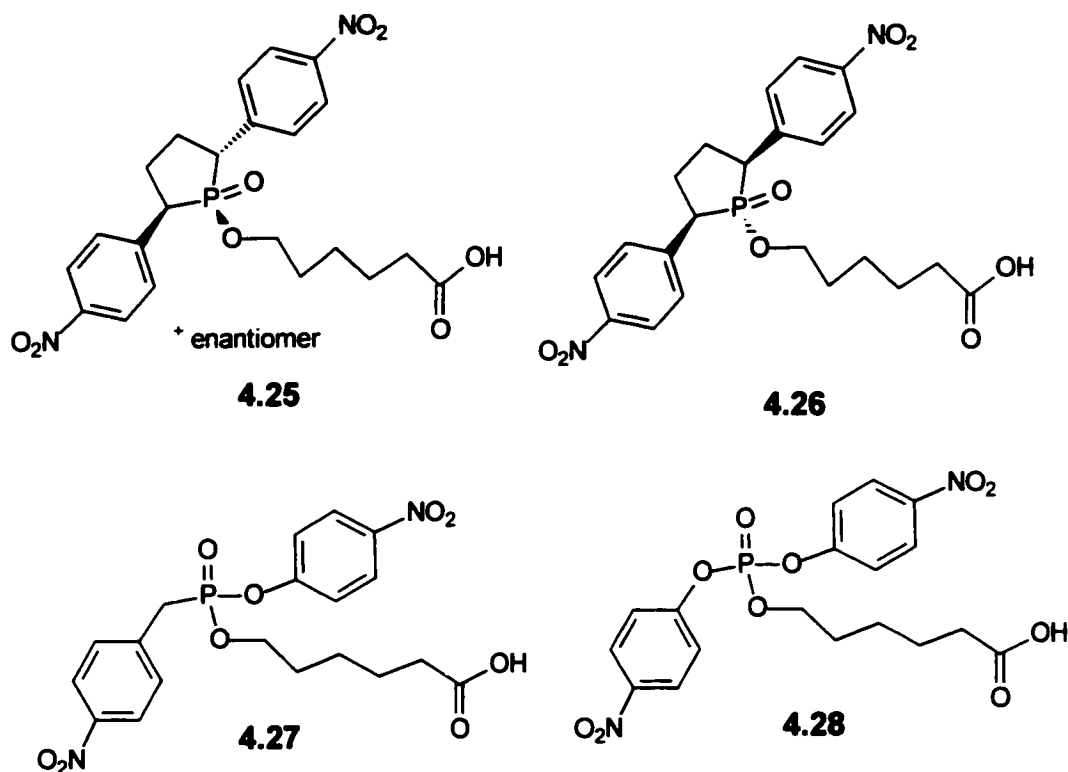
Calorimetric studies suggest that the rate enhancement is mainly a result of the release of ring strain at the transition state.^{22,23}



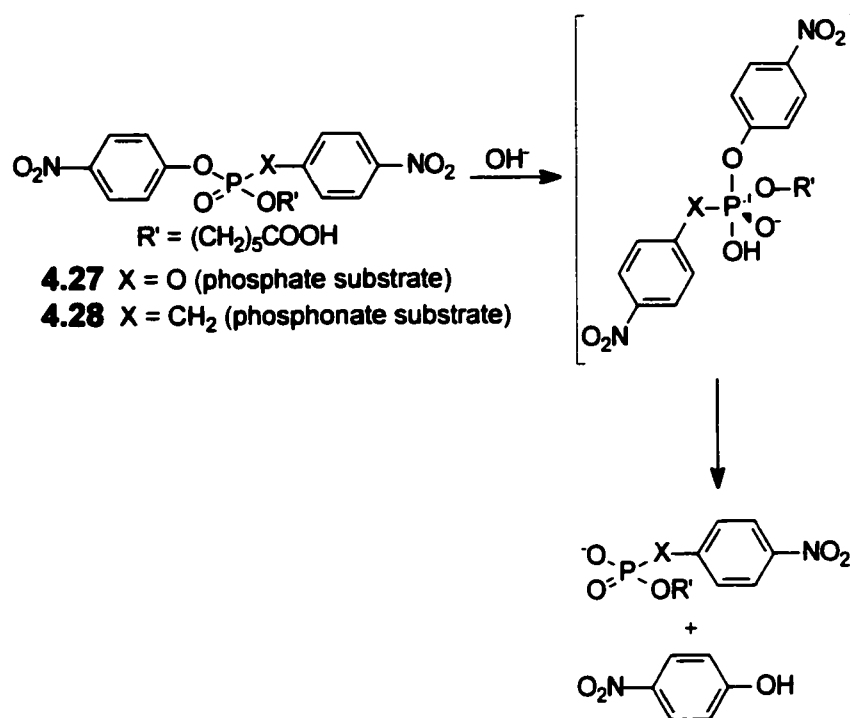
Scheme 4.5. Hydrolysis of a cyclic phosphate ester.

X-ray crystallographic studies have demonstrated that the endocyclic O-P-O bond angle in MEP (**4.23**) is 98° ²⁴ which is considerably less than ideal tetrahedral bond angle of 109° . In the TBP transition state (**4.24**), the strain is relieved when the ring spans an apical and equatorial position and the O-P-O bond is 90° which is ideal for the TBP geometry. The strain hypothesis has been challenged on the basis of theoretical calculations conducted by Chang *et al.*²⁵ These authors suggest the source of the rate enhancement is a result of differential solvation effects between the ground state and the transition state. Nevertheless, the fact that the endocyclic O-P-O bond angle in MEP is indeed distorted towards the ideal equatorial-axial TBP transition state bond angle of 90° found during phosphate ester hydrolysis is undisputable.

Our approach to obtaining phosphohydrolase abzymes is to use cyclic five-membered phosphinate esters as TSA's. We will test this approach by raising abzymes to compounds **4.25** and **4.26**. Abzymes specific for these TSAs will be examined for their ability to hydrolyze esters **4.27** and **4.28**.



There are several features of these TSA's which warrant mention. First, we expect the C-P-C bond angle of **4.25** and **4.26** to be compressed towards the ideal equatorial-axial TBP bond angle of 90° found during the hydrolysis of phosphate esters **4.27** and **4.28** (Scheme 4.6). This is based on the work of Alver²⁶ and Chiu²⁴ who reported the crystal structures of cyclic phosphinates and phosphates and found the C-P-C/O-P-O bond angles to be $95\text{-}98^\circ$. Second, the phosphoryl bond is fairly polar²⁷ and has the potential to elicit complementary charges in the binding site which may potentially stabilize developing charges in the transition state. Third, *p*-nitrophenyl groups are used since they are strong antigenic determinants and would therefore provoke a strong immune response and be strongly recognized by the individual antibodies. This feature also allows us to incorporate *p*-nitrophenol in the substrates which facilitates kinetic studies.



Scheme 4.6. Hydrolysis of substrates for antibodies raised against **4.25** and **4.26**.

A six carbon linker is used to join the TSA's to the carrier proteins and is attached to the phosphorous atom, away from the aryl rings, in order to minimize interference with antibody recognition. Finally, by utilizing both the *trans* (**4.25**, phenyl groups *trans* to one another) and *cis* (**4.26**, phenyl groups *cis* to one another) isomers of the TSA, crucial antigenic determinants can be ascertained. For example, if an antibody raised to the *cis* hapten binds equally well to the *trans* hapten (or vice versa) then this would imply that the antibody does not bind strongly to both phenyl rings and would probably not catalyze the reaction. Here we report the synthesis of **4.25** and **4.26** and our attempts to obtain phosphohydrolase abzymes using these compounds as TSA's.

4.2 Experimental

General

The general details for the synthesis, purification, and characterization of compounds is as described in section 2.2. HPLC purifications were performed on a Waters LC 450 System using an Altech normal phase silica preparative HPLC column (250 mm x 22 mm i.d. with 10 μ Econosil silica, cat. no. 6259). All of the phospholanate esters reported here were analyzed by HPLC using the above system equipped with an Altech normal phase silica analytical HPLC column (10 μ Econosil silica, cat. no. 60090) and were found to exhibit a single peak in the HPLC chromatogram.

4.2.1 Synthesis of Transition State Analogues

(\pm)-trans-1-ethoxy-2,5-diphenyl-2,3-dihydro-1H-1 λ^5 -phosphol-1-one

(4.42) and (\pm)-cis-1-ethoxy-2,5-diphenyl-2,3-dihydro-1H-1 λ^5 -phosphol-1-one

(4.43): Method A: 1,4 diphenyl-1,3-butadiene (2.06 g, 10 mmol, 1 equiv) was combined with 2,6-di-tert-butyl-4-methyl phenol (10 mg, 2 mol%) in a 15 mL ACE Glass pressure tube (cat. no. 8648-75) equipped with a stir bar and then flushed thoroughly with Ar. Phosphorous trichloride (0.545 mL, 6.33 mmol, 0.66 equiv) and tris(2-chloroethyl) phosphite (0.635 mL, 3.33 mmol, 0.33 equiv) was added to the tube under a stream of Ar. The glass bomb was rapidly sealed and the thick, mainly solid mixture was vigorously shaken by hand for about 30 seconds to mix the contents. The tube was immersed in an oil bath, stirred vigorously, and slowly heated to 170°C and maintained at this temperature for 19 hrs during which time the solid diene melted and the solution reaction became an orange

colour. **CAUTION: This procedure must be performed in a fumehood behind a blast shield.** In addition to several broad beaks, the ^{31}P NMR of the crude reaction mixture exhibited 2 sharp peaks of approximately equal magnitude at 68.6 and 69.7 ppm. After removing the oil bath and allowing the tube to cool to room temperature, the tube was fitted with a septum and dry benzene (20 mL) was added to the crude reaction mixture under argon. The solution was transferred very slowly over a period of 30 min via syringe to an ice cold solution of dry ethanol (5.8 mL, 100 mmol, 10 equiv) and triethylamine (1.7 mL, 10 mmol, 1 equiv) in dry benzene (20 mL) and the reaction was stirred overnight at room temperature under Ar. The volume of the crude reaction mixture was reduced to one quarter by rotary evaporation and diluted with ether (75 mL) which resulted in the precipitation of triethylamine hydrochloride which was removed by suction filtration. The filter cake was washed with ether and the filtrate was washed with 0.1 N HCl (3 x 50 mL), 5% NaHCO_3 (3 x 50 mL), brine (3 x 50 mL) and then dried (MgSO_4) and concentrated *in vacuo* to yield a crude orange oil which was subjected to silica gel column chromatography. Flash chromatography on silica, (9:1 CH_2Cl_2 :EtOAc, $R_f = 0.4$) of the crude reaction yielded **4.42** as a pale yellow solid (577 mg, 19.2%): mp 82-86 °C; ^1H NMR δ 1.23 (3H, t, $J = 6.9$ Hz), 2.81-2.96 (1H, m), 3.10-3.54 (2H, m), 3.98-4.23 (2H, m), 7.03 (1H, t, $J = 3.3$ Hz), 7.42 (8 H, m), 7.65 (2H, d, $J = 6.2$ Hz); ^{31}P NMR δ 60.41 (s); ^{13}C NMR δ 142.20 (d, $J = 36.1$), 138.35 (br d), 136.95 (d, $J = 4.6$ Hz), 133.59 (d, $J = 9.1$ Hz), 128.70, 128.39 (d, $J = 11.5$ Hz), 126.96, 126.68 (d, $J = 5.5$ Hz), 61.58 (d, $J = 6.4$ Hz), 42.28 (d, $J = 92.8$ Hz), 35.57 (d, $J = 17.8$ Hz), 16.66 (d, $J = 5$ Hz); MS, m/z

(relative intensity) 298 (64), 270 (36), 205 (100), 104 (31), 91 (41), 77 (30); HRMS calcd for $C_{18}H_{19}O_2P$ 298.1123, found 298.1127. From the same column **4.43** (9:1 CH_2Cl_2 :EtOAc, $R_f = 0.6$) was obtained as a white solid (533 mg, 17.8%): mp 102-104 °C; 1H NMR δ 0.91 (3H, t, $J = 5.9$ Hz), 2.84-3.93 (5.5H, m), 7.08 (0.5H, t, $J = 3.75$ Hz), 7.35 (8H, m), 7.71 (2H, d, $J = 7$ Hz); ^{31}P NMR δ 60.05 (s); ^{13}C NMR δ 142.23 (d, $J = 35.7$ Hz), 137.58, 136.12 (d, $J = 6.5$ Hz), 135.20, 133.14 (br d), 128.70 (d, $J = 6.2$ Hz), 128.34, 126.92, 126.66 (d, $J = 3.7$), 61.58 (d, $J = 6.4$), 43.44 (d, $J = 90.6$), 33.19 (d, $J = 16.4$) 16.16; MS, m/z (relative intensity) 298 (100), 270 (66), 254 (47), 205 (50), 194 (83), 91 (43), 77 (30); HRMS calcd for $C_{18}H_{19}O_2P$ 298.1123, found 298.1134. **Method B:** The above McCormack reaction can also be performed in a similar manner as described above using dry benzene as solvent (approximately 3 mL of benzene per gram of diene) and heating the reaction in the sealed tube for 72 hours at 190 °C. This procedure produces **4.42** and **4.43** in a 2:1 ratio in yields that are slightly higher than that obtained by method A. **CAUTION: When performing the reaction using benzene as solvent, for safety reasons, the total volume of the reaction in the pressure tube must not be greater than half the total capacity of the pressure tube. The reaction must be performed in a fumehood behind a blast shield.**

(±)-1-ethoxy-trans-2,5-diphenyl-1 λ^5 -phospholan-1-one (**4.33**) and (meso)-trans-1-ethoxy-cis-2,5-diphenyl-1 λ^5 -phospholan-1-one (**4.34**): A solution of **4.42** (1.530 g, 5.03 mmol) in ethanol (20 mL) containing 10% Pd/C (100 mg) was hydrogenated overnight at 30 psi under a H_2 atmosphere using a

Parr hydrogenation apparatus. The Pd catalyst was removed by filtration and the filtrate concentrated *in vacuo* leaving a pale yellow oil which was subjected to column chromatography on silica (9:1 CH₂Cl₂:EtOAc) to give pure **4.33** and **4.34**. Overall yield was 99 %. **4.33** was obtained as a white solid (9:1 CH₂Cl₂:EtOAc, R_f = 0.5) (432 mg, 27 %): R_f = 0.5; mp 103-105 °C; ¹H NMR δ 0.93 (3H, t, J = 7.2 Hz), 2.07-2.60 (4H, m), 3.09-3.52 (3H, m), 3.66-3.85 (1H, m), 7.35 (10H, cm); ³¹P NMR δ 61.73 (s); ¹³C NMR δ 137.13 (d, J = 5.5 Hz), 128.70 (d, J = 5.5 Hz), 127.52, 126.68, 61.37 (d, J = 6.4 Hz), 43.59 (d, J = 85.1 Hz), 29.57 (d, J = 14.6 Hz), 16.69; MS, m/z (relative intensity) 300 (87), 206 (42), 196 (36), 104 (100), 91 (28), 78 (22); HRMS calcd for C₁₈H₂₁O₂P 300.1279, found 300.1272. **4.34** was obtained as a white solid (9:1 CH₂Cl₂:EtOAc, R_f = 0.3) (1.10 g, 72 %): mp 69-72 °C; ¹H NMR δ 1.24 (3H, t, J = 7.1 Hz), 2.33-2.46 (4H, m), 3.21-3.37 (2H, m), 4.00 (2H, m), 7.35 (10H, m); ³¹P NMR δ 62.37 (s); ¹³C NMR δ 136.69 (bd), 136.22 (d, J = 2.7 Hz), 128.76, 128.56, 128.14 (d, J = 4.6 Hz), 126.81, 61.24 (d, J = 7.3 Hz), 46.68 (d, J = 84.1 Hz), 45.50 (d, J = 86.9 Hz), 30.40 (d, J = 12.8 Hz), 27.85 (d, J = 9.0 Hz), 16.26 (d, J = 4.6 Hz); MS, m/z (relative intensity) 300 (91), 206 (41), 196 (26), 104 (100), 91 (30), 78 (20). HRMS calcd for C₁₈H₂₁O₂P 300.1279, found 300.1294.

(meso)-cis-1-ethoxy-cis-2,5-diphenyl-1λ⁵-phospholan-1-one (4.35): A solution of **4.43** (820 mg, 2.75 mmol) in ethanol (20 mL) containing 10% Pd/C (60 mg) was hydrogenated overnight at 30 psi under a H₂ atmosphere using a Parr hydrogenation apparatus. The Pd catalyst was removed by filtration and the filtrate concentrated *in vacuo* leaving a pale yellow solid. Silica gel

chromatography (EtOAc R_f = 0.40) yielded pure **4.35** as a white solid (674 mg, 82 %): mp 133-137 °C; $^1\text{H NMR}$ δ 0.64 (3H, t, J = 7 Hz), 2.42 (4H, m), 3.22-3.54 (4H, m), 7.31 (10H, m); $^{31}\text{P NMR}$ δ 65.14 (s); $^{13}\text{C NMR}$ δ 135.54 (d, J = 5.5 Hz), 128.41, 127.94 (d, J = 3.7 Hz), 126.63, 61.20 (d, J = 7.4 Hz), 43.96 (d, J = 82.4 Hz), 27.45 (d, J = 12.8 Hz), 15.90; MS, m/z (relative intensity) 300 (64), 206 (48), 196 (18), 104 (100), 91 (29), 78 (25); HRMS calcd for $\text{C}_{18}\text{H}_{21}\text{O}_2\text{P}$ 300.1279, found 300.1290.

General procedure for the nitration of 2,5-diphenyl-1 λ^5 -phospholan-1-one esters 4.33-4.35: To an ice cold solution of **4.33**, **4.34** or **4.35** (100 mg, 0.33 mmol, 1 equiv) in H_2SO_4 (1.5 mL) was added a solution of $\text{HNO}_3:\text{H}_2\text{SO}_4$ (1:1, 0.0180 mL, 0.86 mmol, 2.6 equiv HNO_3) dropwise of a period of 1 min. The reaction was stirred at 0 °C for 30 min and then poured into a beaker containing ice which upon melting left a suspension. CHCl_3 (20 mL) was added and the two layers were separated. The aqueous layer was further extracted with CHCl_3 (3 x 20 mL) and the combined organics phases were washed with brine (2 x 30 mL), dried (MgSO_4) and concentrated *in vacuo* leaving an oily solid residue. Pure nitrated esters (**4.46**, **4.47** and **4.48**) were obtained by either silica gel chromatography or recrystallization of the crude residue.

(\pm)-1-ethoxy-trans-2,5-di(4-nitrophenyl)-1 λ^5 -phospholan-1-one (4.46): Obtained in 55 % yield as a white solid from **4.33** using the general procedure described above. Purification was achieved using flash chromatography on silica (4:1 EtOAc:hexanes, R_f = 0.7): mp 179-180 °C; $^1\text{H NMR}$ δ 0.98 (3H, t, J = 7 Hz), 2.22 (2H, m), 2.56 (2H, m), 3.45 (3H, m), 3.83 (1H, m), 7.54 (4H, dd, J = 8 Hz, J

= 2.1 Hz), 9.24 (4H, d, $J = 8.4$ Hz); ^{31}P NMR 59.7 (s); ^{13}C NMR δ 147.32, 144.00, 143.46 (br d, $J = 13.8$ Hz), 129.45 (d, $J = 5.5$ Hz), 128.90, 123.73, 62.10 (d, $J = 5.4$ Hz), 46.7 (d, $J = 84.2$ Hz), 45.5 (d, $J = 86.1$ Hz), 30.37, (d, $J = 11$ Hz), 27.73 (d, $J = 11$ Hz.), 16.30; MS, m/z (relative intensity) 390 (100), 362 (28), 296 (61), 149 (86), 119 (51), 103 (55), 77 (58); HRMS calcd for $\text{C}_{18}\text{H}_{19}\text{N}_2\text{O}_6\text{P}$ 390.0981, found 390.0994.

(meso)-trans-1-ethoxy-cis-2,5-di(4-nitrophenyl)-1 λ^5 -phospholan-1-one

(4.47): Obtained in 64 % yield as a white solid from **4.34** using the general procedure described above. Purification was achieved by recrystallization in EtOAc:hexanes. mp 190-192 °C; ^1H NMR δ 1.24 (3H, t, $J = 7.2$ Hz), 2.45 (6H, m), 3.40 (2H, m), 4.03 (2H, m), 7.52 (4H, dd, $J = 2$ Hz, $J = 7$ Hz), 8.22 (4H, d, $J = 8.7$ Hz); ^{31}P NMR δ 60.49 (s); ^{13}C (CDCl_3) δ 147.32, 144.16 (d, $J = 5.4$ Hz), 129.45, 123.73, 62.26 (d, $J = 7.3$ Hz), 43.66 (d, $J = 86.1$ Hz), 29.31 (d, $J = 12.8$ Hz), 16.60; MS, m/z (relative intensity) 390 (100), 362, (26), 296 (77), 148 (95), 119 (44), 103 (37), 77 (36) ; HRMS calcd for $\text{C}_{18}\text{H}_{19}\text{N}_2\text{O}_6\text{P}$ 390.0981, found 390.0989.

(meso)-cis-1-ethoxy-cis-2,5-di(4-nitrophenyl)-1 λ^5 -phospholan-1-one

(4.48): Obtained in 75 % yield as a white solid from **4.35** using the general procedure described above. Purification was achieved using flash chromatography on silica (EtOAc, $R_f = 0.3$): mp 180-182 °C; ^1H NMR δ 0.65 (3H, t, $J = 7$), 2.45 (4H, m), 3.38 (2H, m), 3.59 (2H, m), 7.51 (4H, dd, $J = 2.2$ Hz, $J = 9.1$ Hz), 8.21 (4H, d, $J = 8.8$ Hz); ^{31}P NMR δ 59.9 (s); ^{13}C NMR δ 147.28, 143.54 (d, $J = 8.2$ Hz), 128.63 (d, $J = 4.6$ Hz), 123.62, 62.15 (d, $J = 7.3$ Hz), 44.10 (d, $J = 81.5$

Hz), 26.88 (d, $J = 7.9$ Hz), 15.94 (d, $J = 3.7$ Hz); MS, m/z (relative intensity) 390 (35), 362 (20), 296 (50), 149 (100), 119 (42), 103 (39), 77 (42); HRMS calcd for $C_{18}H_{19}N_2O_6P$ 390.0981, found 390.0992.

General procedure for the deprotection of esters 4.33-4.35 and 4.46-4.48: Trimethyl silyl iodide (1.2 equiv) was added dropwise to a solution of the ester (4.33-4.35 or 4.46-4.48) in dry CH_2Cl_2 (approx. 1 mmol ester/mL of solvent) and the reaction stirred for 2 hrs under an Ar atmosphere. Additional CH_2Cl_2 was added and the product was extracted into a 0.1 N sodium hydroxide solution. The two layers were immediately separated and the aqueous layer rapidly acidified to pH 1 (pH paper) with 6 N hydrochloric acid which resulted in the formation of the desired acid product as a precipitate. The product (4.44-4.45 or 4.49-4.50) was recovered by suction filtration. In some instances, further purification by HPLC was necessary.

(±)-1-hydroxy-trans-2,5-diphenyl-1 λ^5 - phospholan-1-one (4.44):

Obtained in a 90% yield as a white solid from 4.33 using the general procedure for ester deprotection described above. mp 220-223 °C; 1H NMR (CD_3OD) δ 2.10-2.59 (4H, m), 3.22-3.42 (2H, m), 7.20-7.42 (10H, m); ^{31}P NMR (CD_3OD) δ 63.49 (s); ^{13}C (CD_3OD) δ 138 (d, $J = 4.6$ Hz), 128.51 (d, $J = 4.6$ Hz), 128.06, 126.04, 45.46 (d, $J = 85.1$ Hz), 28.85 (d, $J = 11$ Hz); MS, m/z (relative intensity) 272 (46), 168 (18), 104 (100), 91 (28), 78 (25); HRMS calcd for $C_{16}H_{17} O_2P$ 272.0966, found 292.0972.

1-hydroxy-cis-2,5-diphenyl-1 λ^5 - phospholan-1-one (4.45): Obtained in a 90% yield as a white solid from 4.34 or 4.35 using the general procedure for

ester deprotection described above. mp 169-171 °C; ^1H NMR (DMSO- d_6) δ 2.13-2.44 (4H, m), 3.20-3.37 (2H, m), 7.16-7.39 (10H, m); ^{31}P NMR (DMSO- d_6) δ 60.32 (s); ^{13}C (DMSO- d_6) δ 138 (d, J = 6.5 Hz), 128.42 (d, J = 5.5 Hz), 128.08, 126.01, 43.23 (d, J = 84.2 Hz), 27.61 (d, J = 12.9 Hz); MS, m/z (relative intensity) 272 (57), 168 (23), 104 (100), 91 (24), 78 (25); HRMS calcd for $\text{C}_{16}\text{H}_{17}\text{O}_2\text{P}$ 272.0966, found 292.0976.

(\pm)-1-hydroxy-trans-2,5-di(4-nitrophenyl)-1 λ^5 - phospholan-1-one

(4.49): Obtained in a 90% yield as amorphous yellow solid from **4.49** using the general procedure for ester deprotection described above. mp 271-273 °C; ^1H NMR (DMSO- d_6) δ 2.04-2.45 (4H, m), 3.40-3.64 (2H, m), 7.62 (4H, d, J = 5.8 Hz), 8.27 (4H, d, J = 5.8 Hz); ^{31}P NMR (DMSO- d_6) δ 58.60 (s); ^{13}C (DMSO- d_6) δ 146.26, 129.68 (d, J = 5.4 Hz), 123.17, 45.68 (d, J = 82.2 Hz), 28.54 (d, J = 10 Hz); MS, m/z (relative intensity) 362 (100), 298 (36), 149 (54), 119 (38), 103 (26), 77 (29); HRMS calcd for $\text{C}_{16}\text{H}_{15}\text{N}_2\text{O}_6\text{P}$ 362.0668, found 362.0671.

1-hydroxy-cis-2,5-di(4-nitrophenyl)-1 λ^5 - phospholan-1-one (4.50):

Obtained in a 90% yield as an amorphous light yellow solid from **4.47** or **4.48** using the general procedure for ester deprotection described above. Purification was achieved via HPLC (isocratic, 99:1 CHCl_3 :MeOH, retention time = 13 min). mp 278-281 °C; ^1H NMR (DMSO- d_6) δ 2.06-2.48 (4H, m), 3.45-3.64 (2H, m), 7.62 (4H, d, J = 7.3 Hz), 8.22 (4H, d, J = 8.8 Hz); ^{31}P NMR (DMSO- d_6) δ 59.17 (s); ^{13}C (DMSO- d_6) δ 146.24, 129.56 (d, J = 4.5 Hz), 123.15, 43.71 (d, J = 82.4 Hz), 28.52 (d, J = 3.3 Hz), MS, m/z (relative intensity) 362 (36), 298 (19), 149 (100), 133 (43), 119 (20), 103 (32), 77 (43); HRMS calcd for $\text{C}_{16}\text{H}_{15}\text{N}_2\text{O}_6\text{P}$ 362.0668,

found 362.0681.

Allyl 6-hydroxyhexanoate (4.52): To a solution of tetrabutyl ammonium hydroxide (50 mL of a 20% w/w solution, 39 mmol, 1 equiv) was added ϵ -caprolactone (4.40 g, 39 mmol, 1 equiv). This mixture was stirred at 65 °C for 6 hrs after which the water was removed by high vacuum rotary evaporation. The resulting crude salt was dried under high vacuum for 18 hrs. The crude white salt that was produced (3.74 g, 10 mmol) was dissolved in dry DMF (15 mL) and allyl chloride (0.895 mL, 11 mmol, 1.1 equiv) was added and the solution stirred overnight for 12 hrs at room temperature. The reaction was diluted with water (75 mL) and extracted with EtOAc (4 x 50 mL). The organic phase was washed with 5% NaHCO₃ (3 x 250 mL), saturated brine (3 x 250 mL), dried (MgSO₄), and concentrated by rotary evaporation. Flash chromatography on silica gel (3:2 EtOAc:hexanes, R_f = 0.4) yielded the desired product **4.52** as a clear colourless oil (1.58 g, 90%): ¹H NMR δ 1.39-1.68 (6H, m), 2.29 (2H, t, *J* = 7.3 Hz), 3.55 (2H, t, *J* = 6.4 Hz), 4.49 (2H, d, *J* = 5.8 Hz), 5.28 (2H, t, *J* = 10.3 Hz), 5.57-5.91 (1H, m).

Benzyl 6-hydroxyhexanoate (4.58): To an aqueous solution of 20% tetrabutylammonium hydroxide (100 mL, 77.1 mmol, 1 equiv) was added ϵ -caprolactone (8.79 g, 77.1 mmol, 1 equiv) and the solution heated to 65 °C for 2 hours during which time the solution became homogeneous. The solution was concentrated by rotary evaporation leaving a white solid that was dried under high vacuum for several hours. The solid was dissolved in dry DMF (80 mL) and benzylchloride (10.7 g, 84.8 mmol, 1.1 equiv) was added and the reaction stirred

for 24 hrs. The reaction mixture was diluted with water (80 mL) and the extracted with ether (4 x 150 mL). The ether layers were combined and dried (Na_2SO_4), then concentrated leaving a pale yellow oil. Flash chromatography on silica, (3:2 hexanes:EtOAc, $R_f = 0.3$) of the oil yielded pure **4.58** as a colourless oil (15.2 g, 89%): ^1H NMR δ 1.33-1.71 (7H, m), 1.91 (1H, s), 2.37 (2H, t, $J = 7.3$ Hz), 3.60 (2H, t, $J = 5.8$ Hz), 5.10 (2H, s), 7.34 (5H, s); ^{13}C NMR δ 173.43, 136.23, 128.50, 128.08, 66.05, 62.30, 34.25, 32.30, 25.34, 24.71; MS, m/z (relative intensity) 223 (3), 194 (12), 115 (59), 108 (52), 91 (100); HRMS: calcd for $\text{C}_{13}\text{H}_{18}\text{O}_3$ m/z 222.1256 (M^+), found 222.1252.

Benzyl 6-(*t*-butyldimethylsilyloxy)hexanoate (4.59): To a solution of **4.58** (7.0 g, 31.5 mmol) and imidazole (5.14 g, 75.6 mmol, 2.4 equiv) in dry DMF (15 mL) was added *t*-butyldimethylsilylchloride (5.69 g, 37.8 mmol, 1.2 equiv) in portions. The reaction was stirred under argon overnight. The reaction was diluted with ether (400 mL) and washed with water (2 x 200 mL), 10 % NaHCO_3 (2 x 200 mL), saturated brine (2 x 200 mL), dried (MgSO_4) and concentrated leaving a pale yellow oil. Flash chromatography on silica (9:1 hexanes:EtOAc, $R_f = 0.6$) of the crude oil yielded pure **4.58** as a colourless oil (9.71 g, 92%): ^1H NMR δ 0.044 (6H, s); 0.89 (9H, s); 1.36-1.71 (6H, m); 2.37 (2H, t, $J = 7.3$ Hz); 3.59 (2H, t, $J = 5.9$ Hz); 5.12 (2H, s); 7.36 (5H, s); ^{13}C NMR δ 173.17, 136.47, 136.38, 128.46, 128.04, 65.94, 62.90, 34.34, 32.48, 25.97, 25.53, 24.82, 18.29, -5.30; MS, m/z (relative intensity) 279 (13), 171 (4), 91 (100); HRMS: calcd for $\text{C}_{15}\text{H}_{23}\text{O}_3\text{Si}$ m/z 279.1416 ($\text{M}^+ - \text{C}_4\text{H}_9$), found 279.1411.

6-(*t*-Butyldimethylsilyloxy)hexanoic acid (4.60): To a solution of **4.59**

(9.71 g, 28.8 mmol) in EtOAc (100 mL) was added 5% Pd/C (400 mg). The flask was fitted with a balloon filled with H₂ and the reaction stirred for 16 hours. The reaction was filtered through filter paper, concentrated, diluted with 50 mL EtOAc. The solution was filtered again, concentrated and residual solvent removed under high vacuum leaving pure **4.60** as a colourless oil (6.79 g, 95%). ¹H NMR δ 0.044 (6H, s), 0.89 (9H, s), 1.39-1.69 (6H, m), 2.36 (2H, t, *J* = 7.3 Hz), 3.61 (2H, t, *J* = 5.9 Hz), 11.05 (1H, bs); ¹³C NMR δ 179.18, 62.85, 33.97, 32.39, 25.89, 25.40, 24.51, 18.23, -5.39; MS, *m/z* (relative intensity) 231 (2), 229 (4), 213 (7), 189 (37), 171 (89), 75 (100); HRMS: calcd for C₁₁H₂₃O₃Si *m/z* 231.1416 (M⁺ - CH₃), found 231.1416.

***t*-Butyl 6-hydroxyhexanoate (4.57)**: To a solution of **4.60** (2 g, 8.1 mmol) in dry CH₂Cl₂ (8 mL) was added DMAP (198 mg, 20 mol%) and *t*-BuOH (3.10 mL, 32.4 mmol, 4 equiv). The solution was cooled to 0 °C. DCC was added (1.76 g, 8.5 mmol, 1.05 equiv) in portions over 5 minutes. The solution was stirred for 1 hour at 0 °C and then allowed to warm to room temperature then stirred for another 24 hrs. The reaction was filtered and the filtrate concentrated leaving a pale yellow oil. The oil was dissolved in ether (150 mL) and washed with water (2 x 75 mL), 10% NaHCO₃ (1 x 75 mL), saturated brine (1 x 75 mL), dried (MgSO₄) and concentrated to approximately 10 mL. The solution was filtered and the filtrate concentrated leaving a yellow oil. The oil was distilled (b.p. 65-68 °C, 100 microns) to give 1.65 g of a colourless oil. In addition to the desired *t*-butyl ester of **4.60**, the ¹H NMR of the distilled material indicated that small amounts (approximately 5%) of both DCC and DCU were present. 1.3 g

(approximately 4.13 mmol of **4.60**) of the impure distilled oil was dissolved in dry THF (6 mL). To this was added TBAF (12 mL of a 1.0 M solution in THF, 12 mmol) and the solution stirred for 36 hours. The solution was diluted with ether (150 mL) and then washed with water (5 x 100 mL), 10 % NaHCO₃ (2 x 100 mL), saturated brine (1 x 100 mL), dried (MgSO₄) and concentrated leaving a yellow oil. Flash chromatography on silica (7:3 hexanes:EtOAc, R_f = 0.25) of the oil yielded pure **4.57** as a pale yellow oil (636 mg, 42%): ¹H NMR δ 1.36-1.63 (6H, m), 1.41 (9H, s), 1.86 (1H, s), 2.20 (2H, t, J = 7.3 Hz), 3.60 (2H, bt); ¹³C NMR δ 173.14, 79.90, 61.99, 35.37, 32.17, 27.95, 25.17, 24.71; MS, m/z (relative intensity) 132 (8), 115 (48), 97 (34), 69 (35), 57 (100); HRMS: calcd for C₁₁H₂₃O₃Si m/z 132.0777 (M⁺ - C₄H₉), found 132.0786.

(±)-allyl 6-([trans-2,5-di(4-nitrophenyl)-1-oxo-1λ⁵-phospholan-1-yl]oxy)hex-anoate (4.55): **4.49** (250 mg, 0.69 mmol, 1 equiv) was suspended in dry CH₂Cl₂ (5 mL). Oxalyl chloride (0.180 mL, 2.07 mmol, 3 equiv) was added dropwise over a period of 1 min. A catalytic drop of DMF was added. The reaction was stirred for 3 hrs at room temperature under an Ar atmosphere. The solvent was removed by rotary evaporation and the crude acid chloride dried under high vacuum for 12 hrs. The crude acid chloride was suspended in dry benzene (1 mL). A solution of the protected linker **4.52** (119 mg, 0.69 mmol, 1 equiv) and 2,6-lutidine (0.81 mL, 0.69 mmol, 1 equiv) in dry benzene (1 mL) was added dropwise over 2 min. The reaction was stirred at room temperature for 24 hrs. The solution was diluted with Et₂O which caused the precipitation of the lutidine hydrochloride salt which was removed by vacuum filtration. The

filtrate was concentrated by rotary evaporation. The product **4.55** was obtained as a clear colourless oil (104 mg, 29%) by flash chromatography on silica gel (3:2 EtOAc:hexanes, $R_f = 0.3$): $^1\text{H NMR } \delta$ 1.04-1.55 (6H, m), 2.09-2.75 (6H, m), 3.20-3.85 (4H, m), 4.38 (2H, d, $J = 5.5$ Hz), 5.25 (2H, t, $J = 14.1$ Hz), 5.57 (1H, m), 7.51 (4H, d, $J = 8.4$ Hz), 8.19 (4H, d, $J = 8.5$ Hz); $^{31}\text{P NMR } \delta$ 59.92 (s).

(meso)-trans-allyl 6-[[1-oxo-cis-2,5-di(4-nitrophenyl)-1 λ^5 -phospholan-1-yl]oxy]hexan-oate (4.56): **4.50** (273 mg, 0.75 mmol, 1 equiv) was suspended in dry CH_2Cl_2 (1.55 mL). Oxalyl chloride (0.197 mL, 2.25 mmol, 3 equiv) was added dropwise over a period of 1 min. A catalytic drop of DMF was added. The reaction was stirred at room temperature for 3 hrs under an Ar atmosphere. The solvent was removed by rotary evaporation and the acid chloride product dried under high vacuum overnight. The crude acid chloride was suspended in dry benzene (1 mL). A solution of the allyl protected linker arm **4.52** (143 mg, 0.69 mmol, 1 equiv) and 2,6-lutidine (0.86 mL, 75 mmol, 1 equiv) in dry benzene (1 mL), was added dropwise over a period of 2 min. The reaction was stirred at room temperature for 24 hrs. The reaction was diluted with Et_2O in order to induce precipitation of the lutidine hydrochloride salt which was removed by vacuum filtration. The filtrate was concentrated *in vacuo*. Flash chromatography of the crude (7:3 CH_2Cl_2 :EtOAc, $R_f = 0.8$) yielded the desired product **x** as a clear colourless oil (56 mg, 20% yield). $^1\text{H NMR } \delta$ 1.21-1.74 (6H, m), 2.23-2.64 (6H, m), 3.34-3.54 (2H, m), 3.90 (2H, m), 4.58 (2H, d, $J = 5.5$ Hz), 5.25 (2H, t, $J = 13.4$ Hz), 5.80 (1H, m), 7.52 (4H, d, $J = 8.8$ Hz), 8.20 (4H, d, $J = 8.8$ Hz); $^{31}\text{P NMR } \delta$ 60.68 (s).

(±)-tert-butyl 6-{{trans-2,5-di(4-nitrophenyl)-1-oxo-1λ⁵-phospholan-1-yl]oxy}hex-anoate (4.62) from 4.49 via the Mitsunobu procedure: **4.57** (39 mg, 0.21 mmol, 1.5 eq), **4.49** (50 mg, 1.4 mmol, 1.0 equiv), triphenylphosphine (54.3 mg, 0.21 mmol, 1.5 equiv), and diisopropylazidodicarboxylate (DIAD) (0.041 mL, 0.21 mmol, 1.5 equiv) were dissolved in dry THF (1.5 mL). The solution was stirred for 30 min at room temperature followed by removal of the solvent by rotary evaporation. Flash chromatography on silica (1:1 EtOAc:hexanes, R_f = 0.5) of the crude residue yielded pure **4.62** as a clear colourless oil (60.1 mg, 82%): ¹H NMR δ 1.00-1.48 (15H, m), 2.00-2.74 (6H, m), 3.19-3.86 (4H, m), 7.45-7.58 (4H, m), 8.23 (4H, dd, J = 0.9 Hz, J = 6.9 Hz); ³¹P NMR δ 59.77 (s), ¹³C δ 172.42, 147.41, 143.84 (d, J = 3.7 Hz), 143.21 (d, J = 6.4 Hz), 129.50 (d, J = 5.5 Hz), 128.82 (d, J = 4.6 Hz), 123.80, 123.77, 80.08, 65.77 (d, J = 7.3 Hz), 46.83 (d, J = 83.3 Hz), 45.51 (d, J = 86 Hz), 35.17, 30.50, 30.24, 28.11, 27.77, 27.57, 24.89, 24.38; MS, m/z (relative intensity) 476 (12), 459 (65), 363 (89), 280 (48), 216 (54), 57 (100); HRMS calcd for C₂₆H₃₄N₂O₈P (-C₄H₈) 476.1348, found 476.1351.

(±)-6-{{trans-2,5-di(4-nitrophenyl)-1-oxo-1λ⁵-phospholan-1-yl]oxy}hexanoic acid (4.25): **4.62** (35 mg, mmol) was dissolved in 20% TFA/CH₂Cl₂ (1.5 mL) and stirred overnight at room temperature. The CH₂Cl₂ and TFA was removed by rotary evaporation. Flash chromatography on silica (4:1 EtOAc:hexanes, R_f = 0.5) on the crude residue yielded pure **4.25** as a clear colourless oil (25 mg, 80%): ¹H NMR δ 1.09-1.65 (6H, m), 2.05-2.75 (6H, m), 3.17-3.98 (4H, m), 7.52 (4H, m), 8.22 (4H, m), ³¹P NMR δ 60.17 (s); ¹³C NMR δ

175.92, 147.44, 143.65 (d, $J = 3.7$ Hz), 143.11 (d, $J = 6.4$ Hz), 129.53 (d, $J = 5.5$ Hz), 128.87 (d, $J = 3.7$ Hz), 123.82, 65.83 (d, $J = 7.3$ Hz), 46.64 (d, $J = 84.2$ Hz), 45.50 (d, $J = 85.1$ Hz), 33.23, 30.33, 30.02, 24.80, 24.02; MS m/z (relative intensity) 477, 444 (8), 363 (83), 280 (84), 216 (53), 149 (54), 119 (56), 69 (82); HRMS calcd for $C_{22}H_{25}N_2O_8P$ (-OH) 459.1321, found 459.1327.

(meso)-cis-tert-butyl 6-[[1-oxo-cis-2,5-diphenyl-1 λ^5 -phospholan-1-yl]oxy]hexanoate (4.64): 4.57 (60 mg, 0.33 mmoles, 1.5 eq) triphenyl phosphine (87 mg, 0.33 mmoles, 1.5 eq), 4.45 (60 mg, 0.22 mmoles, 1 equiv), and DIAD (65 μ l, 67 mg, 0.33 mmoles, 1.5 eq) were dissolved in dry THF (1.5 ml) and stirred at room temperature for 30 min. The solvent was removed under reduced pressure. Flash chromatography of the crude residue on silica (3:2 EtOAc: hexanes, $R_f = 0.4$) yielded 4.64 as a clear colourless oil (58.5 mg, 60%): 1H NMR δ 0.65-0.85 (2H, br m), 0.89-1.04 (2H, br m), 1.20-1.26 (3H, br m), 1.439, (7H, s), 1.75 (1H, s), 1.97 (3H, t, $J = 8.1$ Hz), 2.35-2.48 (4H, br m), 3.11-3.20 (2H, br m), 3.38-3.54 (2H, br m), 7.20-7.35 (10H, br m); ^{31}P NMR δ 61.75 (s); ^{13}C NMR δ 172.94, 136.29 (d, $J = 8.1$ Hz), 128.43 (d, $J = 2.2$ Hz), 127.80 (d, $J = 5.1$ Hz), 126.65 (d, $J = 3.0$ Hz), 79.83, 64.69 (d, $J = 7.4$ Hz), 43.74 (d, $J = 82.0$ Hz), 35.24, 29.87 (d, $J = 5.1$ Hz), 28.05, 27.48 (d, $J = 7.2$ Hz), 24.44, 24.34; MS, m/z (relative intensity) 443 (18), 387 (58), 272 (49), 104 (100);) HRMS calcd for $C_{26}H_{35}O_4P$ 442.2273, found 442.2264.

(meso)-trans-tert-butyl 6-[[1-oxo-cis-2,5-diphenyl-1 λ^5 -phospholan-1-yl]oxy]hexan-oate (4.70): To a solution of 4.45 (120 mg, 0.55 mmol, 1 equiv) in dry CH_2Cl_2 (2 mL) was added oxalyl chloride (0.144 mL, 1.65 mmol, 3 equiv)

dropwise over a period of 1 min and the solution was stirred for 3 hrs. The solvent was removed by rotary evaporation and the crude acid chloride subjected to high vacuum for 12 hrs. The crude acid chloride was dissolved in dry benzene (1 mL) and a solution of **4.57** (125 mg, 0.66 mmol, 1.1 equiv) and triethylamine (0.100 mL, 0.72 mmol, 1.2 equiv) in dry benzene (1 mL) was added dropwise over a period of 2 min and the reaction was stirred for 24 hrs. Ether was added which resulted in the precipitation of triethylamine hydrochloride which was removed by vacuum filtration and the filtrate was concentrated by rotary evaporation. Flash chromatography on silica (9:1 CH₂Cl₂:EtOAc, R_f = 0.6) on the crude residue yielded pure **4.70** as a clear colourless oil (140 mg, 57%): ¹H NMR δ 1.23-1.65 (15H, m), 2.18 (2H, t, J = 7.3 Hz), 2.40 (4H, m), 3.29 (2H, m), 3.91 (2H, q, J = 6.6 Hz), 7.35 (10H, m); ³¹P NMR δ 62.56 (s); ¹³C NMR δ 172.66, 137.07 (d, J = 4.6 Hz), 128.75, 128.63, 128.50, 126.68, 79.92, 65.18 (d, J = 6.5), 43.51 (d, J = 86.0 Hz), 35.39, 30.49 (d, J = 5.5 Hz), 29.51 (d, J = 14.7 Hz), 28.15, 25.13, 24.62; MS, m/z (relative intensity) 442, 386 (99), 369 (33), 272 (60), 104 (100); HRMS calcd for C₂₆H₃₅O₄P 442.2297, found 442.2293.

(meso)-trans-6-[[cis-2,5-di(4-nitrophenyl)-1-oxo-1λ⁵-phospholan-1-yl]oxy]hexanoic acid (4.26): **4.70** (120 mg, 0.27 mmol, 1 equiv) was dissolved in 0.5 mL of H₂SO₄ at 0 °C. A solution of HNO₃/H₂SO₄ (1:1, 0.062 mL, 2.6 equiv HNO₃) was added and the reaction was stirred at 0 °C for 30 min. The reaction was poured into a beaker containing ice which upon melting left a suspension. CHCl₃ (5 mL) was added and the two layers were separated. The aqueous layer was further extracted with CHCl₃ (4 x 10 mL) and the combined organics were

washed with brine (2 x 15 mL), dried (MgSO_4) and concentrated *in vacuo* leaving an oily solid residue. Attempts to obtain pure product by subjecting the crude residue to silica gel flash chromatography were unsuccessful. Final purification of the desired product was accomplished using HPLC (isocratic, 7:3 EtOAc:hexanes, retention time = 18 min) to give **4.26** as a clear colourless oil (51 mg, 44 %): $^1\text{H NMR}$ δ 1.23-1.68 (6H, m), 2.24 (2H, t, $J = 7$ Hz), 2.35-2.60 (4H, m), 3.35-3.57 (2H, m), 3.87-4.03 (2H, dd, $J = 6.6$ Hz, $J = 7.7$ Hz), 7.52 (4H, dd, $J = 1.8$ Hz, $J = 6.9$ Hz), 8.19 (4H, dd, $J = 8.4$ Hz); $^{31}\text{P NMR}$ (CDCl_3) δ 61.11 (s); $^{13}\text{C NMR}$ δ 176.79, 147.28, 143.97 (d, $J = 7.3$ Hz), 129.46 (d, $J = 5.5$ Hz), 123.84, 66.23 (d, $J = 7.3$ Hz), 43.56 (d, $J = 84.2$ Hz), 33.48, 30.30 (d, $J = 5.5$ Hz), 29.26 (d, $J = 14.7$ Hz), 24.96, 24.1; MS, m/z (relative intensity) 363(53), 280(57), 149(52); HRMS calcd for $\text{C}_{22}\text{H}_{25}\text{N}_2\text{O}_8\text{P}$ 477.1427, found 477.1432.

4.2.2 *Cis* TSA (**4.26**) Isomerization Studies

General Procedure: Solutions of the *cis* TSA **4.26** (500 μM) were made up in the media as indicated below and partitioned into smaller aliquot (0.5 μL each). Reaction aliquots were quenched at arbitrary time intervals with HCl solutions (1 M) and extracted with EtOAc. In order to determine the relative amounts of *cis* and *trans* isomers, aliquots of the EtOAc layer were analyzed using a normal phase analytical HPLC column from Altech on Waters LC4000 systems. An isocratic mobile phase of 100% EtOAc (0-5 min: 1 mL/min, 6-20 min: 2 mL/min) was used for separation with the UV detector set at 280 nm.

0.1 M NaOH: A 500 μM solution of *cis* TSA **4.26** in 0.1 M NaOH was prepared and partitioned into fractions (500 μL). Reaction aliquots were

quenched with HCl solutions (100 μ L of a 1 M solution) at time intervals of 10 min, 1 hr, 24 hrs. The quenched reactions were extracted with EtOAc (500 μ L). The organic layer was analyzed by HPLC.

pH 7.5: A 500 μ M solution of *cis* TSA 4.26 in 50 mM sodium phosphate buffer at pH 7.5 was prepared and partitioned into fractions (500 μ L). Reaction aliquots were quenched with HCl solutions (40 μ L of a 1 M solution) at time intervals of 25 min, 1, 3, 7, and 11 days. The quenched reactions were extracted with EtOAc (500 μ L). The organic layer was analyzed by HPLC.

pH 8.5: A 500 μ M solution of *cis* TSA 4.26 in 20 mM sodium bicarbonate buffer at pH 8.5 was prepared and partitioned into fractions (500 μ L). Reaction aliquots were quenched with HCl solutions (100 μ L of a 1 M solution) at time intervals of 20 min, 3.5 and 8 days. The quenched reactions were extracted with EtOAc (500 μ L). The organic layer was analyzed by HPLC.

4.2.3 Conjugation of TSA's to Carrier Proteins

To a solution of TSA 4.25 or 4.26 (~6 mg, ~0.013 mol) in DMF:water (3 mL of a 3:2), was added *N*-hydroxysulfosuccinimide (~3.5 mg, ~0.016 mol) and EDC (~3.1 mg, ~0.016 mol). The reaction was stirred for 3 hrs at room temperature. The reaction was divided into two equal aliquots (1.5 mL each). Two separate solutions of the carrier proteins BSA (6.3 mg) and KLH (6.1 mg) in potassium phosphate buffer at pH 7.5 (3 mL of a 50 mM solution) were prepared. Each aliquot was added to a carrier protein solution. The reactions were slowly mixed on a 180° shaker for 16 hrs at 4°C. The unconjugated hapten was removed by dialysis (4 x 1 L, 3 hrs each) in potassium phosphate buffer (50 mM, pH 7.5).

The extent of conjugation was measured for the BSA reactions using the method of Habeeb³⁹ and found to be 11 for the *trans* hapten **4.25**, and 19 for the *cis* hapten **4.26**. No measurements were performed on the KLH solutions due to their cloudy appearance. The carrier protein-TSA conjugates were stored at -20°C.

4.2.4 Synthesis of Antibody Substrates

6-[[di(4-nitrophenoxy)phosphoryl]oxy]hexanoic acid (4.27): To a solution of *tert*-butyl-6-hydroxy-hexanoate (**4.57**) (125 mg, 0.66 mmoles) in dry THF (4 mL) was added bis(4-nitrophenyl)-phosphate (150 mg, 0.44 mmoles), triphenyl phosphine (173 mg, 0.66 mmoles), and (DIAD) (130 μ l, 130 mg, 0.66 mmoles). This reaction was stirred under argon for 30 minutes. The solvent was removed by rotary evaporation and the crude chromatographed on silica (19:1 CH₂Cl₂:EtOAc, R_f = 0.7). Due to slow product breakdown, it was not possible to separate the *tert*-butyl-6-[[di(4-nitrophenoxy)phosphoryl]oxy]hexanoate product from trace amounts of 4-nitrophenol, triphenyl phosphine, and triphenyl phosphine oxide. For this reason, the impure product was deprotected in a 1 mL solution of trifluoroacetic acid:methylene chloride (1:5) overnight. The solvent was removed by rotary evaporation and the product obtained by flash chromatography on silica (1:1 hexanes:EtOAc, R_f=0.2) **4.27** as a white solid (146 mg, 73% overall yield): mp 77-78 °C; ¹H NMR δ 1.20-1.90 (7H, c m), 2.35 (2H, t, *J* = 7 Hz), 4.34 (2H, q, *J* = 6.6 Hz), 7.40 (4H, d, *J* = 9.2 Hz), 8.26 (4H, d, *J* = 7.3 Hz); ³¹P NMR δ -15.83 Hz (s); ¹³C NMR δ 178.16, 154.74 (d, *J* = 6.4 Hz), 145.40, 125.81, 120.71 (d, *J* = 4.7 Hz), 70.49, 33.57, 29.81, 24.84, 24.02; MS,

m/z (relative intensity) 341 (80), 316 (51), 139 (100), 109 (82), 65 (70); HRMS calcd for C₁₈H₁₉O₁₀N₂P 455.08556, found 455.0830.

dimethyl (4-nitrobenzyl)phosphonate (4.72): To a solution of 4-nitrobenzyl bromide (3 g, 13.8 mmoles) in dry benzene (4 mL) was added trimethyl phosphite (6mL, 5.70 g, 45 mmoles). The reaction was refluxed overnight. Removal of excess trimethyl phosphite was performed by vacuum distillation (35 Torr, 60 °C). The remaining crude was purified by flash chromatography on silica (EtOAc, R_f = 0.5) to give **4.72** as a clear oil (3.08 g, 90% yield): ¹H NMR δ 3.26 (2H, d, J = 22.3 Hz), 3.71 (6H, d, J = 10.9 Hz), 7.47 (2H, dd, J = 2.6 Hz, J = 8.8 Hz), 8.19 (2H, d, J = 8.8 Hz); ³¹P NMR δ 24.47 (s); ¹³C NMR δ 147.12, 139.48 (d, J = 9.1 Hz), 130.53 (d, J = 6.4 Hz), 123.51 (d, J = 2.7 Hz), 57.79 (d, J = 7.3 Hz), 32.82 (d, J = 138.2 Hz); MS, m/z (relative intensity) 246 (15), 229 (25), 228 (100), 109 (88), 198 (37), 90 (51); HRMS calcd for C₉H₁₂O₅NP 245.0453, found 245.0447.

methyl hydrogen (4-nitrobenzyl)phosphonate (4.73): A mixture composed of dimethyl (4-nitrobenzyl)phosphonate (2.5 g, 10.2 mmoles) and sodium hydroxide (816 mg, 20.4 mmoles) in water (60 mL) was heated at 75 °C until homogeneous. The solution was acidified to pH 1 with concentrated hydrochloric acid (6M). The product precipitated out of solution and was obtained by vacuum filtration as a white solid (2.12 g, 90% yield). mp 132-134 °C; ¹H NMR (DMSO-*d*₆) δ 3.19 (2H, d, J = 22.8 Hz), 3.59 (3H, d, J = 11.3 Hz), 7.44 (2H, dd, J = 2.5 Hz, J = 8.8 Hz), 8.17 (2 H, d, J = 8 Hz); ³¹P NMR 25.48 (s); ¹³C NMR δ 146.28, 142.02 (d, J = 9.2 Hz), 130.90 (d, J = 5.5 Hz), 123.13, 51.72 (d, J

= 6.4 Hz), 33.30 (d, $J = 131.8$); MS, m/z (relative intensity) 231 (50), 214 (100), 184 (31), 136 (31), 107 (62), 89 (52); HRMS calcd for $C_8H_{10}O_5NP$ 231.0297, found 231.0314.

methyl (4-nitrophenyl) (4-nitrobenzyl) phosphonate (4.74): Methyl hydrogen 4-nitrobenzyl-phosphonate (4.73) was (1 g, 4.33 mmoles) was suspended in dry methylene chloride (40 mL). To the suspension was added 4-nitrophenol (722 mg, 5.19 mmoles) and 1-[3-(dimethylamino)propyl]-3-ethyl carbodiimide hydrochloride (EDC) coupling agent (995 mg, 5.19 mmoles). The reaction was stirred under argon for 72 hrs. Additional CH_2Cl_2 was added to dilute the reaction. The organic layer was washed with aliquots of 5% sodium bicarbonate, 0.1 N HCl, and saturated brine before being dried over magnesium sulphate. The product was purified by recrystallization in hexanes-ethyl acetate (64%). mp 112-114 °C; 1H NMR δ 3.48 (2H, d, $J = 22.7$ Hz), 3.80 (3H, d, $J = 11$ Hz), 7.29 (2H, d, $J = 8.8$ Hz), 7.51 (2H, dd, $J = 2.9$ Hz, $J = 5.9$ Hz), 8.22 (4H, d, $J = 8.8$ Hz); ^{31}P NMR δ 20.94; ^{13}C NMR δ 155.31 (d, $J = 8.2$ Hz), 147.48, 144.90, 138.09 (d, $J = 9.1$ Hz), 130.78 (d, $J = 6.4$ Hz), 125.61, 123.86, 120.85 (d, $J = 4.6$ Hz), 53.91 (d, $J = 6.4$ Hz), 33.55 (d, $J = 139.1$ Hz); MS, m/z (relative intensity) 352 (100), 335 (41), 305 (27), 257 (34), 136 (49); HRMS calcd for $C_{14}H_{13}O_7N_2P$ 352.0460, found 352.0450.

4-nitrophenyl hydrogen (4-nitrobenzyl)-phosphonate (4.75): Methyl(4-nitrophenyl) (4-nitrobenzyl) phosphonate (4.74) (1.83 g, 5.4 mmoles) was dissolved in butanone (40 mL) with sodium bromide (833 mg, 8.10 mmoles). The reaction was refluxed overnight. The sodium salt product was obtained by

cooling the solution and isolating the precipitate by vacuum filtration. The sodium salt was dissolved in water and the solution was acidified with 6 N HCl to pH 2. The resulting precipitate was isolated by vacuum filtration and dried under vacuum (535 mg, 93% yield). ^1H NMR ($\text{DMSO-}d_6$) 3.54 (2H, dd, $J = 8.1$ Hz, $J = 23$ Hz), 7.38 (2H, d, $J = 8$ Hz), 7.59 (2H, d, $J = 5.9$ Hz), 8.19 (4H, d, $J = 9.5$ Hz); ^{31}P NMR δ 21.66; ^{13}C NMR δ 156.20, 146.44, 143.68, 141.11 (d, $J = 9.1$ Hz), 131.07 (d, $J = 6.4$ Hz), 125.48, 123.19, 121.07 (d, $J = 4.6$ Hz), 34.35 (d, $J = 133.6$ Hz); MS, m/z (relative intensity) 338 (33), 228 (18), 210 (24), 139 (100), 109 (83); HRMS calcd for $\text{C}_{13}\text{H}_{11}\text{O}_7\text{N}_2\text{P}$ 338.0304, found 338.0310.

6-([4-nitrobenzyl](4-nitrophenoxy)phosphoryl]oxy)hexanoic acid (4.28): To a solution of tert-butyl-6-hydroxy-hexanoate (4.57) (156 mg, 0.83 mmoles) in dry THF (1.5 mL) was added 4-nitrophenyl hydrogen (4-nitrobenzyl)-phosphonate (4.75) (180 mg, 0.55 mmoles), triphenyl phosphine (218 mg, 0.83 mmoles), and DIAD (180 μl , 180mg, 0.83 mmoles). The reaction was stirred for 1 hr. The solvent was removed by rotary evaporation and the crude purified by silica gel chromatography (3:2 EtOAc:hexanes, $R_f = 0.7$). Due to decomposition of the product upon the column the crude product, containing traces of 4-nitrophenol, triphenyl phosphine, and triphenyl phosphine oxide impurities, was used in the deprotection step. The crude product was stirred in 1 mL solution of 20% trifluoroacetic acid in methylene chloride overnight. The solvent was removed by rotary evaporation and the product chromatographed on silica (4:1 EtOAc:hexanes, $R_f = 0.6$) to yield the product as a thick oil (159 mg, 64% overall yield): ^1H NMR ($\text{DMSO-}d_6$) δ 0.75-1.75 (7H, c m), 2.30 (2H, t, $J = 7.2$ Hz), 3.52 (2H,

$J = 22.7$ Hz), 4.15 (2H, m), 7.29 (2H, d, $J = 9.6$ Hz), 7.51 (2H, dd, $J = 2.6$ Hz, 8.20 (4H, d, $J = 8.8$ Hz); ^{31}P NMR δ 19.7; ^{13}C NMR 177.47, 155.16 (d, $J = 7.1$ Hz), 147.50, 144.93, 138.07 (d, $J = 9.1$ Hz), 130.85 (d, $J = 5.5$ Hz), 125.63, 123.84, 121.00, 67.83 (d, $J = 7.3$ Hz), 33.80 (d, $J = 138.1$), 33.61, 29.92 (d, $J = 4.6$ Hz), 24.84, 24.07; MS, m/z (relative intensity) 339 (64), 314 (58), 139 (77), 109 (51), 97 (66), 69 (100); HRMS calcd for $\text{C}_{19}\text{H}_{21}\text{O}_9\text{N}_2\text{P}$ 453.1063, found 453.1086.

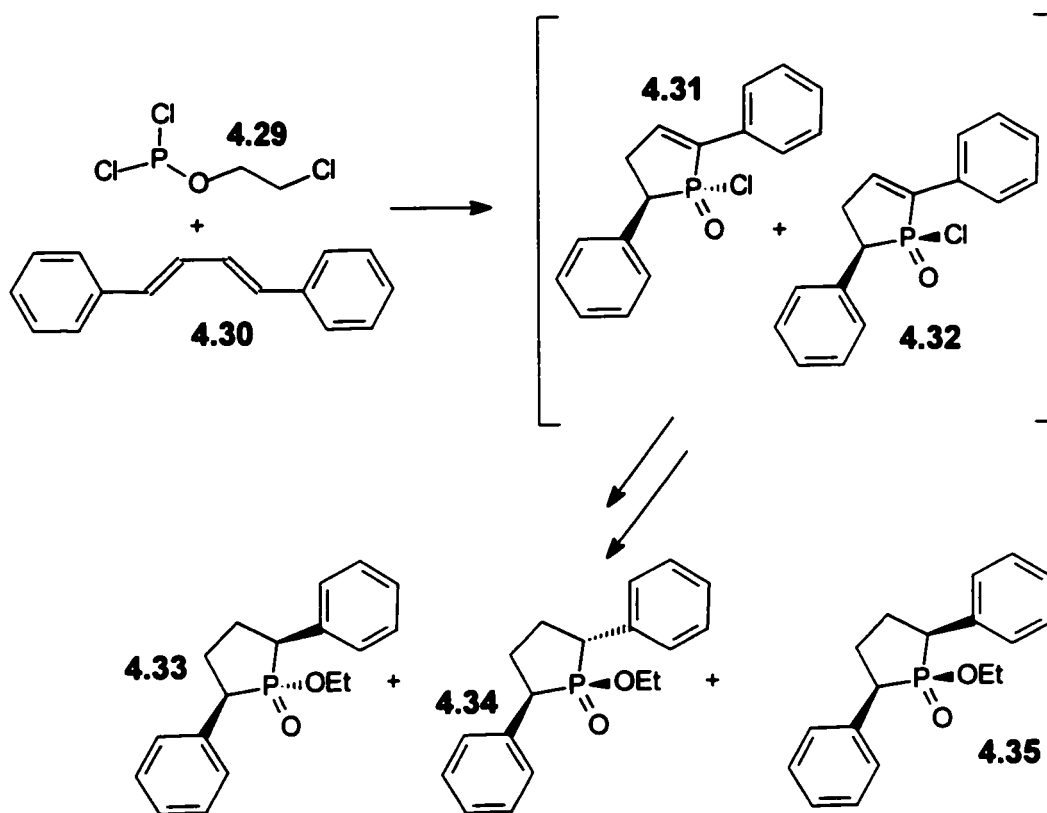
4.2.5 Antibody Substrate Hydrolysis Studies

A 20 μL aliquot of 1 mM stock solution of phosphate substrate **4.27** or phosphonate substrate **4.28** in DMF was added to a reduced volume cuvette containing 980 μL of buffer solution composed of 10 mM CHES, 50 mM NaCl at pH 9.0 which was preincubated at 25 $^\circ\text{C}$. The cuvette was incubated at 25 $^\circ\text{C}$ and the hydrolysis reaction followed by measuring the absorbance at 400 nm every 30 min using a Cary 1B UV-Vis spectrophotometer for 72 hrs. The data was fitted to the first order rate equation using the GraFit program. Each reaction was performed in duplicate. The half-life of each substrate was calculated by averaging the first order rate constants from the duplicate assays and using the equation $t_{1/2} = (\ln 2)/k$.

4.3 Results and Discussion

4.3.1 Synthesis of Transition State Analogues

Our approach to preparing TSA's **4.25** and **4.26** was based upon earlier work from within our laboratory by Professor Scott Taylor.²⁸ Employing the phosphite (**4.29**) used by Modritzer and coworkers²⁹ for performing McCormack reactions, Taylor had shown that 2,5-biarylphospholanates, such as **4.33-4.35**, could be prepared by reacting diene **4.30** with phosphite **4.29** in a pressure tube at 170 °C to give the acid chlorides **4.31-4.32** as a starting point (Scheme 4.7).

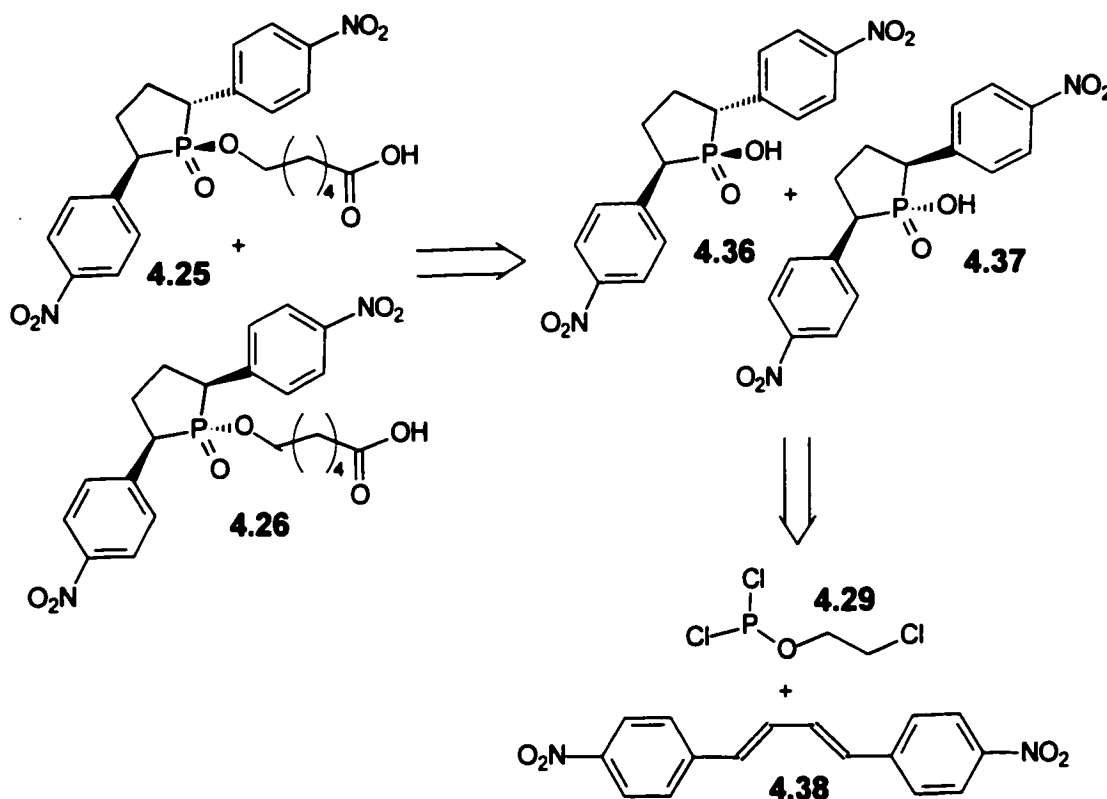


Scheme 4.7. Towards the synthesis of intermediates **4.33-4.35**.

The McCormack reaction is a [4 + 2] cycloaddition reaction and, therefore, usually yields the 3,4-dihydro products. However, when the reaction is performed at high temperature (as was the case here) the double bond can

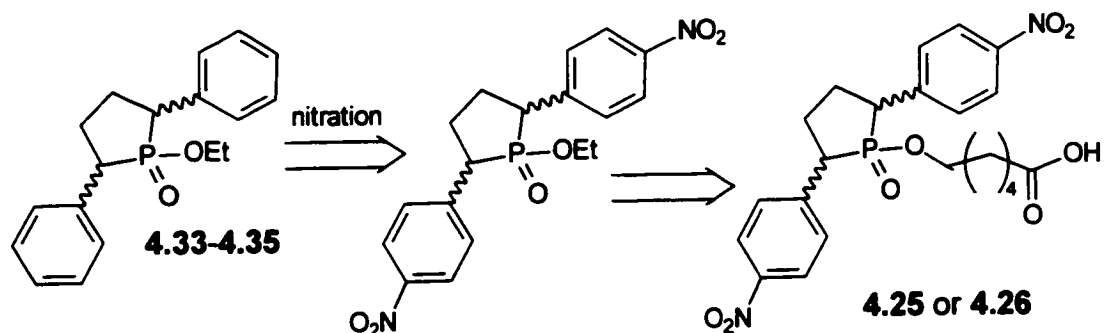
migrate and the 2,3-dihydro products dominate.³⁰ The acid chlorides could be readily esterified by reaction with an alcohol in the presence of a tertiary amine. Taylor also demonstrated that the double bond can be hydrogenated to give the cyclic five-membered phosphinates as a mixture of isomers (Scheme 4.7).²⁸ These ethyl esters with the intact phospholanate rings serve as the precursors for the desired TSA's.

On the basis of these studies, we considered two approaches to the desired nitrated TSA's. The first route was to incorporate the bis *para*-nitro functionalities at the beginning of the synthesis in the McCormack reaction using the nitrated diene **4.38** as outlined in Scheme 4.8.



Scheme 4.8. Retrosynthesis of **4.25** and **4.26** starting with nitrated diene **4.38**.

The alternative strategy consisted of introducing the nitro groups after the McCormack reaction as shown in Scheme 4.9. We decided to attempt the approach outlined in Scheme 4.8 first. This route was attractive since it avoided the need to nitrate at the bis-*para* positions (as in Scheme 4.9). When this project began, we only foresaw a remote possibility of performing the bis *para*-nitration in a regioselective manner.

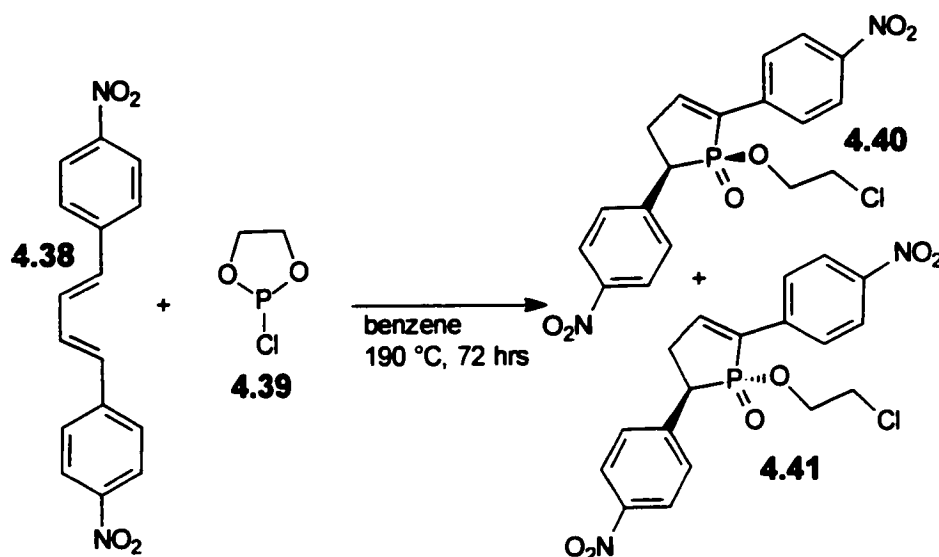


Scheme 4.9. Alternative approach to TSA's 4.25 and 4.26.

The McCormack reaction conditions worked out by Taylor involved heating the diene 4.30 and phosphite 4.29 neat in a pressure tube at 170 °C. However, this was not possible with the nitrated diene 4.38 due to its high melting point. We therefore modified the procedure slightly by performing the reaction in benzene, a solvent commonly used for McCormack reactions, and heating the reactants in a pressure tube at 190 °C. However, we were unable to detect any of the desired cycloaddition products.

Since cyclic phosphites have been reported to be more reactive in the McCormack reaction than their acyclic counterparts,^{31,32,33} we performed the reaction with ethylene chloro phosphite (4.39) as the dienophile as shown in Scheme 4.10. In this case, we were able to detect products 4.40 and 4.41 by

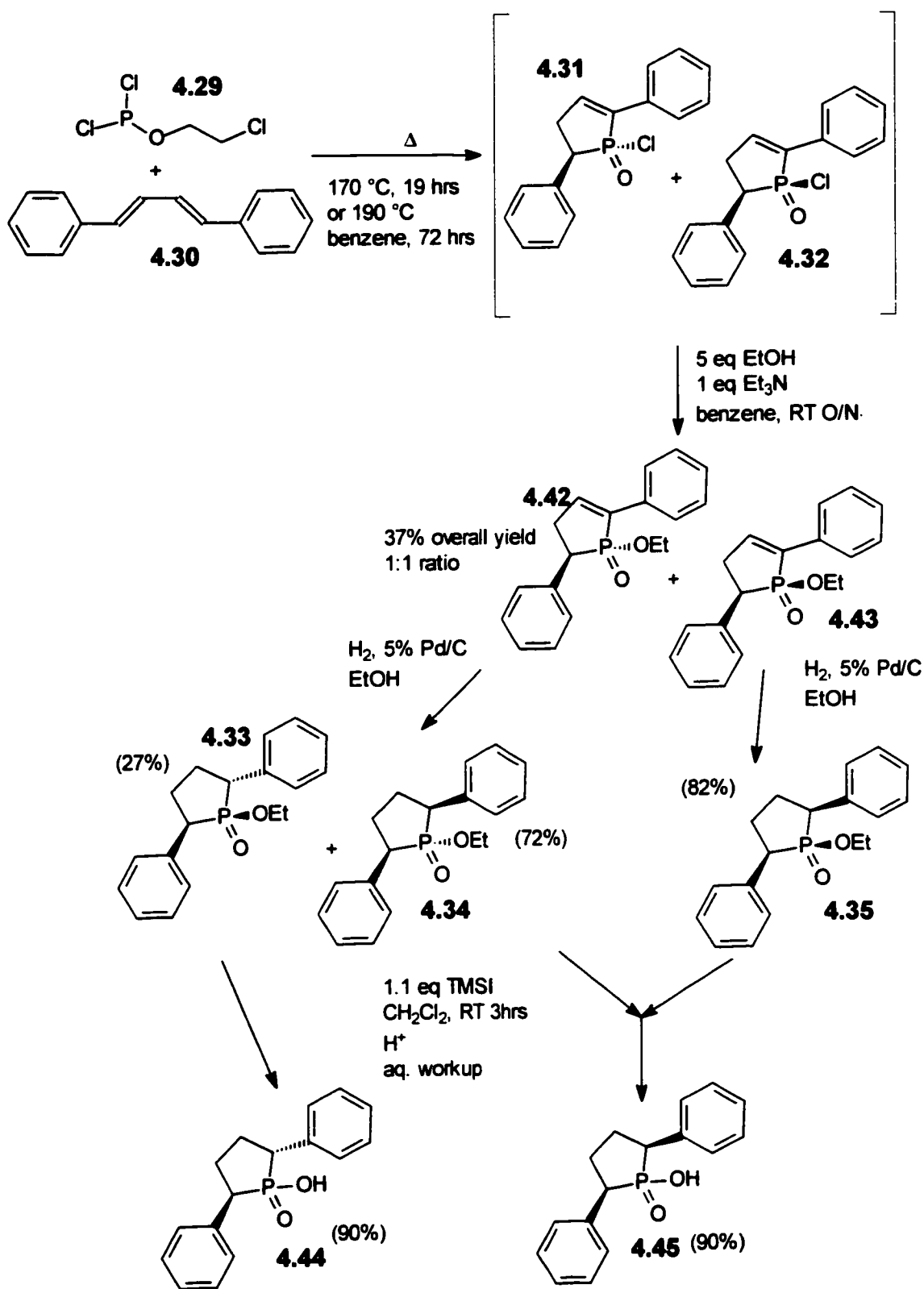
mass spectroscopy and ^{31}P NMR but the overall yields were very low (typically 2-3% with a high of 11%).



Scheme 4.10. McCormack reaction with nitrated diene.

The products from the McCormack reaction shown in Scheme 4.10 were also very difficult to isolate and the reactions were characterized by the formation of significant amounts of unidentified polymeric material. These poor results may be attributed to two key factors which are the well documented reaction of phosphites with nitro groups^{34,35} to form nitrenes and the deactivating effect of nitro groups on dienes in cycloaddition reactions. Since these two effects would be present regardless of the phosphite employed, we decided to pursue the other avenue towards preparing the desired products which involved the selective bis *para* nitration of certain selected precursors as outlined in Scheme 4.9.

The first step was to prepare compounds **4.31-4.32** (Scheme 4.11) using Taylor's original conditions.



Scheme 4.11. Synthesis of unnitrated precursors **4.33-4.35**.

As described above, Taylor's synthesis begins with the cycloaddition of a diene, which was 1,4-diphenyl-1,3-butadiene (**4.30**) in our case, with 2-chloroethyl dichlorophosphite (**4.29**), which was generated *in situ* by the disproportionation of trichlorophosphite and tris-(2-chloroethyl) phosphite. Although Taylor performed these reactions neat, it was found here that the reaction could also be performed in benzene in a sealed tube, at 190 °C. Although the yields were not dramatically improved (37% neat vs 39% in benzene), these conditions decrease the amount of polymeric byproduct which made the eventual purification of the esters **4.42** and **4.43** easier.

As shown in Scheme 4.11, the resulting isomeric phosphinyl chlorides are not isolated but rather esterified with ethanol in benzene in the presence of triethylamine. The resulting two isomeric ethyl esters are isolated in an overall 37% yield in an approximately 1:1 ratio and can be distinguished from one another by ¹H NMR.

As a result of a shielding effect by the phenyl ring at the 5-position of the phospholene ring in the *cis* isomer **4.43**, in which the ethyl and 5-phenyl groups reside on the same side of the phospholene ring, the methyl protons appear at about 0.9 ppm and the two methylene protons are fairly complex multiplets with shifts of 3.45 and 3.85 ppm. In **4.42**, the *trans* isomer, the methyl protons have a shift of 1.20 ppm and the methylene protons appear at 4.1 ppm as a complex multiplet. This is due to the absence of the shielding effect since the 5-phenyl and the ethyl groups are located on opposite faces of the phospholene ring.

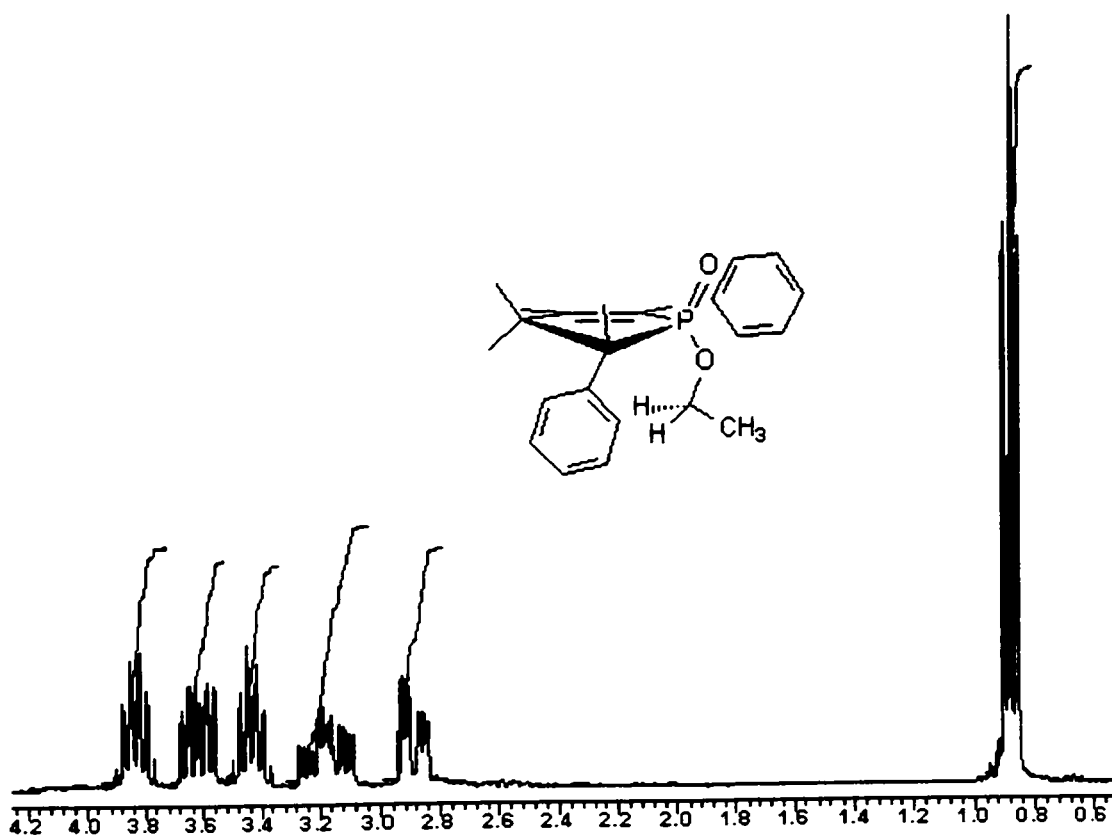


Figure 4.5. ¹H NMR of 4.43.

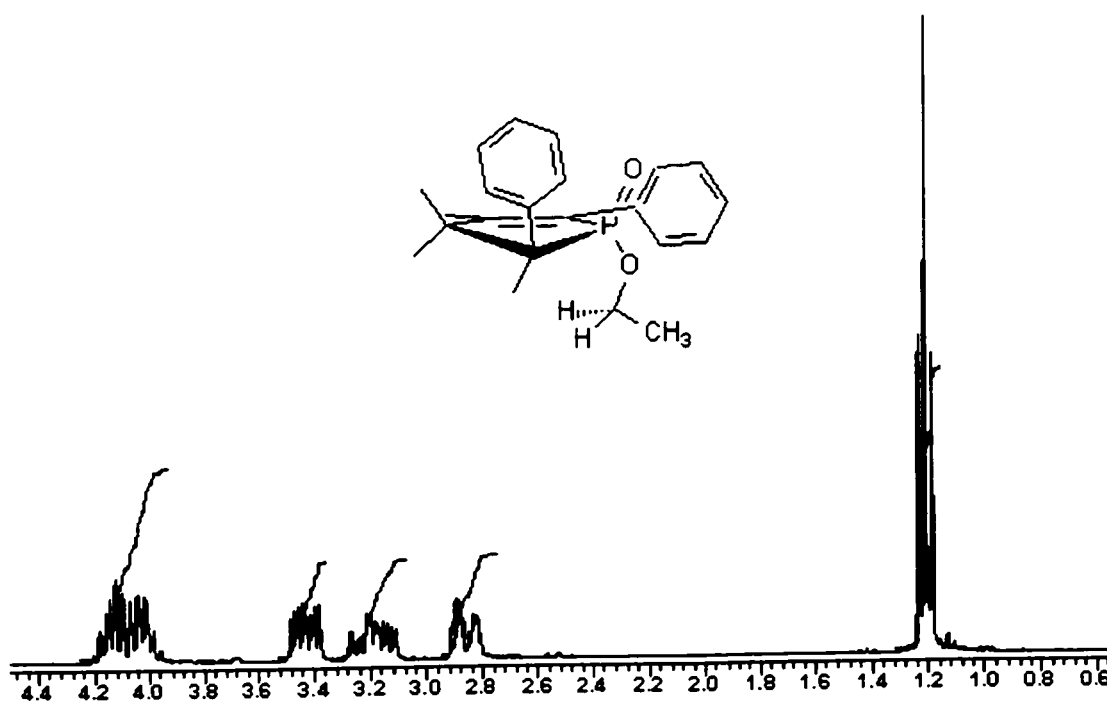


Figure 4.6. ¹H NMR of 4.42.

Hydrogenation of **4.43** resulted in exclusively the 'all *cis*' compound **4.35** where the phenyl groups and the ethyl group are the same side of the phospholanate ring (Scheme 4.11). The overall yield for this latter reaction was 82%. Two isomers, **4.33** and **4.34**, were formed upon hydrogenation of the *trans* isomer **4.42**. The 'phenyl *cis*' isomer **4.34** was formed in a 72% yield whereas the 'phenyl *trans*' compound **4.33** was isolated in a 27% yield. The ratio in which the products were formed indicates that steric factors dictated the stereochemical outcome of the reaction. These three isomers were once again distinguishable by ^1H NMR and readily separable using silica gel chromatography.

The 'all *cis*' isomer **4.35** is a meso compound and could be differentiated from the other isomers by the shift of the methylene and methyl protons (Figure 4.7) of the ethyl group.

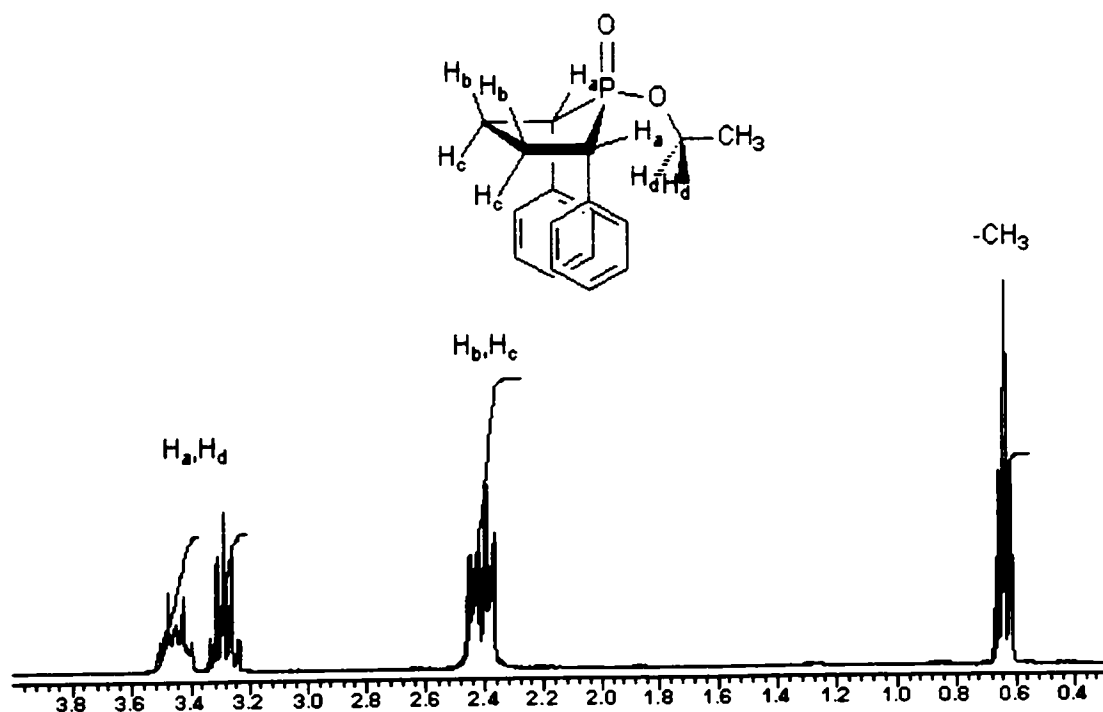


Figure 4.7. ^1H NMR spectra of **4.35**.

The shift of the methylene protons (δ 3.30) are significantly upfield from that of a typical phosphorous ethyl ester (δ 3.9-4.4) due to the shielding effect cause by the proximity to the two aryl rings. This shielding also affects the methyl group (δ 0.65) which is also noticeably different from characteristic values (δ 0.9-1.25).

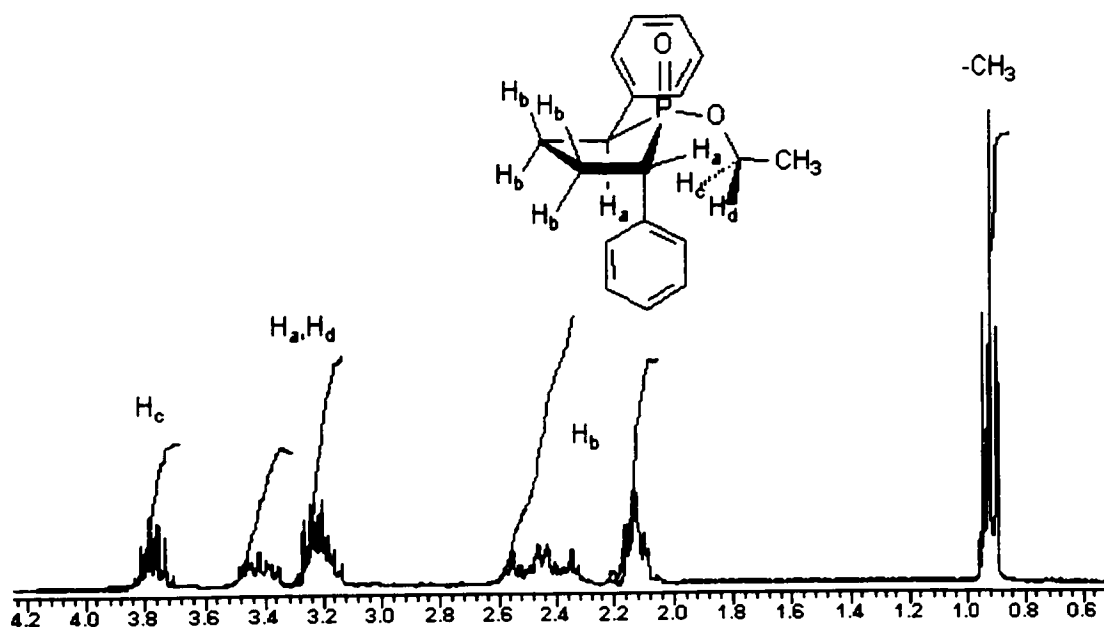


Figure 4.8. ^1H NMR spectra of **4.33**.

The 'phenyl *trans*' isomer **4.33** is a chiral compound with a fairly complex ^1H NMR spectrum. when compared to the isomers **4.34** and **4.35** as seen in Figure 4.8. Since the ethyl group is only proximal to one of the phenyl groups, the shielding effect is not as prominent in the chemical shifts of the methylene and methyl protons. The methylene protons are also not located in equivalent environments. One of the protons is always closer to the phenyl ring than the

other resulting in an upfield shift (δ 3.20) relative to the proton away from the ring (δ 3.80). The methyl protons do show some of the shielding effect (δ 0.95), but it is not as pronounced as in 4.35.

The phenyl *trans* precursor 4.33 and all subsequent derivatives exist as enantiomers due to the chiral centers at the 2 and 5 positions. No effort was made to isolate any of these materials in an enantiomerically enriched form for the purpose of synthesizing the TSA's. Enantiomerically pure material was not deemed necessary since there is no chirality at the phosphorous atom and the substrates lack any chiral carbon centers.

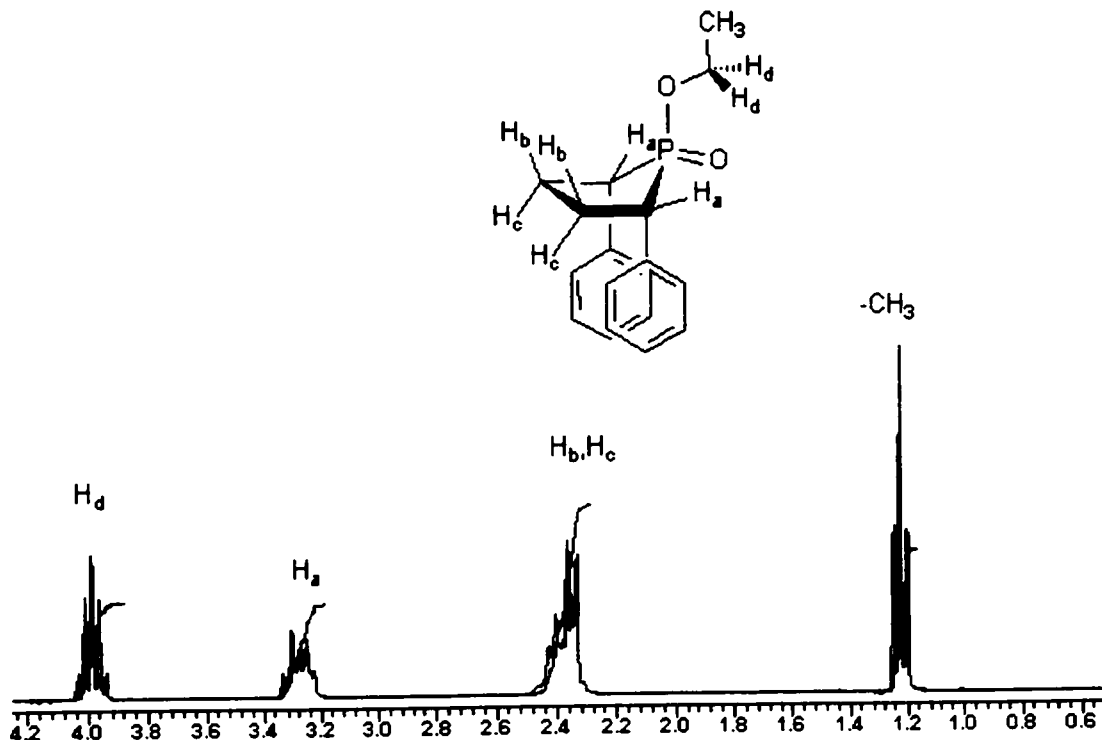


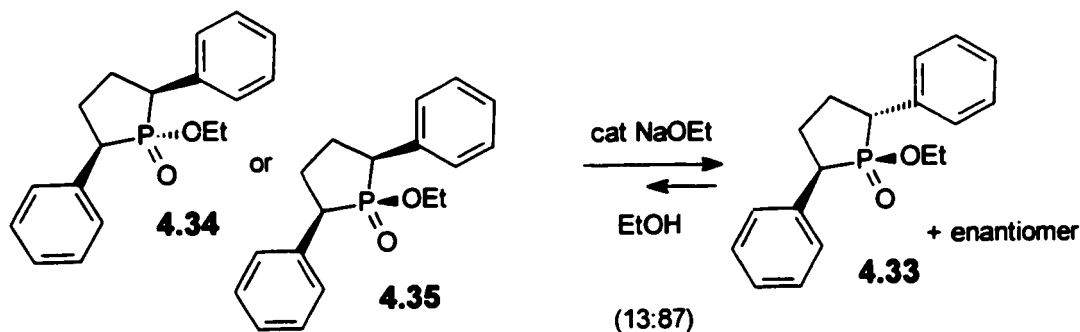
Figure 4.9. ¹H NMR spectra of 4.34.

The 'phenyl *cis*' isomer 4.34 is also a meso compound, but unlike the 'all *cis*' compound 4.35 no shielding effect is present in the ¹H NMR since the phenyl

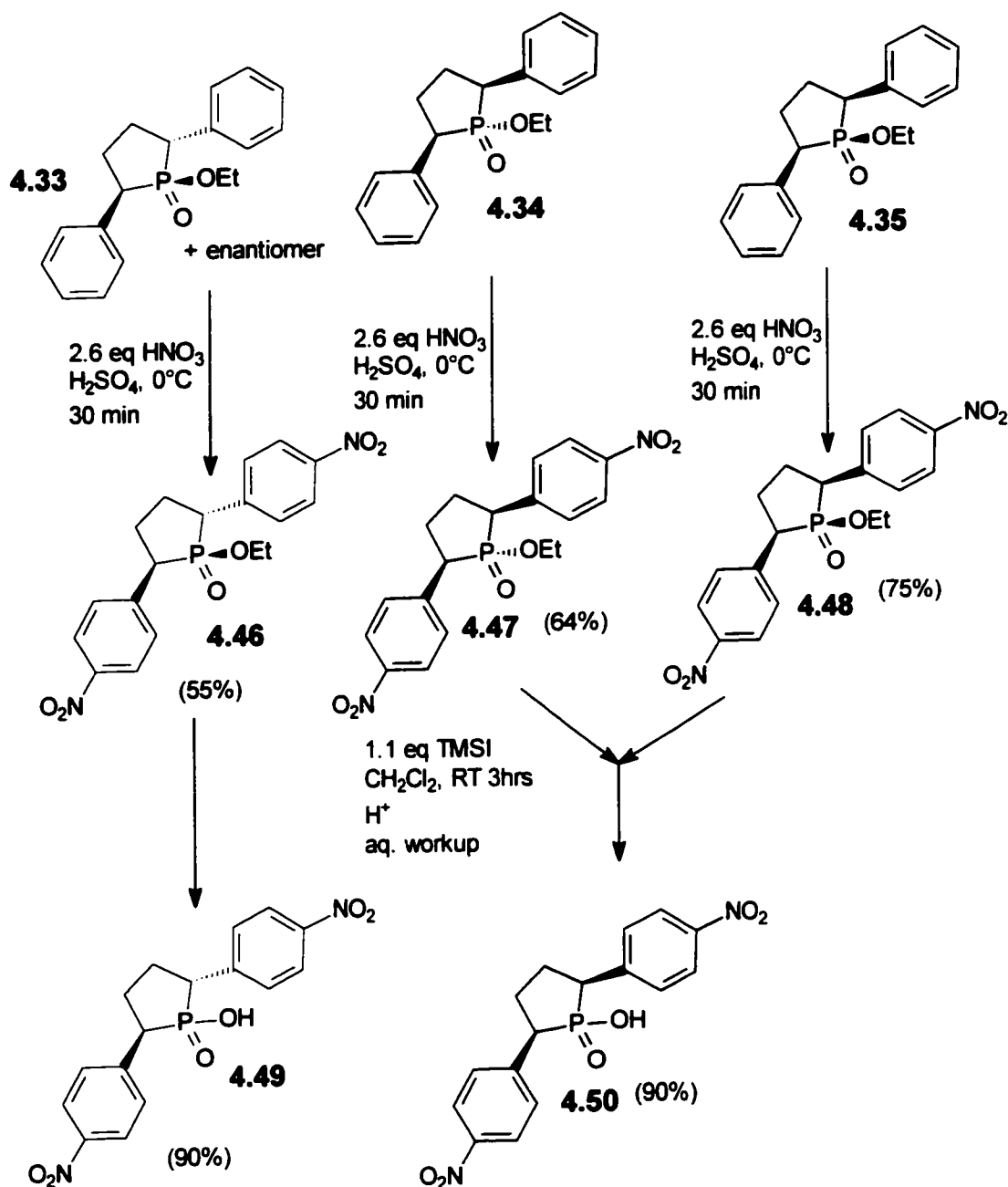
rings are oriented away from the ethyl group (Figure 4.9). As a result, the methylene protons (δ 4.0) fall into the range of the typical phosphorous ethyl ester as do the shift for the methyl protons (δ 1.25).

The stereochemical relationship between alkoxy substituents on the phosphorous atom and the phenyl rings of all the subsequent phospholanate esters described in this chapter which originated from isomers **4.33**–**4.35** could be readily determined in a similar fashion. The shifts of the $-\text{CH}_2\text{-O-P-}$ protons served as a simple diagnostic tool for assigning the relative positions of any P alkoxy substituent and the phenyl rings.

The hydrogenation of **4.42** and **4.43** provided predominantly the precursors for the *cis* isomer where both phenyl groups reside on the same face of the ring. In order to prepare more of the *trans* precursor, we found that it was possible to isomerize either **4.34** and **4.35**, using a catalytic amount of sodium ethoxide, to an equilibrium ratio of 87:13 in favour of the more thermodynamically stable *trans* compound (Scheme 4.12).²⁸ The isomerization occurs by deprotonation/protonation at the 2- and 5-positions on the phospholanate ring which are α to both the phosphorous atom and the phenyl group.



Scheme 4.12. Isomerization of **4.34** or **4.35** to *trans* compound **4.33**.



Scheme 4.13. Nitration of **4.33-4.34** and deprotection of the resulting products.

Though many electrophilic aromatic nitration conditions have been developed, no single method appeared to exhibit complete selectivity for the *para* position.³⁶ In order to introduce the bis *para* nitro groups, we examined classical

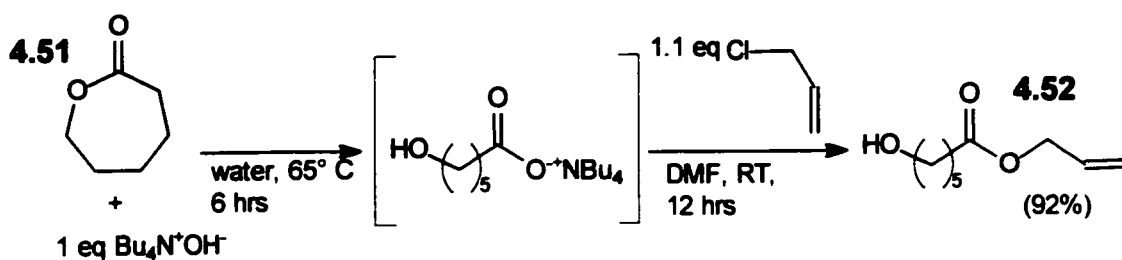
nitration conditions, since it appeared to be an economical method of favouring *para* nitration. These conditions consisted of reacting the esters **4.33-4.35** with a H₂SO₄/HNO₃ mixture at 0 °C for 30 minutes. To our surprise, we were able to achieve the bis-*para* nitration in reasonable to good yields which varied with each substrate. As outlined in Scheme 4.13, the lowest yield obtained was 55% for the nitration of the 'phenyl *trans*' compound (**4.33** to **4.46**), followed by 64% for the 'phenyl *cis*' (**4.34** to **4.47**), and 75% for the 'all *cis*' (**4.35** to **4.48**). These yields appear to reflect increased steric hindrance at the *ortho* positions therefore minimizing the competing side reaction of *ortho* nitration.

Deprotection of the ethyl esters **4.33-4.35** and **4.46-4.48** was easily accomplished by reaction with TMSI to form the silyl ester intermediates which were hydrolyzed to yield the free acids **4.44-4.45** and **4.49-4.50**. The aryl *cis* esters converged to produce the same *cis* acid as outlined in Scheme 4.11 and Scheme 4.13.

With the free acids in hand, the next step of the synthesis was the attachment of the linker chain to the phosphinic acids in an esterification reaction. Thus, the linker arm with the acid moiety protected with an allyl group was prepared as we anticipated that, after esterification, the allyl group could be removed under mild conditions.

The allyl protected linker arm was prepared in two steps, as shown in Scheme 4.14, by reaction of ϵ -caprolactone (**4.51**) with 1 equivalent of aqueous tetra butyl-ammonium hydroxide at 65 °C for 6 hours. The resulting salt was dried under high vacuum to remove traces of water and reacted with 1.1

equivalents of allyl chloride in DMF at room temperature for 12 hours. The resulting allyl protected ester (**4.52**) was obtained in a 92% overall yield.

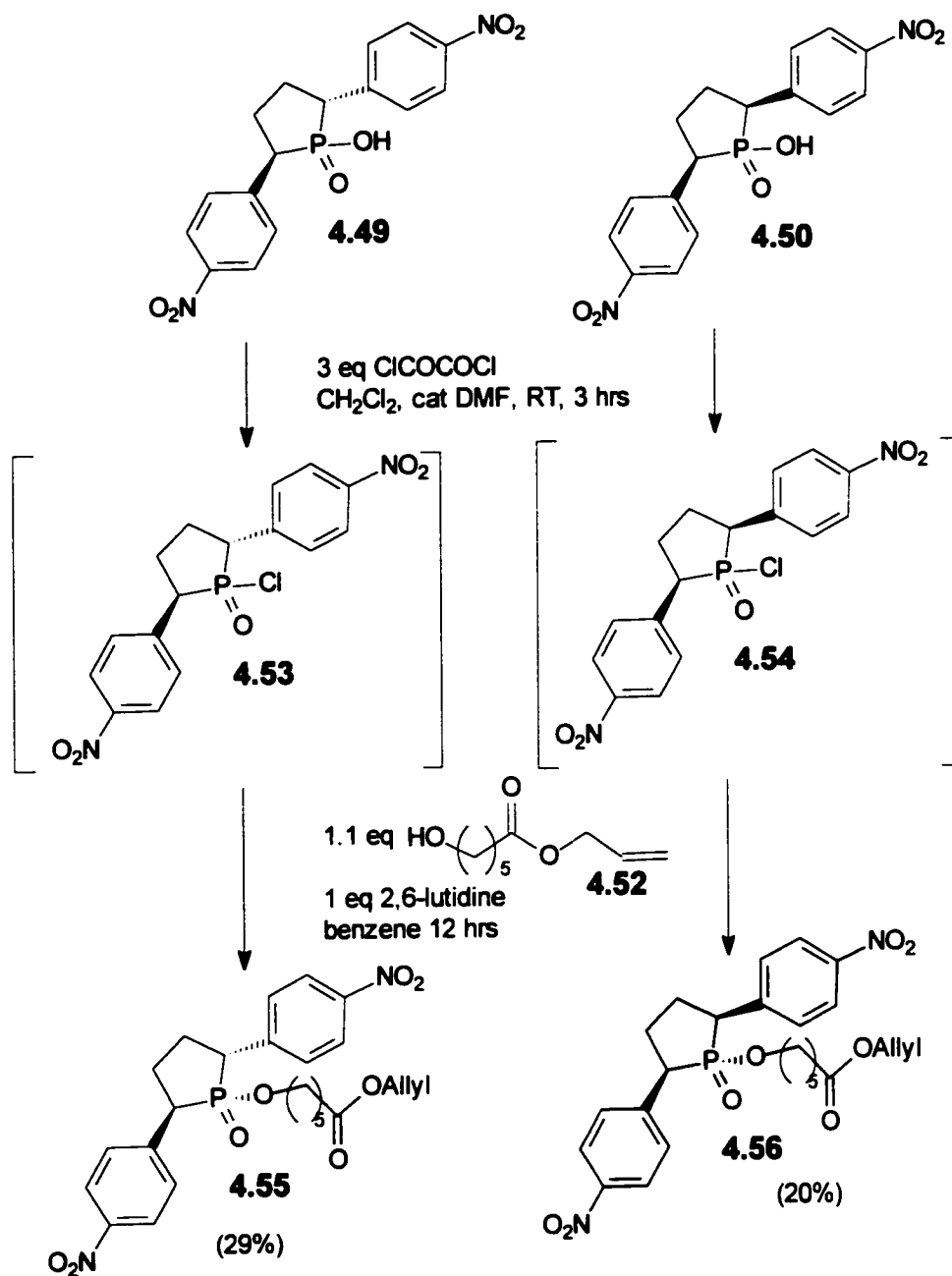


Scheme 4.14. Synthesis of allyl protected linker **4.52**.

In order to attach the **4.52** to the free acids, we converted the acids **4.49** and **4.50** to the acid chlorides by reaction of the free acids with 3 equivalents of oxalyl chloride in CH_2Cl_2 in the presence of a catalytic amount of DMF at room temperature for 3 hours (Scheme 4.15). The acid chlorides were not isolated but instead reacted directly with 1.1 equivalents of the linker arm **4.52** in benzene in the presence of 2,6-lutidine for 12 hours at room temperature.

The allyl protected *trans* TSA precursor **4.55** was obtained in a low 29% yield while the *cis* counterpart **4.56** was isolated in an even lower 20% yield. Part of the low yield of the *cis* compound **4.56** was due to the fact that significant amounts of the *trans* isomer **4.55** were detected and were not easily separable from the desired *cis* product. Taylor²⁸ examined this reaction with the unnitrate *cis* analogue and found that isomerization did not occur. Thus, isomerization with **4.50** appears to be due to the *para* nitro groups which lowered the pK_a of the benzylic protons on the phospholane ring, therefore, making them more acidic. Therefore, even with a sterically hindered base such 2,6-lutidine base, isomerization to the more thermodynamically stable *trans* isomer occurs.

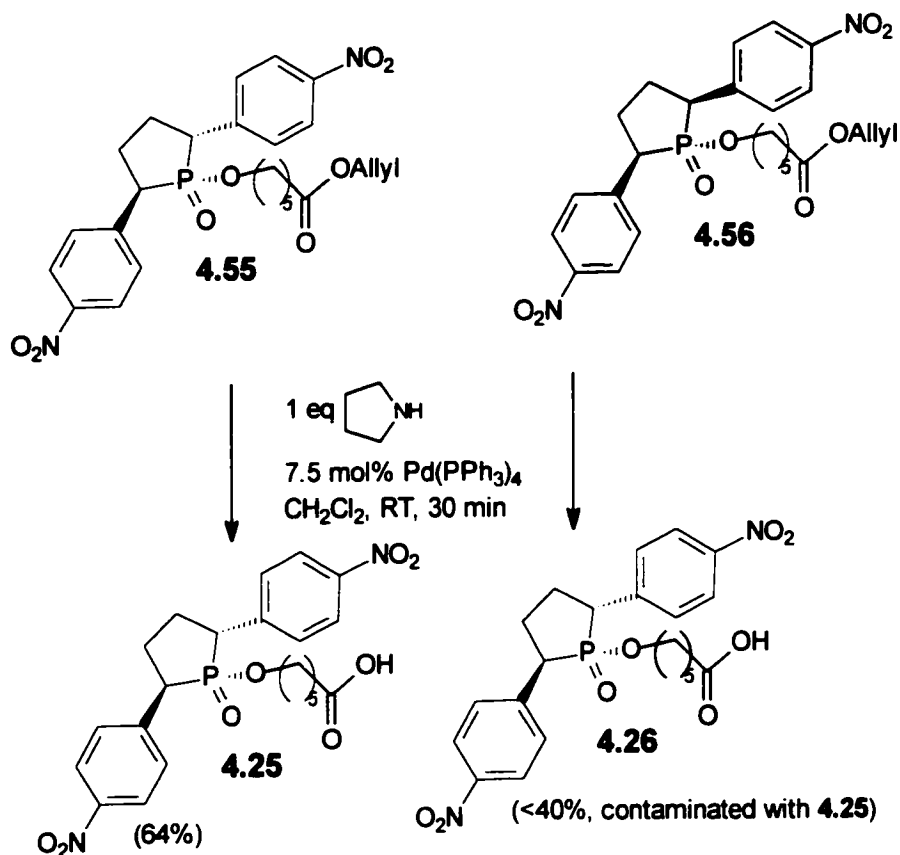
Despite the low yields obtained in these reactions, there was a sufficient amount of material for attempts at removing the allyl protecting group.



Scheme 4.15. Attachment of allyl protected linker arm **4.52**.

The palladium catalyzed removal of the allyl group was first attempted on the *trans* compound **4.55** using pyrrolidine in the presence of a catalytic amount

of $\text{Pd}(\text{PPh}_3)_4$. As seen in Scheme 4.16, the yield in the case of the *trans* compound was 64% however, this material was difficult to purify and was contaminated with trace amounts of triphenyl phosphine and its oxide which could not be removed even after several attempts at chromatographic separation.



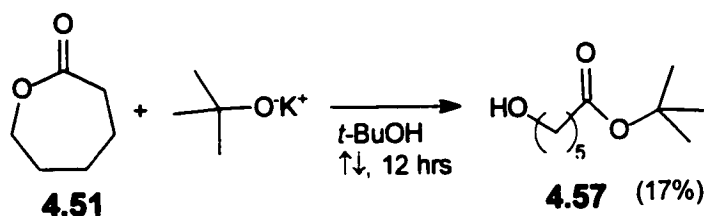
Scheme 4.16. Removal of allyl group from **4.55** and **4.56**.

When the deprotection was attempted on the *cis* precursor **4.56**, the results were even more disappointing. The yields were low (<40%) and contamination by triphenyl phosphine and its oxide was once again a problem. The acidity of the benzylic compounds became a factor once more since significant amounts of the *trans* compound **4.25** was present due to abstraction

of the acidic protons by pyrrolidine. The separation of the deprotected compounds **4.25** and **4.26** was not possible using silica gel chromatography.

The above results led us to two conclusions. The low yield from the esterification reaction meant that we required a more efficient method of attaching the linker arm to the phospholanic acids. These conditions would require the absence of any base due to the ease with which isomerization to the *trans* isomer was occurring in the presence of the *para* nitro groups on the aryl ring. In addition to a new esterification route, the removal of the allyl group produced side products that were difficult to remove, therefore, necessitating a new protecting group for the acid functionality.

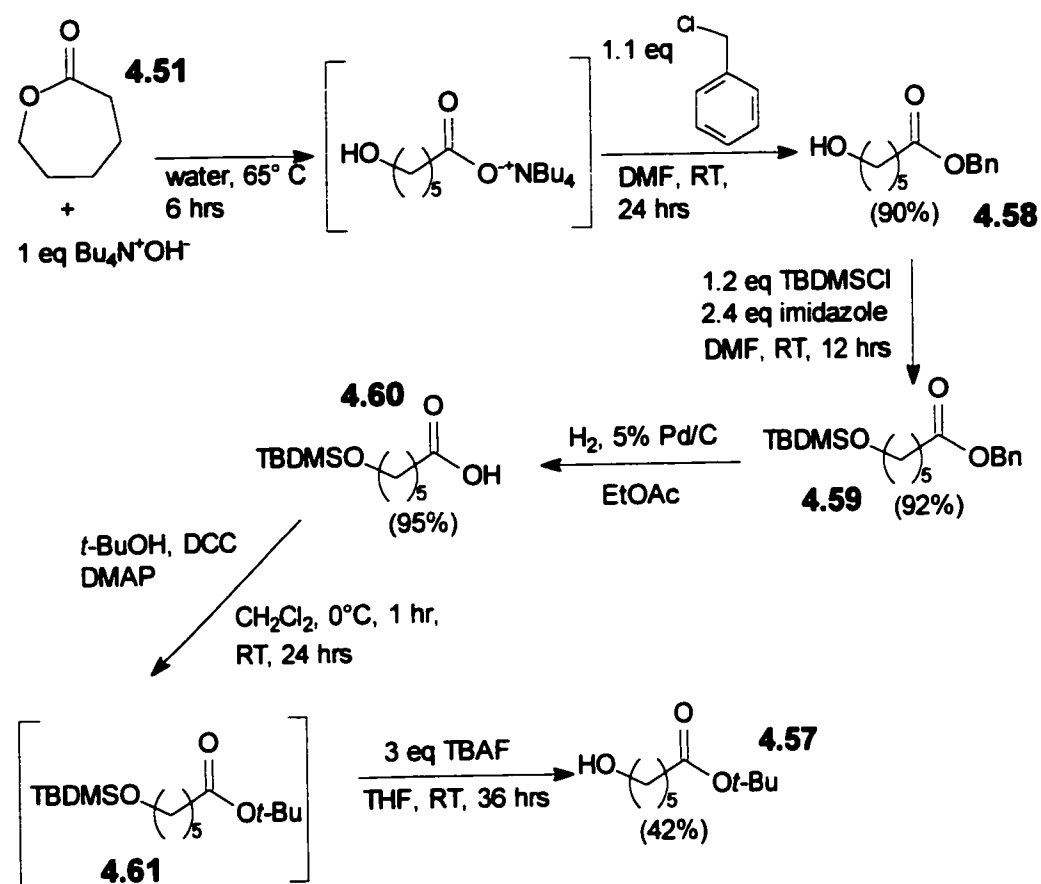
To address the problem of the protecting group, we decided to employ the *t*-butyl group since it can be removed under mild acidic conditions. The *t*-butyl protected compound **4.57** is a literature compound previously reported by Larock *et al.*³⁷ Larock's synthesis, shown in Scheme 4.17, was attractive since it was fairly straight forward and employed readily available and inexpensive reagents and a 76% yield was reported for the reaction.



Scheme 4.17. Larock's method for preparing ester **4.57**.

In our hands, Larock's procedure failed to provide the reported yields of greater than 80%. Besides the extremely low recovery of products, the material was contaminated with the *isobutyl*-protected isomer which was detectable in

both the ^1H and ^{13}C NMR. The *tert*-butyl alcohol that we employed was not contaminated with the isobutyl compound. We are unable to explain how this isomerization occurs during the reaction. No mention was made of this in Larock's paper, however, the compound was not well characterized by Larock and only ^1H NMR data was reported. Thus, in order to obtain pure **4.57**, an alternative route was required.



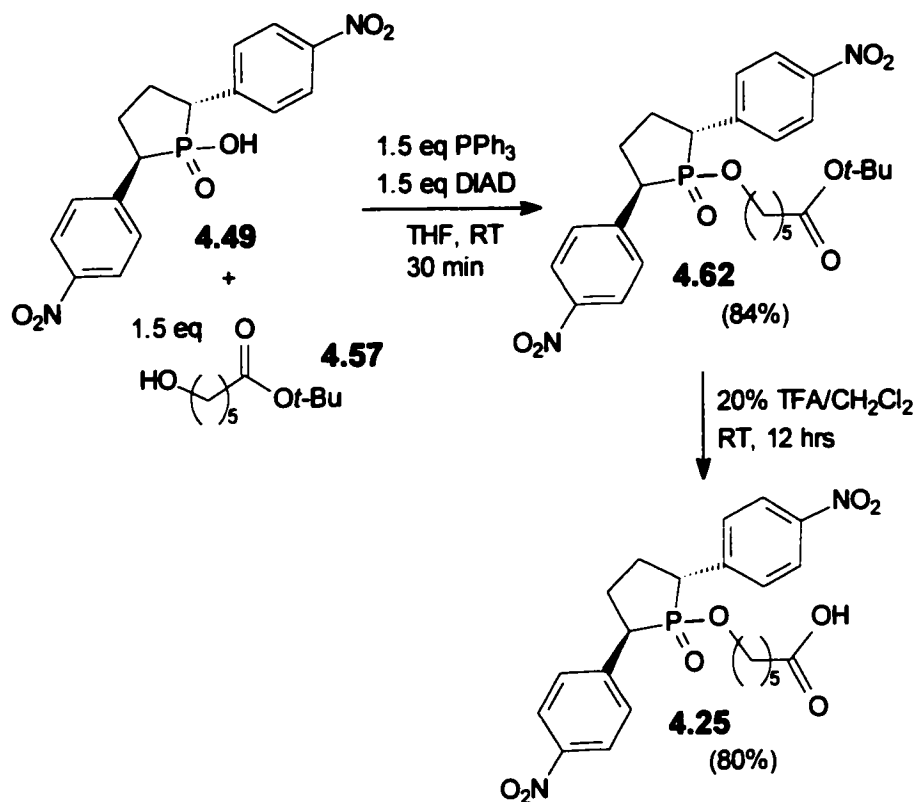
Scheme 4.18. Synthesis of *t*-butyl protected linker arm **4.57**.

The synthesis of pure *t*-butyl protected linker chain is shown in Scheme 4.18 and begins with ϵ -caprolactone (**4.51**) which was converted to the tetra-butyl ammonium salt. The salt was reacted *in situ* with benzyl chloride to give the benzyl protected **4.58** in 90% yield. The alcohol functionality was then protected

as the *tert*-butyl-dimethyl silyl ether by reaction with TBDMS chloride in the presence of imidazole. The diprotected intermediate **4.59** was obtained in a 92% yield. Hydrogenolysis removed the benzyl group to yield the free acid (**4.60**, 95% yield) which was then reprotected as the *t*-butyl ester via a DCC coupling with *t*-butanol. The product **4.61** was difficult to purify due to the presence of trace amounts of DCC and its byproduct DCU. The slightly impure product was converted to the free alcohol using TBAF which facilitated the isolation of the desired product **4.57** in a 42% yield. Although this route required six steps, the final product was obtained in high purity.

In order to improve the yields of the coupling between the linker arm and phosphonic acids, we used the Mitsunobu reaction conditions developed by Campbell³⁸ for the esterification of phosphonic acids. These conditions appeared attractive since the reported yields were high (>80%) and the conditions did not require any exogenous base.

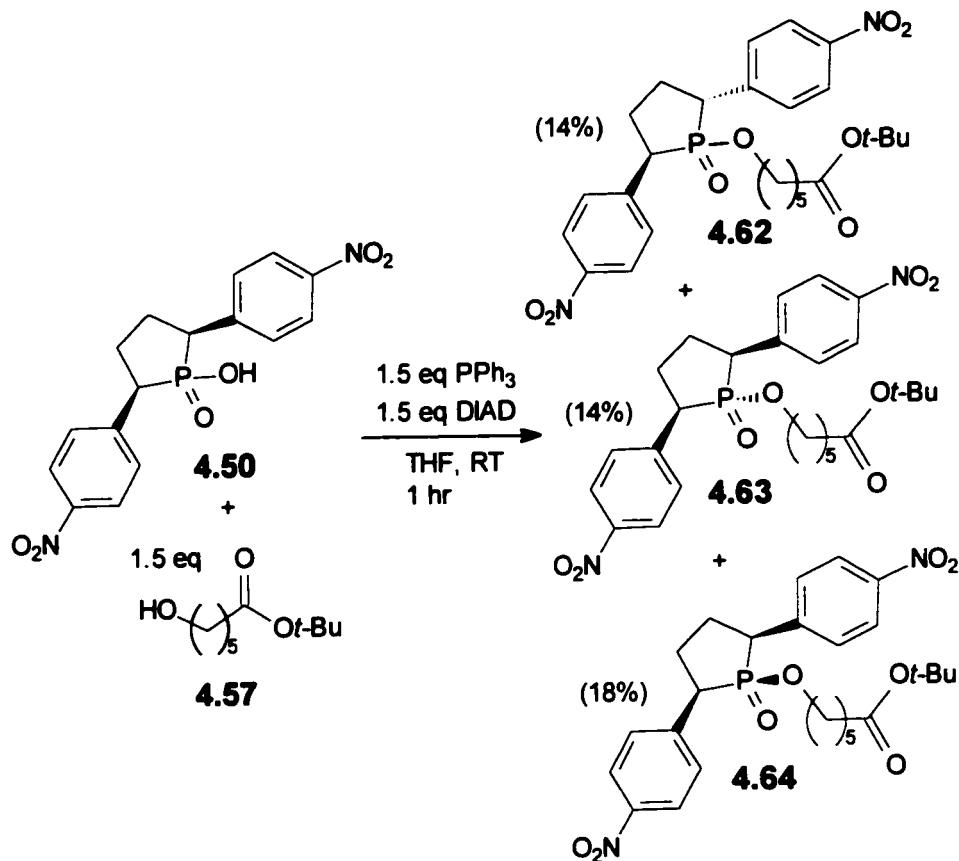
The reaction of the *trans* acid **4.49** with 1.5 equivalents of each of the reagents DIAD, triphenyl phosphine, and the alcohol **4.57** produced the *t*-butyl protected precursor in an 84% yield. Removal of the *t*-butyl protecting group was performed by stirring **4.62** in 20% TFA/CH₂Cl₂ at room temperature for 12 hours to give the final *trans* TSA **4.25** in an 80% yield (Scheme 4.19).



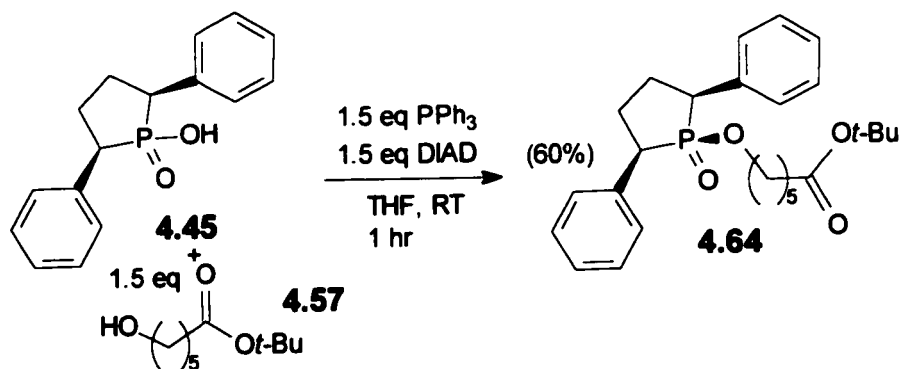
Scheme 4.19. Synthesis of *trans* TSA **4.25**.

When the same Mitsunobu conditions were applied to the *cis* acid **4.50**, as shown in Scheme 4.20, the desired 'aryl *cis*' product **4.63** was obtained in an 14% yield. Also isolated were the 'all *cis*' (**4.64**) (18%) and the 'aryl *trans*' (**4.62**) products (14%). These results were surprising since no exogenous base was present during the coupling to promote the isomerization of the 'aryl *cis*' compound **4.63** to the more stable *trans* isomer **4.62**. The only basic species generated during the course of the reaction is the betaine formed between triphenyl phosphine and DIAD. Adding to the ambiguity of the results was the formation of equivalent amounts of the 'all *cis*' product **4.64**.

In order to better understand the results presented in Scheme 4.20, the Mitsunobu coupling was repeated using the unnitrated *cis* acid **4.45** (Scheme 4.21).



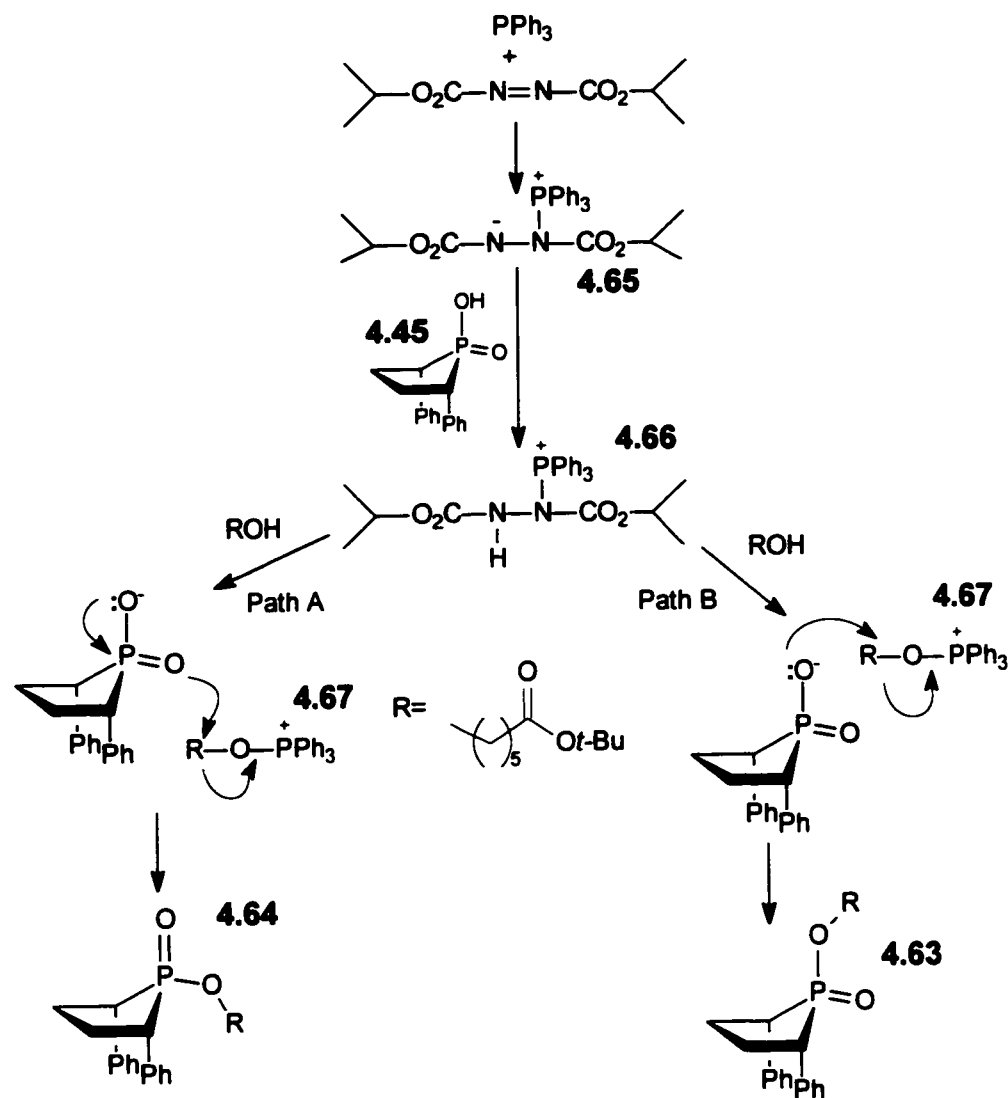
Scheme 4.20. Mitsunobu reaction with nitrated *cis* phospholanic acid **4.50**.



Scheme 4.21. Mitsunobu reaction of unnitrated phospholanic acid **4.45**.

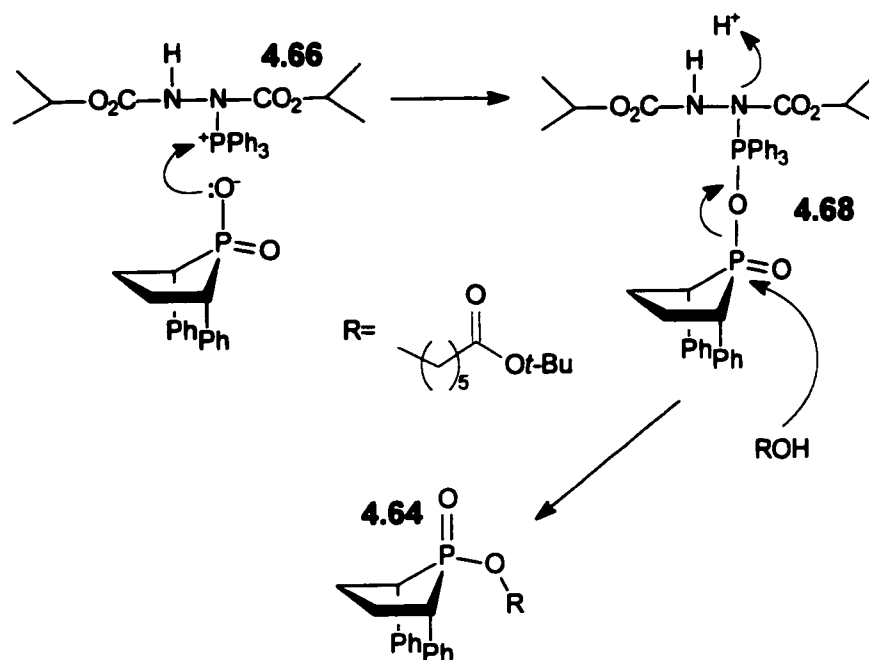
Interestingly, the product resulting from the Mitsunobu coupling of **4.47** with the unnitrated 'phenyl *cis*' acid **4.45** was exclusively the 'all *cis*' isomer **4.64**. These results appear to indicate that the multiple products arising from the coupling of the nitrated *cis* acid (Scheme 4.20) were due to the presence of the *para* nitro groups which once again facilitated the deprotonation of the benzylic protons. It is most likely that the all *cis* product **4.64** was formed as the initial product in Scheme 4.20, and the other two isomers, **4.62** and **4.63** arose due to isomerization with the triphenylphosphine-DIAD betaine acting as a base.

The results in Scheme 4.21 appear to contradict the currently accepted mechanism for the Mitsunobu esterification of phosphonic acids which is outlined in Scheme 4.22.³⁸ The betaine **4.65** which is formed between triphenylphosphine and DIAD deprotonates the phosphonic acid to give the protonated betaine **4.66**. The alcohol reacts with **4.66** and forms the alkoxyphosphonium salt **4.67**. The deprotonated acid acts as a nucleophile and attacks the oxygen bearing carbon atom to give triphenyl phosphine oxide and form the final ester bond. To account for the 'all *cis*' product, attack upon the alkoxyphosphonium salt would have to occur on the more sterically hindered face of the phospholane ring *cis* to the 2,5-phenyl rings as represented by path A in Scheme 4.22. The mechanism does not explain the absence of 'phenyl *cis*' products which would form as a result of path B where the nucleophilic attack occurs upon the less hindered side away from the bulky 2,5 substituents.



Scheme 4.22. Mechanism of Mitsunobu reaction.

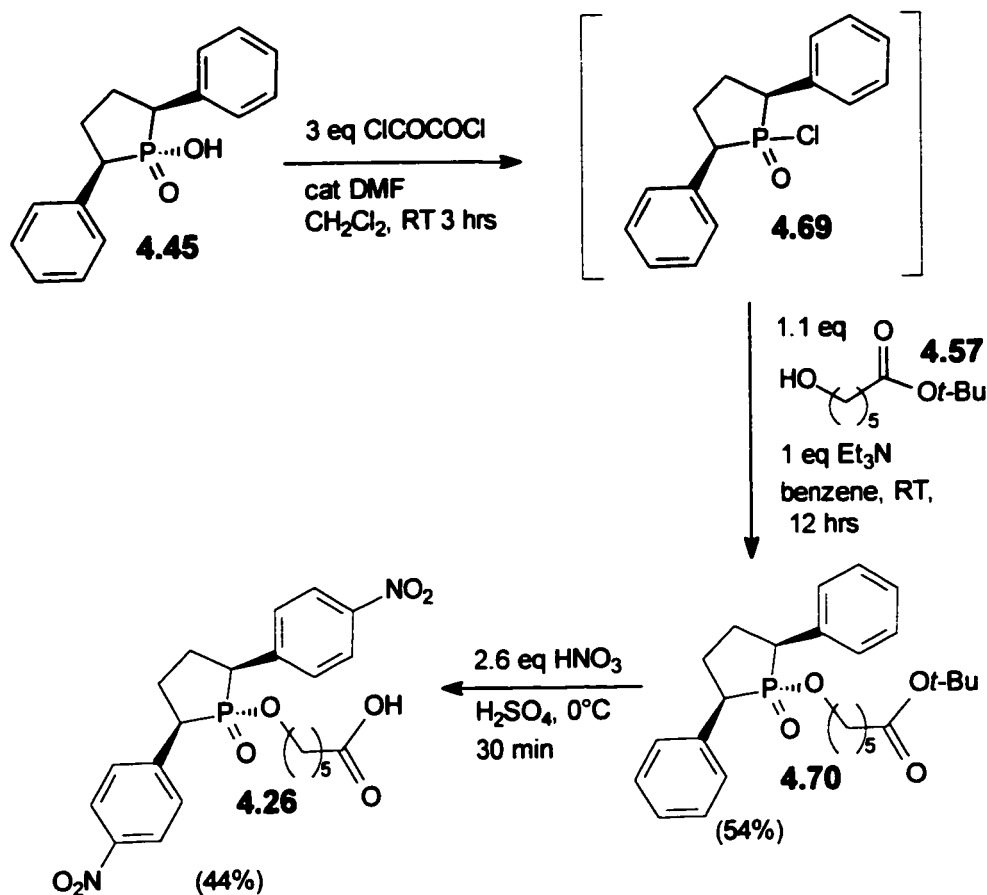
An alternative is outlined in Scheme 4.23, where deprotonation of the acid by the betaine is once again the initial step of the reaction. However, rather than form the alkoxy phosphonium salt with the alcohol, the protonated betaine **4.66** and the phosphonic acid form an adduct on the less hindered face of the phospholane ring away from the 2,5-phenyl rings due to the steric bulk of triphenyl phosphine and DIAD.



Scheme 4.23. Alternative mechanism for the Mitsunobu reaction.

An in-line attack on phosphorus by the alcohol gives the final 'all cis'. As with the mechanisms outlined in Scheme 4.22, this one also has some points of contention. Here, the in-line attack on phosphorous would require that the five-membered ring occupy a diequatorial orientation at the TBP transition state which is rather unfavorable due to ring strain. However, this would be the case for any in-line attack on a five-membered cyclic phosphinate.

We believe that it would be possible to distinguish between the above mechanisms by using ¹⁸O labeled alcohol (eg. ethanol) and follow the incorporation of the isotope in the resulting products. If the mechanism in Scheme 4.22 is correct, the label would be present in the triphenyl phosphine oxide whereas according to Scheme 4.23, it would be found in the ester product. ³¹P NMR and mass spectroscopy could be used to readily determine the final location of the label.



Scheme 4.24. Synthesis of *cis* TSA **4.26**.

Regardless of the details of the mechanism of the Mitsunobu reaction, it was obvious that the incorporation of the bis *para* nitro groups into the *cis* TSA precursors was creating several unforeseen problems. In order to avoid these difficulties, we decided to nitrate at a later stage of the synthesis as shown in Scheme 4.24. We started with the unnitrated *cis* acid **4.45**, and formed the acid chloride **4.69**. The acid chloride was not isolated but instead reacted with the *t*-butyl protected linker arm **4.57**. Surprisingly, this gave us almost exclusively the unnitrated 'phenyl *cis*' isomer **4.70** in which the linker arm is in the correct geometry *trans* to the 2,5-phenyl rings. This may be due to the reaction of the *in situ* generated chloroiminium ion with the least sterically hindered phosphoryl

oxygen. The resulting adduct then reacts with the chloride ion to give exclusively the acid chloride **4.69**. This then reacts by inversion of configuration with the linker arm to give ester **4.70**. Using the classical nitration conditions, we found that it was possible to introduce the bis *para* nitro groups and deprotect the *t*-butyl group in a single step to give the desired *cis* TSA **4.26** in 44% yield.

4.3.2 Hapten Isomerization Studies

The problems surrounding the isomerization of the nitrated *cis* compounds to the *trans* compounds during the syntheses raised concerns regarding their the stability of the *cis* compound during conjugation to the carrier proteins and the immunization process. In effect, if isomerization did occur during these processes, we would actually be raising antibodies to pure *trans* hapten **4.25** and a mixture of *cis* and *trans* material **4.26** and **4.25**. To alleviate these concerns, we chose to study the rate of isomerization under circumstances approximating an *in vivo* environment as well as the conditions required for conjugation to the carrier proteins.

Though the isomers have slightly different ^{31}P chemical shifts, the use NMR spectroscopy suffered from two major disadvantages for purposes of this study. The first drawback was the amount of material that was required. Due to sensitivity issues, a minimum of approximately 20-30 mg of material would be required for each study. The studies would have to be conducted in buffered aqueous solutions at physiological pH. The NMR pulse and decoupling sequences often cause such solutions to heat up therefore possibly increasing

the rate of isomerization. The use of HPLC appeared to be a more accurate and sensitive method.

We found that the two isomers could be resolved using a normal phase silica analytical HPLC column (Figure 4.10). The *cis* TSA 4.26 was found to elute slightly earlier than the *trans* isomer 4.25 with a retention time of 3.9 minutes (Figure 4.10a) compared to 5.9 minutes (Figure 4.10b). Co-injection of the two compounds showed that baseline resolution was possible (Figure 4.10c).

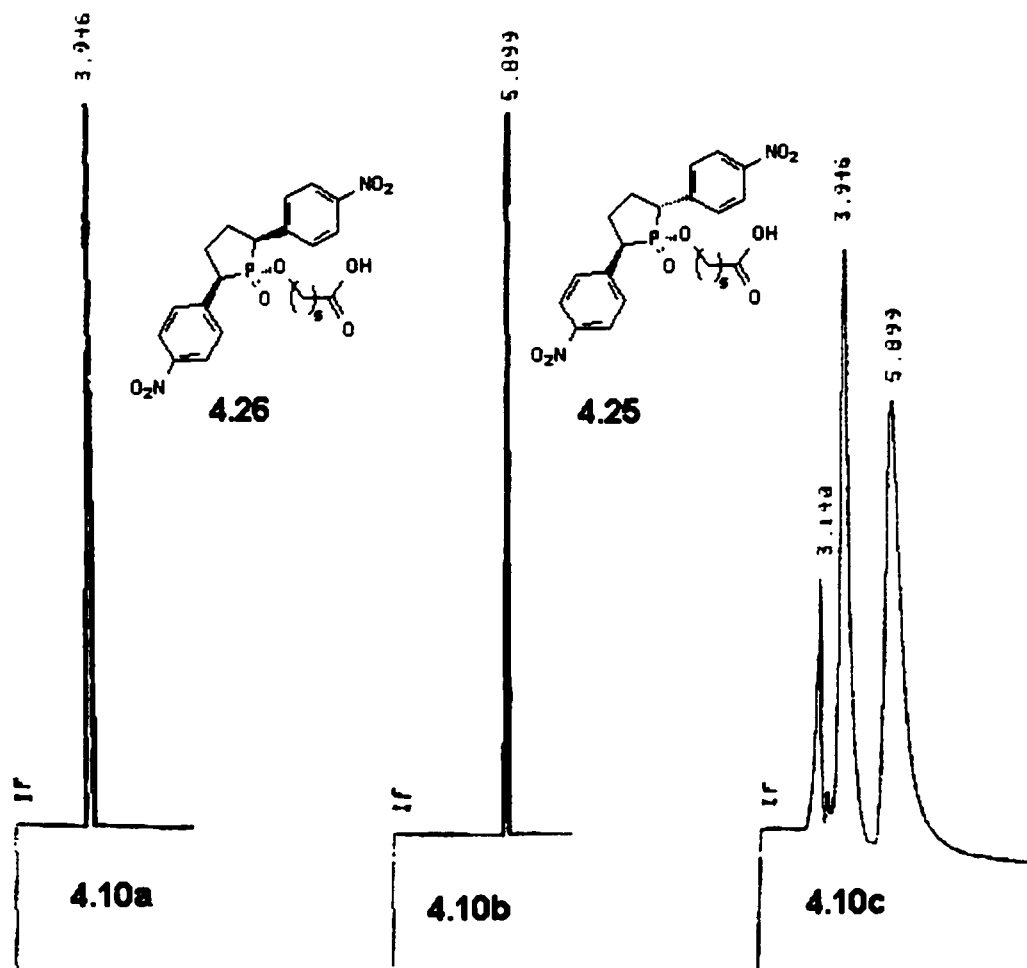


Figure 4.10. HPLC chromatograms of 4.26 and 4.25.

In order to study the isomerization, a 500 μM solution of the *cis* TSA **4.26** in 0.1 M NaOH was prepared. To perform the analysis, aliquots were withdrawn and quenched with HCl at various time intervals. The solutions were extracted with EtOAc and then injected into the HPLC for analysis (Figure 4.11).

Immediately obvious is the increase in retention times, which can be attributed to the fact that the times indicated in Figure 4.10 were from a pure EtOAc solutions whereas the injections from the EtOAc extracts are most likely saturated with water. The data for aliquots quenched at 10 min, 1 hour and 1 day is presented in Figure 4.11 and Table 4.1. In 0.1 M NaOH, the isomerization to the *trans* isomer **4.25** occurs very rapidly as the equilibrium ratio of 3:1 (*trans:cis*) is reached within 10 minutes. This ratio differs slightly from the levels observed when the isomerization was conducted in EtOH with NaOEt as a base (see Scheme 4.12).

Table 4.1. Percentages of the *cis* (**4.26**) and *trans* (**4.25**) isomers in 0.1 M NaOH at various time intervals.

Incubation Period	% <i>cis</i> Isomer 4.26	% <i>trans</i> Isomer 4.25
10 minutes	24	76
1 hour	22	78
1 day	26	74

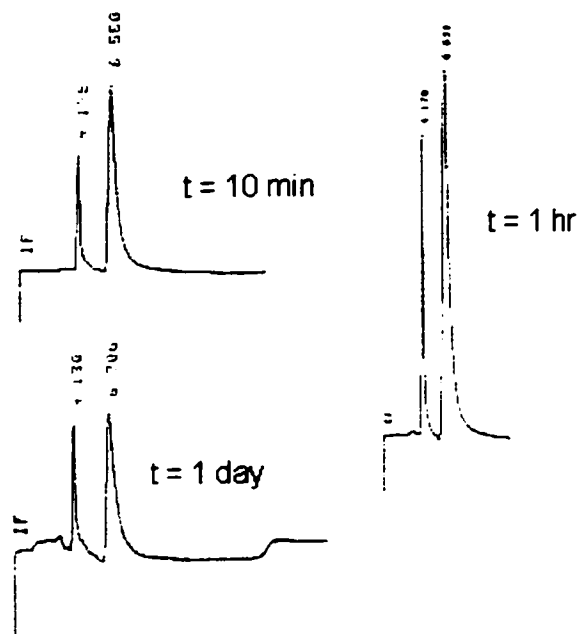


Figure 4.11. HPLC chromatograms of *cis* TSA **4.26** in 0.1 M NaOH.

To simulate *in vivo* conditions as well as the conditions used for the conjugation process, the extent of isomerization was studied in 20 mM sodium phosphate buffer at pH 7.5 (approximating physiological pH).

Table 4.2. Percentages of the *cis* (**4.26**) and *trans* (**4.25**) isomers in 20 mM sodium phosphate buffer, pH 7.5, at various time intervals.

Incubation Period	% <i>cis</i> Isomer 4.26	% <i>trans</i> Isomer 4.25
25 minutes	100	0
1 day	100	0
3 days	97	3
1 week	92	8
11 days	86	14

The chromatograms for the analyses conducted after incubation periods of 25 minutes, 1, 3, 7, and 11 days are shown in Figure 4.12 and summarized in Table 4.2.

The data in Table 4.2 shows that at pH 7.5, after a week only 8% of the *cis* isomer **4.26** has undergone isomerization. Thus, during the immunization with the *cis* hapten, sufficient quantities of the *cis* hapten should remain to elicit *cis* specific antibodies.

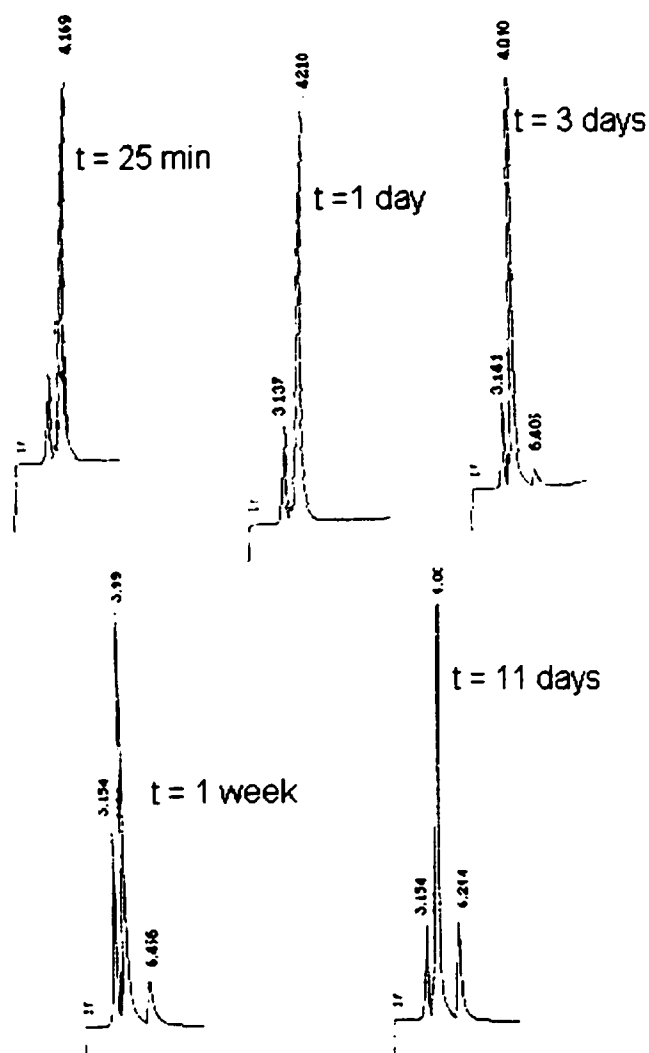


Figure 4.12. HPLC chromatograms of *cis* TSA **4.26** in 20 mM sodium phosphate buffer, pH 7.5.

Table 4.3. Percentages of the *cis* (4.26) and *trans* (4.25) isomers in 20 mM sodium bicarbonate buffer, pH 8.5, at various time intervals.

Incubation Period	% <i>cis</i> Isomer 4.26	% <i>trans</i> Isomer 4.25
20 minutes	100	0
3.5 days	48	52
8 days	29	71

A final isomerization experiment was conducted in 20 mM NaHCO₃ buffer at pH 8.5 in order to simulate the conditions often used for the screening of monoclonal antibodies for hapten binding. Chromatograms from this study are presented in Figure 4.13 and summarized in Table 4.3. At pH 8.5, the rate of isomerization increases significantly with 52% of the hapten in the *trans* form after 3.5 days.

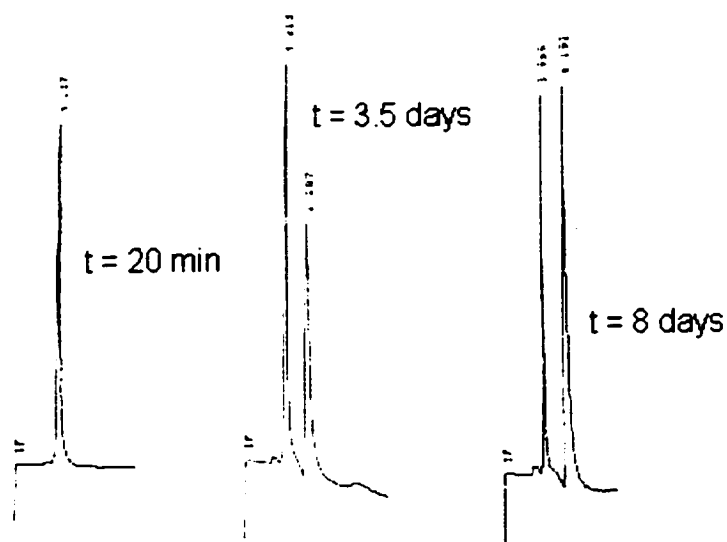


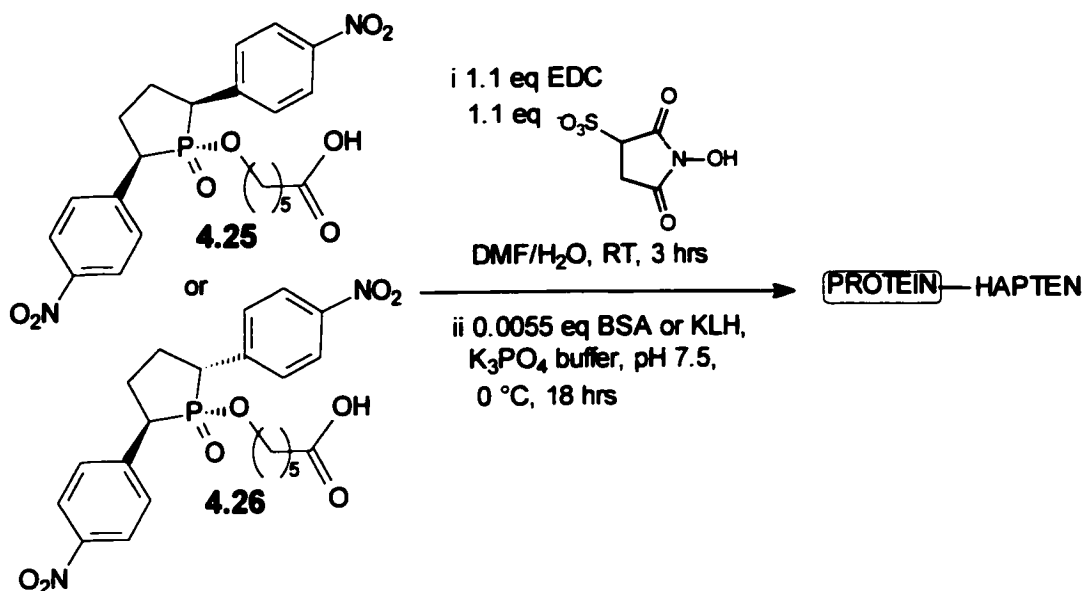
Figure 4.13. HPLC chromatogram of *cis* TSA 4.26 in 20 mM NaHCO₃ buffer, pH 8.5.

After 8 days, only 29% of the *cis* isomer remains. These results indicate that the screening of the monoclonal antibodies for hapten binding has to be conducted below pH 8.5.

4.3.3 Conjugation of TSA's to Carrier Proteins

As small molecules, TSA's **4.25** and **4.26** will not elicit antibodies themselves, but instead must be conjugated to carrier proteins in order to provoke an immune response. Common proteins used for the production and screening of monoclonal antibodies are BSA (bovine serum albumin) and KLH (keyhole limpet hemocyanin) since they are inexpensive and commercially available. We conjugated both TSA's to both carrier proteins for a total of four TSA-protein conjugates. Two carrier proteins are used since one (KLH) is used for immunization and the other (BSA) for antibody screening in order to ensure that the antibodies are recognizing the TSA's and not the carrier protein.

The conjugation of the carrier proteins was performed by forming the activated N-hydroxy sulfosuccinimide esters of the free acids of the linker arm via an EDC coupling (Scheme 4.25) in a DMF/water cosolvent system at room temperature for 3 hours. The resulting activated esters were not isolated but instead reacted with the free amino groups of the solvent accessible lysine side chains of BSA and KLH in 50 mM potassium phosphate buffer for 18 hours. The hapten conjugates were purified by dialysis which removed the unconjugated TSA's and the byproducts from the coupling reactions.



Scheme 4.25. Conjugation of TSA's to carrier proteins.

The method described by Habeeb³⁹ was used to determine the number of *cis* and *trans* haptens attached to BSA. The protein concentration of the conjugates was determined by using the bicinchoninic acid (BCA) protein assay. In order to perform the BCA assay, solution of unconjugated BSA of equal concentration is made up and reacted with 2,4,6-trinitrobenzene sulfonic acid (TNBS) as is an aliquot of each of BSA•4.25 and BSA•4.26 solutions. The TNBS reacts with the free amino residues. TNBS-lysine adducts absorb at a wavelength of 562 nm. Unconjugated BSA has 33 solvent accessible lysine residues whereas the BSA conjugates have fewer since some of the accessible lysine sites are occupied by the TSA's. A measure of the extent of loading is made by comparing the absorbance of the control (unreacted BSA) with the conjugated proteins. Our results indicated that there were 19 and 11 haptens attached to the BSA for the *cis* and *trans* conjugates respectively. This same analysis was not performed with the KLH conjugates due their cloudy

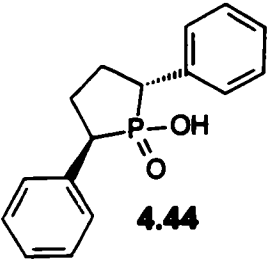
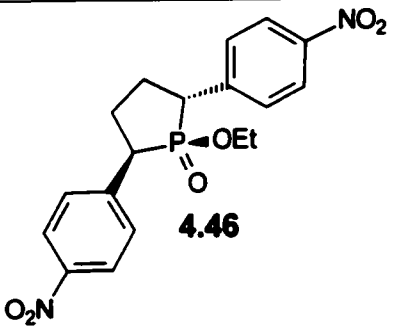
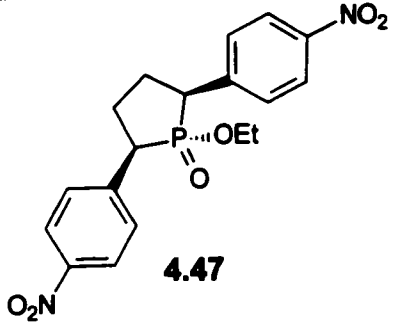
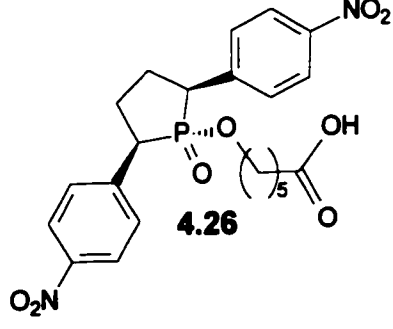
appearance which interferes with the assay. Determination of only the extent of BSA conjugation is standard practice and it is usually presumed that the KLH conjugations proceed to the same extent.

4.3.4 Crystal Structure Data

A crucial aspect of our hapten design was the C-P-C bond angle in the phospholane ring. The only report of a crystal structure of a similar compound is that of phospholanic acid by Alver *et al.*²⁶ in which the C-P-C angles is 95°. For cyclic phosphates, the O-P-O bond has been determined to be 98°. ²⁴ We expected our compounds to have bond angles in this range. We were able to crystallize several of our phosphinates for the purposes of x-ray structural analysis. These compounds included the *trans* unnitrated phospholanic acid **4.44**, the *trans* nitrated ethyl ester **4.46**, the nitrated *cis* ethyl ester **4.47**, and the *cis* TSA **4.26**. The crystal structures were acquired by Dr. Alan Lough, from the Department of Chemistry of the University of Toronto. The x-ray structures are presented as Figures 4.14-4.17 and the crucial bond angles are summarized in Table 4.4.

The bond angles ranged from 94 to 98° which demonstrates that these compounds have endocyclic C-P-C bond angles that are compressed towards the ideal equatorial-axial TBP transition state bond angle of 90° found during phosphate ester hydrolysis. Additional crystallographic data for these compounds are included in Appendix A.

Table 4.4. Endocyclic C-P-C bond angles of **4.44**, **4.46**, **4.47**, and **4.26**.

Compound	Bond Angle
 <p style="text-align: center;">4.44</p>	97.7°
 <p style="text-align: center;">4.46</p>	97.4°
 <p style="text-align: center;">4.47</p>	94.0°
 <p style="text-align: center;">4.26</p>	96.8°

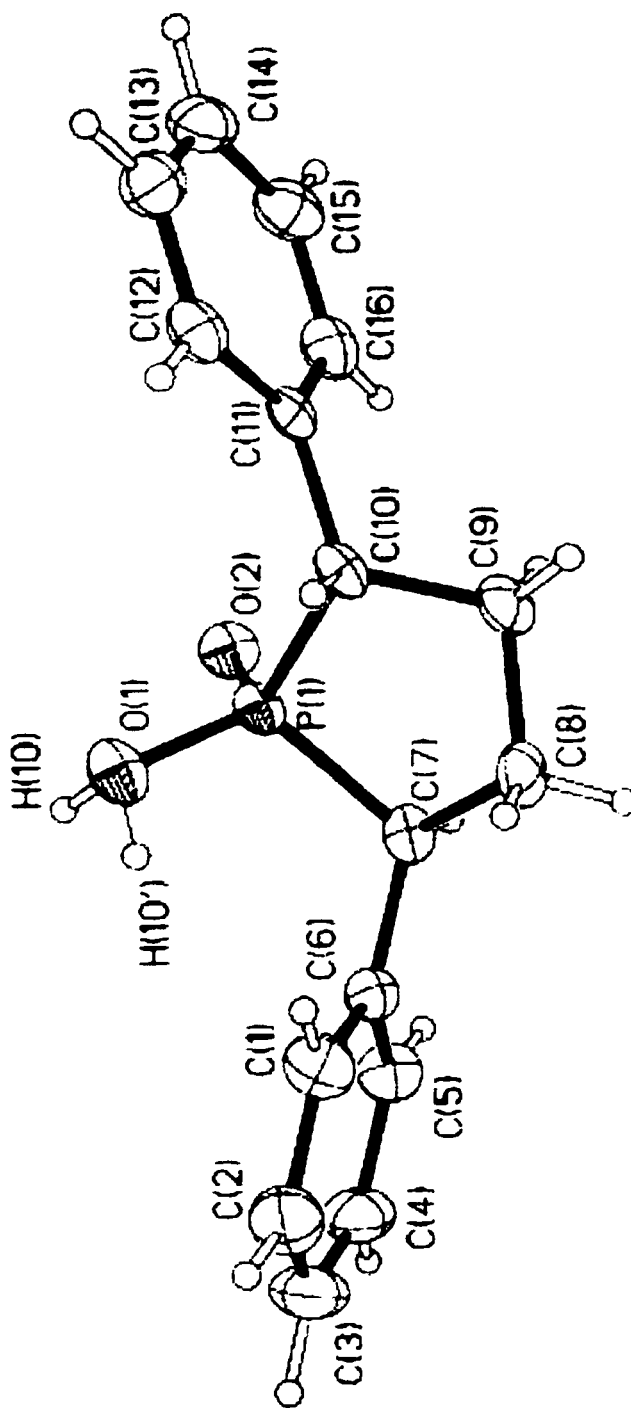


Figure 4.14. Crystal structure of 4.44.

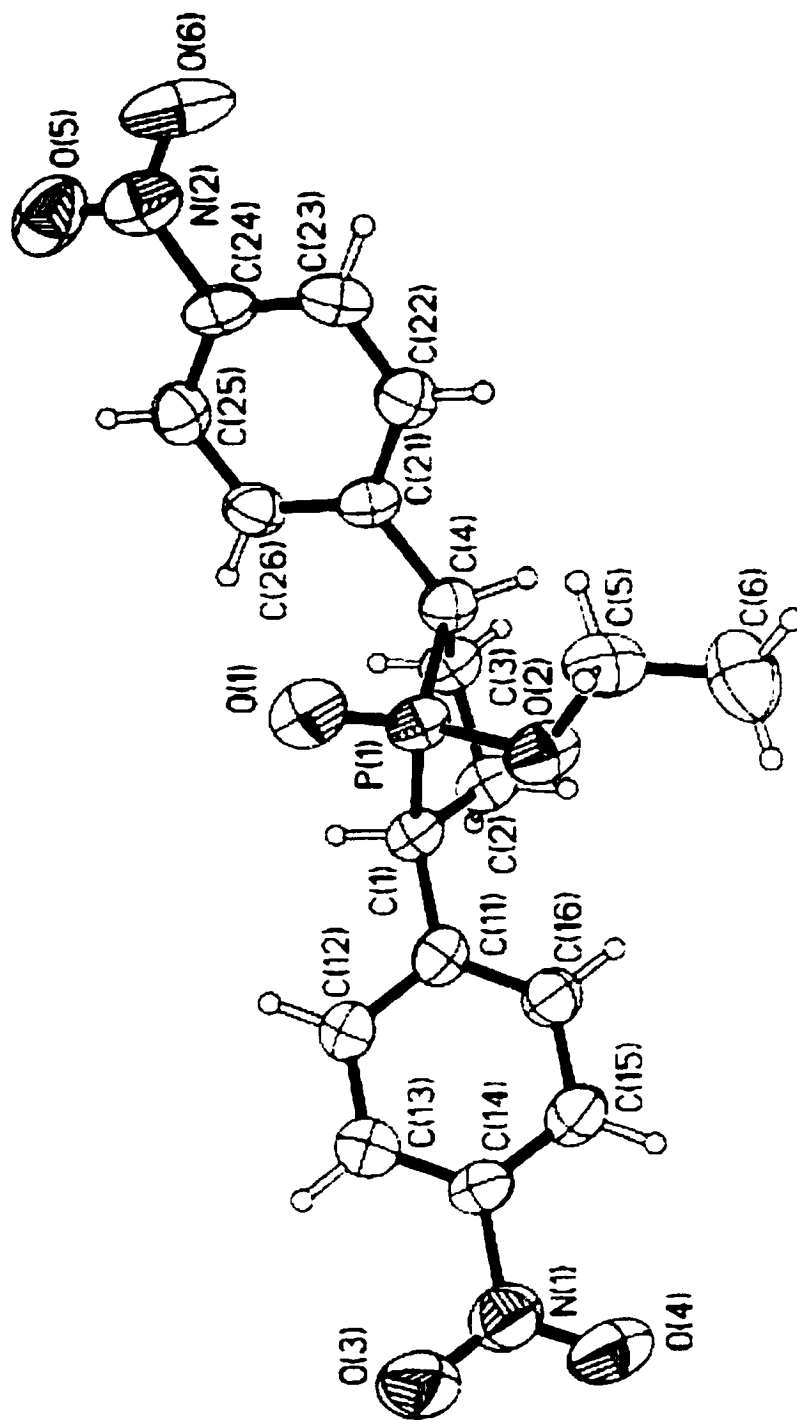


Figure 4.15. Crystal structure of 4.46.

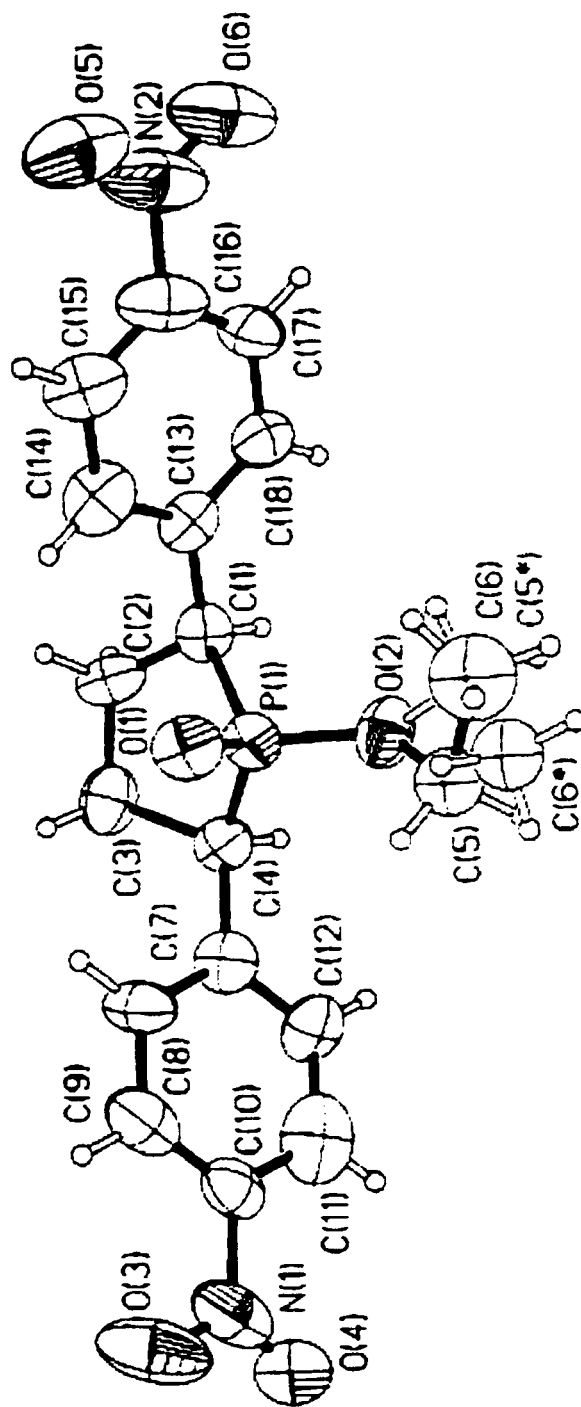


Figure 4.16. Crystal structure of 4.47.

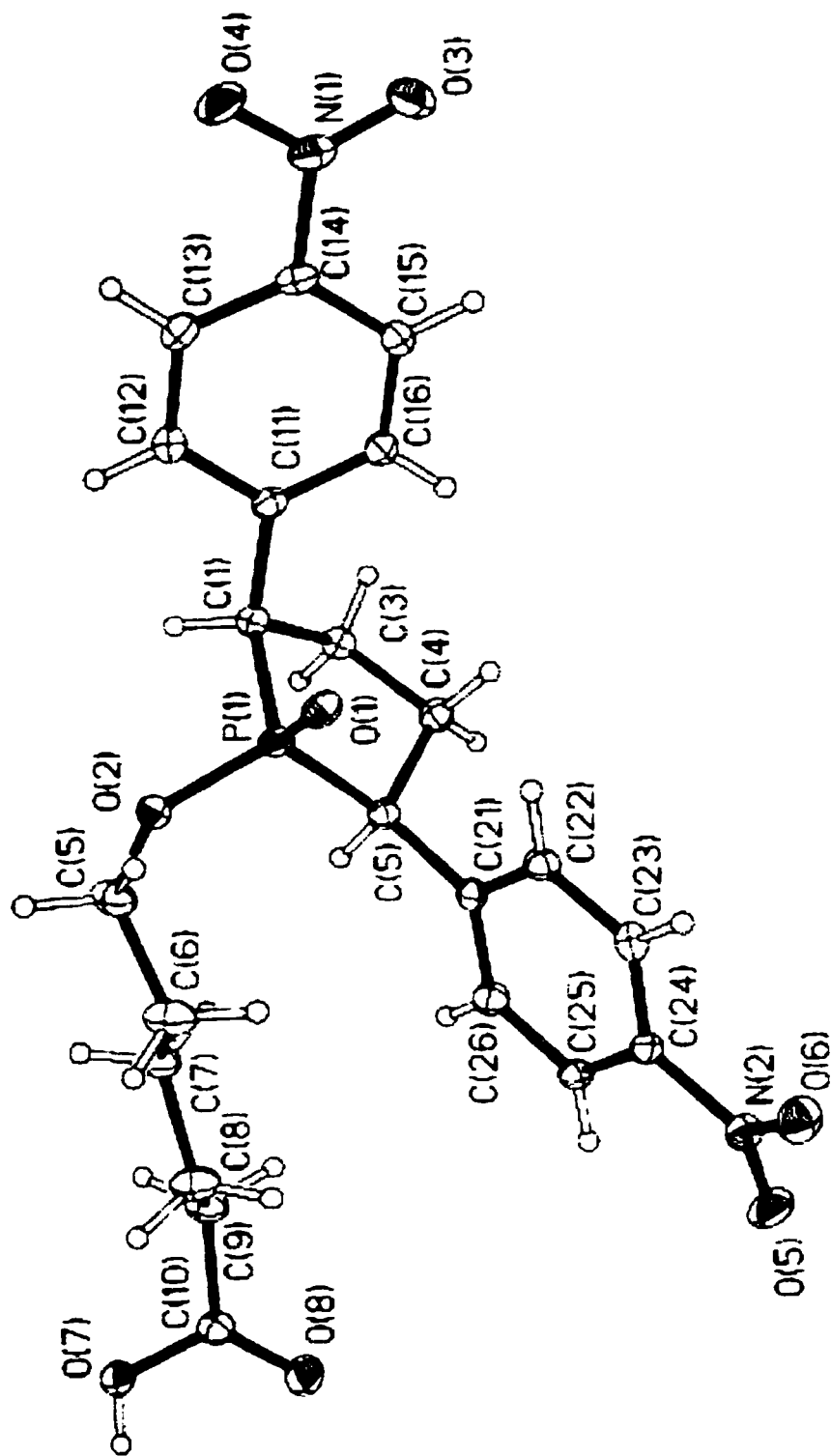
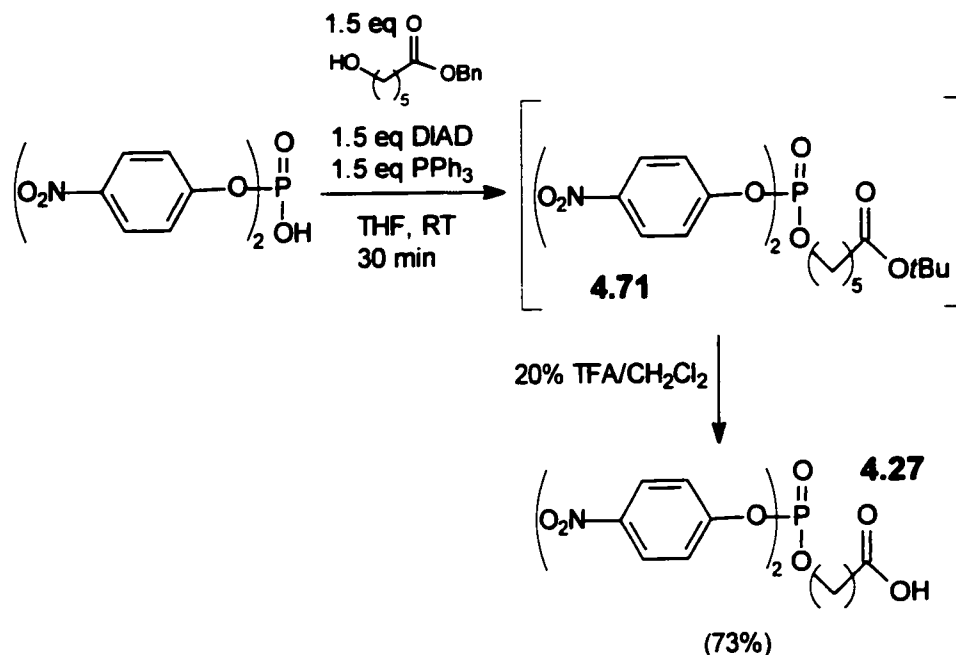


Figure 4.17. Crystal structure of *cis* TSA 4.26.

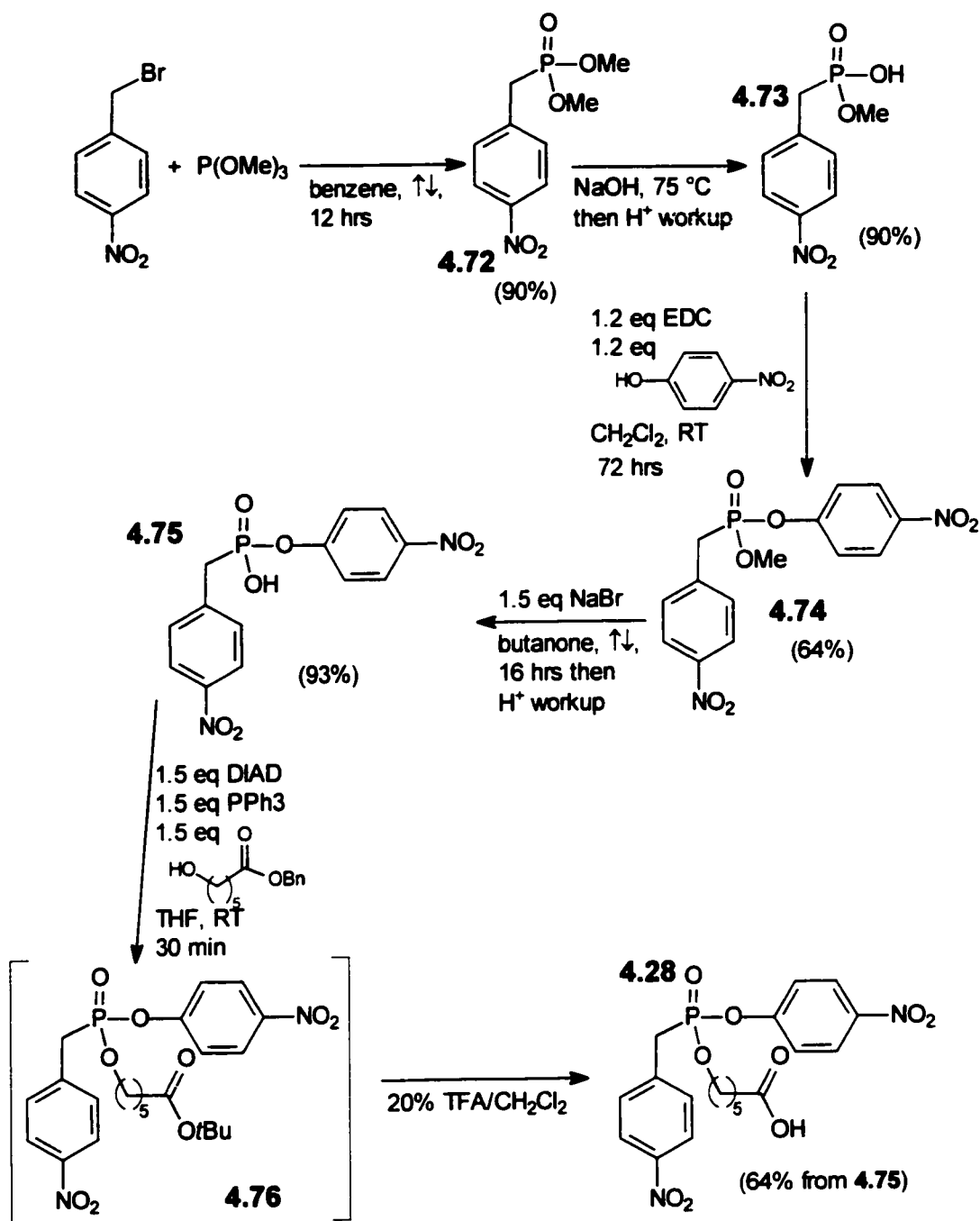
4.3.5 Synthesis of Antibody Substrates

The intended model substrates for the antibodies **4.27** and **4.28**, are not commercially available and thus had to be synthesized.



Scheme 4.26. Synthesis of phosphate substrate **4.27**.

The preparation of the phosphate substrate was fairly straightforward as outlined in Scheme 4.26. Starting with commercially available bis (*para* nitrophenyl) phosphate, the *t*-butyl protected linker arm was attached using a Mitsunobu reaction. The resulting ester **4.71** was contaminated with trace amounts of triphenyl phosphine oxide which persisted even after several attempts at purification by chromatography. The impure product was deprotected in 20% TFA/CH₂Cl₂ to give the substrate **4.27**. Upon removal of the *t*-butyl group, the final product **4.27** could be easily separated from the contaminants and isolated pure in an overall 73% yield.



Scheme 4.27. Synthesis of phosphonate substrate **4.28**.

Preparation of the phosphonate substrate required more synthetic steps as outlined in Scheme 4.27. *Para*-nitro benzyl bromide was reacted with trimethyl phosphite in an Arbuzov reaction to produce dimethyl *para*-nitrobenzyl phosphonate in a 90% yield. Basic hydrolysis of **4.72** removed one of the methyl

groups to produce the intermediate Na salt which, upon acidification produced the monoacid **4.73**. An EDC mediated coupling between **4.73** and *para*-nitrophenol produced the phosphonate ester **4.74** in a 64% yield. Conversion of **4.74** to the free acid was accomplished by removal of the methyl group with NaBr in refluxing butanone followed by acidification to obtain the acid **4.75** in a 93% yield. The *t*-butyl protected linker arm was once again attached using a Mitsunobu reaction. As encountered during the synthesis of the phosphate substrate, the intermediate *t*-butyl protected compound **4.76** was difficult to purify. The partially purified precursor was deprotected in 20% TFA/CH₂Cl₂ to yield the desired phosphonate substrate **4.28** in a 64% yield.

4.3.6 Antibody Substrate Hydrolysis Studies

Prior to determining if the hydrolysis of substrates **4.27** and **4.28** could be catalyzed by an abzyme, we studied the rates of the uncatalyzed reactions in order to determine the stability of the substrates. The half lives of substrates **4.27** and **4.28** were studied at pH 9.0 in 10.0 mM CHES buffer containing 50.0 mM NaCl. The hydrolysis reactions were followed using spectrophotometry by recording the increase in absorbance at 400 nM over a period of 72 hours. The data was fitted to a first order rate equation using the Grafit⁴⁰ software package in order to determine the first order rate constant. Under these conditions, the phosphate (**4.27**) and phosphonate (**4.28**) substrates were found to have half lives of 14 and 29 hours respectively.

Sample absorbance plots for the hydrolysis of the phosphonate and phosphate substrates are presented in Figure 4.18. These studies demonstrate

that the intended substrates are sufficiently stable for screening the antibodies for catalytic activity.

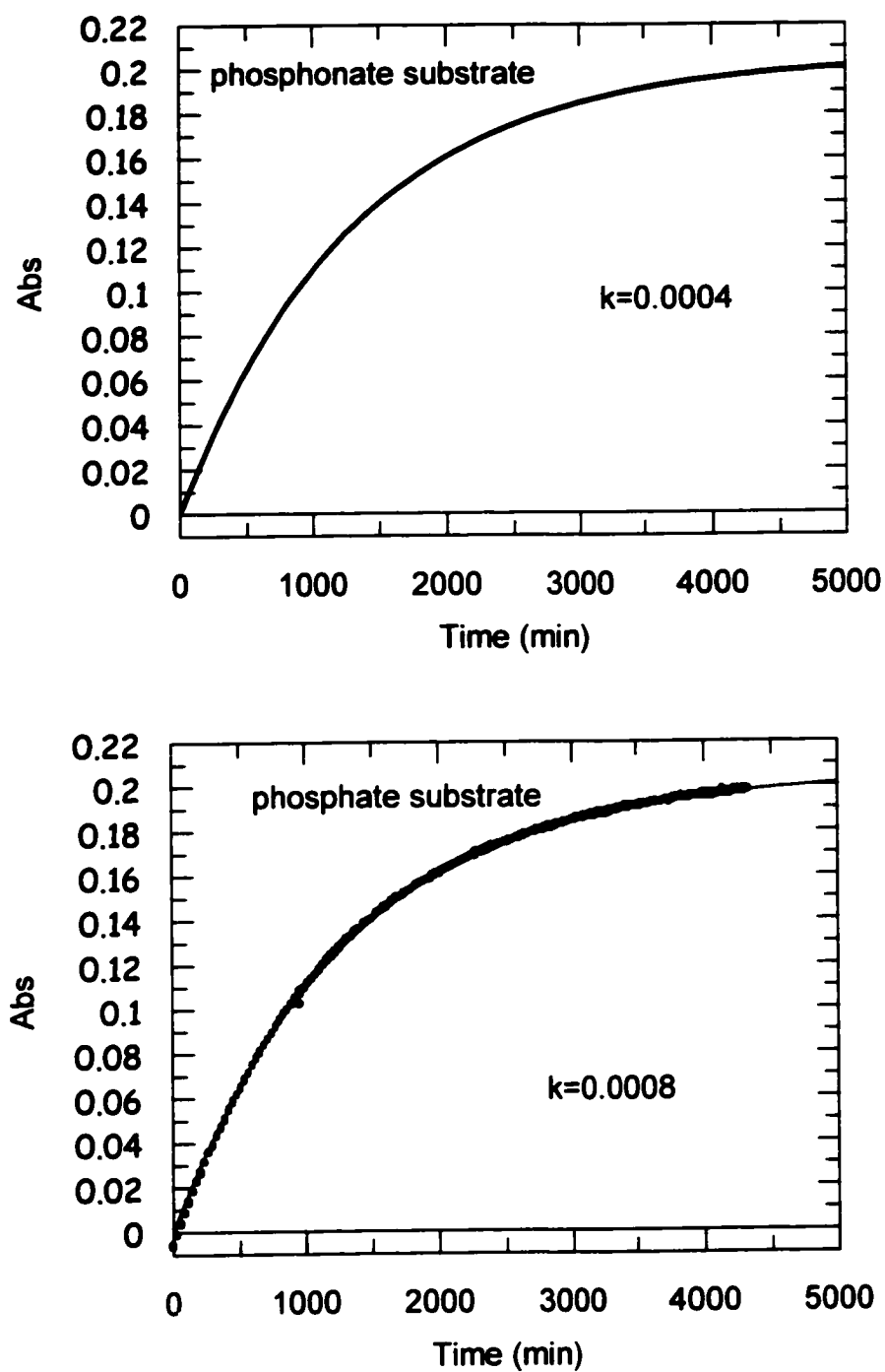


Figure 4.18. Plot of absorbance as a function of time for hydrolysis of 4.27 and 4.28.

4.3.7 Antibody Production and Catalytic Screening

Monoclonal antibodies were raised against the haptens **4.25** and **4.26** using hybridoma technology, by Krista Wooller, an M.Sc. student in the laboratory of Prof. Jeremy Lee of the Department of Biochemistry at the University of Saskatchewan. A total of seven hybridoma cell lines which produced antibodies capable of binding the TSA's were obtained. Only one of the seven cell lines was capable of distinguishing between the *cis* and *trans* haptens with a preference for the *trans* **4.25**. This antibody, Jel 541, was originally raised against the *cis* hapten **4.26** and was found to be an IgM class antibody. Thus, it appears that isomerization of the *cis* hapten to the *trans* hapten occurred during the immunization process. SRIA experiments, performed by Krista Wooller, revealed that Jel 541 binds the *trans* TSA **4.25** approximately 100 times tighter than the *cis* isomer **4.26**.

All seven antibodies were screened for catalytic activity using substrates **4.27** and **4.28**, by Krista Wooller. At a concentration of approximately 0.50 μM of antibody and 500 μM of substrate in 10 mM Hepes buffer at pH 7, only Jel 541 was found to catalyze the hydrolysis of the phosphonate substrate **4.28** as indicated by an increase in absorbance at 400 nm (Figure 4.19). Jel 541 also catalyzed the hydrolysis of the phosphate substrate **4.27** to a lesser extent (data not shown) and was capable of functioning at pH 9.0 (Figure 4.20). The preference for the phosphonate substrate **4.28** can be attributed to closer resemblance of **4.28** to the TSA's used to generate the antibodies.

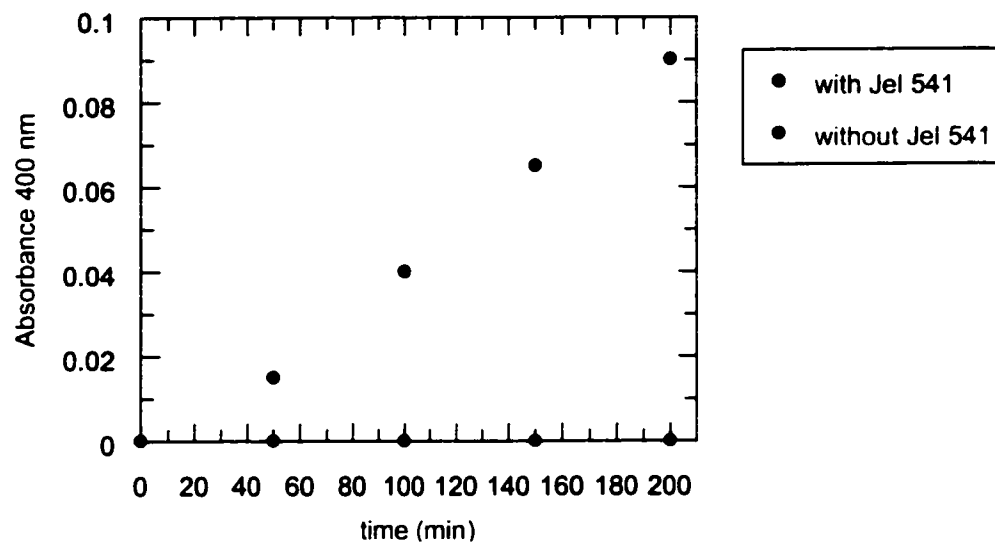


Figure 4.19. Hydrolysis of phosphonate substrate **4.28** (500 μ M) in the presence and absence of Jel 541 (500 nM) in 10 mM HEPES buffer, pH 7.0.

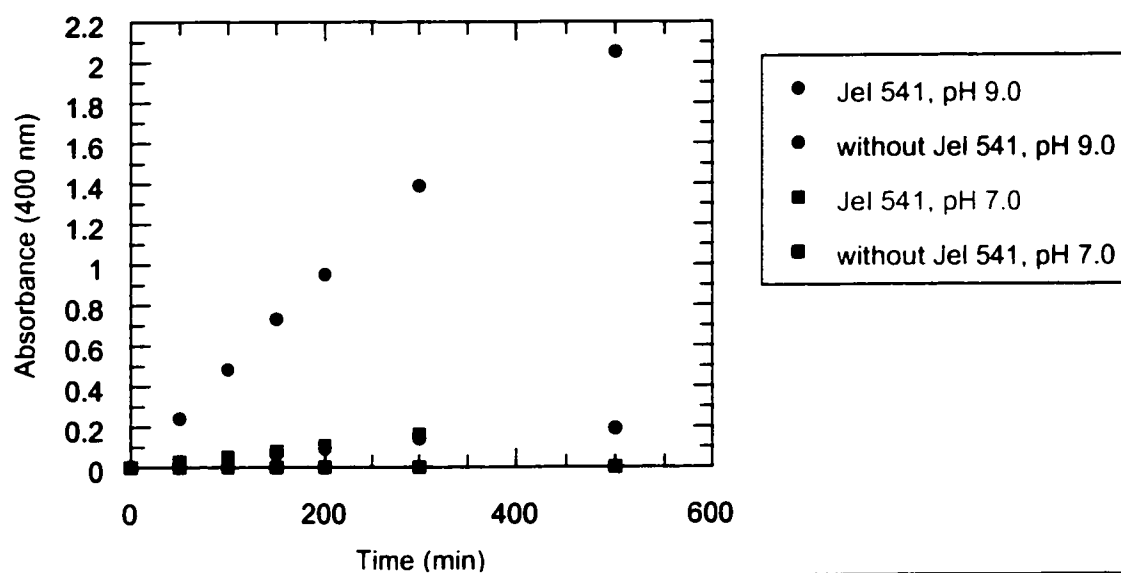


Figure 4.20. Hydrolysis of phosphonate substrate **4.28** (500 μ M) in the presence and absence of Jel 541 (500 nM) in 10 mM HEPES buffer, pH 7.0 and 10 mM CHES buffer, pH 9.0.

The likelihood that the observed activity was due to Jel 541 and not a contaminant can be ruled out on the basis of three observations: (1) Jel 541 catalyzes the hydrolysis of the more stable phosphonate substrate **4.28** faster

than the phosphate substrate **4.27**, (2) all seven antibodies were purified in the same manner and only Jel 541 exhibited catalytic activity, and (3) the activity of Jel 541 was inhibited by the presence of the *trans* TSA **4.25**.

Unfortunately, we were unable to obtain accurate kinetic data with Jel 541. It was found that this antibody was rather unstable and had a tendency to precipitate out of solution during the time course of the reaction. This is not unusual for IgM class antibodies which have very high molecular weights (about 10^3 kDa, ten binding sites) and often exhibit low solubility. Attempts in the Lee lab to convert the Jel 541 Mab to smaller, more manageable Fab fragments were unsuccessful. It is clear that an IgG class antibody will be necessary to fully evaluate this approach to abzyme-catalyzed phosphate ester hydrolysis.

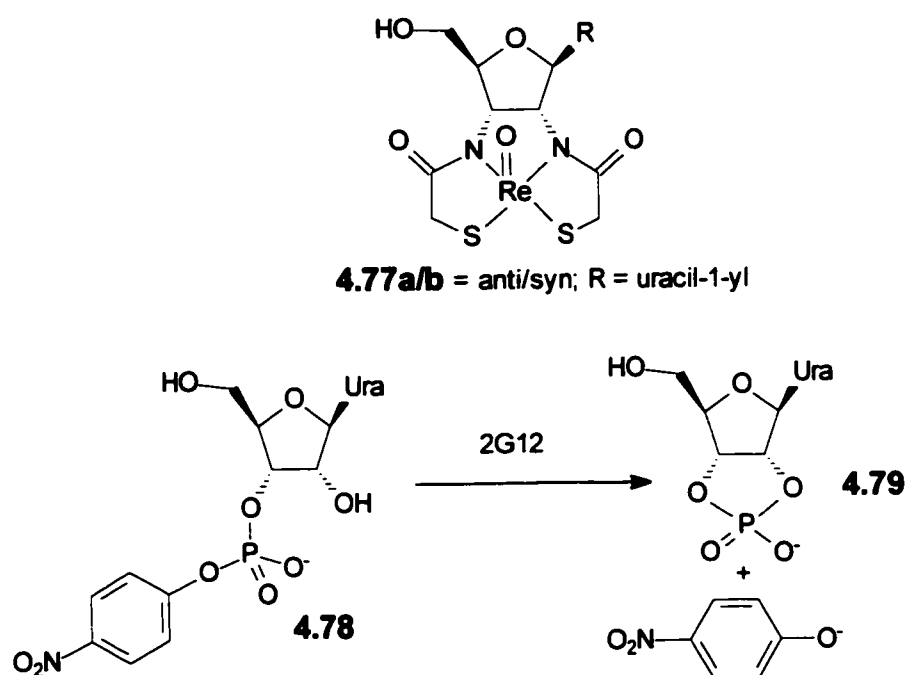
4.4 Summary

A series of novel phospholates, for the ultimate purpose of obtaining phosphatase abzymes by employing **4.25** and **4.26** as TSA's, were synthesized. The potential for our TSA design was demonstrated by Jel 541, an IgM class antibody which exhibited the ability to catalyze the hydrolysis of the model substrates **4.27** and **4.28**. This is the first demonstration of antibody-catalyzed hydrolysis of a phosphonate ester. Nevertheless, further studies will be necessary to fully evaluate this approach to obtaining phosphohydrolase abzymes.

4.5 Current State of Phosphatase Abzymes

During the course of our studies, several papers appeared on antibody-catalyzed phosphate ester hydrolysis. Janda *et al.* reported two different

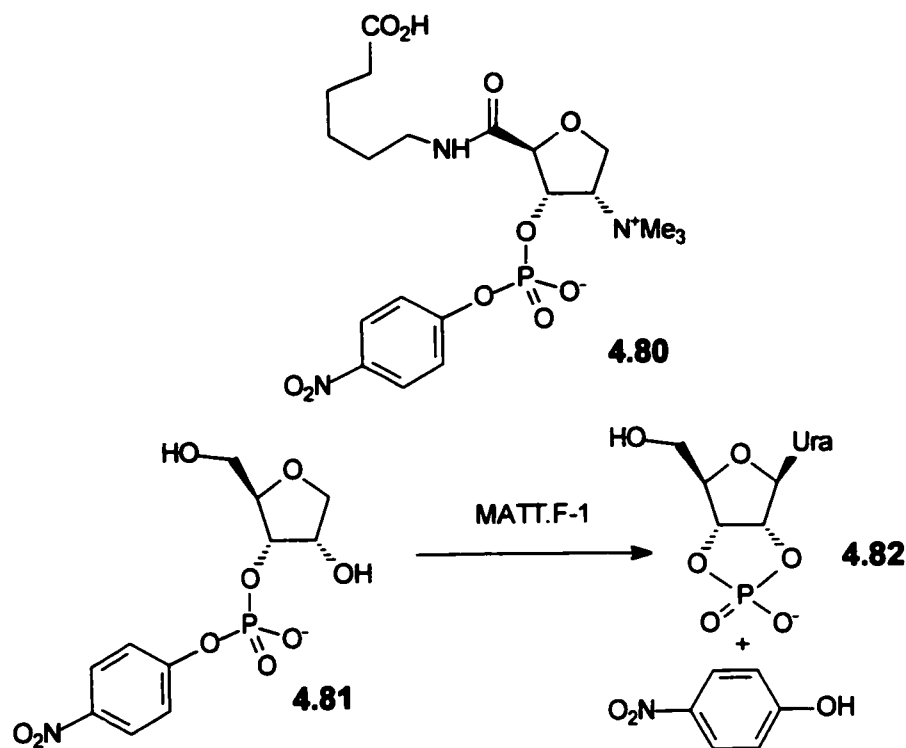
approaches towards hapten design for obtaining phosphodiesterase abzymes. In order to mimic the potentially trigonal bipyramidal (TBP) or distorted TBP/square pyramidal (SP) transition state that is believed to be utilized by RNase A during the hydrolysis of P-O^{5'} bond of RNA, Janda and coworkers employed the pentacoordinate oxorhenium (V) metallochelates **4.77a/b** as haptens (Scheme 4.28).⁴¹ These species are water stable and possess a negatively charged pentacoordinate structure which most likely exists in a distorted TBP/SP geometry.



Scheme 4.28. Phosphodiester hydrolysis by 2G12.

A total of 50 monoclonal antibodies were raised separately against **4.77a** and **4.77b**, of which only 3, originally raised against **4.77a**, were found to be catalytic. Antibody 2G12 was found to be the most active in catalyzing the hydrolysis of uridine-3'-(*p*-nitrophenyl phosphate) **4.78** (Scheme 4.28). A more detailed characterization of the kinetic parameters of 2G12 at pH 6 showed $k_{\text{cat}} =$

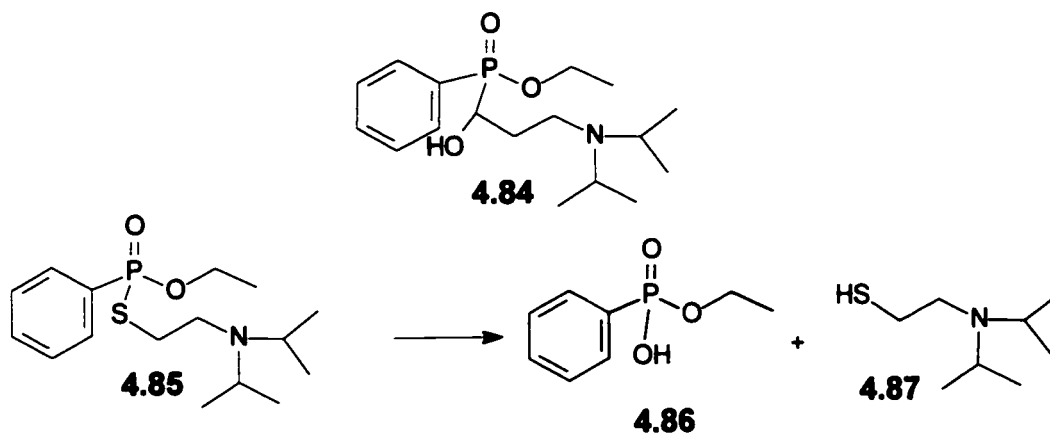
$1.53 \times 10^{-3} \text{ s}^{-1}$, a K_m of $240 \mu\text{M}$, and a K_i of approximately 400 nM for both **4.77a** and **4.77b**. The similar K_i values for the anti/syn isomers suggests that 2G12 recognizes primarily the common Re core. In comparison to the uncatalyzed reaction, 2G12 exhibits a 312 fold rate enhancement. This work is the first example of an abzyme capable of hydrolyzing phosphodiesteres.



Scheme 4.29. Phosphodiester hydrolysis by MATT.F-1.

Further work from Janda's lab provided a more efficient phosphatase abzyme.⁴² Compound **4.80** was used as a haptent in a 'bait and switch' approach towards raising antibodies to catalyze the hydrolysis of the activated phosphodiester substrate **4.81**. In the 'bait and switch' strategy, the positive charge on the haptent is meant to elicit a complementary charged residue in the antibody combining site. The complementary charge may assist in a catalytic fashion when the haptent is 'switched' to the substrate. The positive charge on

levels of AchE activity was correlated with more effective hydrolysis of VX by the polyclonal antibodies, since only VX, and not its hydrolysis products, inhibits AchE. Mice that were immunized with **4.83** produced sera that appeared to degrade VX as indicated by higher levels of AchE activity relative to non-immunized mice. The sera from immunized mice showed 8-12% more AchE activity which was decreased by the presence of 50 μM **4.83** and completely diminished when the concentration of **4.83** was increased to 150 μM . Due to the small volumes of sera collected from the immunized mice, purification of the polyclonal antibodies was not possible therefore making it impossible to characterize the protective effect in any greater detail.



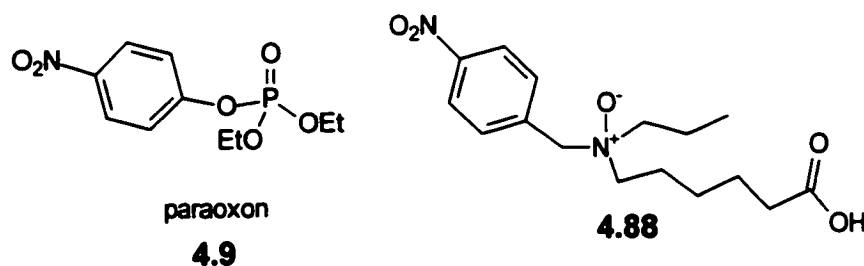
Scheme 4.30. Hydrolysis of VX analog **4.85** by PAR 15.

To avoid working with the extremely toxic VX material, Vayron *et al.* raised antibodies against **4.84** for the purposes of catalyzing the hydrolysis of **4.85**, a less toxic analogue of VX (Scheme 4.30). A total of 13 monoclonal antibodies capable of binding **4.84** were raised of which only one, PAR 15 displayed catalytic activity. Due to the poor solubility of **4.85**, it was impossible to perform saturation kinetics therefore precluding the determination of the kinetic

parameters of PAR 15 (k_{cat} , K_m). Vayron and coworkers do report that PAR 15 is capable of multiple turnovers and exhibits a linear Lineweaver-Burke plot which permitted the evaluation of k_{cat}/K_m as $0.36 \text{ M}^{-1} \cdot \text{min}^{-1}$.

Though the initial results lack detail, the initial work by Vayron *et al.* demonstrate the potential application of catalytic antibodies for the *in vivo* detoxification of organophosphorous toxins. In order to continue towards an actual animal or clinical trial, a new hapten design strategy is required that would increase both the affinity for the substrates and the catalytic activity.

In an effort to obtain antibodies with augmented catalytic activity for paraoxon hydrolysis, Janda *et al.*⁴⁵ employed a novel amine-oxide hapten **4.88** which possessed greater flexibility than its predecessor (antibody 3H5, see section 4.1.4).¹⁸ Once again, the principle of hapten-charge complementarity was employed. The more flexible hapten was meant to allow for a greater range of binding and recognition modes.



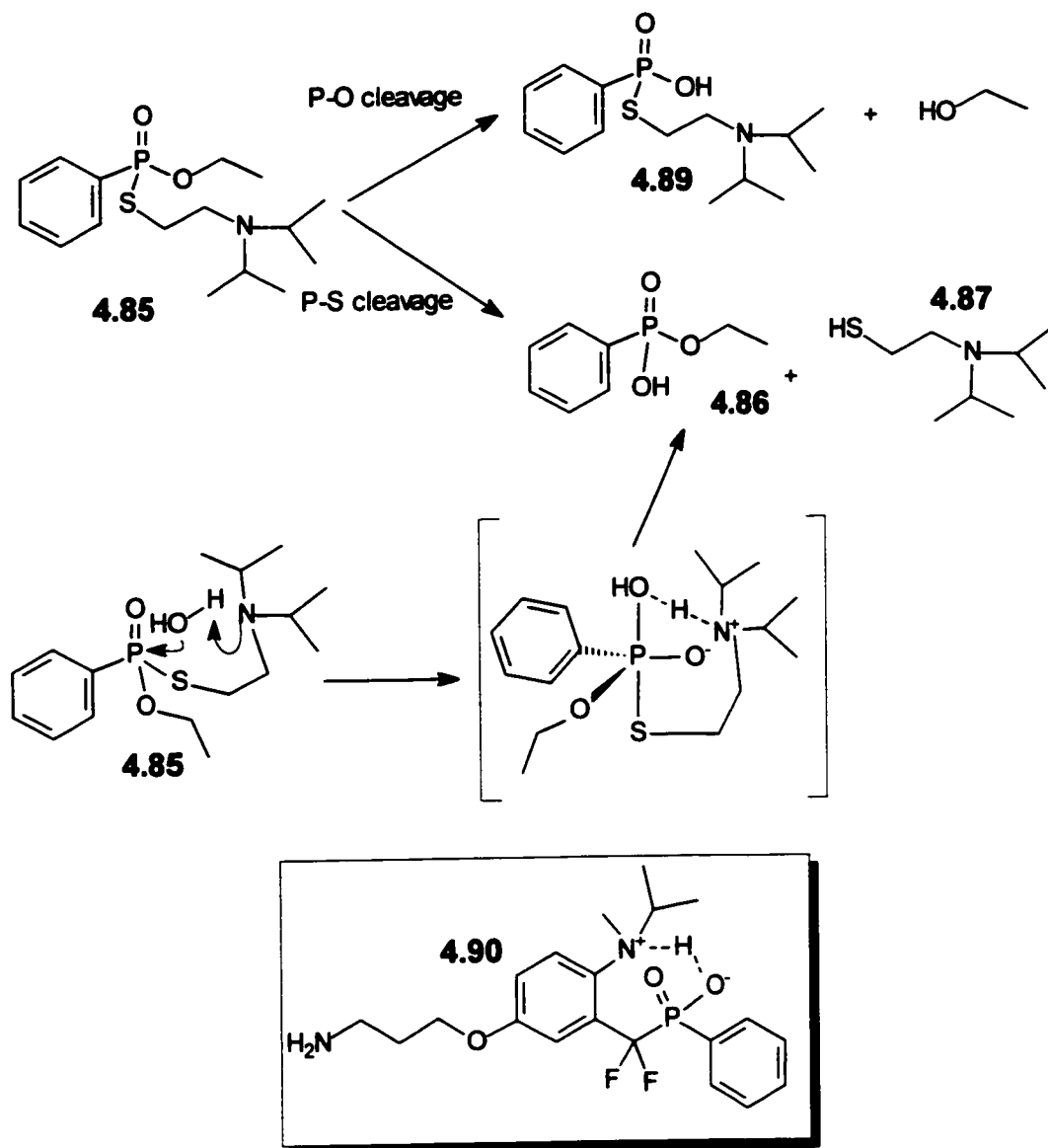
A total of 20 monoclonal antibodies were found to bind to **4.88**, of which 7 displayed catalytic activity. The most active, 1H9, was characterized in greater detail and found to have a k_{cat} of $3.73 \times 10^{-4} \text{ min}^{-1}$ and a K_m of 1.12 mM at an optimal pH of 8.77. The rate acceleration ($k_{\text{cat}}/k_{\text{uncat}}$) was 56 which represented a significant decrease from antibodies raised against the more constrained hapten

(see Section 4.1.4). Though the constrained hapten **4.22** elicited fewer catalysts (1 out of 25 versus 7 out of 20), the abzymes raised against the flexible hapten were far less catalytically active. Janda suggests that additional catalytic impetus might be provided by the way of ground state destabilization in the case of the abzyme raised against the more constrained TSA **4.22**.

Once again targeting VX analog **4.85** as a substrate, Vayron *et al.* synthesized a second hapten **4.90**, which included an α,α -difluorophosphate moiety.⁴⁶ This second generation TSA was designed to have the antibody favour hydrolysis of the P-S bond since cleavage of the P-O bond results in the toxic byproduct **4.89**, whereas the cleavage of the P-S bond produces a harmless product **4.86** (Scheme 4.31).

In order to favour P-S versus P-O bond cleavage, hapten **4.90** is supposed to mimic the pathway in which the amino functionality acts as a base to activate a water molecule towards nucleophilic attack upon the P atom. The S atom would occupy the apical position of the TBP TS therefore acting as the leaving group to result in P-S bond cleavage (Scheme 4.31). There are several structural features which Vayron makes special mention of. The incorporation of the charged N atom is meant to force folding of the S alkyl side chain in order for the substrate to attain a reactive form. In addition, the charged N atom may elicit complementary charges in the antibody binding site which can stabilize charges in the transition state therefore utilizing a 'bait and switch' strategy. The α,α -difluorophosphate functionality is used to mimic the P-S bond due to its successful implementation in inhibitors of PTPases in place of P-O bonds. To

date, Vayron *et al.* have yet to report any catalysts arising from immunization with **4.90**.



Scheme 4.31. P-O versus P-S hydrolysis of **4.85**.

4.6 Future Work

Antibody Jel 541 demonstrates that our hapten design can elicit phosphatase abzymes. Much more insight would be gained by obtaining an IgG counterpart to Jel 541. Recent work in Prof. Jeremy Lee's labs has involved a

second trial at immunizing mice with the *trans* hapten **4.25** in an effort to raise an IgG antibody capable of hydrolyzing substrates **4.27** and **4.28**. This work is currently at the stage of raising the hybridoma cell lines. Any catalysts resulting from the second immunization trial will be sent to the Taylor lab for detailed characterization of its kinetic parameters.

4.7 References

- 1 Tramantano, A.; Janda, K. D.; Lerner, R.A. *Science* **1986**, *234*, 1566-1570.
- 2 Pollack, S.J.; Jacobs, J.W.; Schultz, P.G. *Science* **1986**, *234*, 1570-1573.
- 3 Coordinates were downloaded from the Brookhaven Protein Data Bank,
Access code 1gt. Authours: Harris, L.J.; Larson, S.B.; Hasel, K. W.;
McPherson, A.
- 4 Schultz, P. G.; Lerner, R. A.; Benkovic, S. J.; *Chem. & Eng. News* **1990**, 24-40.
- 5 Janeway, Jr., C. A. *Sci. Am.* **1993**, *269*, 73-79.
- 6 Köhler, G.; Milstein, C. *Nature* **1975**, *256*, 495-497.
- 7 Griffiths, A. D.; Williams, S. C.; Hartley, O.; Tomlinson, I. M.; Waterhouse, O.;
Crosby, W. L.; Kontermann, R. E.; Jones, P. T.; Low, N. M.; Allison, T. J.;
Prospero, T. D.; Hoogenboom, H. R.; Nissim, A.; Cox, J. P. L.; Harrison, J. L.;
Zaccolo, M.; Gherardi, E.; Winter, G. *EMBO J.* **1994**, *13*, 3245.
- 8 Pauling, L. *Am. Sci.* **1948**, *36*, 519.
- 9 Jencks, W.P. "*Catalysis in Chemistry and Enzymology*" McGraw-Hill, New
York, **1969**.
- 10 Fersht, A. "Enzyme Strucure and Mechanism" W. H. Freeman and Co., New
York, **1985**, 319-322.
- 11 Raso, V.; Stollar, B. D. *Biochemistry* **1975**, *14*, 584.
- 12 Raso, V.; Stollar, B. D. *Biochemistry* **1975**, *14*, 590.
- 13 Blackburn, G. M.; Datta, A.; Denham, H.; Wentworth, P. *Adv. Phys. Org.*
Chem. **1998**, *31*, 249-392.
- 14 Thomas, N. R. *Nat. Prod. Rep.* **1996**, *13*, 479.

-
- 15 Stevenson, J. D.; Thomas, N. R. *Nat. Prod. Rep.* **2000**, *17*, 535.
- 16 Scanlan, T. S.; Prudent, J. R.; Schultz, P. G. *J. Am. Chem. Soc.* **1991**, *113*, 9397-9398.
- 17 Rosenblum, J. S.; Lo, L-C.; Li, T.; Janda, K. D.; Lerner, R. A. *Angew. Chem. Int. Ed. Engl.* **1995**, 2275-2277.
- 18 Lavey, B. J.; Janda, K. D. *J. Org. Chem.* **1996**, *61*, 7633-7636.
- 19 Lavey, B. J.; Janda, K. D. *Bioorg. Med. Chem. Lett.* **1996**, *6*, 1523-1524.
- 20 Thatcher, G. R. J.; Kluger, R. H. *Adv. Phys. Org. Chem.* **1989**, *25*, 99-265.
- 21 Westheimer, F. H. *Acc. Chem. Res.* **1968**, *1*, 70-78.
- 22 Kluger, R. H.; Taylor, S. D. *J. Am. Chem. Soc.* **1990**, *112*, 6669-6671.
- 23 Taylor, S. D.; Kluger, R. H. *J. Am. Chem. Soc.* **1992**, *114*, 3067-3071.
- 24 Chiu, Y. H.; Lipscomb, W. N. *J. Am. Chem. Soc.* **1969**, *91*, 4150.
- 25 Chang, N-y.; Lim, C. *J. Am. Chem. Soc.* **1998**, *120*, 2156.
- 26 Alver, E.; Kjøge, H. M. *Acta. Chim.Scand.* **1969**, *23*, 1101.
- 27 Prezdho, V. V.; Prezdho, O. V.; Vaschenko, E. V. *J. Mol. Struct.* **1996**, *385*, 137.
- 28 S. D. Taylor, unpublished results.
- 29 Modritzer, K. *Synth. React. Inorg. Met-Org. Chem.* **1975**, *5*, 45.
- 30 L. D. Quin. "The Heterocyclic Chemistry of Phosphorus" Chapter 2; Wiley, New York, **1981**.
- 31 Quin, L.D.; Barket, T. P. *Chem. Commun.*, **1967**, 914.
- 32 Razumova, N. A.; Evtikhov, Z. L.; Petrov, A. A. *J. Gen. Chem. USSR* **1969**, *39*, 1388.

-
- 33 Razumova, N.A.; Bagrov, F.V.; Petrov, A. A. *J. Gen. Chem. USSR* **1969**, *39*, 2305.
- 34 Cadogan, J. I. G. *Quart. Rev., Chem. Soc.*, **1962**, *16*, 208.
- 35 Cadogan, J. I. G. *Acc. Chem. Res.* **1972**, *5*, 303.
- 36 Olah, G.A.; Malhotra, R.; Narang, S.C. "Nitration Methods and Mechanisms" VCH Publishers, New York, **1989**.
- 37 Larock, R. C.; Leach, D. R. *J. Org. Chem.* **1984**, *49*, 2144-2147.
- 38 Campbell, D. A.; Bermak, J. C. *J. Org. Chem.* **1994**, *59* 658.
- 39 Habeeb, A. F. S. A. *Anal. Biochem.* **1966**, *14*, 328.
- 40 Grafit 3.03 **1994** from Erithacus Software Ltd and Microsoft.
- 41 Weiner, D. P.; Wiemann, T.; Wolfe, M. M.; Wentworth Jr, P.; Janda, K. D. *J. Am. Chem. Soc.* **1997**, *119*, 4088-4089.
- 42 Wenworth Jr., P.; Liu, Y.; Wentworth, A. D.; Fan, P.; Foley, M. J.; Janda, K. D. *Proc. Natl. Acad. Sci. USA* **1998**, *95*, 5971-5975.
- 43 Renard, P-Y.; Vayron, P.; Taran, F.; Mioskowski, C.; *Tetrahedron Lett.* **1999**, *40*, 281-284.
- 44 Vayron P.; Renard P. Y.; Taran F.; Creminon C.; Frobert Y.; Grassi J.; Mioskowski C. *Proc. Natl. Acad. Sci. USA.* **2000**, *97*, 7058-63.
- 45 Spivak, D. A.; Hoffman, T. Z.; Moore, A. H.; Taylor, M. J.; Janda, K. D. *Bioorg. Med. Chem. Lett.* **1999**, *7*, 1145-1150.
- 46 Vayron, P.; Renard, P-Y.; Valleix, A.; Mioskowski, C. *Chem. Eur. J.* **2000**, *6*, 1050-1063.

Appendix

A.1 Supplementary Crystallographic Data for 4.26	A.iii
Crystal data and structure refinement for 4.26.	A.iii
Atomic coordinates and equivalent isotropic displacement parameters for 4.26.	A.iv
Bond lengths and angles for 4.26.	A.v
Anisotropic displacement parameters for 4.26.	A.vi
Hydrogen coordinates and isotropic displacement parameters for 4.26.	A.vii
A.2 Supplementary Crystallographic Data for 4.44	A.viii
Crystal data and structure refinement for 4.44.	A.viii
Atomic coordinates and equivalent isotropic displacement parameters for 4.44.	A.ix
Bond lengths and angles for 4.44.	A.x
Anisotropic displacement parameters for 4.44.	A.xi
Hydrogen coordinates and isotropic displacement parameters for 4.44.	A.xii
A.3 Supplementary Crystallographic Data for 4.47	A.xiii
Crystal data and structure refinement for 4.47.	A.xiii
Atomic coordinates and equivalent isotropic displacement parameters for 4.47.	A.xiv

	A.ii
Bond lengths and angles for 4.47.	A.xv
Anisotropic displacement parameters for 4.47.	A.xvi
Hydrogen coordinates and isotropic displacement parameters for 4.47.	A.xvii
A.4 Supplementary Crystallographic Data for 4.46	A.xviii
Crystal data and structure refinement for 4.46.	A.xviii
Atomic coordinates and equivalent isotropic displacement parameters for 4.46.	A.xix
Bond lengths and angles for 4.46.	A.xx
Anisotropic displacement parameters for 4.46.	A.xxi
Hydrogen coordinates and isotropic displacement parameters for 4.46.	A.xxii

A.1 Supplementary Crystallographic Data for 4.26

Crystal data and structure refinement for (meso)-trans-6-[[cis-2,5-di(4-nitrophenyl)-1-oxo-1 λ^5 -phospholan-1-yl]oxy]hexanoic acid (4.26).

Identification code	k9856a
Empirical formula	C ₂₂ H ₂₅ N ₂ O ₈ P
Formula weight	476.41
Temperature	150(2) K
Wavelength	0.71073 Å
Crystal system	Monoclinic
Space group	P2 ₁ /c
Unit cell dimensions	$a = 12.0218(5)$ Å $\alpha = 90^\circ$ $b = 20.7060(5)$ Å $\beta = 95.0730(10)^\circ$ $c = 8.8267(6)$ Å $\gamma = 90^\circ$
Volume, Z	2188.6 (2) Å ³ , 4
Density (calculated)	1.446 Mg/m ³
Absorption coefficient	0.179 mm ⁻¹
F(000)	1000
Crystal size	0.21 x 0.06 x 0.04 mm
θ range for data collection	4.21 to 26.38°
Limiting indices	$-15 \leq h \leq 14$, $-25 \leq k \leq 0$, $0 \leq l \leq 11$
Reflections collected	16453
Independent reflections	4423 ($R_{\text{int}} = 0.092$)
Absorption correction	Scalepack
Refinement method	Full-matrix least-squares on F ²
Data / restraints / parameters	4423 / 0 / 303
Goodness-of-fit on F ²	1.004
Final R indices [$I > 2\sigma(I)$]	R1 = 0.0484, wR2 = 0.1045
R indices (all data)	R1 = 0.0939, wR2 = 0.1207
Extinction coefficient	0.0027(8)
Largest diff. peak and hole	0.412 and -0.262 eÅ ⁻³

Atomic coordinates [$\times 10^4$] and equivalent isotropic displacement parameters [$\text{\AA}^2 \times 10^3$] for (meso)-trans-6-[[cis-2,5-di(4-nitrophenyl)-1-oxo-1 λ^5 -phospholan-1-yl]oxy]hexanoic acid (4.26). U(eq) is defined as one third of the trace of the orthogonalized U_{ij} tensor.

	x	y	z	U(eq)
P(1)	7181(1)	477(1)	2729(1)	24(1)
O(1)	6973(2)	875(1)	4070(2)	29(1)
N(1)	9214(2)	3453(1)	3195(3)	35(1)
C(1)	8123(2)	840(1)	1444(3)	26(1)
O(2)	6105(1)	295(1)	1668(2)	29(1)
N(2)	7672(2)	-1585(1)	8812(3)	31(1)
O(3)	10098(2)	3566(1)	3945(3)	50(1)
C(3)	9121(2)	365(1)	1480(3)	27(1)
O(4)	8524(2)	3877(1)	2823(2)	45(1)
C(4)	9192(2)	-19(1)	2975(3)	27(1)
O(5)	7814(2)	-2172(1)	8829(2)	43(1)
C(5)	8063(2)	-254(1)	3170(3)	24(1)
C(5)	5012(2)	198(1)	2250(4)	39(1)
O(6)	7503(2)	-1267(1)	9938(2)	40(1)
C(6)	4896(3)	-466(1)	2872(4)	41(1)
O(7)	3942(2)	-2959(1)	848(2)	40(1)
C(7)	5163(2)	-1010(1)	1850(3)	34(1)
O(8)	5242(2)	-3246(1)	2657(2)	45(1)
C(8)	4858(3)	-1676(1)	2348(4)	39(1)
C(9)	5368(2)	-2207(1)	1472(3)	35(1)
C(10)	4866(2)	-2856(1)	1739(3)	29(1)
C(11)	8435(2)	1530(1)	1919(3)	25(1)
C(12)	7803(2)	2039(1)	1279(3)	30(1)
C(13)	8056(2)	2672(1)	1690(3)	30(1)
C(14)	8952(2)	2785(1)	2742(3)	28(1)
C(15)	9599(2)	2292(1)	3389(3)	31(1)
C(16)	9328(2)	1668(1)	2978(3)	31(1)
C(21)	7873(2)	-594(1)	4655(3)	24(1)
C(22)	7911(2)	-255(1)	6031(3)	27(1)
C(23)	7833(2)	-577(1)	7381(3)	26(1)
C(24)	7732(2)	-1242(1)	7364(3)	24(1)
C(25)	7701(2)	-1591(1)	6031(3)	27(1)
C(26)	7763(2)	-1263(1)	4682(3)	28(1)

Bond lengths [Å] and angles [°] for (meso)-trans-6-[[cis-2,5-di(4-nitrophenyl)-1-oxo-1λ⁵-phospholan-1-yl]oxy]hexanoic acid (4.26).

P(1)-O(1)	1.482(2)	P(1)-O(2)	1.574(2)
P(1)-C(5)	1.830(2)	P(1)-C(1)	1.834(3)
N(1)-O(3)	1.224(3)	N(1)-O(4)	1.231(3)
N(1)-C(14)	1.466(3)	C(1)-C(11)	1.526(3)
C(1)-C(3)	1.549(3)	O(2)-C(5)	1.468(3)
N(2)-O(6)	1.223(3)	N(2)-O(5)	1.228(3)
N(2)-C(24)	1.469(3)	C(3)-C(4)	1.536(3)
C(4)-C(5)	1.534(4)	C(5)-C(21)	1.508(3)
C(5)-C(6)	1.490(4)	C(6)-C(7)	1.497(4)
O(7)-C(10)	1.320(3)	C(7)-C(8)	1.503(3)
O(8)-C(10)	1.203(3)	C(8)-C(9)	1.504(4)
C(9)-C(10)	1.501(3)	C(11)-C(12)	1.389(3)
C(11)-C(16)	1.390(4)	C(12)-C(13)	1.388(3)
C(13)-C(14)	1.378(4)	C(14)-C(15)	1.377(4)
C(15)-C(16)	1.374(3)	C(21)-C(26)	1.393(3)
C(21)-C(22)	1.400(3)	C(22)-C(23)	1.377(4)
C(23)-C(24)	1.383(3)	C(24)-C(25)	1.378(4)
C(25)-C(26)	1.378(3)		
O(1)-P(1)-O(2)	114.89(10)	O(1)-P(1)-C(5)	114.58(11)
O(2)-P(1)-C(5)	109.22(10)	O(1)-P(1)-C(1)	115.01(11)
O(2)-P(1)-C(1)	104.47(11)	C(5)-P(1)-C(1)	96.83(11)
O(3)-N(1)-O(4)	122.8(2)	O(3)-N(1)-C(14)	118.8(2)
O(4)-N(1)-C(14)	118.4(2)	C(11)-C(1)-C(3)	114.7(2)
C(11)-C(1)-P(1)	111.4(2)	C(3)-C(1)-P(1)	104.3(2)
C(5)-O(2)-P(1)	122.6(2)	O(6)-N(2)-O(5)	123.8(2)
O(6)-N(2)-C(24)	118.2(2)	O(5)-N(2)-C(24)	118.1(2)
C(4)-C(3)-C(1)	109.2(2)	C(5)-C(4)-C(3)	106.2(2)
C(21)-C(5)-C(4)	114.5(2)	C(21)-C(5)-P(1)	118.4(2)
C(4)-C(5)-P(1)	101.8(2)	O(2)-C(5)-C(6)	111.8(2)
C(5)-C(6)-C(7)	116.1(3)	C(6)-C(7)-C(8)	116.4(2)
C(7)-C(8)-C(9)	113.5(2)	C(10)-C(9)-C(8)	112.7(2)
O(8)-C(10)-O(7)	122.7(2)	O(8)-C(10)-C(9)	125.0(3)
O(7)-C(10)-C(9)	112.3(2)	C(12)-C(11)-C(16)	118.7(2)
C(12)-C(11)-C(1)	119.1(2)	C(16)-C(11)-C(1)	122.2(2)
C(13)-C(12)-C(11)	120.7(3)	C(14)-C(13)-C(12)	118.5(2)
C(15)-C(14)-C(13)	122.2(2)	C(15)-C(14)-N(1)	119.1(2)
C(13)-C(14)-N(1)	118.7(2)	C(16)-C(15)-C(14)	118.4(3)
C(15)-C(16)-C(11)	121.4(2)	C(26)-C(21)-C(22)	118.7(2)
C(26)-C(21)-C(5)	119.8(2)	C(22)-C(21)-C(5)	121.5(2)
C(23)-C(22)-C(21)	120.6(2)	C(22)-C(23)-C(24)	119.1(2)
C(25)-C(24)-C(23)	121.8(2)	C(25)-C(24)-N(2)	119.3(2)
C(23)-C(24)-N(2)	118.8(2)	C(26)-C(25)-C(24)	118.6(2)
C(25)-C(26)-C(21)	121.2(2)		

Anisotropic displacement parameters [$\text{\AA}^2 \times 10^3$] for (meso)-trans-6-[[cis-2,5-di(4-nitrophenyl)-1-oxo-1 λ^5 -phospholan-1-yl]oxy]hexanoic acid (4.26). The anisotropic displacement factor exponent takes the form: $-2\pi^2 [(ha^*)^2U_{11} + \dots + 2hka^*b^*U_{12}]$.

	U11	U22	U33	U23	U13	U12
P(1)	25(1)	17(1)	29(1)	2(1)	1(1)	1(1)
O(1)	33(1)	22(1)	32(1)	2(1)	4(1)	6(1)
N(1)	44(2)	24(1)	37(2)	2(1)	8(1)	-2(1)
C(1)	27(2)	25(1)	25(1)	2(1)	0(1)	-1(1)
O(2)	25(1)	26(1)	35(1)	3(1)	-1(1)	-2(1)
N(2)	28(1)	35(1)	31(1)	6(1)	1(1)	-2(1)
O(3)	48(1)	34(1)	65(2)	-7(1)	-10(1)	-7(1)
C(3)	26(2)	27(1)	29(2)	-2(1)	4(1)	-1(1)
O(4)	61(2)	23(1)	49(1)	4(1)	0(1)	9(1)
C(4)	27(1)	22(1)	31(2)	0(1)	2(1)	7(1)
O(5)	58(1)	28(1)	43(1)	11(1)	3(1)	-1(1)
C(S)	26(1)	18(1)	28(2)	-2(1)	0(1)	0(1)
C(5)	22(2)	26(1)	68(2)	0(1)	7(2)	1(1)
O(6)	48(1)	45(1)	29(1)	-2(1)	6(1)	0(1)
C(6)	38(2)	28(1)	59(2)	-4(1)	18(2)	-3(1)
O(7)	43(1)	31(1)	43(1)	9(1)	-11(1)	-9(1)
C(7)	33(2)	24(1)	45(2)	-1(1)	5(1)	-3(1)
O(8)	51(1)	29(1)	51(1)	7(1)	-14(1)	-2(1)
C(8)	44(2)	23(1)	53(2)	-1(1)	16(2)	-4(1)
C(9)	36(2)	22(1)	48(2)	-3(1)	6(1)	-5(1)
C(10)	32(2)	21(1)	35(2)	-3(1)	3(1)	1(1)
C(11)	27(2)	24(1)	25(1)	4(1)	4(1)	-2(1)
C(12)	29(2)	31(1)	29(2)	2(1)	-2(1)	0(1)
C(13)	31(2)	27(1)	33(2)	6(1)	3(1)	4(1)
C(14)	31(2)	20(1)	34(2)	2(1)	8(1)	0(1)
C(15)	28(2)	28(1)	37(2)	1(1)	-4(1)	-2(1)
C(16)	32(2)	23(1)	38(2)	3(1)	-6(1)	2(1)
C(21)	20(1)	23(1)	28(1)	1(1)	-2(1)	2(1)
C(22)	28(2)	20(1)	31(2)	-2(1)	0(1)	0(1)
C(23)	25(1)	28(1)	24(1)	-4(1)	-1(1)	5(1)
C(24)	22(1)	25(1)	26(1)	4(1)	2(1)	-2(1)
C(25)	29(2)	18(1)	33(2)	2(1)	-1(1)	-2(1)
C(26)	33(2)	19(1)	31(2)	-3(1)	2(1)	0(1)

Hydrogen coordinates [$\times 10^4$] and isotropic displacement parameters [$\text{\AA}^2 \times 10^3$] for (meso)-trans-6-[[cis-2,5-di(4-nitrophenyl)-1-oxo-1 λ^5 -phospholan-1-yl]oxy]hexanoic acid (4.26).

	x	y	z	U(eq)
H(1B)	7740(2)	848(1)	392(3)	31
H(3A)	9019(2)	66(1)	605(3)	33
H(3B)	9823(2)	609(1)	1404(3)	33
H(4A)	9706(2)	-390(1)	2924(3)	32
H(4B)	9468(2)	260(1)	3840(3)	32
H(5A)	7800(2)	-571(1)	2337(3)	29
H(5B)	4417(2)	271(1)	1419(4)	46
H(5C)	4913(2)	518(1)	3061(4)	46
H(6A)	4118(3)	-521(1)	3136(4)	49
H(6B)	5390(3)	-501(1)	3827(4)	49
H(7A)	5975(2)	-1002(1)	1740(3)	40
H(7B)	4774(2)	-930(1)	831(3)	40
H(8A)	4035(3)	-1722(1)	2227(4)	47
H(8B)	5104(3)	-1727(1)	3441(4)	47
H(9A)	5263(2)	-2105(1)	372(3)	42
H(9B)	6180(2)	-2224(1)	1771(3)	42
H(12A)	7190(2)	1952(1)	553(3)	36
H(13A)	7622(2)	3020(1)	1256(3)	36
H(15A)	10219(2)	2381(1)	4102(3)	38
H(16A)	9761(2)	1323(1)	3428(3)	37
H(22A)	7991(2)	202(1)	6032(3)	32
H(23A)	7848(2)	-345(1)	8312(3)	31
H(25A)	7637(2)	-2049(1)	6041(3)	32
H(26A)	7731(2)	-1498(1)	3755(3)	33
H(7O)	3688(35)	-3346(20)	900(46)	89(14)

A.2 Supplementary Crystallographic Data for 4.44

Crystal data and structure refinement for (\pm)-1-hydroxy-trans-2,5-diphenyl-1 λ^5 -phospholan-1-one (**4.44**).

Identification code	s9739
Empirical formula	C ₁₆ H ₁₇ O ₂ P
Formula weight	272.27
Temperature	293(2) K
Wavelength	0.71073 Å
Crystal system	Monoclinic
Space group	C2
Unit cell dimensions	$a = 22.559(2)$ Å $\alpha = 90^\circ$ $b = 5.7077(5)$ Å $\beta = 105.445(2)^\circ$ $c = 11.3422(9)$ Å $\gamma = 90^\circ$
Volume, Z	1407.7(2) Å ³ , 4
Density (calculated)	1.285 mg/m ³
Absorption coefficient	0.190 mm ⁻¹
F(000)	576
Crystal size	0.15 x 0.15 x 0.25 mm
θ range for data collection	1.86 to 28.27°
Limiting indices	$-29 \leq h \leq 24$, $-7 \leq k \leq 6$, $-14 \leq l \leq 15$
Reflections collected	4459
Independent reflections	2778 ($R_{\text{int}} = 0.0445$)
Absorption correction	Semi-empirical
Refinement method	Full-matrix least-squares on F ²
Data / restraints / parameters	2778 / 1 / 192
Goodness-of-fit on F ²	1.032
Final R indices [$I > 2\sigma(I)$]	$R_1 = 0.0605$, $wR_2 = 0.1210$
R indices (all data)	$R_1 = 0.0878$, $wR_2 = 0.1335$
Absolute structure parameter	-0.1(2)
Extinction coefficient	0.0022(11)
Largest diff. peak and hole	0.420 and -0.485 eÅ ⁻³

Atomic coordinates [$\times 10^4$] and equivalent isotropic displacement parameters [$\text{\AA}^2 \times 10^3$] for (\pm)-1-hydroxy-trans-2,5-diphenyl-1 λ^5 -phospholan-1-one (4.44).
 U(eq) is defined as one third of the trace of the orthogonalized U_{ij} tensor.

	x	y	z	U(eq)
P(1)	1809(1)	2296(2)	392(1)	22(1)
O(1)	1954(1)	-325(5)	649(3)	29(1)
O(2)	2013(1)	3274(5)	-670(2)	27(1)
C(1)	2519(2)	1179(9)	3435(4)	37(1)
C(2)	3004(2)	340(9)	4373(4)	44(1)
C(3)	3566(2)	1477(9)	4637(4)	48(1)
C(4)	3645(2)	3394(9)	3974(4)	46(1)
C(5)	3158(2)	4265(8)	3043(4)	33(1)
C(6)	2589(2)	3124(7)	2771(3)	26(1)
C(7)	2065(2)	4110(7)	1760(3)	24(1)
C(8)	1461(2)	4692(8)	2103(4)	31(1)
C(9)	949(2)	4851(8)	917(4)	31(1)
C(10)	983(2)	2612(7)	189(3)	23(1)
C(11)	593(2)	2488(8)	-1114(3)	24(1)
C(12)	210(2)	564(7)	-1507(4)	29(1)
C(13)	-169(2)	434(8)	-2681(4)	37(1)
C(14)	-170(2)	2204(10)	-3502(3)	39(1)
C(15)	224(2)	4097(9)	-3146(4)	38(1)
C(16)	606(2)	4234(8)	-1966(4)	32(1)

Bond lengths [Å] and angles [°] for (±)-1-hydroxy-trans-2,5-diphenyl-1λ⁵-phospholan-1-one (4.44).

P(1)-O(2)	1.506(3)	P(1)-O(1)	1.542(3)
P(1)-C(10)	1.824(3)	P(1)-C(7)	1.827(4)
C(1)-C(6)	1.374(6)	C(1)-C(2)	1.392(6)
C(2)-C(3)	1.385(7)	C(3)-C(4)	1.366(7)
C(4)-C(5)	1.397(6)	C(5)-C(6)	1.398(5)
C(6)-C(7)	1.519(5)	C(7)-C(8)	1.550(5)
C(8)-C(9)	1.526(5)	C(9)-C(10)	1.534(6)
C(10)-C(11)	1.506(5)	C(11)-C(16)	1.394(6)
C(11)-C(12)	1.395(6)	C(12)-C(13)	1.380(6)
C(13)-C(14)	1.373(6)	C(14)-C(15)	1.388(7)
C(15)-C(16)	1.388(6)		
O(2)-P(1)-O(1)	114.6(2)	O(2)-P(1)-C(10)	112.5(2)
O(1)-P(1)-C(10)	106.1(2)	O(2)-P(1)-C(7)	111.9(2)
O(1)-P(1)-C(7)	112.7(2)	C(10)-P(1)-C(7)	97.7(2)
C(6)-C(1)-C(2)	121.0(4)	C(3)-C(2)-C(1)	119.5(4)
C(4)-C(3)-C(2)	120.1(4)	C(3)-C(4)-C(5)	120.7(5)
C(4)-C(5)-C(6)	119.5(4)	C(1)-C(6)-C(5)	119.2(4)
C(1)-C(6)-C(5)	122.2(4)	C(5)-C(6)-C(7)	118.5(4)
C(6)-C(7)-C(S)	116.7(3)	C(6)-C(7)-P(1)	116.0(3)
C(S)-C(7)-P(1)	103.5(3)	P(9)-C(8)-C(7)	107.5(3)
C(B)-C(9)-C(10)	106.9(3)	C(11)-C(10)-C(9)	117.8(4)
C(11)-C(10)-P(1)	115.3(2)	C(9)-C(10)-P(1)	102.1(2)
C(16)-C(11)-C(12)	117.8(3)	C(16)-C(11)-C(10)	122.2(4)
C(12)-C(11)-C(10)	120.0(4)	C(13)-C(12)-C(11)	121.6(4)
C(14)-C(13)-C(12)	120.2(4)	C(13)-C(14)-C(15)	119.4(4)
C(16)-C(15)-C(14)	120.6(4)	C(15)-C(16)-C(11)	120.4(4)

Anisotropic displacement parameters [$\text{\AA}^2 \times 10^3$] for (\pm)-1-hydroxy-trans-2,5-diphenyl-1 λ^5 -phospholan-1-one (4.44). The anisotropic displacement factor exponent takes the form: $-2\pi^2 [(ha^*)^2U_{11} + \dots + 2hka^*b^*U_{12}]$.

	U11	U22	U33	U23	U13	U12
P(1)	12(1)	24(1)	32(1)	1(1)	10(1)	0(1)
O(1)	16(1)	31(2)	44(2)	2(1)	15(1)	1(1)
O(2)	17(1)	36(2)	32(1)	1(1)	13(1)	-4(1)
C(1)	35(3)	38(3)	38(2)	7(2)	10(2)	0(2)
C(2)	61(3)	43(3)	32(2)	11(2)	18(2)	9(2)
C(3)	39(3)	66(4)	33(2)	6(2)	-1(2)	15(2)
C(4)	30(3)	66(3)	37(2)	-3(2)	-2(2)	5(2)
C(5)	24(2)	40(3)	36(2)	1(2)	9(2)	-5(2)
C(6)	21(2)	32(2)	26(2)	0(2)	8(2)	0(2)
C(7)	20(2)	22(2)	34(2)	-1(2)	12(2)	-5(2)
C(S)	26(2)	36(3)	36(2)	-9(2)	14(2)	5(2)
C(9)	18(2)	36(3)	40(2)	-1(2)	10(2)	4(2)
C(10)	13(2)	26(2)	34(2)	4(2)	12(1)	2(2)
C(11)	13(2)	30(2)	31(2)	-3(2)	11(1)	6(2)
C(12)	21(2)	33(3)	37(2)	1(2)	14(2)	5(2)
C(13)	28(2)	45(3)	39(2)	-11(2)	12(2)	2(2)
C(14)	25(2)	57(3)	34(2)	-5(3)	4(2)	8(3)
C(15)	31(2)	48(3)	38(2)	8(2)	14(2)	6(2)
C(16)	22(2)	33(2)	43(2)	0(2)	14(2)	0(2)

Hydrogen coordinates [$\times 10^4$] and isotropic displacement parameters [$\text{\AA}^2 \times 10^3$]
for (\pm)-1-hydroxy-trans-2,5-diphenyl-1 λ^5 -phospholan-1-one (4.44).

	x	y	z	U(eq)
H(10)	2285(13)	-636(24)	517(53)	33(18)
H(10')	2121(25)	-509(15)	1379(9)	33(18)
H(1)	2142(2)	411(9)	3254(4)	44(13)
H(2)	2950(2)	-973(9)	4818(4)	51(14)
H(3)	3891(2)	935(9)	5268(4)	50(14)
H(4)	4027(2)	4125(9)	4143(4)	70(17)
H(5)	3212(2)	5594(8)	2608(4)	42(13)
H(7)	2214(2)	5584(7)	1498(3)	35(12)
H(SA)	1369(2)	3475(8)	2625(4)	49(14)
H(SB)	1502(2)	6169(8)	2540(4)	12(9)
H(9A)	1006(2)	6222(8)	453(4)	21(10)
H(9B)	552(2)	4967(8)	1091(4)	56(14)
H(10)	855(2)	1314(7)	631(3)	19(9)
H(12)	211(2)	-659(7)	-966(4)	12(9)
H(13)	-425(2)	-856(8)	-2918(4)	63(16)
H(14)	-431(2)	2136(10)	-4288(3)	45(12)
H(15)	232(2)	5283(9)	-3703(4)	25(11)
H(16)	872(2)	5499(8)	-1742(4)	29(11)

A.3 Supplementary Crystallographic Data for 4.47

Crystal data and structure refinement for (meso)-trans-1-ethoxy-cis-2,5-di(4-nitrophenyl)-1 λ^5 -phospholan-1-one (4.47).

Identification code	k98l0a	
Empirical formula	C ₁₈ H ₁₉ N ₂ O ₆ P	
Formula weight	390.32	
Temperature	293(2) K	
Wavelength	0.71073 Å	
Crystal system	Orthorhombic	
Space group	Pna2 ₁	
Unit cell dimensions	a = 16.7742(3) Å	alpha = 90°
	b = 5.4009(11) Å	beta = 90°
	c = 21.019(2) Å	gamma = 90°
Volume, Z	1904.2(4) Å ³ , 4	
Density (calculated)	1.361 Mg/m ³	
Absorption coefficient	0.181 mm ⁻¹	
F(000)	816	
Crystal size	0.21 x 0.03 x 0.04 mm	
θ range for data collection	2.43 to 26.17°	
Limiting indices	20 ≤ h ≤ 20, -6 ≤ k ≤ 6, -25 ≤ l ≤ 26	
Reflections collected	21719	
Independent reflections	3503 (R _{int} = 0.103)	
Refinement method	Full-matrix least-squares on F ²	
Data / restraints / parameters	3503 / 11 / 211	
Goodness-of-fit on F ²	1.006	
Final R indices [I > 2σ(I)]	R1 = 0.0671, wR2 = 0.1725	
R indices (all data)	R1 = 0.1367, wR2 = 0.2068	
Absolute structure parameter	0.4(3)	
Extinction coefficient	0.015(4)	
Largest diff. peak and hole	0.270 and -0.191 eÅ ⁻³	

Atomic coordinates [$\times 10^4$] and equivalent isotropic displacement parameters [$\text{\AA}^2 \times 10^3$] for (meso)-trans-1-ethoxy-cis-2,5-di(4-nitrophenyl)-1 λ^5 -phospholan-1-one (4.47). U(eq) is defined as one third of the trace of the orthogonalized U_{ij} tensor.

	x	y	z	U(eq)
P(1)	1440(1)	5347(2)	1329(2)	73(1)
N(1)	1242(6)	2931(15)	-1818(4)	127(3)
N(2)	1196(8)	3199(23)	4459(4)	166(5)
O(1)	1217(2)	2724(4)	1332(4)	90(1)
O(2)	2346(2)	5867(5)	1332(4)	101(1)
O(3)	875(6)	989(13)	-1905(3)	173(4)
O(4)	1525(5)	4236(18)	-2228(4)	156(4)
O(5)	872(7)	1199(21)	4572(4)	184(5)
O(6)	1612(7)	4324(18)	4836(4)	184(4)
C(1)	977(5)	7165(13)	1969(4)	74(2)
C(2)	198(6)	7692(14)	1724(3)	90(2)
C(3)	129(4)	7625(18)	1003(4)	103(3)
C(4)	1016(5)	7143(14)	717(4)	80(2)
C(5)	2894(9)	4044(29)	1051(6)	107(5)
C(6)	3190(13)	2721(41)	1623(9)	167(8)
C(5*)	3044(10)	4661(36)	1618(7)	162(9)
C(6*)	3385(1)	2731(3)	1195(2)	114(5)
C(7)	1078(1)	6010(3)	55(2)	88(2)
C(8)	633(1)	3955(3)	-125(2)	96(3)
C(9)	687(1)	3050(3)	-743(2)	117(3)
C(10)	1187(1)	4199(3)	-1180(2)	93(2)
C(11)	1632(1)	6254(3)	-1000(2)	145(4)
C(12)	1577(1)	7159(3)	-382(2)	97(3)
C(13)	1018(1)	6088(3)	2611(2)	77(2)
C(14)	591(1)	3951(3)	2752(2)	105(3)
C(15)	649(1)	2892(3)	3353(2)	108(3)
C(16)	1133(1)	3970(3)	3813(2)	115(3)
C(17)	1559(1)	6107(3)	3672(2)	101(3)
C(18)	1502(1)	7166(3)	3071(2)	100(3)

Bond lengths [Å] and angles [°] for (meso)-trans-1-ethoxy-cis-2,5-di(4-nitrophenyl)-1 λ ⁵-phospholan-1-one (4.47).

P(1)-O(1)	1.465(3)	P(1)-O(2)	1.546(3)
P(1)-C(4)	1.760(9)	P(1)-C(1)	1.837(7)
N(1)-O(4)	1.212(5)	N(1)-O(3)	1.229(5)
N(1)-C(10)	1.508(9)	N(2)-O(6)	1.219(5)
N(2)-O(5)	1.232(5)	N(2)-C(16)	1.424(9)
O(2)-C(5 [*])	1.467(10)	O(2)-C(5)	1.471(9)
C(1)-C(2)	1.433(12)	C(1)-C(13)	1.471(9)
C(2)-C(3)	1.520(8)	C(3)-C(4)	1.626(12)
C(4)-C(7)	1.524(8)	C(5)-C(6)	1.484(12)
C(5 [*])-C(6 [*])	1.484(12)	C(7)-C(12)	1.39
C(7)-C(8)	1.39	C(8)-C(9)	1.39
C(9)-C(10)	1.39	C(10)-C(11)	1.39
C(11)-C(12)	1.39	C(13)-C(14)	1.39
C(13)-C(18)	1.39	C(14)-C(15)	1.39
C(15)-C(16)	1.39	C(16)-C(17)	1.39
C(17)-C(18)	1.39		
O(1)-P(1)-O(2)	115.2(2)	O(1)-P(1)-C(4)	115.7(4)
O(2)-P(1)-C(4)	107.5(4)	O(1)-P(1)-C(1)	113.9(4)
O(2)-P(1)-C(1)	108.3(4)	C(4)-P(1)-C(1)	94.0(2)
O(4)-N(1)-O(3)	125.9(7)	O(4)-N(1)-C(10)	113.1(7)
O(3)-N(1)-C(10)	119.3(7)	O(6)-N(2)-O(5)	124.4(8)
O(6)-N(2)-C(16)	121.1(9)	O(5)-N(2)-C(16)	114.0(9)
C(5 [*])-O(2)-P(1)	134.9(10)	C(5)-O(2)-P(1)	119.4(8)
C(2)-C(1)-C(13)	116.7(6)	C(2)-C(1)-P(1)	103.2(5)
C(13)-C(1)-P(1)	116.2(4)	C(1)-C(2)-C(3)	115.0(8)
C(2)-C(3)-C(4)	107.6(8)	C(7)-C(4)-C(3)	117.7(7)
C(7)-C(4)-P(1)	114.7(5)	C(3)-C(4)-P(1)	100.8(6)
O(2)-C(5)-C(6)	101.9(11)	O(2)-C(5 [*])-C(6 [*])	112.0(9)
C(12)-C(7)-C(8)	120.0	C(12)-C(7)-C(4)	117.8(3)
C(8)-C(7)-C(4)	122.2(3)	C(9)-C(8)-C(7)	120.0
C(10)-C(9)-C(8)	120.0	C(11)-C(10)-C(9)	120.0
C(11)-C(10)-N(1)	124.9(4)	C(9)-C(10)-N(1)	115.0(4)
C(10)-C(11)-C(12)	120.0	C(7)-C(12)-C(11)	120.0
C(14)-C(13)-C(18)	120.0	C(14)-C(13)-C(1)	120.0(3)
C(18)-C(13)-C(1)	119.9(3)	C(15)-C(14)-C(13)	120.0
C(14)-C(15)-C(16)	120.0	C(17)-C(16)-C(15)	120.0
C(17)-C(16)-N(2)	114.1(5)	C(15)-C(16)-N(2)	125.7(5)
C(16)-C(17)-C(18)	120.0	C(17)-C(18)-C(13)	120.0

Anisotropic displacement parameters [$\text{\AA}^2 \times 10^3$] for (meso)-trans-1-ethoxy-cis-2,5-di(4-nitrophenyl)-1 λ^5 -phospholan-1-one (4.47). The anisotropic displacement factor exponent takes the form: $-2\pi^2 [(ha^*)^2U_{11} + \dots + 2hka^*b^*U_{12}]$.

	U11	U22	U33	U23	U13	U12
P(1)	83(1)	50(1)	85(1)	-3(2)	-2(2)	-1(1)
N(1)	125(7)	133(8)	124(8)	-42(6)	-47(6)	31(6)
N(2)	207(12)	204(12)	85(7)	-13(8)	-5(8)	100(10)
O(1)	122(2)	47(1)	100(2)	-11(4)	7(4)	2(1)
O(2)	79(2)	95(2)	130(3)	28(4)	15(4)	10(2)
O(3)	292(11)	103(6)	124(6)	-52(5)	-37(7)	5(6)
O(4)	144(6)	217(11)	107(7)	-30(6)	5(4)	-15(6)
O(5)	216(10)	211(11)	126(7)	34(7)	43(7)	70(9)
O(6)	240(10)	215(11)	98(7)	-9(6)	-22(6)	68(8)
C(1)	80(6)	47(4)	95(6)	-13(4)	4(4)	15(4)
C(2)	131(7)	71(5)	67(5)	0(4)	18(4)	S(S)
C(3)	74(5)	101(6)	134(7)	3(5)	12(4)	20(4)
C(4)	102(7)	56(4)	83(5)	-16(4)	13(4)	-19(4)
C(7)	106(7)	62(5)	96(6)	10(4)	-1(5)	1(4)
C(S)	140(8)	85(6)	62(4)	3(4)	-9(4)	-12(5)
C(9)	112(7)	121(8)	117(7)	-26(5)	-33(5)	8(6)
C(10)	78(5)	103(6)	99(6)	-12(5)	-21(5)	19(5)
C(11)	120(8)	108(8)	207(12)	42(9)	-1(8)	24(6)
C(12)	94(5)	71(5)	127(7)	-14(5)	27(5)	19(4)
C(13)	83(5)	57(5)	92(6)	7(4)	17(4)	21(4)
C(14)	135(8)	49(5)	131(7)	10(4)	16(6)	5(5)
C(15)	167(9)	58(4)	100(6)	-7(4)	22(6)	20(5)
C(16)	167(10)	103(7)	77(6)	-10(5)	3(6)	60(6)
C(17)	104(6)	121(8)	77(5)	14(5)	-17(4)	7(5)
C(18)	102(6)	117(8)	81(5)	-7(5)	13(4)	-6(5)

Hydrogen coordinates [$\times 10^4$] for (meso)-trans-1-ethoxy-cis-2,5-di(4-nitrophenyl)- $1\lambda^5$ -phospholan-1-one (4.47).

	x	y	z	U(eq)
H(1A)	1263	8745	1987	89
H(2A)	39	9321	1871	108
H(2B)	-174	6503	1901	108
H(3A)	-81	9185	847	124
H(3B)	-229	6308	874	124
H(4A)	1295	8736	709	97
H(5A)	3326	4848	8241	128
H(5B)	2617	2930	7641	128
H(6A)	3677	3474	1765	250
H(6B)	3287	1017	1519	250
H(6C)	2798	2817	1955	250
H(5*1)	2890	3912	2019	194
H(5*2)	3448	5900	1705	194
H(6*1)	3027	1347	1174	170
H(6*2)	3889	2194	1362	170
H(6*3)	3460	3402	777	170
H(8A)	299	3186	168	115
H(9A)	390	1675	-863	140
H(11A)	1966	7023	-1293	174
H(12A)	1875	8534	-262	117
H(14A)	267	3229	2445	126
H(15A)	363	1462	3448	130
H(17A)	1883	6829	3980	121
H(18A)	1787	8596	2977	120

A.4 Supplementary Crystallographic Data for 4.46

Crystal data and structure refinement for (\pm)-1-ethoxy-trans-2,5-di(4-nitrophenyl)-
1 λ^5 -phospholan-1-one (4.46).

Identification code	k9840a
Empirical formula	C ₁₈ H ₁₉ N ₂ O ₆ P
Formula weight	390.32
Temperature	293(2) K
Wavelength	0.71073 Å
Crystal system	Monoclinic
Space group	P2 ₁ /c
Unit cell dimensions	a = 21.304(4) Å alpha = 90° b = 10.849(4) Å beta = 100.44(1)° c = 8.298(2) Å gamma = 90°
Volume, Z	1886.1(7) Å ³ , 4
Density (calculated)	1.375 Mg/m ³
Absorption coefficient	0.183 mm
F(000)	816
Crystal size	0.11 x 0.12 x 0.25 mm
θ range for data collection	1.94 to 20.89°
Limiting indices	-21 $\leq h \leq$ 20, -10 $\leq k \leq$ 0, 0 $\leq l \leq$ 7
Reflections collected	6958
Independent reflections	1922 (R _{int} = 0.076)
Absorption correction	None
Refinement method	Full-matrix least-squares on F ²
Data / restraints / parameters	1922 / 0 / 246
Goodness-of-fit on F ²	1.088
Final R indices [$ I > 2\sigma(I)$]	R1 = 0.0662, wR2 = 0.1471
R indices (all data)	R1 = 0.1053, wR2 = 0.1701
Extinction coefficient	0.004(2)
Largest diff. peak and hole	0.222 and -0.269 eÅ ⁻³

Atomic coordinates [$\times 10^4$] and equivalent isotropic displacement parameters [$\text{\AA}^2 \times 10^3$] for (\pm)-1-ethoxy-trans-2,5-di(4-nitrophenyl)-1 λ^5 -phospholan-1-one (4.46). U(eq) is defined as one third of the trace of the orthogonalized U_{ij} tensor.

	x	y	z	U(eq)
P(1)	7389(1)	1178(2)	8092(2)	71(1)
O(1)	7112(2)	2373(5)	7459(6)	98(2)
C(1)	8007(3)	1247(6)	9870(7)	71(2)
N(1)	10429(3)	2806(8)	8553(9)	111(2)
O(2)	7732(2)	418(5)	6884(5)	94(2)
N(2)	4240(3)	1523(7)	8181(10)	101(2)
C(2)	7937(3)	5(6)	10721(7)	79(2)
C(3)	7225(3)	-164(6)	10662(7)	80(2)
O(3)	10567(3)	3879(7)	8781(10)	154(3)
O(4)	10758(3)	2069(7)	8035(9)	153(3)
C(4)	6870(3)	94(6)	8898(7)	72(2)
O(5)	4101(3)	2257(6)	9198(10)	135(2)
C(5)	7377(3)	-105(8)	5363(8)	99(2)
O(6)	3865(3)	1045(8)	7110(8)	159(3)
C(6)	7679(4)	-1285(8)	5049(10)	131(3)
C(11)	8654(3)	1628(7)	9566(7)	70(2)
C(12)	8834(3)	2849(7)	9735(8)	83(2)
C(13)	9414(4)	3236(7)	9404(9)	93(2)
C(14)	9806(3)	2404(8)	8911(8)	77(2)
C(15)	9654(3)	1183(8)	8731(8)	85(2)
C(16)	9064(3)	806(7)	9054(8)	80(2)
C(21)	6180(3)	487(6)	8713(7)	65(2)
C(22)	5718(3)	-37(6)	7559(8)	80(2)
C(23)	5091(4)	286(7)	7370(8)	86(2)
C(24)	4920(3)	1186(7)	8374(9)	75(2)
C(25)	5368(4)	1746(6)	9516(8)	81(2)
C(26)	6004(3)	1407(6)	9701(8)	78(2)

Bond lengths [Å] and angles [°] for (±)-1-ethoxy-trans-2,5-di(4-nitrophenyl)-1λ⁵-phospholan-1-one (4.46).

P(1)-O(1)	1.480(5)	P(1)-O(2)	1.576(4)
P(1)-C(1)	1.793(6)	P(1)-C(4)	1.822(6)
C(1)-C(11)	1.502(8)	C(1)-C(2)	1.542(8)
N(1)-O(4)	1.194(8)	N(1)-O(3)	1.207(8)
N(1)-C(14)	1.477(9)	O(2)-C(5)	1.463(7)
N(2)-O(6)	1.199(8)	N(2)-O(5)	1.235(8)
N(2)-C(24)	1.475(9)	C(2)-C(3)	1.519(7)
C(3)-C(4)	1.547(7)	C(4)-C(21)	1.512(8)
C(5)-C(6)	1.476(10)	C(11)-C(16)	1.369(8)
C(11)-C(12)	1.380(8)	C(12)-C(13)	1.381(9)
C(13)-C(14)	1.343(9)	C(14)-C(15)	1.365(9)
C(15)-C(16)	1.393(8)	C(21)-C(22)	1.366(8)
C(21)-C(26)	1.386(8)	C(22)-C(23)	1.362(8)
C(23)-C(24)	1.374(9)	C(24)-C(25)	1.360(9)
C(25)-C(26)	1.385(8)		
O(1)-P(1)-O(2)	115.6(3)	O(1)-P(1)-C(1)	116.2(3)
O(2)-P(1)-C(1)	100.9(3)	O(1)-P(1)-C(4)	117.8(3)
O(2)-P(1)-C(4)	106.1(3)	C(1)-P(1)-C(4)	97.4(3)
C(11)-C(1)-C(2)	119.0(5)	C(11)-C(1)-P(1)	115.6(4)
C(2)-C(1)-P(1)	102.9(4)	O(4)-N(1)-O(3)	124.0(8)
O(4)-N(1)-C(14)	118.9(8)	O(3)-N(1)-C(14)	117.1(8)
C(5)-O(2)-P(1)	121.7(4)	O(6)-N(2)-O(5)	125.1(8)
O(6)-N(2)-C(24)	118.8(8)	O(5)-N(2)-C(24)	116.0(8)
C(3)-C(2)-C(1)	105.6(5)	C(2)-C(3)-C(4)	108.9(4)
C(21)-C(4)-C(3)	116.6(5)	C(21)-C(4)-P(1)	115.1(4)
C(3)-C(4)-P(1)	103.8(4)	O(2)-C(5)-C(6)	108.4(6)
C(16)-C(11)-C(12)	118.4(6)	C(16)-C(11)-C(1)	122.0(7)
C(12)-C(11)-C(1)	119.6(6)	C(11)-C(12)-C(13)	121.0(6)
C(14)-C(13)-C(12)	119.0(7)	C(13)-C(14)-C(15)	122.5(6)
C(13)-C(14)-N(1)	119.6(8)	C(15)-C(14)-N(1)	118.0(8)
C(14)-C(15)-C(16)	117.9(6)	C(11)-C(16)-C(15)	121.2(7)
C(22)-C(21)-C(26)	118.5(6)	C(22)-C(21)-C(4)	121.2(6)
C(26)-C(21)-C(4)	120.3(6)	C(23)-C(22)-C(21)	122.7(6)
C(22)-C(23)-C(24)	118.3(6)	C(25)-C(24)-C(23)	120.7(6)
C(25)-C(24)-N(2)	121.1(8)	C(23)-C(24)-N(2)	118.2(8)
C(24)-C(25)-C(26)	120.5(6)	C(25)-C(26)-C(21)	119.2(6)

Anisotropic displacement parameters [$\text{\AA}^2 \times 10^3$] for (\pm)-1-ethoxy-trans-2,5-di(4-nitrophenyl)-1 λ^5 -phospholan-1-one (4.46). The anisotropic displacement factor exponent takes the form: $-2\pi^2 [(ha^*)^2U_{11} + \dots + 2hka^*b^*U_{12}]$.

	U11	U22	U33	U23	U13	U12
P(1)	65(1)	91(2)	59(1)	10(1)	17(1)	0(1)
O(1)	93(3)	105(4)	99(3)	42(3)	23(3)	8(3)
C(1)	60(4)	78(5)	75(4)	8(4)	14(3)	6(4)
N(1)	88(6)	105(7)	141(6)	24(5)	28(4)	7(5)
O(2)	76(3)	143(4)	63(3)	-11(3)	17(2)	1(3)
N(2)	81(6)	123(7)	103(6)	37(5)	28(4)	-13(5)
C(2)	72(5)	97(6)	69(4)	23(4)	13(3)	7(4)
C(3)	76(5)	96(5)	71(5)	20(4)	22(3)	3(4)
O(3)	113(5)	114(5)	247(8)	29(6)	65(5)	-11(4)
O(4)	96(5)	156(7)	224(8)	3(5)	76(5)	-5(4)
C(4)	68(4)	85(5)	64(4)	1(3)	18(3)	-3(4)
O(5)	109(5)	126(6)	185(7)	36(5)	67(5)	20(4)
C(5)	89(5)	152(8)	54(4)	-12(4)	4(4)	-19(5)
O(6)	66(4)	281(9)	123(5)	23(5)	2(3)	-20(5)
C(6)	176(9)	107(7)	102(6)	-12(5)	1(6)	13(7)
C(11)	76(5)	85(6)	52(4)	1(3)	17(3)	10(4)
C(12)	75(5)	81(6)	98(5)	-15(4)	25(4)	4(4)
C(13)	84(6)	84(6)	113(6)	-5(4)	24(5)	-8(5)
C(14)	59(5)	89(6)	85(5)	15(4)	17(4)	0(5)
C(15)	74(5)	88(7)	97(5)	9(4)	23(4)	15(4)
C(16)	74(5)	78(5)	92(5)	6(4)	21(4)	3(4)
C(21)	57(4)	85(5)	55(4)	8(3)	12(3)	-6(4)
C(22)	79(5)	89(5)	73(5)	-4(4)	21(4)	-7(4)
C(23)	75(6)	108(6)	71(5)	-5(4)	4(4)	-25(5)
C(24)	54(5)	96(6)	75(5)	28(4)	15(4)	-7(4)
C(25)	91(6)	81(5)	77(5)	-6(4)	28(4)	-1(5)
C(26)	72(5)	87(6)	75(5)	-16(4)	16(4)	-13(4)

Hydrogen coordinates [$\times 10^4$] and isotropic displacement parameters [$\text{\AA}^2 \times 10^3$]
for (\pm)-1-ethoxy-trans-2,5-di(4-nitrophenyl)-1 λ^5 -phospholan-1-one (4.46).

	x	y	z	U(eq)
H(1B)	7876	1882	10580	85
H(2A)	8106	-662	10149	95
H(2B)	8163	21	11846	95
H(3A)	7078	400	11422	96
H(3B)	7139	-999	10978	96
H(4A)	6876	-674	8280	86
H(5A)	7386	459	4460	119
H(5B)	6936	-242	5462	119
H(6A)	7465	-1621	4025	197
H(6B)	7648	-1854	5917	197
H(6C)	8120	-1147	5000	197
H(12A)	8560	3421	10077	100
H(13A)	9533	4061	9520	111
H(15A)	9935	621	8404	102
H(16A)	8947	-18	8918	96
H(22A)	5837	-639	6874	96
H(23A)	4786	-92	6582	103
H(25A)	5247	2360	10177	98
H(26A)	6310	1793	10480	93